Numerical Methods for Multi-Marginal Optimal Transportation

Luca Nenna

THÈSE DE DOCTORAT

de l'Université de recherche Paris Sciences et Lettres
PSL Research University

Préparée à l'Université Paris-Dauphine

Numerical Methods for Multi-Marginal Optimal Transportation

École Doctorale de Dauphine — ED 543

Spécialité **Sciences**

COMPOSITION DU JURY :

M. Jean-David BENAMOU
INRIA-Université Paris Dauphine
Directeur de thèse

M. Guillaume CARLIER
Université Paris-Dauphine
Co-Directeur de thèse

M. Alfred GALICHON
New York University
Rapporteur

M. Dejan SLEPČEV
Carnegie Mellon University
Rapporteur

M. Yann BRENIER
CNRS-Ecole Polytechnique
Président du jury

Mme Virginie EHRLACHER
École des Ponts
Membre du jury

M. Christian LÉONARD
Université Paris Ouest
Membre du jury

M. Mathieu LEWIN
CNRS-Université Paris-Dauphine
Membre du jury

Soutenue le 5/12/2016
par Luca NENNA

Dirigée par **Jean-David BENAMOU**
Guillaume CARLIER

DAUPHINE UNIVERSITÉ PARIS | PSL RESEARCH UNIVERSITY PARIS

per aspera ad astra

Remerciements

Tout d'abord, je voudrais remercier très chaleureusement Jean-David Benamou et Guillaume Carlier pour avoir accepté d'encadrer ma thèse. Pendant ces trois années, ils m'ont appris, avec une patience presque divine, une quantité extraordinaire de choses et m'ont fait découvrir un domaine des mathématiques que j'ignorais. Si en mai 2013 j'avais fait un choix différent, si j'avais choisi de faire un doctorat dans un endroit différent et, surtout, avec des directeurs de thèse différents, je ne serais pas si heureux (et fier) du travail accompli et plein d'énergie pour tout le travail qui m'attend. Encore merci pour m'avoir fait grandir tant sur le plan mathématique que sur le plan humain.

I am deeply thankful to Alfred Galichon and Dejan Slepčev for accepting to be referees of this thesis. I am glad that they appreciated this work and I have found their comments and suggestions very inspiring.

Je tiens également à remercier Yann Brenier (merci pour les discussions sur les mathématiques, la politique et les trains...ça a été un vrai plaisir!!), Virginie Ehrlacher, Christian Léonard et Mathieu Lewin qui m'ont fait l'honneur d'être les membres de mon jury.

Durant ma thèse, j'ai eu le plaisir et l'honneur de travailler avec des gens extraordinaires et notre travail fait partie de cette thèse. Je remercie Marco Cuturi (le guru de la régularisation entropique) et Gabriel Peyré (on devrait te dédier une thèse pour comprendre comme tu arrives à faire tout ce que tu fais, mais pour l'instant je te remercie pour le sexy colormaps). Je remercie Adrien Blanchet pour les discussion sur Cournot-Nash. Je remercie Simone Di Marino et Augusto Gerolin pour le papier qu'on a écrit ensemble, pour les papiers qu'on ecrira et, surtout, pour l'amitié. Merci aussi à Paola Gori-Giorgi, Mike Seidl et Klaas Giesbertz.

Un moka-merci à l'equipe MOKAPLAN, aux moka-jeunes (Aude, Bernhard, Clarice, Lénaïc, Jean, Maxime, Quentin, Simon, Jonathan, Xavier), aux moka-senior (Vincent, François-Xavier), aux mokamis (Quentin, Jean-Marie) qui m'ont offert un super moka-cadre de moka-travail! En particulier je tiens à remercier Simon et Maxime, sans qui le travail, la vie et la thèse n'auraient pas été pareils, et Aude, Lénaïc et Jean pour avoir lu et corrigé la version française de l'introduction. Pour conclure les moka-remerciements, je dois remercier le plus important des mokamis, un mokaVIP : Filippo Santambrogio. Merci pour ta bonne humeur, ta sagesse et les dîners chez toi. Un grand merci aussi à toute l'équipe du CEREMADE. Merci en particulier à Marco, Clara, Thibaut, Is-

abelle, Raphaël B., Camille, Daniela, Pierre, Fang, Roméo, Raphaël D., Arnaud, Michaël, les moka-jeunes pour toutes les pauses et les sorties après le séminaire pour aller boire plusieurs coups. Merci aux italiens (Dario, Margherita, Riccardo, ...) pour les muffins.

Durant ces trois années, j'ai aussi effectué une mission d'enseignement à l'Université Paris-Dauphine et je tiens à remercier toute l'équipe du MIDO ainsi que les professeurs pour qui j'effectuais des TD et TP : Guillaume Legendre, Amic Frouvelle et Daniela Tonon. Ce fut vraiment très agréable de travailler avec eux.

Vorrei ringraziare i poli-amici (Silvia, Laura, Marco, Usu e Judy) per le vacanze e i week-end tra Londra e Parigi (nonché per 5 anni di università). É infine doversoso che una parte di questi ringraziamenti sia dedicata alle persone che nel corso della mia vita non hanno mai smesso di appoggiarmi e credere in me. Un grazie particolare va ai red cats (Daniele, Laura, Valerio, Monica e Claudio e ovviamente il gatto rosso) per tutte le avventure che abbiamo condiviso e per tutte quelle che verranno. É di conforto sapere che, nonostante la distanza, sarete sempre pronti a ritrovarci, a fare una vacanza insieme e ad ascoltare le mie (numerose) lamentele. Grazie anche a Roberta, Sara, Gianluca e Simona per gli aperitivi durante i miei soggiorni italiani. Un grazie anche a Marco, Stefano, a Zuffada senior e alla zia Lucy per avermi riempito la valigia di Esse alla fine di (quasi) ogni week-end, piú o meno lungo, passato in Italia. Grazie a tutta la mia famiglia per il sostengo incondizionato. In particolare tengo a ringraziare Antonietta, Roger e Frank per numerosi pranzi domenicali passati insieme a mangiare moules-frites. Se oggi posso definire Parigi "casa" questo é stato possibile anche grazie a voi. Infine un grazie enorme ai miei genitori per avermi sempre appoggiato e creduto in me senza riserve. E ovviamente grazie per avermi riempito il frigorifero tutte le volte che siete venuti a trovarmi a Parigi.

Contents

Introduction **1**

Introduction **11**

I Entropic Regularization **21**

1 A Survey on Optimal Transportation **25**
1.1 The Continuous Setting 25
1.1.1 The Benamou-Brenier formulation 29
1.2 The Discrete setting 30

2 Regularized Optimal Transport **33**
2.1 The continuous setting 33
2.1.1 The Schrödinger problem 34
2.2 The discrete setting 37

3 Bregman's Projection Algorithm **41**
3.1 Bregman alternate projections 41
3.2 The Iterative Proportional Fitting Procedure (aka the Sinkhorn algorithm) 42
3.2.1 The Convergence of the IPFP in the Hilbert's metric . . . 45
3.3 Dykstra's Algorithm 47

4 Applications **49**
4.1 Optimal Transport Barycenters 49
4.2 Matching for Teams 54
4.3 Partial Transport 58
4.4 Capacity Constrained Transport 59

5 Entropic Cournot-Nash equilibria **63**
5.1 Cournot-Nash equilibria 63
5.2 A variational approach to Cournot-Nash equilibria 64
5.3 Entropic regularization 66
5.4 A proximal splitting algorithm 67
5.4.1 A class of convex problems 68
5.4.2 A semi-implicit scheme for more general nonconvex cases 70
5.5 Numerical results 70
5.5.1 Dimension one 71

5.5.2 Dimension two 72
5.6 Extension to several populations 72
5.6.1 A class of two-populations models 72

II Multi-Marginal Optimal Transportation 79

6 From Euler equations to Multi-Marginal optimal transport 83
6.1 Incompressible Euler Equations and Arnold's Principle 83
6.2 Brenier's Principle and Generalized Solutions 86
6.2.1 Generalized incompressible flows 86
6.2.2 The hydrostatic approximation 88
6.2.3 Existence and Consistency with classical solutions 90
6.3 Brenier's principle and Multi-Marginal Optimal Transport 92
6.4 A Brenier's principle with viscosity 95

7 A Review on Multi-Marginal Optimal Transportation 101
7.1 The Multi-Marginal OT problem: the continuous setting 101
7.1.1 The Dual problem 103
7.1.2 Geometry of the Optimal Transport sets 105
7.1.3 Some symmetric cases 106
7.1.4 The Gangbo-Swiech cost 110
7.2 The Multi-Marginal OT problem: the discrete setting 112
7.3 Hidden multi-marginal optimal transport problems 113
7.3.1 The multi-marginal Wasserstein Barycenter 113
7.3.2 The multi-marginal Matching for teams problem 114
7.4 Regularized Multi-Marginal OT and generalization of the IPFP . 114
7.5 Applications 116
7.5.1 Wasserstein Barycenter 116
7.5.2 Partial Optimal Transport 117
7.5.3 Generalized Solutions of Euler Equations 118
7.5.4 1 dimension experiments 120
7.5.5 2 dimension experiment: the Beltrami flow 121
7.5.6 2 dimension experiment: the unit disk 123

8 Repulsive Optimal Transport 137
8.1 Multi-marginal OT with repulsive Harmonic Cost 137
8.2 Numerical Results: MM-OT with repulsive Harmonic Cost . . . 145
8.3 Multi-marginal OT for the Determinant 147
8.4 Numerical Results: MM-OT with Determinant Cost 151

III Application to Density Functional Theory 153

9 Density Functional Theory and Multi-Marginal Optimal Transport 157
9.1 Brief introduction to Quantum Mechanics of K-body systems . . 157
9.2 Probabilistic Interpretation and Marginals 160
9.3 Density Functional Theory (DFT) 161
9.4 "Semi-classical limit" and Optimal Transport problem 163

9.5 Multi-marginal OT with Coulomb Cost 166
9.5.1 General theory: duality, equivalent formulations and many particles limit 166
9.5.2 Regularized Optimal Transport and Hohenberg-Kohn functional 168

10 The Seidl's Conjecture and Counterexamples **173**
10.1 The Monge problem: deterministic examples and counterexamples 173
10.2 Counterexample 177

11 Numerical Results **185**
11.1 1−dimensional density: analytical solutions and numerical examples 185
11.1.1 1−dimensional for $K = 2$ 185
11.1.2 1−dimensional for $K \geqslant 3$ 186
11.2 d−dimensional radial symmetric density 190
11.2.1 $N = 2$ electrons in dimension $d \geqslant 3$: analytical examples 190
11.2.2 $K = 2$ electrons in dimension $d = 3$: Helium atom 190
11.2.3 $K = 3$ electrons in dimension $d = 3$ radial case : Lithium atom 191
11.3 Numerical Counterexamples to Seidl's conjecture 192
11.3.1 The Thin Shell 192
11.3.2 Some others numerical counterexamples 194

Contributions **201**

Bibliography **201**

Introduction

Le transport optimal (TO) est un domaine de recherche très dynamique et il y a tant d'exemples et d'applications qu'il est difficile de choisir l'un d'entre eux pour introduire ce sujet fascinant; nous mentionnons les manuels "old and new" comme [3, 61, 105, 115, 116]. Nous avons décidé d'introduire le problème du transport optimal classique, et certaines de ses variantes que nous traiterons tout au long de ce manuscrit, en utilisant un exemple donné par Villani dans [116].

Situons notre contexte à Paris et prenons en considération l'ensemble des boulangeries qui produisent des pains au chocolat (le lecteur peut bien sur choisir la viennoiserie qui lui plaît le plus). Ces derniers doivent être livrés chaque matin aux cafés dans lesquels les clients pourront les goûter. La production et la consommation de pains au chocolat sont décrites par μ et ν, respectivement. Nous supposons que la quantité total de la production et de la consommation est le même. Le problème du transport optimal consiste alors à transporter la quantité de pains au chocolat produite par la boulangerie $x \in X$ ($X \subset \mathbb{R}^d$ est l'ensemble des boulangeries) à un café $y \in Y$ ($Y \subset \mathbb{R}^d$ est l'ensemble des cafés) de sorte que le coût de transport $c(x, y)$, par exemple la distance entre la boulangerie et le café, soit minimal. Le problème introduit par Monge dans [94] consiste à chercher un transport $y = T(x)$ qui nous indique le café y où l'intégralité des pains au chocolat produits par x seront délivrés. Dans le chapitre 1 nous montrerons que ce problème est difficile à traiter et qu'on a besoin d'une relaxation (connu sous le nom de problème de *Monge-Kantorovich*) : on permet, par exemple, qu'une partie des pains au chocolat produite en x soit envoyée au café y_1 et l'autre à y_2. Dans ce cas, nous cherchons un couplage optimal $\gamma(x, y)$ qui nous indique comment la masse en x est répartie sur chaque $y \in Y$. Si le couplage optimal $\gamma(x, y)$ consiste à assigner le même café y à tous les pains au chocolat produits par la boulangerie x, alors on dit que le couplage est *déterministe* et qu'un transport optimal T existe. Lorsque le coût $c(x, y)$ est la distance au carré, l'existence d'un couplage déterministe a été prouvée par Yann Brenier dans [21].

Beaucoup de questions se posent à ce stade: que se passe-t-il si l'offre et la demande de pains au chocolat sont différentes? Et si le camion, représenté par γ, peut transporter une quantité de marchandises plus petite que celle produite en x et que celle demandée par le café y? De plus, nous pouvons également ajouter une troisième catégorie, par exemple les hôtels, de sorte que maintenant nous devons minimiser le coût de transport des pains au chocolat aux cafés et aux hôtels qui se trouvent à Paris. Ce problème peut-il encore être interprété comme un problème de TO? Peut-on introduire une méthode numérique capable

de résoudre toutes ces variantes du transport optimal? Cette thèse s'attache à répondre à ces questions et à quelques autres portant sur des modèles de transport optimal qui apparaissent en physique, notamment en physique quantique et en mécanique des fluides. De plus, nous souhaitons souligner trois thèmes récurrents. Le premier traite de la régularisation entropique des problèmes de transport optimal. L'idée principale, que nous détaillerons dans la suite, est de "relâcher" le problème de Monge-Kantorovich en ajoutant un bruit. Cela nous permet de remplacer le problème de Monge-Kantorovich par un problème strictement convexe qui admet une solution unique. En outre, le plus grand avantage de cette régularisation réside dans le fait que nous pouvons introduire un algorithme (assez simple à coder) pour calculer la solution. Dans ce cas, nous ne pouvons plus nous attendre à des plans de transport déterministes. En effet considèrons γ comme le camion qui livre les pains au chocolat à chaque cafés. Ajouter une régularisation entropique revient à faire boire au conducteur de γ beaucoup de bières. Ce dernier essaiera de suivre le chemin le moins cher entre les boulangeries et les cafés mais, étant ivre, il suivra une trajectoire aléatoire, livrant ainsi les pains au chocolat à plusieurs cafés voisins. Remarquons que la régularisation entropique nous permet de définir un algorithme puissant, mais, comme le lendemain d'une soirée alcolisée, présente aussi quelques inconvénients: par exemple, si le problème non régularisé admet un plan optimal déterministe, alors nous l'approcherons toujours avec un plan non déterministe (ou étalé). Il est clair que l'étalement de plan approximatif dépendra de l'amplitude du paramètre de régularisation (équivalente au nombre de bières bues par le conducteur).

Cela nous conduit au deuxième thème: l'existence d'un plan non-déterministe. Nous avons dit que le problème régularisé présente des solutions non déterministes à cause du type de régularisation que nous avons introduit. En effet, de telles solutions apparaissent également pour des problèmes non régularisés. Nous verrons que dans le cas du transport multi-marges, et son application aux équations d'Euler généralisées et à la théorie de la fonctionnelle de la densité (TFD), il peut y avoir plusieurs solutions optimales parmi lesquelles il y a à la fois des plans déterministes et non-déterministes.

Le troisième thème traite ensuite du problème de transport optimal multi-marges. Ne considérons plus uniquement les boulangeries et les cafés, mais prenons également en compte les hôtels, les restaurants, etc. et cherchons un couplage $\gamma(x_1, \cdots, x_K)$ nous indiquant la quantité de pains au chocolat envoyée par la boulangerie x_1 au café x_2, à l'hôtel x_3, etc. Cet exemple peut paraître simple, mais nous pouvons remarquer que le transport optimal multi-marges apparaît plus *général* que le TO classique, car il nous permet de modéliser l'interaction entre les boulangeries et tous les clients possibles, à savoir des cafés, des restaurants, des hôtels, etc.

Avoir plusieurs marges augmente évidemment la difficulté du problème et sa résolution, en particulier avec la formulation de Monge, est une tâche délicate. Cela donne toutefois lieu à des solutions présentant une structure surprenante et qui n'ont pas d'équivalent dans le cas du transport à deux marges. Nous montrerons par exemple qu'il existe pour le coût harmonique répulsif un plan optimal déterministe qui se concentre sur des transports "fractals".

Décrivons maintenant en détail les principaux résultats mathématiques inclus dans cette thèse.

Partie I: régularisation entropique du transport optimal classique

Dans la partie I nous abordons le problème de transport optimal standard et certaines de ses variantes telles que le barycentre de Wasserstein, le transport optimal partiel, le transport optimal avec une contrainte de capacité et une application pour calculer les équilibres de Cournot-Nash. Le but principal est d'introduire une méthode numérique qui nous permet de résoudre tous ces problèmes. Cette partie comprend les chapitres 1, 2, 3, 4 et 5.

Le chapitre 1 est un panorama de la théorie du transport optimal (classique): nous introduisons le problème de Monge-Kantorovich

$$\inf \left\{ \int_{X\times Y} c(x,y) d\gamma(x,y) \mid \gamma \in \Pi(\mathbb{R}^d; \mu, \nu) \right\}, \qquad (\mathcal{MK})$$

ainsi que quelques résultats qui seront utiles tout au long de la thèse. Nous verrons comment tous ces concepts et résultats sont modifiés dans le cas du transport optimal multi-marges (TOMM) dans les parties II et III.

Le chapitre 2 est consacré à l'étude de la régularisation entropique du problème de Monge-Kantorovich

$$\inf \left\{ \int_{X\times Y} c(x,y) d\gamma(x,y) + \varepsilon \, \mathrm{H}(\gamma|\mu\otimes\nu) \mid \gamma \in \Pi(\mathbb{R}^d; \mu, \nu) \right\}, \qquad (\mathcal{MK}_\varepsilon)$$

où $\varepsilon > 0$ est un paramètre de régularisation et

$$\mathrm{H}(\gamma|\mu\otimes\nu) := \begin{cases} \displaystyle\int_{X\times Y} \left(\log\left(\frac{d\gamma}{d\mu\otimes\nu}\right) - 1 \right) d\gamma & \text{if} \gamma \ll \mu\otimes\nu \\ +\infty & \text{sinon} \end{cases} \qquad (0.1)$$

est l'entropie relative. Nous verrons que grâce à l'entropie, le problème $(\mathcal{MK}_\varepsilon)$ est strictement convexe et admet une solution unique qui a une forme presque explicite. De plus, comme souligné par C. Léonard dans de nombreux travaux, voir [84, 85] par exemple, la régularisation de $(\mathcal{MK})$ lorsque le coût est la distance au carré est en relation avec le problème introduit par Schrödinger dans [107, 108].

L'idée de régulariser le problème de transport optimal, d'un point de vue numérique, à l'aide d'un terme d'entropie a été introduite indépendamment par Cuturi [46] et Galichon et Salanié [63]. Dans [BCC$^+$15], nous étendons cette idée à d'autres problèmes de transport optimal. Dans le chapitre 3, nous allons voir que, en utilisant l'algorithme des projections alternées, nous utilisons la même méthode numérique pour approcher des solutions de plusieurs problèmes variationnels liés au transport optimal (voir aussi partie II et III). Les chapitres

3, 4 et 5 représentent une contribution importante de cette thèse car ils donnent une méthode numérique simple, robuste et flexible.

Nous donnons maintenant une brève description de cette méthode. Après quelques calculs algébriques simples, le problème $(\mathcal{MK}_\varepsilon)$ peut être réécrit comme la minimisation de la divergence KL de Kullback-Leibler, qui est en fait l'entropie relative

$$\inf \left\{ \mathrm{KL}\left(\gamma|\eta_\varepsilon\right) \mid \gamma \in \Pi(\mathbb{R}^d; \mu, \nu) \right\}, \tag{KL}$$

où $\mathrm{KL}\left(\gamma|\eta_\varepsilon\right) := \mathrm{H}(\gamma|\eta_\varepsilon)$ et $\eta_\varepsilon = \frac{1}{L} \exp\left(c(x,y)/\varepsilon\right)\mu \otimes \nu$ avec L tel que η est une mesure de probabilité. La distance (KL) peut être placée dans le cadre plus général des distances de Bregman [18]. On peut alors résoudre le problème en utilisant l'algorithme des projections alternées de Bregman ou sa généralisation (nécessaire lorsque les ensembles convexes ne sont pas affines) connue sous le nom d'algorithme de Dykstra. Notez que l'ensemble $\Pi(\mathbb{R}^d; \mu, \nu)$ peut être vu comme l'intersection de deux ensembles convexes $\mathcal{C}_i$, chacun étant associé à une contrainte de marginale.

L'idée de l'algorithme des projections alternées est de construire une suite de plans $\gamma^{(n)}$ telle que le $(n+1)-$ième terme est la projection, pour la divergence KL, de $\gamma^{(n)}$ sur l'ensemble $\mathcal{C}_{[n+1]}$ où $[\cdot]$ désigne le modulo. Dans le cas du problème classique (TO), l'ensemble convexe $\mathcal{C}_i$ est un sous-espace affine et nous montrerons que l'algorithme de Bregman/Dykstra peut être reformulé comme l'algorithme connu sous le nom de IPFP (Iterative Proportional Fitting Procedure) ou Sinkhorn.

Le chapitre 4 est basé sur [BCC$^+$15]. Nous montrons ici que l'algorithme de Bregman peut être appliqué pour résoudre différents types de (TO):

- Supposons que nous avons K marginales μ_i qui modélisent la consommation de pains au chocolat des cafés, des hôtels, des restaurants, des supermarchés, etc et nous voulons trouver une quantité optimale de production ν qui est proche de chaque μ_i afin de minimiser le coût transport des marchandises. La distribution ν est le barycentre des mesures μ_i dans l'espace de Wasserstein (voir [1]).
- Si nous ne pouvons déplacer qu'une fraction des pains au chocolat ou si les cafés ne peuvent accepter qu'une partie des biens produits, alors nous avons un problème connu sous le nom de transport optimal partiel (voir [27] et [54]).
- Supposons maintenant que nous ne pouvons pas transporter de x à y une quantité de biens plus grande qu'une limite donnée $\theta(x,y)$, alors nous imposons une contrainte supplémentaire, une "contrainte de capacité" , sur le plan de transport: cela nous conduit au transport optimal avec une contrainte de capacité introduit par Korman et McCann dans [79, 80].

Notons que tous ces problèmes de transport optimal sont intrinsèquement différents, mais en utilisant la régularisation entropique, nous pouvons les reformuler tous en termes de minimisation de la divergence de Kullback-Leibler et appliquer l'algorithme de Bregman.

Cette partie s'achève avec le chapitre 5, consacré au calcul des équilibres de Cournot-Nash. Ceci est basé sur un travail en commun avec Adrien Blanchet et Guillaume Carlier [BCN16b]. Le problème peut être décrit comme suit: les acteurs hétérogènes doivent chacun choisir une stratégie (ou une probabilité par rapport aux stratégies, c'est-à-dire que des stratégies mixtes sont autorisées) afin de minimiser un coût, sur lequel on fait deux hypothèses majeures. D'une part, chaque joueur a une influence négligeable sur le coût. D'autre part, les interactions entre les joueurs sont de type champ moyen: ce qui importe n'est pas vraiment qui joue quoi, mais plutôt combien de joueurs jouent une strategie donnée. Il existe différents effets de champ moyen, de nature différente et qui peuvent être soit répulsifs (c'est-à-dire favorisant la dispersion des stratégies) soit attractifs (favorisant la concentration des stratégies). La congestion (le coût d'une stratégie est plus élevée si il y a beaucoup de joueurs qui la choisissent) est un exemple typique d'effet dispersif. Plus récemment, Blanchet et Carlier [15] (voir aussi [14]) ont souligné le fait que pour une classe de coûts séparables, les équilibres de Cournot-Nash peuvent être obtenus en minimisant une certaine fonctionnelle sur l'ensemble des mesures sur l'espace des stratégies. Cette fonctionnelle comporte généralement deux termes: un coût de transport optimal et une fonctionnelle intégrale plus classique qui peut capturer à la fois la congestion et les effets attractifs (comme dans [83]). Plus précisément, nous avons le problème de minimisation suivant

$$\inf_{\nu}\{\mathcal{MK}_c(\mu,\nu)+E(\nu)\}, \tag{CN}$$

où $\mathcal{MK}_c(\mu,\nu)$ est le problème $(\mathcal{MK})$ avec un coût c et $E(\nu)$ est une fonctionnelle qui capture à la fois la congestion et les effets attractifs. Le but de ce chapitre est de montrer qu'une extension de l'algorithme de Bregman/Dykstra, récemment proposé par Peyré [100] pour les flots gradients dans l'espace de Wasserstein, peut être parfaitement adaptée au calcul des équilibres de Cournot-Nash. Notons que jusqu'à présent les tentatives de résolution numérique de (CN) ont été faites dans le cas du coût quadratique, en raison de la structure spéciale des solutions optimales. Ici, grâce à la régularisation entropique et par conséquent à l'algorithme de Bregman/Dykstra, nous sommes capables de calculer les équilibres de Cournot-Nash quelle que soit la fonction de coût c dans $\mathcal{MK}_c$. Enfin, nous présentons quelques simulations numériques qui donnent des indications intéressantes sur la topologie des équilibres et nous proposons également une extension du modèle à plusieurs populations.

Partie II: des équations d'Euler au transport optimal répulsif

Cette partie est consacrée au problème du transport optimal multi-marges (TOMM). Nous verrons que ce type de problème apparaît de façon très naturelle dans de nombreux contextes en physique comme en dynamique des fluides et en théorie de la fonctionnelle de la densité (TFD). La deuxième contribution importante de la thèse est de donner un cadre unificateur des applications du transport optimal multi-marges en physique. Par ailleurs, nous introduisons une classe de problèmes de transport optimal, le transport optimal répulsif (qui trouve son application principale en TDF), pour lequel nous résumons les résultats existants

dans la littérature et donnons de nouveaux, comme l'existence de transports fractals.

Le chapitre 6 traite des problèmes variationnels associés aux équations d'Euler incompressibles. Nous nous concentrons surtout sur le principe variationnel introduit par Brenier dans [20, 19] car il peut être considéré comme un précurseur du problème multi-marges. Ce chapitre est basé sur un travail en commun avec Jean-David Benamou et Guillaume Carlier [BCN16a].

Soient $u : [0,T] \times \mathcal{D} \to \mathbb{R}^d$ le champ de vitesse et $p : [0,T] \times \mathcal{D} \to \mathbb{R}$ le champ de pression. On peut écrire les équations d'Euler de la façon suivante

$$\begin{cases} \partial_t u + (u \cdot \nabla)u + \nabla p = 0 & \text{dans } [0,T] \times \mathcal{D} \\ \mathrm{div}(u) = 0 & \text{dans } [0,T] \times \mathcal{D} \\ u \cdot n = 0 & \text{sur } [0,T] \times \partial\mathcal{D}, \end{cases} \tag{0.2}$$

où n est le vecteur unitaire normal à $\partial\mathcal{D}$. Le mouvement d'un fluide incompressible à l'intérieur de $\mathcal{D}$ peut aussi être décrit d'un point de vue Lagrangien: on regarde alors le mouvement des particules du fluide par rapport à leur position initiale. Nous supposons donc que le champ de vitesse u est une solution régulière du système (6.1) et on note par $g : [0,T] \times \mathcal{D} \to \mathbb{R}^d$ la solution de

$$\begin{cases} \partial_t g(t,x) = u(t, g(t,x)) & (t,x) \in [0,T] \times \mathcal{D} \\ g(0,x) = x & x \in \mathcal{D}. \end{cases} \tag{0.3}$$

Puisque u est à divergence nulle, pour chaque temps t le flot $g(t,\cdot)$ est un difféomorphisme qui préserve la mesure (on note $g(t,\cdot) \in \mathbb{S}\mathrm{Diff}(\mathcal{D})$) c'est à dire $g(t,\cdot)_\sharp \mathcal{L}_\mathcal{D} = \mathcal{L}_\mathcal{D}$. Si l'on écrit (0.10) en fonction de g on obtient

$$\begin{cases} \partial_{tt} g(t,x) = -\nabla p(t, g(t,x)) & \text{dans } [0,T] \times \mathcal{D} \\ g(0,x) = x & x \in \mathcal{D} \\ g(t,\cdot) \in \mathbb{S}\mathrm{Diff}(\mathcal{D}) \end{cases} \tag{0.4}$$

Dans [6], Arnold a interprété l'équation ci-dessus comme une équation géodésique dans l'espace $\mathbb{S}\mathrm{Diff}(\mathcal{D})$: on peut ainsi chercher la solution de (0.12) en minimisant

$$\int_0^T \int_\mathcal{D} \frac{1}{2} |\dot{g}(t,x)|^2 dx dt \tag{$\mathcal{A}$}$$

parmi les chemins $g(t,\cdot) \in \mathbb{S}\mathrm{Diff}(\mathcal{D})$ avec configuration initiale $g(0,\cdot) = g_\star$ et configuration finale $g(T,\cdot) = g^\star$ (par invariance on peut prendre $g_\star$ égale à l'identité Id). Dans [51], Ebin et Marsden ont prouvé que, lorsque $\mathcal{D}$ est une variété compacte sans frontière, le problème de minimisation $(\mathcal{A})$ a une solution unique, qui est aussi une solution des équations d'Euler, si $g_\star$ et $g^\star$ sont suffisamment proches dans une norme de Sobolev adéquate. Malgré ces résultats, Shnirelman a prouvé dans [112, 111] que quand $d \geqslant 3$ l'infimum n'est pas atteint et que quand $d = 2$ il existe une configuration finale $\gamma^\star \in \mathbb{S}\mathrm{Diff}(\mathcal{D})$ qui ne peut pas être reliée à Id par un chemin d'énergie finie. Ces résultats motivent l'étude des formulations relaxées du problème d'Arnold, introduites

par Brenier dans [20]: il considère les mesures de probabilité γ sur $\Omega(\mathcal{D})$, l'espace des chemins absolument continus ω, et minimise

$$\int_{\Omega(\mathcal{D})} \int_0^1 \frac{1}{2} |\dot{\omega}(t)|^2 dt d\gamma(\omega), \tag{$\mathcal{E}$}$$

sous les contraintes

$$(e_0, e_T)_\sharp \gamma = (\mathrm{Id}, g^\star)_\sharp \mathcal{L}_\mathcal{D}, \quad (e_t)_\sharp \gamma = \mathcal{L}_\mathcal{D}, \ \forall t \in [0,T], \tag{0.5}$$

où $e_t(\omega) := \omega(t)$ indique la projection à l'instant t. Brenier a appelé γ un *flot incompressible généralisé* dans $[0,T]$ entre Id et $g^\star$. On remarque que le problème $(\mathcal{E})$ ressemble à un problème de Monge-Kantorovich avec un nombre infini de marges. Dans la section 6.3 nous présentons une discrétisation temporelle du problème de Brenier obtenue en fixant le nombre K de pas de temps (à savoir le nombre de marges) :

$$\begin{aligned} \inf \Big\{ \int_\Omega \sum_{i=1}^K |\omega(t_i) - \omega(t_{i-1})|^2 d\gamma \mid \\ \gamma \in \mathcal{P}(\Omega), \ (e_i)_\sharp \gamma = \mathcal{L}_D, \ (e_0, e_T)_\sharp \gamma = (\mathrm{Id}, g^\star)_\sharp \mathcal{L}_\mathcal{D} \Big\}, \end{aligned} \tag{$\mathcal{E}_K$}$$

et nous prouvons que le problème discret $(\mathcal{E}_K)$ converge vers $(\mathcal{E})$ quand $K \to \infty$.

On conclut ce chapitre en décrivant un modèle, introduit d'abord par Léonard et ses co-auteurs dans [5] (et ensuite dans [BCN16a]) qui peut être vu comme un principe de Brenier avec viscosité. On peut retrouver ce modèle à partir de la régularisation entropique de $(\mathcal{E}_K)$: la version régularisée de $(\mathcal{E}_K)$ peut être vue comme une discrétisation temporelle d'un problème avec un nombre infini de marges. En effet, nous retrouvons un problème de minimisation d'une entropie relative (définie comme dans $(\mathcal{MK}_\varepsilon)$) où la mesure de référence est une mesure de Wiener. En d'autres termes, nous obtenons un problème de Schrödinger avec un nombre infini de marges, ce qui peut être considéré comme une extension du problème avec deux marges.

Le chapitre 7 est consacré à l'introduction du transport optimal multi-marges et à la présentation d'une généralisation de l'algorithme IPFP à ce cas. Ce chapitre est basé sur [BCC+15, BCN16a]. Soit K le nombre de marges. Le problème de Monge-Kantorovich multi-marges devient

$$\inf \left\{ \int_{\mathbb{R}^{dK}} c(x_1, \dots, x_K) d\gamma(x_1, \cdots, x_K) \mid \gamma \in \Pi(\mathbb{R}^{dK}; \mu_1, \cdots, \mu_K) \right\}, \tag{$\mathcal{MK}_K$}$$

où $\Pi(\mathbb{R}^{dK}; \mu_1, \cdots, \mu_K)$ est l'ensemble des couplages $\gamma(x_1, \cdots, x_K)$ ayant $\mu_1, \cdots, \mu_K$ comme marges. Le problème de Monge correspondant devient alors

$$\inf \left\{ \int_{\mathbb{R}^{dK}} c(x, T_2(x), \cdots, T_K(x)) d\mu_1(x) \mid T = \{T_i\}_{i=1}^K \in \mathcal{T}_K \right\}, \tag{$\mathcal{M}_K$}$$

où

$$\mathcal{T}_K := \{T = \{T_i\}_{i=1}^K \mid T_i : \mathbb{R}^d \to \mathbb{R}^d \ (T_i)_\sharp \mu_1 = \mu_i, \forall i = 2, \cdots, K, \ T_1 = \mathrm{Id}\}.$$

Ces problèmes multi-marges sont apparus pour la première fois dans le travail de Gangbo et Święch [66] qui ont résolu le cas du coût quadratique et ont prouvé l'existence de solutions de Monge (c'est-à-dire d'applications de transport optimales). Au cours des dernières années, les problèmes multi-marges ont suscité beaucoup d'intérêt, car ils apparaissent naturellement dans de nombreux contextes différents, tels que l'économie [32], [96] et la théorie de la fonctionnelle de la densité [26, 43, 49, 60, 44] comme nous le verrons dans la dernière partie. Dans la section 7.5, nous présentons des simulations numériques pour différents types de problèmes de transport optimal multi-marges. Nous soulignons que cela est possible grâce à une extension de l'algorithme IPFP proposé par l'auteur [BCC$^+$15, BCN15, BCN16a, DMGN15].

Le chapitre 8 est basé sur un travail en commun avec Simone Di Marino et Augusto Gerolin [DMGN15]. Ici, nous avons essayé de donner un cadre général pour une classe particulière de fonctions de coût : les coûts répulsifs. Comme nous l'expliquerons dans la dernière partie de cette thèse, la principale motivation qui nous a amenés à étudier ce type de problème de transport optimal provient de la théorie de la fonctionnelle de la densité où certains coûts, comme le coût de Coulomb ou le coût harmonique répulsif, jouent un rôle central . Du point de vue mathématique, le cas intéressant est celui où toutes les marges du couplage γ dans $(\mathcal{MK}_K)$ sont absolument continues par rapport à la mesure de Lebesgue et sont identiques. En particulier, puisque les coûts sont *"repulsifs"*, si des solutions de type Monge existent, elles doivent suivre la règle *"plus c'est loin, mieux c'est !"*, ce qui veut dire que nous cherchons à déplacer la masse autant que possible.

Le résultat principal de cette section est contenu dans le théorème 8.1.6 où nous montrons qu'il existe des transports optimaux pour le problème de Monge lorsque le coût est donné par

$$c(x_1, \cdots, x_K) = -\sum_{i<j} |x_i - x_j|^2$$

et ces transports ont la particularité d'avoir une structure fractale quand $k \geqslant 3$. On note que c'est un résultat surprenant qui n'a pas de version équivalente dans le cas de deux marges.

Partie III: rencontre entre transport optimal et la théorie de la fonctionnelle de la densité

La dernière partie de cette thèse est consacrée à exploiter la connexion entre la théorie de la fonctionnelle de la densité et le transport optimal multi-marges. On peut décrire la structure d'une molécule avec N électrons en étudiant l'équation de Schrödinger pour une fonction d'onde $\psi \in \mathrm{L}^2(\mathbb{R}^{3K}; \mathbb{C})$ (négligeons pour le moment la variable de spin). La limite de cette approche est dans la complexité du calcul numérique : pour prédire le comportement d'une molecule H_2O (10 électrons) en discrétisant $\mathbb{R}$ en une grille de 10 points, nous devons résoudre l'équation de Schrödinger sur une grille de 10^{30} points. C'est pourquoi Hohenberg, Kohn et Sham ont introduit, dans [73] et [78], la

théorie de la fonctionnelle de la densité (TFD) comme méthode d'approximation numérique pour résoudre l'équation de Schrödinger plus efficacement. L'idée principale de la DFT est de calculer seulement la densité électronique

$$\rho(x_1) = \int \gamma_K(x_1, x_2 \cdots, x_K) dx_2 \cdots dx_K,$$

où $\gamma_K = |\psi(x_1, \cdots, x_K)|^2$ est la densité de probabilité jointe des électrons aux positions $x_1, \cdots, x_K \in \mathbb{R}^3$, au lieu de la fonction d'onde ψ. Un cas intéressant pour la DFT est lorsque la répulsion entre les électrons domine sur l'énergie cinétique. Alors, le problème peut être reformulé comme un problème de transport optimal (OT) comme souligné dans les travaux pionniers de Buttazzo, De Pascale et Gori-Giorgi [26] et Cotar, Friesecke et Klüppelberg [43].

Dans le chapitre 9, nous introduisons la théorie de la fonctionnelle de la densité et le transport optimal multi-marges avec le coût de Coulomb. Dans la théorie de la fonctionnelle de la densité [73] l'énergie totale d'un système (avec N électrons) est obtenue en minimisant la fonctionnelle suivante par rapport à la densité électronique $\rho(x)$:

$$E(\rho) = \min_{\rho \in \mathcal{R}} F_{HK}(\rho) + \int_{\mathbb{R}^3} v(x)\rho(x)dx \tag{0.6}$$

où $\mathcal{R} := \{\rho : \mathbb{R}^3 \to \mathbb{R} | \rho \geqslant 0, \sqrt{\rho} \in \mathrm{H}^1(\mathbb{R}^3), \int_{\mathbb{R}^3} \rho(x)dx = K\}$,
$v := -\dfrac{Z}{|x - R|}$ est le potentiel d'interaction électron-noyau (Z et R sont la charge et la position du noyau), F_{HK} est la fonctionnelle Hohenberg-Kohn qui est définie comme la valeur minimale parmi toutes les fonctions ψ qui donnent ρ:

$$F_{HK}(\rho) = \min_{\psi \to \rho} \hbar^2 T(\psi) + V_{ee}(\psi), \tag{0.7}$$

où $\hbar^2$ est un facteur constant,

$$T(\psi) = \frac{1}{2} \int \cdots \int \sum_{i=1}^{K} |\nabla_{x_i} \psi|^2 dx_1 \cdots dx_K$$

est l'énergie cinétique et

$$V_{ee}(\psi) = \int \cdots \int \sum_{i=1}^{N} \sum_{j>i}^{N} \frac{1}{|x_i - x_j|} |\psi|^2 dx_1 \cdots dx_K$$

est l'interaction électron-électron. Si l'on considère la limite *semi-classique*

$$\lim_{\hbar \to 0} \min_{\psi \to \rho} \hbar^2 T(\psi) + V_{ee}(\psi)$$

et si l'on suppose avoir le droit d'échanger minimum et limite (Cotar, Friesecke et Klüppelberg dans [43] l'ont prouvé pour $K = 2$), alors on obtient la fonctionnelle suivante:

$$V_{ee}^{SCE}(\rho) = \min_{\psi \to \rho} \int \cdots \int \sum_{i=1}^{K} \sum_{j>i}^{K} \frac{1}{|x_i - x_j|} |\psi|^2 dx_1 \cdots dx_K \tag{0.8}$$

où V_{ee}^{SCE} est l'énergie minimale de répulsion de Coulomb dont le minimiseur caractérise l'état de *Strictly Correlated Electrons* (SCE). On peut noter que, en notant $\gamma = |\psi|^2$, V_{ee}^{SCE} correspond au problème de Monge-Kantorovich avec le coût de Coulomb. Puisque le coût est à symétrie radiale, si les marges ρ sont également à symétrie radiale, alors (0.16) peut être réduit à un problème unidimensionnel avec le coût donné par la minimisation sur les angles de $\sum_{i=1}^{K}\sum_{j>i}^{K}\frac{1}{|x_i-x_j|}$. Dans la section 9.5.2, nous prouvons que

$$F_{HK}(\rho) \geqslant \min\left\{\mathrm{H}(\gamma|\eta) \mid \gamma \in \Pi_K(\mathbb{R}^{dK};\rho)\right\}$$

où $\eta := \frac{1}{L}\exp\left(-\sum_{i<j}\frac{1}{\varepsilon|x_i-x_j|}\right)\otimes_{i=1}^{K} dx_i$ et $\varepsilon = \dfrac{\pi\hbar^2}{2}$. Cela nous montre que la régularisation entropique, introduite pour des raisons "numériques", a en fait un sens "physique" en ce sens qu'elle tient compte des effets dus à l'énergie cinétique.

Le chapitre 10 est basé sur un travail en commun ([SDMG$^+$]) avec Simone Di Marino, Augusto Gerolin, Klaas Giesbertz, Paola Gori-Giorgi et Michael Seidl. Nous y donnons un contre-exemple (nous renvoyons le lecteur aussi à [41] pour d'autres contre-exemples) à la conjecture de Seidl 0.0.1.

Le dernier chapitre 11 est consacré aux simulations numériques pour le (TOMM) avec coût de Coulomb obtenues avec l'IPFP. Ce chapitre est basé sur [BCN15, DMGN15, SDMG$^+$]. Remarquons que la section 11.3 est liée au chapitre 10 car nous y présentons des contre-exemples numériques à la conjecture 0.0.1.

Introduction

Optimal Transportation is a very dynamic research field and there are so many examples and applications that it is actually difficult to choose one among them in order to introduce this fascinating subject; we refer the reader to some "old and new" textbooks such as [3, 61, 105, 115, 116]. Here, we have decided to introduce the classical optimal transport problem, and some of its variants which we deal with throughout the thesis, by using an example given by Villani in [116].

Imagine that we are in Paris and consider the bakeries, producing pain au chocolat (the reader is free to choose his favorite French pastry), which should be transported each morning to the local cafés where customers will enjoy eating them. The production and the consumption of pain au chocolat are described by a distribution μ and ν, respectively; we assume that the total amount of the production and the consumption is the same. Then, the Optimal Transportation problem consists in transporting the amount of pain au chocolat produced by the bakery $x \in X$ ($X \subset \mathbb{R}^d$ is the set of bakeries) to a café $y \in Y$ ($Y \subset \mathbb{R}^d$ is the set of cafés) such that the transport cost $c(x, y)$, for instance the distance between the bakery and the café, is minimized. The problem introduced by Monge in [94] deals with searching for a transport map $y = T(x)$ which tells us the café y where *all* the amount of pain au chocolat produced by x is sent. In chapter 1, we will recall that this problem is actually difficult to treat and a relaxation (known as the *Monge-Kantorovich* problem) is needed: we allow to split the "mass" at x such that, as an example, a fraction is sent to y_1 and the other one to y_2. So, in this second case we are looking for an optimal coupling $\gamma(x, y)$ which tells us how mass at x is distributed to all $y \in Y$. In the case in which the "cheapest" coupling $\gamma(x, y)$ is to assign the same café y to all the pain au chocolat produced by the bakery x, then we say that the optimal coupling is *deterministic* and an optimal map exists. When cost $c(x, y)$ is the squared distance the existence of such a deterministic coupling was proved by Yann Brenier in [21].

Many questions arise at this point: what happens if the supply and the demand of pain au chocolat are different? and if the truck, represented by γ, can transport a quantity of goods smaller than the one produced at x and requested by the café y? Moreover, we can also add a third category, e.g. the hotels, so that now we have to minimize the cost of sending the pain au chocolat to both the cafés and the hotel in Paris. Can this problem still be interpreted as an OT problem? Can we introduce a numerical method which is able to solve all these variants of Optimal Transport? This thesis is, actually, devoted to answer these

questions and a few other ones dealing with optimal transport models arising in Physics, especially in Quantum Physics and Fluid Dynamics. Moreover, there are three recurring themes that we wish to highlight. The first one deals with the entropic regularization of Optimal Transport problems. The main idea, that we will detail in the following, is to "relax" the Monge-Kantorovich problem by adding a noise. This enable us to replace the Monge-Kantorovich problem by a strongly convex problem which admits a unique solution. Furthermore, the greatest advantage of this regularization lies on the fact that we can introduce a simple algorithm to compute the solution. In this case we cannot expect deterministic transport plans anymore: if we consider γ as the truck which delivers the pain au chocolat to each cafés, then adding an entropic regularization is equivalent to make the driver of γ drink many beers. Thus, the driver will try to follow the cheapest path between the bakeries and the cafés but, since he is drunk, he will follow a random trajectory, delivering pain au chocolat to several nearby cafés. Notice that the entropic regularization allow us to define a powerful algorithm, but, as an hangover, has also some drawbacks: for instance, if the unregularized problem admits a deterministic optimal plan, then we always approximate it with a non-deterministic (or spread) plan. It is clear that the "spreadness" of the approximate plan will depend on the magnitude of the regularization parameter (roughly speaking it depends on the number of beers drunk by the driver).

This leads to the second theme: the existence of non-deterministic plan. We have said that the regularized problem has solutions which are non-deterministic and this is due to the kind of regularization we have introduced. Indeed these kinds of solutions arise also in the case of un-regularized problems. We will see that in the case of multi-marginal transportation, and its application to generalized Euler equations and Density Functional theory, there could be many optimal solutions among which there are both deterministic and non-deterministic plans.

Then, the third theme deals with multi-marginals optimal transport problem. Instead of considering only bakeries and cafés, we take into account also hotels, restaurants, etc and we look for a coupling $\gamma(x_1, \cdots, x_K)$ which tells us the amount of pain au chocolat sent by the bakery x_1 to the café x_2, the hotel x_3, etc. Even if this is a simple example, we can notice that the multi-marginal optimal transport appears more *general* than the classic OT as it let us model the interaction between the bakeries and all the possible customers which include cafés, restaurants, hotel etc.

The multi-marginality character of the problem obviously increases its difficulty and treat it, especially the Monge formulation, is a delicate task. However this also gives rise to solutions with a surprising structure which have not a counterpart in the two marginals case. For instance, we will show that for the repulsive harmonic cost, there exists a deterministic optimal plan which is concentrated on "fractal" maps.

Now we shall describe in details the main mathematical results included in the present thesis. We shall see how they are presented with respect to the chapters as well.

Part I: entropic regularization of classic optimal transport

In part I we address the standard optimal transport problem and some of its variants such as Wasserstein barycenter, Partial optimal transport, Optimal Transport with capacity constraint and an application to compute Cournot-Nash equilibria. The main purpose is to introduce a numerical method which is used to solve all these problems. This part is composed by chapters 1, 2, 3, 4 and 5.

Chapter 1 is a survey on (classical) Optimal Transport Theory: we introduce the Monge-Kantorovich problem

$$\inf\left\{\int_{X\times Y} c(x,y)d\gamma(x,y) \mid \gamma\in\Pi(\mathbb{R}^d;\mu,\nu)\right\}, \tag{$\mathcal{MK}$}$$

as well as some results which will be useful throughout the thesis. Especially, we will see how all these concepts and results will be modified in the case of the Multi-Marginal Optimal Transport (MMOT) in parts II and III.

Chapter 2 is devoted to study the entropic regularization of the Monge-Kantorovich problem

$$\inf\left\{\int_{X\times Y} c(x,y)d\gamma(x,y)+\varepsilon\,\mathrm{H}(\gamma|\mu\otimes\nu) \mid \gamma\in\Pi(\mathbb{R}^d;\mu,\nu)\right\}, \tag{$\mathcal{MK}_\varepsilon$}$$

where $\varepsilon>0$ is a regularization parameter and

$$\mathrm{H}(\gamma|\mu\otimes\nu):=\begin{cases}\displaystyle\int_{X\times Y}\left(\log\left(\frac{d\gamma}{d\mu\otimes\nu}\right)-1\right)d\gamma & \text{if}\gamma\ll\mu\otimes\nu\\ +\infty & \text{otherwise}\end{cases} \tag{0.9}$$

is the relative entropy. We will see that thanks to the entropy, problem ($\mathcal{MK}_\varepsilon$) is strictly convex and admits a unique solution which has an almost explicit form. Moreover, as highlighted by C. Léonard in many works, see for instance [84, 85], the regularization of ($\mathcal{MK}$) when the cost is the quadratic distance is related to the problem introduced by Schrödinger in [107, 108].

The idea of regularizing the optimal transport problem, from a numerical point of view, by means of an entropy term was introduced, independently by Cuturi [46] and Galichon and Salanié in [63]. In [BCC+15] we extend this to other optimal transport problems. In chapter 3 we will see that by using the alternate projections algorithm we use the same numerical method to approximate solutions to several variational problems related to optimal transport (see also part II and III). Chapters 3, 4 and 5 represent an important contribution of this thesis as they give a simple, robust and flexible numerical method.

Let us now give a brief description of this method. After some simple algebraic computations, problem ($\mathcal{MK}_\varepsilon$) can be rewritten as the minimization of the Kullback-Leibler KL divergence, which is indeed the relative entropy,

$$\inf\left\{\mathrm{KL}\left(\gamma|\eta_\varepsilon\right) \mid \gamma\in\Pi(\mathbb{R}^d;\mu,\nu)\right\}, \tag{KL}$$

where $\mathrm{KL}(\gamma|\eta_\varepsilon) := \mathrm{H}(\gamma|\eta_\varepsilon)$ and $\eta_\varepsilon = \frac{1}{L}\exp(-c(x,y)/\varepsilon)\mu\otimes\nu$ with L such that η is a probability measure. The (KL) distance can be placed in the more general framework of Bregman distances [18]. Then, problem (KL) can be solved by using the Bregman alternate projections algorithm or its generalization (needed when the convex sets are not affine) known as Dykstra's algorithm. Notice that the set $\Pi(\mathbb{R}^d;\mu,\nu)$ can be seen as the intersection of two convex set $\mathcal{C}_i$ each of them associated to a marginal constraint.

The idea of the alternate projections algorithm is to build a sequence of plans $\gamma^{(n)}$ such that the $(n+1)-$th term is the projection, with respect to the KL divergence, of $\gamma^{(n)}$ onto the set $\mathcal{C}_{[n+1]}$ where $[\cdot]$ denotes the modulo operation. In the case of the classical (OT) problem the convex set $\mathcal{C}_i$ are affine subspaces and we will show that the Bregman/Dykstra algorithm can be reformulated as the IPFP, Iterative Proportional Fitting Procedure, (or Sinkhorn) algorithm.

Chapter 4 is based on [BCC$^+$15]. Here, we show that the Bregman algorithm can be applied to solve different kinds of (OT):

- Suppose that we have K marginals μ_i which model the consumption of pain au chocolat of cafés, hotels, restaurants, supermarket, etc and we want to find an optimal amount of production ν which is close to each μ_i in order to minimize the cost of transporting the goods. The distribution ν is the barycenter of the measures μ_i in the Wasserstein space (see [1]).

- If we can move only a fraction of pain au chocolat or the cafés can accept only a part of the goods produced, then we have a problem which is known as Partial Optimal Transport (see [27] and [54]).

- Assume now that we cannot transport from x to y a quantity of goods larger than a given limit $\theta(x,y)$, then we are imposing an additional constraint, a "capacity constraint", on the transport plan: this leads us to the so-called Optimal Transport with capacity constraint introduced by Korman and McCann in [79, 80].

Notice that all these optimal transport problems are intrinsically different, but by using the entropic regularization we can recast all of them in terms of minimization of a Kullback-Leibler divergence and apply the Bregman algorithm.

We end this Part with chapter 5, devoted to the computation of Cournot-Nash equilibria. This is based on a joint work with Adrien Blanchet and Guillaume Carlier [BCN16b]. The problem can be described as follows: heterogeneous players each have to choose a strategy (or a probability over strategies, i.e. mixed strategies are allowed) so as to minimize a cost, the latter depending on the choice of the whole population of players only through the distribution of their strategies. In other words, on the one hand, each player has a negligible influence on the cost. On the other hand, the interactions between players are of mean-field type: it does not matter who plays such and such strategy but rather how many players chose it. There are different mean-field effects, of different nature and which can be either repulsive (i.e. favoring dispersion of strategies) or attractive (favoring concentration of strategies). Congestion (the cost of a strategy is higher if it is frequently played) is a typical example of dispersive

effect. More recently, Blanchet and Carlier [15] (also see [14]) emphasized the fact that for a separable class of costs, Cournot-Nash equilibria can be obtained by the minimization of a certain functional on the set of measures on the space of strategies. This functional typically involves two terms: an optimal transport cost and a more standard integral functional which may capture both congestion and attractive effects (as in [83]). More precisely we have the following minimization problem

$$\inf_{\nu}\{\mathcal{MK}_c(\mu,\nu)+E(\nu)\}, \tag{CN}$$

where $\mathcal{MK}_c(\mu,\nu)$ is problem $(\mathcal{MK})$ with a cost c and $E(\nu)$ is a functional which captures both congestion and attractive effects. The purpose of the chapter is to show that a recent extension of the Bregman/Dykstra's algorithm proposed by Peyré [100] for the Wasserstein gradient flows is perfectly well-suited to the computation of Cournot-Nash equilibria. Notice that so far the attempts to solve numerically (CN) were made in the case of the quadratic cost, due to the special structure of the optimal solutions. Here, thanks to the entropic regularization, and consequently the Bregman/Dykstra's algorithm, we are able to compute the Cournot-Nash equilibria whatever the cost function c in $\mathcal{MK}_c$ is. We, finally, present some numerical simulations which give interesting hints on the topology of the equilibria and we also propose an extension of the model to several populations.

Part II: from Euler equations to repulsive optimal transportation

This part is entirely devoted to the Multi-Marginal optimal transportation problem (MMOT). We will see that this kind of problems arises in a very natural way in many contexts in Physics such as Fluid dynamics and Density Functional Theory (DFT). The other important contribution of the thesis is actually to give a unifying framework of applications of multi-marginal optimal transport in Physics. Furthermore, we also introduce a class of optimal transportation problems, the so-called repulsive OT (which finds its principal application in DFT), where we summarize existing results in the literature and we give also some new important ones such as the appearance of fractal optimal transport maps.

Chapter 6 deals with the variational problems for the incompressible Euler equations. We especially focus on the variational principle introduced by Brenier in [20, 19] as it can be considered a forerunner of multi-marginal OT problem. This chapter is partly based on a joint work with Jean-David Benamou and Guillaume Carlier [BCN16a].

Let $u:[0,T]\times\mathcal{D}\to\mathbb{R}^d$ denote the velocity field and $p:[0,T]\times\mathcal{D}\to\mathbb{R}$ the pressure field, then the Incompressible Euler Equations read as

$$\begin{cases}\partial_t u+(u\cdot\nabla)u+\nabla p=0 & \text{in } [0,T]\times\mathcal{D}\\ \operatorname{div}(u)=0 & \text{in } [0,T]\times\mathcal{D}\\ u\cdot n=0 & \text{on } [0,T]\times\partial\mathcal{D},\end{cases} \tag{0.10}$$

where n is the unit external normal to $\partial\mathcal{D}$. The motion of an incompressible fluid inside $\mathcal{D}$ can be described also by a Lagrangian point of view: one can look at the motion of the particles of the fluid with respect to their initial position. Thus, let us assume that the velocity field u is a smooth solution of the system (6.1) and let $g : [0,T] \times \mathcal{D} \to \mathbb{R}^d$ denote the flow map solution of

$$\begin{cases} \partial_t g(t,x) = u(t, g(t,x)) & (t,x) \in [0,T] \times \mathcal{D} \\ g(0,x) = x & x \in \mathcal{D}. \end{cases} \tag{0.11}$$

Since u is divergence free, for each time the map $g(t,\cdot)$ is a measure-preserving diffeomorphism (say $g(t,\cdot) \in \mathbb{S}\mathrm{Diff}(\mathcal{D})$) such that $g(t,\cdot)_\sharp \mathcal{L}_\mathcal{D} = \mathcal{L}_\mathcal{D}$. Writing (0.10) in terms of g leads us to the following equation

$$\begin{cases} \partial_{tt} g(t,x) = -\nabla p(t, g(t,x)) & \text{in } [0,T] \times \mathcal{D} \\ g(0,x) = x & x \in \mathcal{D} \\ g(t,\cdot) \in \mathbb{S}\mathrm{Diff}(\mathcal{D}) \end{cases} \tag{0.12}$$

In [6], Arnold interpreted the equation above as a geodesic equation in the space $\mathbb{S}\mathrm{Diff}(\mathcal{D})$ so that on can look for solution to (0.12) by minimizing

$$\int_0^T \int_\mathcal{D} \frac{1}{2} |\dot{g}(t,x)|^2 dx dt \tag{$\mathcal{A}$}$$

among all the paths $g(t,\cdot) \in \mathbb{S}\mathrm{Diff}(\mathcal{D})$ with prescribed initial $g(0,\cdot) = g_\star$ and final $g(T,\cdot) = g^\star$ configuration (typically, by right invariance, $g_\star$ is take as the identity map Id). In [51], Ebin and Marsden proved that, when $\mathcal{D}$ is a smooth compact manifold with no boundary, the minimization of ($\mathcal{A}$) leads to a unique solution, corresponding also to a solution to Euler equations, if $g_\star$ and $g^\star$ are sufficiently close in a suitable Sobolev norm. Despite this positive results, Shnirelman proved in [112, 111] that when $d \geqslant 3$ the infimum is not attained in general, and that when $d = 2$ there exists a $\gamma^\star \in \mathbb{S}\mathrm{Diff}(\mathcal{D})$ which cannot be connected to Id by a path with finite energy. This negative results motivate the study of relaxed formulations of Arnold's problem, firstly introduced by Brenier in [20]: he considered probability measures γ on $\Omega(\mathcal{D})$, the space of absolutely continuous path ω, and minimize the problem

$$\int_{\Omega(\mathcal{D})} \int_0^1 \frac{1}{2} |\dot{\omega}(t)|^2 dt d\gamma(\omega), \tag{$\mathcal{E}$}$$

under the constraints

$$(e_0, e_T)_\sharp \gamma = (\mathrm{Id}, g^\star)_\sharp \mathcal{L}_\mathcal{D}, \quad (e_t)_\sharp \gamma = \mathcal{L}_\mathcal{D}, \ \forall t \in [0,T], \tag{0.13}$$

where $e_t(\omega) := \omega(t)$ denote the evaluation maps at time t. Brenier called γ *generalized incompressible flow* in $[0,T]$ between Id and $g^\star$. Notice that problem ($\mathcal{E}$) looks like a Monge-Kantorovich problem with an infinite number of marginal. In section 6.3 we provide a time discretization of the Brenier's problem obtained by fixing the number K of time steps (namely the number of marginals)

$$\begin{aligned} \inf \Big\{ \int_\Omega \sum_{i=1}^K |\omega(t_i) - \omega(t_{i-1})|^2 d\gamma \mid \\ \gamma \in \mathcal{P}(\Omega),\ (e_i)_\sharp \gamma = \mathcal{L}_D,\ (e_0, e_T)_\sharp \gamma = (\mathrm{Id}, g^\star)_\sharp \mathcal{L}_\mathcal{D} \Big\}, \end{aligned} \tag{$\mathcal{E}_K$}$$

and we prove that the discrete problem $(\mathcal{E}_K)$ converges to $(\mathcal{E})$ as $K \to \infty$.

This chapter ends with a model, firstly introduced by Léonard and coauthors in [5] (and then in [BCN16a]) which can be seen as a Brenier's principle with viscosity. This model arises, as we have conceived it, by the entropic regularization of $(\mathcal{E}_K)$: roughly speaking, the regularized version of $(\mathcal{E}_K)$ can be seen as a time discretization of a problem with an infinite number of marginals. Indeed, we retrieve a problem which deals with the minimization of a relative entropy (defined as in $(\mathcal{MK}_\varepsilon)$) where the reference measure is a Wiener measure. In other words we obtain a Schrödinger's problem with infinitely many marginals, which can be regarded as an extension of the two marginals problem.

Chapter 7 is devoted to introduce Multi-Marginal optimal transportation and to present a generalization of the IPFP algorithm to this case. This chapter is based on [BCC$^+$15, BCN16a]. Take K marginals, then the Multi-Marginal Monge-Kantorovich problem reads

$$\inf\left\{\int_{\mathbb{R}^{dK}} c(x_1,\dots,x_K)d\gamma(x_1,\dots,x_K) \mid \gamma \in \Pi(\mathbb{R}^{dK};\mu_1,\cdots,\mu_K)\right\}, \quad (\mathcal{MK}_K)$$

where $\Pi(\mathbb{R}^{dK};\mu_1,\cdots,\mu_K)$ denotes the set of couplings $\gamma(x_1,\dots,x_K)$ having μ_i as marginals. The corresponding Monge problem then becomes

$$\inf\left\{\int_{\mathbb{R}^{dK}} c(x,T_2(x),\cdots,T_K(x))d\mu_1(x) \mid T=\{T_i\}_{i=1}^K \in \mathcal{T}_K\right\}, \qquad (\mathcal{M}_K)$$

where

$$\mathcal{T}_K := \{T=\{T_i\}_{i=1}^K \mid T_i:\mathbb{R}^d\to\mathbb{R}^d\ (T_i)_\sharp\mu_1=\mu_i, \forall i=2,\cdots,K,\ T_1=\mathrm{Id}\}.$$

Such multi-marginals problems first appeared in the work of Gangbo and Święch [66] who solved the quadratic cost case and proved the existence of Monge solutions (namely of optimal transport maps). In recent years, there has been a lot of interest in such multi-marginal problems because they arise naturally in many different settings such as economics [32], [96], polar factorization of vector fields and theory of monotone maps [68, 69, 70, 62] and Density Functional Theory [26, 43, 49, 60, 44] as we will see in the last part. In section 7.5 we present numerical simulations for different kinds of multi-marginal optimal transportation problems. We highlight that this is possible thanks to an extension of the IPFP algorithm proposed by the author [BCC$^+$15, BCN15, BCN16a, DMGN15].

Chapter 8 is based on a joint work with Simone Di Marino and Augusto Gerolin [DMGN15]. Here, we tried to give a general framework for a particular class of cost functions, the so-called repulsive costs. As we will explain in the last part of this thesis, the main motivation which led us to study this kind of optimal transport problem arises from the Density Functional Theory where some interesting costs, as the Coulomb one or the repulsive harmonic, play a central role. From a mathematical perspective the interesting case is when all marginals of the coupling γ in $(\mathcal{MK}_K)$ are absolutely continuous with respect to Lebesgue measure and are all the same. In particular, since the cost functions are *"repulsive"*, if Monge-type solutions exists, they should follow the rule *"the*

further, the better!", which means that we want to move the mass as much as we can.

The main result of this section is contained in theorem 8.1.6 where we show that there exists optimal maps for the Monge problem when the cost is given by

$$c(x_1, \cdots, x_K) = -\sum_{i<j} |x_i - x_j|^2$$

and these maps have the particularity of having a fractal structure when $k \geqslant 3$. Notice that this is a surprising result which has not an equivalent version in the 2 marginals case.

Part III: optimal transport meets Density Functional Theory

The last part of the thesis is devoted to exploit the connection between the Density Functional Theory and Multi-Marginal optimal transportation.

Quantum mechanics for a molecule with N electrons can be studied in terms of the many-electron Schrödinger equation for a wave function $\psi \in \mathrm{L}^2(\mathbb{R}^{3K}; \mathbb{C})$ (for now, we neglect the spin variable). The practical limitation of this approach is computational: in order to predict the chemical behavior of H_2O (10 electrons) using a 10 grid-points discretization of $\mathbb{R}$, we need to solve the Schrödinger equation on 10^{30} grid-points. This is why Hohenberg, Kohn and Sham introduced, in [73] and [78], the Density Functional Theory (DFT) as an approximate computational method for solving the Schrödinger equation at a more reasonable cost.

The main idea of the DFT is to compute only the marginal density for one electron

$$\rho(x_1) = \int \gamma_K(x_1, x_2 \cdots, x_K) dx_2 \cdots dx_K,$$

where $\gamma_K = |\psi(x_1, \cdots, x_K)|^2$ is the joint probability density of electrons at positions $x_1, \cdots, x_K \in \mathbb{R}^3$, instead of the full wave function ψ. One scenario of interest for the DFT is when the repulsion between the electrons largely dominates over the kinetic energy. In this case, the problem can, at least formally, be reformulated as an Optimal Transport (OT) problem as emphasized in the pioneering works of Buttazzo, De Pascale and Gori-Giorgi [26] and Cotar, Friesecke and Klüppelberg [43].

In chapter 9 we give a brief introduction to Density Functional Theory and to Multi-Marginal optimal transportation with Coulomb cost. In Density Functional Theory [73] the ground state energy of a system (with N electrons) is obtained by minimizing the following functional w.r.t. the electron density $\rho(x)$:

$$E(\rho) = \min_{\rho \in \mathcal{R}} F_{HK}(\rho) + \int_{\mathbb{R}^3} v(x)\rho(x)dx \tag{0.14}$$

where $\mathcal{R} := \quad \{\rho : \mathbb{R}^3 \to \mathbb{R} | \rho \geqslant 0, \sqrt{\rho} \in \mathrm{H}^1(\mathbb{R}^3), \int_{\mathbb{R}^3} \rho(x)dx = K\}$,

$v := -\dfrac{Z}{|x-R|}$ is the electron-nuclei potential (Z and R are the charge and the position of the nucleus, respectively) and F_{HK} is the so-called Hohenberg-Kohn which is defined by minimizing over all wave functions ψ which yield ρ:

$$F_{HK}(\rho) = \min_{\psi\to\rho} \hbar^2 T(\psi) + V_{ee}(\psi), \tag{0.15}$$

where $\hbar^2$ is a semiclassical constant factor,

$$T(\psi) = \frac{1}{2}\int\cdots\int \sum_{i=1}^{K} |\nabla_{x_i}\psi|^2 dx_1\cdots dx_K$$

is the kinetic energy and

$$V_{ee}(\psi) = \int\cdots\int \sum_{i=1}^{N}\sum_{j>i}^{N} \frac{1}{|x_i-x_j|}|\psi|^2 dx_1\cdots dx_K$$

is the Coulomb repulsive energy operator.

Let us now consider the *Semiclassical* limit

$$\lim_{\hbar\to 0} \min_{\psi\to\rho} \hbar^2 T(\psi) + V_{ee}(\psi)$$

and assume that taking the minimum over ψ commutes with passing to the limit $\hbar \to 0$ (Cotar, Friesecke and Klüppelberg in [43] proved it for $K = 2$), we obtain the following functional

$$V_{ee}^{SCE}(\rho) = \min_{\psi\to\rho} \int\cdots\int \sum_{i=1}^{K}\sum_{j>i}^{K} \frac{1}{|x_i-x_j|}|\psi|^2 dx_1\cdots dx_K \tag{0.16}$$

where V_{ee}^{SCE} is the minimal Coulomb repulsive energy whose minimizer characterizes the state of *Strictly Correlated Electrons* (SCE). Notice that by denoting $\gamma = |\psi|^2$, V_{ee}^{SCE} corresponds to the Monge-Kantorovich problem with the Coulomb cost. Since the cost is radially symmetric, if the marginals ρ are also radially symmetric, then (0.16) can be reduced to $1-$dimensional (MMOT) problem with the cost given by the minimization over the angles of $\sum_{i=1}^{K}\sum_{j>i}^{K} \dfrac{1}{|x_i-x_j|}$. In section 9.5.2 we prove that

$$F_{HK}(\rho) \geqslant \min\left\{\mathrm{H}(\gamma|\eta) \mid \gamma \in \Pi_K(\mathbb{R}^{dK};\rho)\right\}$$

where $\eta := \frac{1}{L}\exp\left(-\sum_{i<j}\frac{1}{\varepsilon|x_i-x_j|}\right)\otimes_{i=1}^{K} dx_i$ and $\varepsilon = \dfrac{\pi\hbar^2}{2}$. This tells us that the entropic regularization, that we have introduced in order to define a numerical method, has indeed a "physical" meaning in the sense that it takes into account effects due to the kinetic energy.

Chapter 10 is based on a joint work ([SDMG$^+$]) with Simone Di Marino, Augusto Gerolin, Klaas Giesbertz, Paola Gori-Giorgi and Michael Seidl. Here, we give a counterexample (we refer the reader also to [41] for other counterexamples) to the following conjecture on the geometrical characterization of the optimal maps in $d > 1$ and with radially symmetric marginals

Conjecture 0.0.1 (Strong Seidl Conjecture)**.** *Let $\mu \in \mathcal{P}(\mathbb{R}^d)$ be an absolutely continuous measure with respect to the Lebesgue measure, with radial symmetry, and let $\rho(r) = |\cdot|_\sharp \mu$. Let $0 = r_0 < r_1 < \ldots < r_{K-1} < r_K = \infty$ such that the intervals $A_i = [r_i, r_{i+1})$ have all the same radial measure $\rho(A_i) = 1/K$. Then let $F(r) = \rho(0, r]$ be the cumulative radial function and let $S : [0, \infty) \to [0, \infty)$ be defined piecewise such that the interval A_i is sent in the interval A_{i+1} in an anti monotone way:*

$$S(r) = F^{-1}(2i/K - F(r)) \qquad \text{if } r_{i-1} \leqslant r < r_i \text{ and } i < K \tag{0.17}$$

$$S(r) = \begin{cases} F^{-1}(F(r) + 1/K - 1) & \text{if } K \text{ is odd} \\ F^{-1}(1 - F(r)) & \text{if } K \text{ is even,} \end{cases} \qquad \text{if } r_{K-1} \leqslant r < r_K. \tag{0.18}$$

Then the optimal maps T_i are defined as $T_1 = \mathrm{Id}$, $T_i = S^{(i-1)}$ ($S^{(i-1)}$ stands for the $(i-1)-$th composition of S with itself).

Furthermore, we will show in the framework of this counterexample, these maps are never optimal and that fractal maps can appear, as for the repulsive harmonic cost.

The last chapter 11 is devoted to present numerical simulations for the (MMOT) with the Coulomb cost obtained by using the IPFP algorithm. This chapter is based on [BCN15, DMGN15, SDMG$^+$]. We remark that the section 11.3 is related to chapter 10 as we present numerical counterexamples to conjecture 0.0.1.

Notations Throughout the thesis, with a textual citation, e.g. [BCC$^+$15], we refer to an original contribution of the author, where as with numbered citations, e.g. [94], to a "standard" reference.

Part I

Entropic Regularization

Résumé

Dans cette partie nous présentons le problème du transport optimal et la régularisation entropique. Nous étudieons plus précisément les méthodes numériques bases sur l'algorithme des projections alternées de Bregman (ainsi que sa généralisation introduite par Dykstra) et les applications au problème du barycentre dans l'espace de Wasserstein, au transport optimal partiel et au transport optimal avec une contrainte de capacité (voir chapitre 4).
Nous présentons enfin une extension de l'algorithme de Dykstra qui nous permet de calculer l'équilibre de Cournot-Nash pour des coûts généraux (voir chapitre 5). Cette partie est basée sur des travaux en commun avec Jean-David Benamou, Adrien Blanchet, Marco Cuturi, Guillaume Carlier et Gabriel Peyré:[BCC$^+$15] and [BCN16b].

Abstract

In this Part we introduce the standard optimal transport problem and the entropic regularization. We focus on numerical methods, based on Bregman's projections algorithm (and its generalization due to Dykstra), and applications to Wasserstein barycenter, Partial Optimal Transport, Optimal Transport with capacity constraint (see chapter 4).
We finally present an extension of Dykstra's algorithm to compute Cournot-Nash equilibria (see chapter 5). This part is, mostly, based on joint works with Jean-David Benamou, Adrien Blanchet, Marco Cuturi, Guillaume Carlier and Gabriel Peyré:[BCC$^+$15] and [BCN16b].

Chapter 1

A Survey on Optimal Transportation

In this section we give a brief survey on Optimal Transportation.

1.1 The Continuous Setting

The birth of Optimal Transportation dates back to 1781 when Monge [94] introduced the following problem:

Problem 1.1.1. *Given two probability measures $\mu \in \mathcal{P}(X)$ and $\nu \in \mathcal{P}(Y)$ and a cost function $c : X \times Y \to [0, +\infty[$, solve*

$$(\mathcal{M}) \quad \inf \left\{ \int_X c(x, T(x)) d\mu(x) \mid T_\sharp \mu = \nu \right\}, \tag{1.1}$$

where X and Y are compact metric spaces, c is a continuous (or semi-continuous) cost function (in [94] Monge used $c(x, y) = |x-y|$), T is a transport map (namely a push-forward, see definition 1.1.2)

Definition 1.1.2 (Push-forward)**.** *The measure denoted $T_\sharp \mu$ is defined through $T_\sharp \mu(A) := \mu(T^{-1}(A))$ for all measurable subset $A \subset Y$ and is called Push-forward.*

Remark 1.1.3 (Change-of-variables formula)*.* Notice that $T_\sharp \mu$ can be equivalently defined by the change-of-variables formula

$$\int_Y f(y) dT_\sharp \mu(y) = \int_X f(T(x)) d\mu(x), \quad \forall f \in \mathcal{C}(Y).$$

When we stay in the Euclidean setting, with two measures μ and ν induced by densities f, g and assume that the map T is $\mathcal{C}^1$ and injective, then the constraint $T_\sharp \mu = \nu$ can be recast as the following PDE

$$g(T(x)) \det(\mathrm{D}\, T(x))) = f(x), \tag{1.2}$$

which is actually the Jacobian condition obtained as a consequence of a change of variable computation. Notice that this equation is highly nonlinear in T

and this is one of the difficulties preventing an easy analysis of the Monge problem. One also remarks that $(\mathcal{M})$ is rigid in the sense that all the mass that is at x must be associated to the same target $T(x)$. In 1942 Kantorovich (see [75, 74]) suggested a relaxed formulation, which allows *mass splitting*, known as the Monge-Kantorovich problem

Problem 1.1.4. *Given $\mu \in \mathcal{P}(X)$ and $\nu \in \mathcal{P}(Y)$ and a cost function $c : X \times Y \to [0, +\infty[$ solve*

$$(\mathcal{MK}) \quad \inf \left\{ \int_{X\times Y} c(x,y) d\gamma(x,y) \mid \gamma \in \Pi(\mathbb{R}^d; \mu, \nu) \right\}, \tag{1.3}$$

where $\Pi(\mathbb{R}^d; \mu, \nu)$ is the set of so-called transport plans

$$\Pi(\mathbb{R}^d; \mu, \nu) := \{\gamma \in \mathcal{P}(X \times Y) \quad | \quad (\pi_x)_\sharp \gamma = \mu, (\pi_y)_\sharp \gamma = \nu\},$$

where π_x and π_y are the two projections of $X \times Y$ onto X and Y, respectively.

We remark that the constraints π_x and π_y mean that we only consider the probability measures γ whose marginals coincide with μ and ν. The probability measures γ are a different way to describe the displacement of the mass of μ: instead of specifying the destination $T(x)$ of the mass originally at x, we specify for each pair (x, y) how much mass goes from x to y. It is clear that if the mass splitting really occurs (which means that there are multiple destinations for the mass at x) then this displacement cannot be described by a map T. Moreover, if there exists a γ of the form $\gamma_T = (\mathrm{Id}, T)_\sharp \mu$ (one can easily check that $\gamma_T \in \Pi(\mathbb{R}^d; \mu, \nu)$ if and only if $T_\sharp \mu = \nu$) then one obtains

$$\int_{X\times Y} c(x,y) d\gamma_T(x,y) = \int_X c(x, T(x)) d\mu(x).$$

Thus, if $(\mathcal{MK})$ admits a minimizer, the so-called *optimal transport plan*, of the form γ_T then T is an *optimal transport map* for $(\mathcal{M})$. Notice that the Monge-Kantorovich problem is more general than the Monge one: as an example, take $\mu = \delta_0$ then it is impossible to transport μ, through a map T satisfying the constraint, onto a target measure which is not itself a Dirac mass. On the contrary, there always exist transport plans in $\Pi(\mathbb{R}^d; \mu, \nu)$ (at least $\gamma = \mu \otimes \nu$) and the following holds

Theorem 1.1.5 (Theorem 1.4, [105])**.** *Let X and Y be compact metric spaces, $\mu \in \mathcal{P}(X)$ and $\nu \in \mathcal{P}(Y)$ and $c : X \times Y \to \mathbb{R}$ a continuous function. Then $(\mathcal{MK})$ admits a solution.*

For the proof, one just needs to show that $\Pi(\mathbb{R}^d; \mu, \nu)$ is compact and that $\gamma \mapsto \int_{X\times Y} c(x,y) d\gamma(x,y)$ is continuous (take the weak convergence in probability measures), and apply Weierstrass's theorem.

Remark 1.1.6. Theorem 1.1.5 still holds if X and Y are Polish spaces and $c : X \times Y \to [0, +\infty]$ is lower semi-continuous (see 1.1 in [105]).

Remark 1.1.7 (A distance between probability measures). Notice that if $c(x, y) = |x-y|^p$, with $p > 1$, then $(\mathcal{MK})$ defines a distance between the probability measures μ and ν.

The Monge-Kantorovich problem is a linear optimization problem under linear constraints, so it is interesting to look at the dual problem and exploit the relations between the two. Introducing the Lagrange multipliers $\varphi \in \mathcal{C}_b(X)$ and $\psi \in \mathcal{C}_b(Y)$ then the Lagrangian associated to $(\mathcal{MK})$ reads as

$$\mathcal{L}(\gamma, \varphi, \psi) = \int_X \varphi(x) d\mu(x) + \int_Y \psi(y) d\nu(y) + \int_{X\times Y} (c(x,y) - \varphi(x) - \psi(y)) d\gamma(x,y) \tag{1.4}$$

and we have now the following problem

$$\inf_{\gamma} \sup_{\varphi,\psi} \mathcal{L}(\gamma, \varphi, \psi). \tag{1.5}$$

Assuming we can interchange sup and inf, we get

$$\sup_{\varphi,\psi} \int_X \varphi(x) d\mu(x) + \int_Y \psi(y) d\nu(y) + \inf_{\gamma \geqslant 0} \int_{X\times Y} (c(x,y) - \varphi(x) - \psi(y)) d\gamma(x,y) \tag{1.6}$$

and the inf in γ can be re-written as a constraint on φ and ψ

$$\inf_{\gamma \geqslant 0} \int_{X\times Y} (c(x,y) - \varphi(x) - \psi(y)) d\gamma(x,y) = \begin{cases} 0 & \varphi(x) + \psi(y) \leqslant c \text{ on } X \times Y, \\ -\infty & \text{otherwise.} \end{cases} \tag{1.7}$$

This lead to the dual formulation of Monge-Kantorovich problem

Problem 1.1.8. *Given two probability measures $\mu \in \mathcal{P}(X)$ and $\nu \in \mathcal{P}(Y)$ and a cost function $c : X \times Y \to [0, +\infty[$, solve*

$$(\mathcal{MK}_d) \quad \sup \left\{ \int_X \varphi(x) d\mu(x) + \int_Y \psi(y) d\nu(y) \mid (\varphi, \psi) \in \mathcal{K}_c \right\}, \tag{1.8}$$

where

$$\mathcal{K}_c := \{\varphi \in \mathcal{C}_b(X), \psi \in \mathcal{C}_b(Y) \mid \varphi(x) + \psi(y) \leqslant c(x,y) \, \forall (x,y) \in X \times Y\}.$$

The optimal φ and ψ, if they exist, are called the *Kantorovich potentials*. By a direct application of the Fenchel-Rockafellar theorem we obtain the following result

Theorem 1.1.9 (Theorem 1.46, [105])**.** *If X, Y are compact spaces and c continuous, then* $\inf(\mathcal{MK}) = \sup(\mathcal{MK}_d)$.

Remark 1.1.10. Notice that the constraint $\varphi(x) + \psi(y) \leqslant c(x,y)$ is saturated (namely the equality holds) $\gamma-$a.e. where γ is solution to $(\mathcal{MK})$.

However an existence result for $(\mathcal{MK}_d)$ is not so straightforward as for the primal one due to lackness of compactness for the class of admissible functions.

Theorem 1.1.11 (Proposition 1.11, [105])**.** *Let X and Y be compact and c continuous. Then there exists a solution (φ, ψ) to $(\mathcal{MK}_d)$ and it has the form $\varphi \in c - conc(X)$, $\psi \in \overline{c} - conc(Y)$ and $\psi = \varphi^c$.*

We remind that for a given function $f : X \to \overline{\mathbb{R}}$, we define its $c-transform$ $f^c : Y \to \overline{\mathbb{R}}$ as

$$f^c(y) = \inf_{x\in X} c(x,y) - f(x),$$

and in an analogous way we define the $\overline{c} - transform$ of $g : Y \to \overline{\mathbb{R}}$ as

$$g^{\overline{c}}(x) = \inf_{y\in Y} c(x,y) - g(y).$$

Then, we say that a function ψ on Y is $\overline{c} - concave$ if there exists f such that $\psi = f^c$ (analogously a function φ on X is $c - concave$ if there exists g on Y such that $\varphi = g^{\overline{c}}$) and we denote by $c - conc(X)$ and $\overline{c} - conc(Y)$ the sets of $c-$ and $\overline{c} - concave$ functions.

Thus, if we take

$$\mathcal{F}(\varphi,\psi) = \int_X \varphi(x)d\mu(x) + \int_Y \psi(y)d\nu(y),$$

then for any admissible pair (φ,ψ), since $\varphi^c \geqslant \psi$, we have

$$\mathcal{F}(\varphi,\varphi^c) \geqslant \mathcal{F}(\varphi,\psi)$$

end the pair (φ,φ^c) is still admissible. If we iterate the concavification trick, we have that the pair $(\varphi^{c\overline{c}},\varphi^c)$ is admissible and

$$\mathcal{F}(\varphi^{c\overline{c}},\varphi^c) \geqslant \mathcal{F}(\varphi,\varphi^c) \geqslant \mathcal{F}(\varphi,\psi).$$

It is now clear that thanks to this trick, the optimization in (1.1.8) can be reduced to pair of the form (φ,φ^c) and $(\varphi^{c\overline{c}},\varphi^c)$

$$(\mathcal{MK}_d) = \sup_{\varphi\in\mathcal{C}_b(X)} \mathcal{F}(\varphi,\varphi^c) = \sup_{\varphi\in\mathcal{C}_b(X)} \mathcal{F}(\varphi^{c\overline{c}},\varphi^c).$$

It turns out that these kinds of pairs form a sufficient rigid set to get compactness and thus prove theorem 1.1.11.

As we have said above when the optimal plan γ has the form $\gamma_T = (\mathrm{Id},T)\sharp\mu$ then T is also an optimal transport map for the Monge problem. Indeed one would like to understand when this *equivalence* between $(\mathcal{M})$ and $(\mathcal{MK})$ holds and thus have existence result for $(\mathcal{M})$. According to this, if we take $X = Y = \Omega \subset \mathbb{R}^d$ and $c(x,y) = h(x-y)$ with $h : \mathbb{R}^d \to \mathbb{R}$ strictly convex then we have strong results, in particular we have existence as well as a representation formula for the optimal T. In [65] Gangbo and McCann establish the following result

Theorem 1.1.12 (Theorem 1.2, [65])**.** *Given $\mu,\nu \in \mathcal{P}(\Omega)$, where $\Omega \in \mathbb{R}^d$ is a compact domain, there exists an optimal transport plan γ for the cost $c(x,y) = h(x-y)$ with h strictly convex. It is unique and of the form $\gamma_T = (\mathrm{Id},T)_\sharp\mu$, provided μ is absolutely continuous and $\partial\Omega$ is negligible. Moreover, there exists a Kantorovich potential φ, and T and the potential φ are linked by*

$$T(x) = x - \mathrm{D}\, h^{-1}(\mathrm{D}\,\varphi(x)) \quad \textit{for a.e.} - x. \tag{1.9}$$

Remark 1.1.13. If $c(x,y) = |x-y|^2$, the so-called quadratic cost, one actually retrieves the result firstly proved by Yann Brenier in [21]. In this case one obtains that the map T has the form $T(x) = x - \mathrm{D}\,\varphi = \mathrm{D}\,u(x)$ where u is a convex function defined as $u(x) = \frac{1}{2}|x|^2 - \varphi(x)$. Moreover, if $\mu = \rho_0\mathcal{L}^d$ and $\nu = \rho_1\mathcal{L}^d$ (where $\mathcal{L}^d$ is the Lebesgue measure) then the Brenier's map ∇u satisfies the Monge-Ampère equation

$$\det(\mathrm{D}^2\,u)\rho_1(\mathrm{D}\,u) = \rho_0. \tag{1.10}$$

In [30, 31] Caffarelli establishes conditions under which the Brenier's map is smooth. We recall here theorem 4.14 of [115] which summarizes the results obtained by Caffarelli

Theorem 1.1.14 (Theorem 4.14, [115]). *Let $\rho_0, \rho_1 \in \mathcal{C}^{0,\alpha}(\Omega)$ $(0 < \alpha < 1)$ be Hölder-continuous functions defined on a bounded open set Ω, bounded from above and below by positive constants. Assume that Ω is convex. Then the unique Brenier solution u of (1.10) belongs to $\mathcal{C}^{2,\alpha}(\Omega) \cap \mathcal{C}^{1,\alpha}(\overline{\Omega})$ and u satisfies the Monge-Ampère equation in the classical sense (hence also in the Alexandroff and viscosity senses).*

Remark 1.1.15. Theorem 1.1.12 holds for all the costs of the form $c(x, y) = |x - y|^p$ with $p > 1$.

Remark 1.1.16. A similar result as the one in theorem 1.1.12 can be derived also for other cost functions, see [34] for more details.

1.1.1 The Benamou-Brenier formulation

So far we have described the so-called static framework, in [10] Benamou and Brenier give a dynamic formulation of optimal transport. Even if the Benamou-Brenier formulation can be generalized to more general convex costs, here we only consider the case of the quadratic cost. Let us consider a source $\mu = \rho_0\mathcal{L}^d$ and a target $\nu = \rho_1\mathcal{L}^d$ measures, where ρ_0 and ρ_1 are the associated densities, then the Monge-Kantorovich problem with the quadratic cost (also called the 2-Wasserstein distance) is defined as above. The idea of the Benamou-Brenier formulation is to compute a curve of measures connecting μ to ν and minimizing some action functional. Indeed this curve is given by the solution of the continuity equation

$$\partial_t \rho + \operatorname{div}(\rho v) = 0, \quad \rho(0, x) = \rho_0. \tag{1.11}$$

Assuming that the velocity v is smooth then the solution of the continuity equation is given by $\rho(t, x) = g(t, x)_\sharp \rho_0$ where $g(t, x)$ is the flow of v

$$\partial_t g(t, x) = v(t, g(t, x)), \quad g(0, x) = x.$$

The curve of measures we are looking for is the one which minimizes the average kinetic energy (the constant speed geodesic in the Wasserstein space) and the Benamou-Brenier problem takes the form

Problem 1.1.17. *given $\mu = \rho_0\mathcal{L}^d$ and $\nu = \rho_1\mathcal{L}^d$ solve*

$$(\mathcal{BB}) \quad \inf \left\{ \int_0^1 \int_{\mathbb{R}^d} |v(t, x)|^2 \rho(t, x) dx dt \mid (\rho, v) \text{ solve } (1.11), \right. \\ \left. \rho|_{t=0} = \rho_0, \rho|_{t=1} = \rho_1 \right\}. \tag{1.12}$$

Remark 1.1.18 (Optimality condition and Hamilton-Jacobi equation). It is interesting to derive the optimality condition of problem (1.12). Indeed by writing down the Lagrangian associated to (1.12) and denoting by φ the Lagrange multiplier of the constraints in (1.12) (namely the continuity equation and the initial and final configurations ρ_0 and ρ_1), it is easy to see that the formal optimality conditions turn out to be

$$v(t, x) = \nabla_x \varphi(t, x),$$

and the Hamilton-Jacobi equation

$$\partial_t \varphi + \frac{|\nabla_x \varphi|^2}{2} = 0.$$

This says that the optimal solution is given by a pressureless potential flow.

We end this section by giving the following theorem which establishes the relationship between the Monge-Kantorovich problem with the quadratic cost and the Benamou-Brenier problem (1.12).

Proposition 1.1.19 (Proposition 1.1,[10])**.** *Given two probability measures $\mu, \nu \in \mathcal{P}(\Omega)$ which are absolutely continuous with respect the Lebesgue measure. Denote by ρ_0 and ρ_1 the associated density. Then the following holds*

$$\inf(\mathcal{MK}_2) = \inf(\mathcal{BB}), \tag{1.13}$$

where $\mathcal{MK}_2$ stands for the Monge-Kantorovich problem with the quadratic cost and $\mathcal{BB}$ is problem (1.12).

Remark 1.1.20 (McCann's interpolant, [92])*.* We have previously said that one can define the geodesic ρ through a map $g(t,x)$ associated to the velocity field $v(x,t)$. If we consider the optimal solution (ρ, v) to $(\mathcal{BB})$ then (see [10] for the details) the flow map $g(t,x)$ is given by $g(t,x) = (1-t)x + t\nabla u(x)$ where $u(x)$ is a Brenier's solution. Thus, one can rewrite $\rho(t,x) = g(t,x)_\sharp \rho_0$ as

$$\rho(t,x) = (1-t)\,\mathrm{Id}_\sharp\,\rho_0 + t\nabla u_\sharp \rho_0, \tag{1.14}$$

which is known as *McCann's interpolant*.

1.2 The Discrete setting

As we have pointed out in the previous section, the Monge-Kantorovich problem is indeed a linear programming problem in infinite dimension. So it is quite natural to discretize it in a way we can exploit this fact. According to this we replace μ and ν with a sum of Dirac masses

$$\mu = \textstyle\sum_{i=1}^N \mu_i \delta_{x_i} \text{ and } \nu = \sum_{i=1}^N \nu_i \delta_{y_i},$$

where $\{x_i\}_{i=1}^N$ and $\{y_i\}_{i=1}^N$ are the gridpoints used to discretize X and Y (for simplicity we have chosen the same number N of points) and $\{\mu_i\}_{i=1}^N$ and $\{\nu_i\}_{i=1}^N$ are the weights associated to the gridpoints, such that $\sum_{i=1}^N \mu_i = 1$ and $\sum_{i=1}^N \nu_i = 1$ (indeed we are imposing that μ and ν belong to the simplex $\Sigma_N := \{p \in \mathbb{R}^N \mid \sum_{i=1}^N p_i = 1\}$). Let us now denote c_{ij} the cost of transporting the mass located at x_i to y_i, the the discrete Monge-Kantorovich problem reads as follows

Problem 1.2.1. *Given $\mu, \nu \in \Sigma_N$ and $C \in \mathbb{R}^N \times \mathbb{R}^N$, such that $(C)_{ij} = c_{ij}$, solve*

$$(\mathcal{DMK}) \quad \inf\left\{ \sum_{i,j=1}^N c_{ij}\gamma_{ij} \mid \gamma \in \Pi_N(\mathbb{R}^{dN}; \mu, \nu) \right\}, \tag{1.15}$$

where $\Pi_N(\mathbb{R}^{dN}; \mu, \nu) := \{\gamma \in \mathbb{R}^N \times \mathbb{R}^N \mid \gamma \geqslant 0,\ \gamma \mathbf{1} = \mu,\ \gamma^T \mathbf{1} = \nu\}$ and $\mathbf{1} = (1, \cdots, 1)$ is a vector in $\mathbb{R}^N$.

The problem is now finite-dimensional and it is, actually, a classical linear problem in the standard form which, for instance, can be solved with the simplex algorithm. Consider now the following measures

$$\mu = \sum_{i}^{N} \delta_{x_i} \text{ and } \nu = \sum_{j}^{N} \delta_{y_j},$$

then notice that a matrix γ admissible for problem (1.2.1) is a matrix such that the sum of entries on each row and each column is 1. Such matrices are usually called *bistochastic*. Problem (1.2.1) is a minimization over the set of bistochastic matrices which is a convex and compact, so the minimum in (1.2.1) is attained at one extreme point. Furthermore, define a permutation matrix as a matrix of the form $\gamma_{ij} = \delta_{j\sigma(i)}$, where σ is a permutation of $\{1, \cdots, N\}$, then the set of permutation matrices is trivially included in the set of bistochastic. Indeed, thanks to the following result established by Birkhoff, we can identify the set of extremal points of the set of bistochastic matrices with the permutation matrices

Theorem 1.2.2 (Birkhoff's theorem)**.** *The set of extreme points of the set of bistochastic matrices coincides with the set of permutation matrices. In particular, the set of bistochastic measures is a polyhedron with $N!$ vertices and every bistochastic matrix is a convex combination of permutation matrices (as a consequence of the Krein-Milman's theorem).*

We end the section by recalling the dual problem of 1.2.1

Problem 1.2.3. *Given $\mu, \nu \in \Sigma_N$ and $C \in \mathbb{R}^N \times \mathbb{R}^N$, such that $(C)_{ij} = c_{ij}$, solve*

$$(\mathcal{DMK}_d) \quad \sup \left\{ \sum_{i=1}^{N} \varphi_i \mu_i + \sum_{j=1}^{N} \psi_j \nu_j \mid (\varphi, \psi) \in \mathcal{K}_c^N \right\}, \tag{1.16}$$

where $\mathcal{K}_c^N := \{\varphi \in \mathbb{R}^N, \psi \in \mathbb{R}^N \mid \varphi_i + \psi_j \leqslant c_{ij} \, \forall (i,j) \in \{1, \cdots, N\}^2\}$.

We briefly remark the advantages and disadvantages of these two approaches:

- $(\mathcal{DMK})$ has N^2 unknowns, but $2N$ linear constraints to verify;
- on the contrary, $(\mathcal{DMK}_d)$ has $2N$ unknowns, but N^2 constraints.

Thus, if N is large the computational cost of the simplex algorithm becomes prohibitive. Other methods have also been found such as the so-called Hungarian algorithm [81] or the Auction algorithm [12].

Chapter 2

Regularized Optimal Transport

2.1 The continuous setting

In this Section we present a regularization of problem (1.3) which consists in replacing the non-negative constraint on the plan γ by a relative entropy penalization. In other words the entropy plays the role of a barrier function on the non-negativity constraint. In Chapter 3, we will show that the main interest of this kind of regularization resides in the algebraic properties which make it the unique possible choice when one wants to solve the regularized problem by using Bregman's projections algorithm. Here, we want to describe the continuous setting of the regularized problem (in analogy to Section 1.1) and highlight that in the special case of the quadratic Monge-Kantorovich problem (namely $c(x,y) = \frac{1}{2}|x-y|^2$) we retrieve the Schrödinger problem [107, 85].

Definition 2.1.1 (Relative entropy)**.** *Let p and r be two probability measures (for instance $p, r \in \mathcal{P}(\mathbb{R}^d \times \mathbb{R}^d)$), such that p is absolutely continuous with respect to r, then the relative entropy of p with respect to r is given by*

$$\mathrm{H}(p|r) = \int_{\mathbb{R}^d \times \mathbb{R}^d} \left(\log(\frac{dp}{dr}) - 1 \right) dp. \tag{2.1}$$

If p and r are absolutely continuous with respect to the Lebesgue measure then (2.1) takes the form

$$\mathrm{H}(p|r) = \int_{\mathbb{R}^d \times \mathbb{R}^d} (\log(\frac{p}{r}) - 1) p dx,$$

where we have identify a measure with the corresponding density.

Remark 2.1.2. We will also use the following definition of relative entropy

$$\mathrm{H}(p|r) = \int_{\mathbb{R}^d \times \mathbb{R}^d} \left(\log(\frac{dp}{dr}) - 1 \right) dp + 1, \tag{2.2}$$

with p, r two probability measure. Notice that in this case $\mathrm{H} \in [0, \infty]$.

Then the entropy regularized variant of problem (1.3) reads as

Problem 2.1.3. *Given $\mu, \nu \in \mathcal{P}(X)$ (for instance $X = \mathbb{R}^d$), absolutely continuous with respect to the Lebesgue measure, a cost function $c : X \times X \to \mathbb{R}$, solve*

$$(\mathcal{MK}_\varepsilon) \quad \inf \left\{ \int_{X\times X} c(x,y) d\gamma(x,y) + \varepsilon \, \mathrm{H}(\gamma|\mu\otimes\nu) \mid \gamma \in \Pi(\mathbb{R}^d;\mu,\nu) \right\}, \quad (2.3)$$

where $\varepsilon > 0$ is the regularization parameter.

One can easily rewrite problem (2.3) in the following compact form

$$(\mathcal{MK}_\varepsilon) \quad \inf \left\{ \int_{X\times X} \mathrm{H}(\gamma|\eta_\varepsilon) \mid \gamma \in \Pi(\mathbb{R}^d;\mu,\nu) \right\}, \quad (2.4)$$

where

$$\eta_\varepsilon = \frac{1}{L} \exp\left(-c(x,y)/\varepsilon\right) \mu\otimes\nu,$$

with $L = \int_{X\times X} \exp\left(-c(x,y)/\varepsilon\right) d\mu\otimes\nu$. Before introducing the Schrödinger problem and its connection to both the regularized and unregularized Monge-Kantorovich problem, let us give the $\Gamma-$convergence result established by Carlier *et al.* in [35]

Theorem 2.1.4. *Given two probability measures $\mu, \nu \in \mathcal{P}(\mathbb{R}^d)$ having finite entropy and finite moment of order $p > 1$, and a cost function $c : \mathbb{R}^d \times \mathbb{R}^d \to \mathbb{R}$ such that $c(x,y) = h(|x-y|)$ and $|x|^p \leqslant h(x) \leqslant 1 + |x|^p$. Define the following functionals*

$$\mathcal{F}_\varepsilon(\gamma) = \begin{cases} \int_{\mathbb{R}^d\times\mathbb{R}^d} c d\gamma + \varepsilon \, \mathrm{H}(\gamma|\mu\otimes\nu) & \text{if } \gamma \in \Pi(\mathbb{R}^d;\mu,\nu) \\ +\infty & \text{otherwise,} \end{cases} \quad (2.5)$$

and

$$\mathcal{F}(\gamma) = \begin{cases} \int_{\mathbb{R}^d\times\mathbb{R}^d} c d\gamma & \text{if } \gamma \in \Pi(\mathbb{R}^d;\mu,\nu) \\ +\infty & \text{otherwise.} \end{cases} \quad (2.6)$$

Then, $\mathcal{F}_\varepsilon$ $\Gamma-$converges to $\mathcal{F}$ w.r.t. the weak topology on $\mathcal{P}(\mathbb{R}^d)$.

Without loss of generality, from now on we consider the quadratic cost function $c(x,y) = \frac{1}{2}|x-y|^2$ in order to clarify the link with the Schrödinger problem. In the next paragraph, mostly based on Léonard's survey [85], we will show that the Monge-Kantorovich problem with the quadratic cost can be seen as the limit of the Schrödinger problem.

2.1.1 The Schrödinger problem

In his seminal works [107, 108] Schrödinger addressed the following problem: knowing the distribution of particles at an initial time t_0 and a final time t_1, identify the most likely flow of density of particles between these two points. It only later became clear that the problem posed by Schrödinger could be recast as a convex optimization problem. As for the Monge-Kantorovich problem we give a static and a dynamic version of the Schrödinger's problem (see [84, 85] for more details).

Problem 2.1.5 (Dynamic Schrödinger's problem)**.** *Denote by R some reference probability measure on the space of continuous paths $\Omega = \mathcal{C}([0,1], \mathbb{R}^d)$ (we define $\omega : [0,1] \to \mathbb{R}^d$ an element of Ω), then the dynamic Schrödinger's problem associated to the reference path measure $R \in \mathcal{P}(\Omega)$ is the following entropy minimization problem*

$$(\mathscr{S}_{dyn}) \quad \inf \left\{ \mathrm{H}(P|R) \mid P \in \mathcal{P}(\Omega),\ (e_0)_\sharp P = \mu,\ (e_1)_\sharp P = \nu \right\}, \tag{2.7}$$

where $e_0 : \Omega \to \mathbb{R}^d$ and $e_1 : \Omega \to \mathbb{R}^d$ are the evaluation maps at time 0 and 1 (notice that in probability e_t is usually denoted as X_t and called canonical process), respectively, and $\mu, \nu \in \mathcal{P}(\mathbb{R}^d)$ are the prescribed initial and final configuration.

If we consider the projection $\eta := (e_0, e_1)_\sharp R \in \mathcal{P}(\mathbb{R}^{2d})$ of R, then we have the following alternative definition of the previous problem.

Problem 2.1.6 (Static Schrödinger's problem)**.** *The static Schrödinger's problem associated with the reference measure $\eta \in \mathcal{P}(\mathbb{R}^{2d})$ is the following problem*

$$(\mathscr{S}_{static}) \quad \inf \left\{ \mathrm{H}(\gamma|\eta) \mid \gamma \in \mathcal{P}(\mathbb{R}^{2d}),\ (\pi_0)_\sharp \gamma = \mu,\ (\pi_1)_\sharp \gamma = \nu \right\}, \tag{2.8}$$

where π_i is the canonical projection.

Remark 2.1.7. Notice that in problem (2.8) we are minimizing over all the probability measures which belong to $\Pi(\mathbb{R}^d; \mu, \nu)$. Thus we can already see problem (2.4) as a static "Schrödinger problem" (up to an additive constant $\log(L)\varepsilon$) where the reference measure is given by $\eta_\varepsilon = \frac{1}{L} \exp\left(-c(x,y)/\varepsilon\right) \mu \otimes \nu$.

Remark 2.1.8 (Static and Dynamic Monge-Kantorovich). One can generalize the static and dynamic Monge-Kantorovich problem to a generic cost function as follows. Take a cost function $c : \mathbb{R}^{2d} \to \mathbb{R}$ then the static Monge-Kantorovich problem is

$$(\mathcal{MK}_{static}) \quad \inf \left\{ \int_{\mathbb{R}^{2d}} c(x,y) d\gamma(x,y) \mid \gamma \in \Pi(\mathbb{R}^d; \mu, \nu) \right\}, \tag{2.9}$$

where the marginals are prescribed. Consider now a cost $C : \Omega \to [0, \infty]$ defined on the path space, then the dynamic Monge-Kantorovich problem can be defined as

$$(\mathcal{MK}_{dyn}) \quad \inf \left\{ \int_{\Omega} C(\omega) dP(\omega) \mid P \in \mathcal{P}(\Omega),\ (e_0)_\sharp P = \mu,\ (e_1)_\sharp P = \nu \right\}. \tag{2.10}$$

One can prove (see theorem 2.8 in [84]) that $\inf(\mathcal{MK}_{static}) = \inf(\mathcal{MK}_{dyn})$ whenever c and C are related by

$$c(x,y) = \inf\{C(\omega) \mid \omega \in \Omega,\ \omega(0) = x,\ \omega(1) = y\},\ \forall (x,y) \in \mathbb{R}^{2d}.$$

Moreover, if $P^\star$ and $\gamma^\star$ are optimal solutions to $(\mathcal{MK}_{dyn})$ and $(\mathcal{MK}_{static})$, respectively, then the following holds

$$\gamma^\star = (e_0, e_1)_\sharp P^\star, \tag{2.11}$$

$$P^\star = \int_{\mathbb{R}^{2d}} \delta_{\Gamma_{xy}} d\gamma^\star(x,y), \tag{2.12}$$

where $(x,y) \mapsto \delta_{\Gamma_{xy}} \in \mathcal{P}(\Omega)$ is any measurable mapping such that for $\gamma^\star-$almost each (x,y), $\delta_{\Gamma_{xy}}$ concentrates on the set of geodesic paths

$$\Gamma_{xy} := \{\omega \in \Omega \mid \omega(0) = x,\ \omega(1) = y,\ C(\omega) = c(x,y)\}.$$

To conclude this remark, notice that if the cost in $(\mathcal{MK}_{dyn})$ is the classical kinetic action functional, namely $C(\omega) = \frac{1}{2}\int_0^1 |\dot{\omega}(t)|^2 dt$ for any path $\omega(t)$, then it is easy to show by using the Jensen's inequality, that the cost in the static formulation is exactly the quadratic one. Moreover, if the hypothesis of Brenier's theorem hold and so there exists a unique minimizer of $(\mathcal{MK}_{static})$ then Γ_{xy} is the constant speed geodesic path, induced by the optimal map, connecting x to y and the marginal $(e_t)_\sharp P^\star$ of $P^\star$ is the McCann's interpolant (1.14) between μ and ν.

Denote by $\Omega^{xy} := \{\omega \in \Omega \mid \omega(0) = x,\ \omega(1) = y\}$ the subspace of Ω such that $\forall \omega \in \Omega^{xy}\ \omega(0) = x$ and $\omega(1) = y$. It follows that a probability measure P^{xy} (usually called the bridge between x and y of the process P) in $\mathcal{P}(\Omega^{xy})$ is a probability measure on Ω such that its initial and final marginals are $(e_0)_\sharp P^{xy} = \delta_x$ and $(e_1)_\sharp P^{xy} = \delta_y$, respectively, and a measure $P \in \mathcal{P}(\Omega)$ can be disintegrated as

$$P = \int_{\mathbb{R}^{2d}} P^{xy} dP_{01}(x,y),$$

where $P_{01} = (e_0, e_1)_\sharp P$. Then, one can prove (see [55]) that $\inf(\mathscr{S}_{dyn}) = \inf(\mathscr{S}_{static}) \in [0,\infty]$ and since the relative entropy is a strictly convex function, if $\inf(\mathscr{S}_{dyn}) < \infty$ then they admit a unique minimizer $P^\star$ and $\gamma^\star$, respectively. Moreover, these solutions are related as follows

$$\gamma^\star = (e_0, e_1)_\sharp P^\star, \tag{2.13}$$

$$P^\star = \int_{\mathbb{R}^{2d}} R^{xy} d\gamma^\star(x,y). \tag{2.14}$$

Notice that in this case the bridge R^{xy} plays the role of $\delta_{\Gamma_{xy}}$ and the time-marginal $(e_t)_\sharp P^\star$ of $P^\star$ is the *entropic interpolant*. In order to improve the resemblance between $(\mathscr{S}_{dyn})$ and $(\mathcal{MK}_{dyn})$, we should find a way to encode the dynamic cost $C(\omega)$ in the reference measure. In [84] the author shows that this can be done by replacing R with a sequence of reference processes R^ε which satisfies a large deviation principle with scale $\frac{1}{\varepsilon}$ as ε tends to 0 and rate function $C(\omega)$. In other words

$$R^\varepsilon \asymp_{\varepsilon\to 0} \exp\left(-\frac{1}{\varepsilon} \inf_{\omega \in A \subset \Omega} C(\omega)\right).$$

In the case of the original Schrödinger problem theorem A.3 in [84] states that C is actually $C(\omega) = \frac{1}{2}\int_0^1 |\dot{\omega}(t)|^2 dt$ (R^ε is the law of a Brownian motion with diffusion coefficient ε) and the density of $\eta_\varepsilon := (e_0, e_1)_\sharp R^\varepsilon$ is given by the density of the Brownian motion between the final and the initial position

$$\eta_\varepsilon = (2\pi\varepsilon)^{-d/2} \exp\left(-\frac{1}{\varepsilon}|y-x|^2/2\right).$$

Thus, as ε tends to 0, Léonard proves that $(\mathscr{S}^\varepsilon_{dyn})$ and $(\mathscr{S}^\varepsilon_{static})$ $\Gamma-$converges to $(\mathcal{MK}_{dyn})$ and $(\mathcal{MK}_{static})$, respectively. Moreover, it is not surprising that the entropic interpolant converges to McCann's interpolant.

Remark 2.1.9. We end this section with a remark about the parameter ε. One can consider ε as a temperature so that the problem posed by Schrödinger deals with finding the way how an heated system of Brownian particles moves from an initial configuration μ to a final one ν, when the temperature is at ε. Thus, the temperature ε defines the level of the kinetic energy of the system and the Schrödinger problem can be seen as a viscous version of Monge-Kantorovich. Indeed, the Monge-Kantorovich is the zero-temperature limit of $(\mathscr{S}_{static})$ (and $(\mathscr{S}_{dyn})$) which corresponds actually to cool down the original system of particles.

2.2 The discrete setting

In this section we introduce the entropic regularization of the discrete Monge-Kantorovich problem; we recall that this kind of problem has been firstly addressed in [46, 63].
As in Section 1.2 we consider the following discretization of μ and ν

$$\mu = \sum_{i=1}^{N} \mu_i \delta_{x_i} \text{ and } \nu = \sum_{i=1}^{N} \nu_i \delta_{y_i},$$

such that $\mu, \nu \in \Sigma_N$. We define the discrete entropy on a coupling $\gamma \in \mathbb{R}^N \times \mathbb{R}^N$ as

$$\mathcal{E}(\gamma) := \sum_{i,j=1}^{N} \gamma_{ij}(\log(\gamma_{ij}) - 1) + i_{\mathcal{D}}(\gamma),$$

with the convention that $0 \log(0) = 0$ and where $i_{\mathcal{D}}$ (with $\mathcal{D} = \mathbb{R}_+^N \times \mathbb{R}_+^N$) is the indicator function

$$i_{\mathcal{D}}(\gamma) = \begin{cases} 0 & if\ \gamma \in \mathcal{D} \\ +\infty & otherwise \end{cases}$$

Then the discrete relative entropy of $\gamma \in \mathbb{R}_+^N \times \mathbb{R}_+^N$ with respect to $\eta \in \mathbb{R}_+^N \times \mathbb{R}_+^N$ has the form

$$\mathrm{H}(\gamma|\eta) := \sum_{i,j=1}^{N} \gamma_{ij}(\log(\frac{\gamma_{ij}}{\eta_{ij}}) - 1).$$

Following the idea described in Section 2.1, we now penalize the problem (1.2.1) by adding an entropy term as follows

$$\min \left\{ \sum_{ij} c_{ij}\gamma_{ij} + \varepsilon\, \mathrm{H}(\gamma|\eta) \mid \gamma \in \mathcal{C} \right\}, \tag{2.15}$$

where $\eta = \mu \otimes \nu$ ($\otimes$ must be understood as an entry-wise operation, i.e. $\mu \otimes \nu := (\mu_i \nu_j)_{ij}$), $\mathcal{C} := \{\gamma \in \mathbb{R}_+^N \times \mathbb{R}_+^N \mid \gamma \mathbf{1} = \mu,\ \gamma^T \mathbf{1} = \nu\}$ and after some algebraic operations (2.15) can be re-written as

$$\min \left\{ \mathrm{H}(\gamma|\overline{\gamma}) \mid \gamma \in \mathcal{C} \right\}, \tag{2.16}$$

where

$$\overline{\gamma}_{ij} = \exp\left(-c_{ij}/\varepsilon\right)\eta_{ij}.$$

Moreover, (2.16) is also known as the minimization of the Kullback-Leibler distance KL, defined as

$$\mathrm{KL}\left(\gamma|\overline{\gamma}\right) := \mathrm{H}(\gamma|\overline{\gamma}). \tag{2.17}$$

Finally, we have the following regularized problem

Problem 2.2.1. *Given $\mu, \nu \in \Sigma_N$ and $C \in \mathbb{R}^N \times \mathbb{R}^N$, such that $(C)_{ij} = c_{ij}$, solve*

$$(\mathcal{KL}) \quad \min \left\{ \mathrm{KL}\left(\gamma | \overline{\gamma}\right) \mid \gamma \in \mathcal{C} \right\}, \tag{2.18}$$

where $\mathcal{C} := \{\gamma \in \mathbb{R}_+^N \times \mathbb{R}_+^N \mid \gamma \mathbf{1} = \mu,\ \gamma^T \mathbf{1} = \nu\}$.

The problem (2.2.1) reads as the projection, in terms of the KL distance, of the point $\overline{\gamma}$ on the set of constraints $\mathcal{C} := \mathcal{C}_1 \cap \mathcal{C}_2$ where

$$\mathcal{C}_1 := \left\{ \gamma \in \mathbb{R}_+^N \times \mathbb{R}_+^N \mid \gamma \mathbf{1} = \mu \right\}, \tag{2.19}$$

$$\mathcal{C}_2 := \left\{ \gamma \in \mathbb{R}_+^N \times \mathbb{R}_+^N \mid \gamma^T \mathbf{1} = \nu \right\}. \tag{2.20}$$

Remark 2.2.2. Problem (2.2.1) can be seen as a discretization of the Schrödinger problem (see [84] for the continuous formulation).

Then, the dual problem of (2.2.1) reads as

Problem 2.2.3. *Given $\mu, \nu \in \Sigma_N$ and $C \in \mathbb{R}^N \times \mathbb{R}^N$, such that $(C)_{ij} = c_{ij}$, solve*

$$(\mathcal{KL}_d) \quad \sup \left\{ \sum_{i=1}^N \varphi_i \mu_i + \sum_{j=1}^N \psi_j \nu_j - \varepsilon \sum_{ij} \exp\left(\frac{\varphi_i + \psi_j - c_{ij}}{\varepsilon}\right) \mid \varphi \in \mathbb{R}^N, \psi \in \mathbb{R}^N \right\}. \tag{2.21}$$

Remark 2.2.4. The dual is actually the unconstrained penalized version of (1.2.3).

The minimization problem (2.2.1) is now a strictly convex problem and we have the following proposition

Proposition 2.2.5. *Problem (2.2.1) admits a unique solution $\gamma^{\varepsilon,\star}$. Moreover, there exist two non-negative vectors $a, b \in \mathbb{R}_+^N$, uniquely determined up to a multiplicative constant, such that $\gamma^{\varepsilon,\star}$ has the form*

$$\gamma_{ij}^{\varepsilon,\star} = a_i \overline{\gamma}_{ij} b_j, \tag{2.22}$$

where $\overline{\gamma}_{ij} = \exp\left(-c_{ij}/\varepsilon\right)\eta_{ij}$.

Proof. The existence and the uniqueness of $\gamma^{\varepsilon,\star}$ follow from the boundedness of $\mathcal{C}$ and the strictly convexity of KL. Notice that problem (2.2.1) can be recast as the following saddle point problem

$$\inf_{\gamma} \sup_{\varphi,\psi} \mathcal{L}(\gamma, \varphi, \psi)$$

where $\varphi, \psi \in \mathbb{R}^N$ are the Lagrange multipliers the Lagrangian $\mathcal{L}$ is given by

$$\begin{aligned} \mathcal{L}(\gamma, \varphi, \psi) = &\sum_{ij} c_{ij} + \varepsilon \sum_{ij} \gamma_{ij}(\log(\gamma_{ij}) - 1) - \cdots \\ &\sum_i \varphi_i (\sum_j \gamma_{ij} - \mu_i) - \sum_j \psi_j (\sum_i \gamma_{ij} - \nu_i), \end{aligned} \tag{2.23}$$

where, for simplicity, we have taken $\eta_{ij} = 1\ \forall (i,j) \in \{1, \cdots, N\}^2$. Notice now that a critical point (γ, φ, ψ) exists. Then the optimality condition w.r.t. γ_{ij} reads as

$$\frac{\partial \mathcal{L}}{\partial \gamma_{ij}} = c_{ij} + \varepsilon \log(\gamma_{ij}) - \varphi_i - \psi_j = 0,$$

so that the optimal $\gamma^{\varepsilon,\star}$ must have the form

$$\gamma_{ij}^{\varepsilon,\star} = a_i \overline{\gamma}_{ij} b_j,$$

where $a_i := \exp(\varphi_i/\varepsilon)$ and $b_j := \exp(\psi_j/\varepsilon)$ and they are uniquely determined, up to a multiplicative constant, by the marginal constraints

$$a_i = \frac{\mu_i}{\sum_j \overline{\gamma}_{ij} b_j} \quad \text{and} \quad b_j = \frac{\nu_j}{\sum_i \overline{\gamma}_{ij} a_i}. \tag{2.24}$$

□

Remark 2.2.6. We refer to equations (2.24) as the *discrete Berstein-Schrödinger equations*.

Remark 2.2.7. The existence of solutions to (2.24) can be also proven by using a different approach, for instance see theorem 3.2.5 in section 3.2.1.

Remark 2.2.8. In section 3.2 we will show that equations (2.24) can be used to define a fixed point iterative algorithm, known as IPFP (*Iterative Proportional Fitting Procedure*) or Sinkhorn.

In Section 1.2 we have pointed out that an optimal solution of the discrete $(\mathcal{MK})$ (assume that the marginals are sum of dirac such that an admissible plan γ belongs to the set of bistochastic matrices) lies on the vertices of the set $\Pi_N(\mathbb{R}^{dN}; \mu, \nu)$ and so it is a permutation matrix. On the contrary the optimal solution $\gamma^{\varepsilon,\star}$ of regularized problem (2.2.1) belongs to the relative interior of the set $\Pi_N(\mathbb{R}^{dN}; \mu, \nu)$ and so it can be seen as a convex combination of the permutation matrices, see theorem 3.2.2 . On one hand, if ε tends to $+\infty$, we find that the optimal solution of the regularized problem is $\gamma^{\varepsilon,\star} = \mu \otimes \nu$; on the other hand if $\varepsilon \to 0$ we expect that $\gamma^{\varepsilon,\star} \to \gamma^\star$. Moreover, if the optimal transport problem admits a unique solution $\gamma^\star$, then $\gamma^{\varepsilon,\star}$ should converge exactly to this solution. If the optimal transport problem admits more than one solution then the optimal $\gamma^{\varepsilon,\star}$ should converge to the one with minimal entropy as $\varepsilon \to 0$. Indeed we have the following convergence result

Theorem 2.2.9 (Cominetti-San Martin,[42])**.** *Let $\gamma^{\varepsilon,\star}$ be the optimal solution of (2.2.1), for a given ε, and $\gamma^\star$ be the optimal transport plan of (1.2.1). Then $\gamma^{\varepsilon,\star} \to \gamma^\star$. Moreover, $\gamma^{\varepsilon,\star}$ has asymptotic expansion*

$$\gamma^{\varepsilon,\star} = \gamma^\star + \eta^\varepsilon,$$

where the error term η^ε converges exponentially fast to 0 as $\varepsilon \to 0$.

Remark 2.2.10. Theorem 2.2.9 says that the convergence of the minimizers of (2.2.1) to the ones of (1.2.1) is exponential

$$\|\gamma^{\varepsilon,\star} - \gamma^\star\| \leqslant M \exp(-\tfrac{\lambda}{\varepsilon}),$$

where the M and λ depend on the cost function c_{ij}, the marginals μ, ν and the number of gridpoints N used for the discretization

Figure 2.1 displays examples of transport plans $\gamma = \gamma^{\varepsilon,\star}$ solving (2.2.1), for two 1-D marginals $(\mu, \nu) \in \mathbb{R}^N \times \mathbb{R}^N$ discretized on a uniform grid $\{x_i\}_{i=1}^N$ of $[0,1]$, and with a ground cost $c_{ij} = \|x_i - x_j\|^2$. The computation is performed with $N = 256$. This figure shows how $\gamma^{\varepsilon,\star}$ converges towards a solution of the original un-regularized transport as $\varepsilon \to 0$.

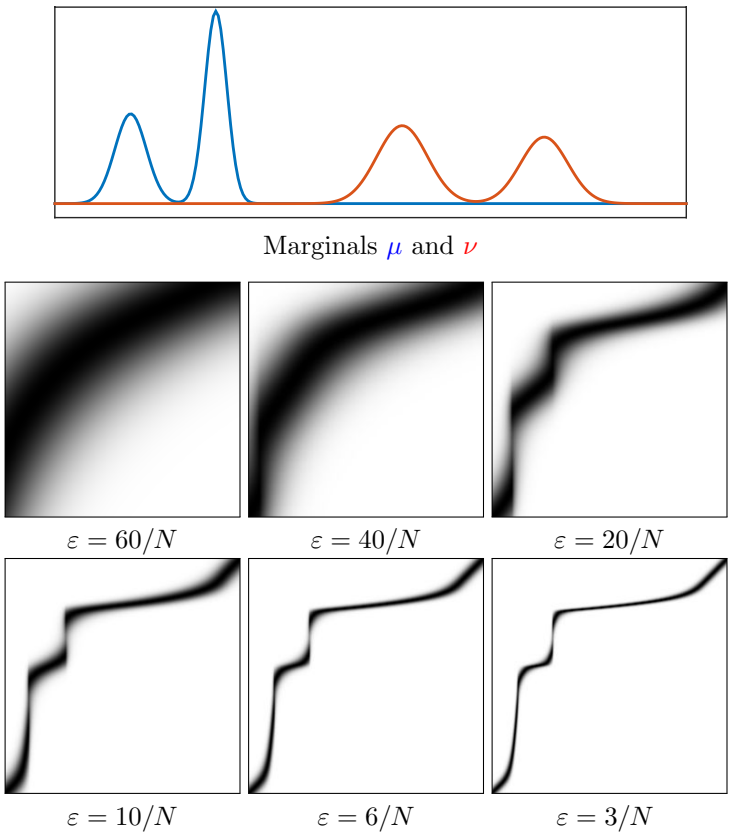

Figure 2.1: *Top: the input densities μ (blue curve) and ν (red curve). Bottom: solution $\gamma^{\varepsilon,\star}$ of (2.2.1) for several values of ε.*

Chapter 3

Bregman's Projection Algorithm

3.1 Bregman alternate projections

Here, we present a numerical method which is not based on linear programming techniques, but on an entropic regularization and the so-called alternate projection method. It has recently been applied to various optimal transport problems (see for instance [BCC$^+$15, BCN15, SDMG$^+$, BCN16b] and [46, 45, 100]) and in Chapter 4 we will present some interesting application.

The initial idea goes back to Von Neumann [95, 117] who proved that the sequence obtained by projecting orthogonally iteratively onto two affine subspaces converges to the projection of the initial point onto the intersection of these affine subspaces. Since the seminal work of Bregman [18], it is by now well-known that one can extend this idea not only to several affine subspaces (the extension to convex sets is due to Dyskstra and we will discuss it in Section 3.3) but also by replacing the Euclidean distance by a general Bregman divergence associated to some suitable f.

Definition 3.1.1 (Bregman divergence)**.** *Given a convex function f of Legendre type, the Bregman divergence associated with f is given by*

$$D_f(x, y) = f(x) - f(y) - \langle \nabla f(y), x - y \rangle, \tag{3.1}$$

where $\langle \cdot, \cdot \rangle$ denote the dot product.

Definition 3.1.2 (Function of Legendre type)**.** *Suppose f is a closed convex proper function on $\mathcal{D} \subset \mathbb{R}^d$ with $int(domf) \neq 0$. Then f is a convex function of Legendre type, if it satisfie every one of the following condition:*

- *f is differentiable on $int(domf)$.*
- *$\lim_{t \to 0^+} \langle \nabla f(x + t(y - x)), y - x \rangle$, $\forall x \in bd(domf)$, $\forall y \in int(domf)$.*
- *f is strictly convex $int(domf)$.*

Then the minimization problem with a Bregman divergence now reads

Problem 3.1.3. *Given a strictly convex and differentiable function f, a point y and a set of constraints $\mathcal{C} = \cap_{l=1}^{M} \mathcal{C}_\ell$, where $\mathcal{C}_\ell$ are convex sets, solve*

$$\min \{D_f(x, y) \mid x \in \mathcal{C}\}. \tag{3.2}$$

If we now take as $f(x)$ the Boltzmann/Shannon entropy

$$f(x) := \sum_i x_i(\log x_i - 1), \quad x \in \mathbb{R}_+^N$$

then the Bregman divergence (restricted to probabilities i.e. imposing the normalization $\sum_i x_i = 1$) is the Kullback-Leibler distance or relative entropy

$$D_f(x, y) = \sum_i x_i \Big(\log \Big(\frac{x_i}{y_i} \Big) - 1 \Big),$$

and if we consider two matrices $A, B \in \mathbb{R}_+^N \times \mathbb{R}_+^N$, $A = (a_{ij})$ and $B = (b_{ij})$ then the Bregman divergence becomes

$$D_f(A, B) = \sum_{ij} a_{ij} \Big(\log \Big(\frac{a_{ij}}{b_{ij}} \Big) - 1 \Big).$$

Thus, the problem 3.1.3 looks like 2.2.1, if we choose properly the set $\mathcal{C}$.

Let us now consider the special case where the convex sets $\mathcal{C}_\ell$ are affine subspaces, then it is possible to solve (3.1.3) by simply using iterative KL projections. Starting from $x^{(0)} = \overline{x}$ (where $\overline{x}$ is a suitable initial point, i.e. $\overline{x} = y$), one computes

$$\forall\, n > 0, \quad x^{(n)} := P^{\mathrm{KL}}_{\mathcal{C}_{[n]}}(x^{(n-1)}), \tag{3.3}$$

where P^{KL} stands for the projection w.r.t. the Kullback-Leibler distance and $[\cdot]$ denotes the mod M function with values in $\{1, \cdots, M\}$. Then one has the following convergence result (for a detailed proof see [7]):

Theorem 3.1.4 (Theorem 4.3, [7])**.** *Let f be a convex function of Legendre type. Suppose $\mathcal{C}_\ell$ with $l = 1, \cdots, M$ are finitely many affine subspaces of $\mathbb{R}^N$ with $\mathcal{C} = \cap_{l=1}^{M} \mathcal{C}_\ell$ and $\mathcal{C} \cap intdomf \neq \emptyset$. Then the sequence $x^{(n)}$ defined as in (3.3) converges to the unique solution of (3.1.3).*

3.2 The Iterative Proportional Fitting Procedure (aka the Sinkhorn algorithm)

Let now consider the problem described in Section 2.2

$$\min \{\mathrm{KL}(\gamma|\overline{\gamma}) \mid \gamma \in \mathcal{C}\}, \tag{3.4}$$

where $\mathcal{C} = \mathcal{C}_1 \cap \mathcal{C}_2$ and

$$\mathcal{C}_1 := \{\gamma \in \mathbb{R}_+^N \times \mathbb{R}_+^N \mid \gamma \mathbf{1} = \mu\}, \tag{3.5}$$

$$\mathcal{C}_2 := \{\gamma \in \mathbb{R}_+^N \times \mathbb{R}_+^N \mid \gamma^T \mathbf{1} = \nu\}. \tag{3.6}$$

It is clear that the set $\mathcal{C}_l$ are affine subspaces of $\mathbb{R}_+^N \times \mathbb{R}_+^N$ and so we can apply the algorithm introduced in the previous Section, being aware of the convergence guaranteed by theorem 3.1.4. Then, the projections $P^{\mathrm{KL}}_{\mathcal{C}_{[n]}}$ can be easily computed as stated in the following proposition

Proposition 3.2.1 ([BCC+15]). *Consider the set $\mathcal{C}_l$ as in 3.5, then for $\overline{\gamma}^{(n)} \in \mathbb{R}_+^N \times \mathbb{R}_+^N$ the projection $\gamma^{(n)} := P^{\mathrm{KL}}_{\mathcal{C}_{[k]}}(\overline{\gamma}^{(n)})$ satisfies $\forall n$*

$$\gamma^{(n)} = \overline{\gamma}^{(n)} \operatorname{diag}\left(\frac{\mu}{\overline{\gamma}^{(n)}\mathbf{1}}\right), \ if \ [n] = 1 \tag{3.7}$$

$$\gamma^{(n)} = \operatorname{diag}\left(\frac{\nu}{{\overline{\gamma}^{(n)}}^T\mathbf{1}}\right)\overline{\gamma}^{(n)}, \ if \ [n] = 2. \tag{3.8}$$

Proof. Let us consider the case $[n] = 1$ (the case $[n] = 2$ is analogous), then the first order condition of the projection $P^{\mathrm{KL}}_{\mathcal{C}_1}(\overline{\gamma}^{(n)})$ states the existence of a Lagrange multiplier $\varphi^{(n)} \in \mathbb{R}^N$ such that

$$\forall n \ \log(\tfrac{\gamma^{(n)}}{\overline{\gamma}^{(n)}}) - \varphi^{(n)} = 0 \text{ which can be re-written as } \gamma^{(n)} = \overline{\gamma}^{(n)} \operatorname{diag}(a^{(n)}),$$

where $a^{(n)} := e^{\varphi^{(n)}/\varepsilon}$. As the optimal $\gamma^{(n)}$ must belong to $\mathcal{C}_1$ we obtain

$$a^{(n)} = \frac{\mu}{\overline{\gamma}^{(n)}\mathbf{1}},$$

and so the projection is

$$\gamma^{(n)} = \overline{\gamma}^{(n)} \operatorname{diag}\left(\frac{\mu}{\overline{\gamma}^{(n)}\mathbf{1}}\right).$$

□

In Section 2.2 we have pointed out that problem (3.4) admits a unique and, almost explicit solution of the form

$$\gamma^{\varepsilon,\star} = \operatorname{diag}(a)\overline{\gamma}\operatorname{diag}(b),$$

where $a, b \in \mathbb{R}^N$ are uniquely determined, up to a multiplicative constant, by the marginal constraints and $\overline{\gamma} := e^{-C/\varepsilon}$. This leads to iterates $\gamma^{(n)}$ which satisfy

$$\gamma^{(n)} = \operatorname{diag}(a^{(n)})\overline{\gamma}\operatorname{diag}(b^{(n)}) \tag{3.9}$$

for two vectors $\left(a^{(n)}, b^{(n)}\right) \in \mathbb{R}^N \times \mathbb{R}^N$ initialized as $a^{(0)} = \mathbf{1}$ and computed with the iterations

$$a^{(n)} = \frac{\mu}{\overline{\gamma}b^{(n)}} \text{ and } b^{(n+1)} = \frac{\nu}{\overline{\gamma}^T a^{(n)}}.$$

This algorithm has been firstly introduced by Sinkhorn in [113] and it is also known as Iterative Proportional Fitting Procedure (IPFP). We remark that the Bregman algorithm iterates on the primal variable, where as the (IPFP) on the dual ones. It is clear that iterating on the dual variable a, b, due to the special structure of the solution, is equivalent to alternatively projecting on $\mathcal{C}_1$ and $\mathcal{C}_2$. Indeed, let us define $\gamma^{(2n)}$ and $\gamma^{(2n+1)}$ as

$$\gamma^{(2n)} := \operatorname{diag}(a^{(n)})\overline{\gamma}\operatorname{diag}(b^{(n)}) \text{ and } \gamma^{(2n+1)} := \operatorname{diag}(a^{(n)})\overline{\gamma}\operatorname{diag}(b^{(n+1)}),$$

then we have

$$\pi_1(\gamma^{(2n)}) = \mu \text{ and } \pi_2(\gamma^{(2n+1)}) = \nu$$

which means that $\gamma^{(2n)} \in \mathcal{C}_1$ and $\gamma^{(2n+1)} \in \mathcal{C}_2$. Moreover, take $\gamma^{(2n-1)} := \mathrm{diag}(a^{(n-1)})\overline{\gamma}\,\mathrm{diag}(b^{(n)})$, which can be written as

$$\overline{\gamma}\,\mathrm{diag}(b^{(n)}) = \frac{\gamma^{(2n-1)}}{\mathrm{diag}(a^{(n-1)})}$$

, then, after some simple algebraic computations, one can re-write $\gamma^{(2n)}$ as

$$\gamma^{(2n)} = \gamma^{(2n-1)}\,\mathrm{diag}(\frac{\mu}{\gamma^{(2n-1)}\mathbf{1}})$$

which corresponds to the Bregman's projection on $\mathcal{C}_1$ (analogously for the projection on $\mathcal{C}_2$).

Figure 3.1 displays examples of transport plans $\gamma = \gamma^{\varepsilon,\star}$ solving (3.4), for two 1-D marginals $(\mu, \nu) \in \mathbb{R}^N \times \mathbb{R}^N$ discretizing continuous densities on a uniform grid $\{x_i\}_{i=1}^N$ of $[0,1]$, and with a ground cost $c_{ij} = \|x_i - x_j\|^2$. The computation is performed with $N = 256$. This figure shows how the iterates of the algorithm $\gamma^{(n)}$ progressively shift mass away from the diagonal during the iterations.

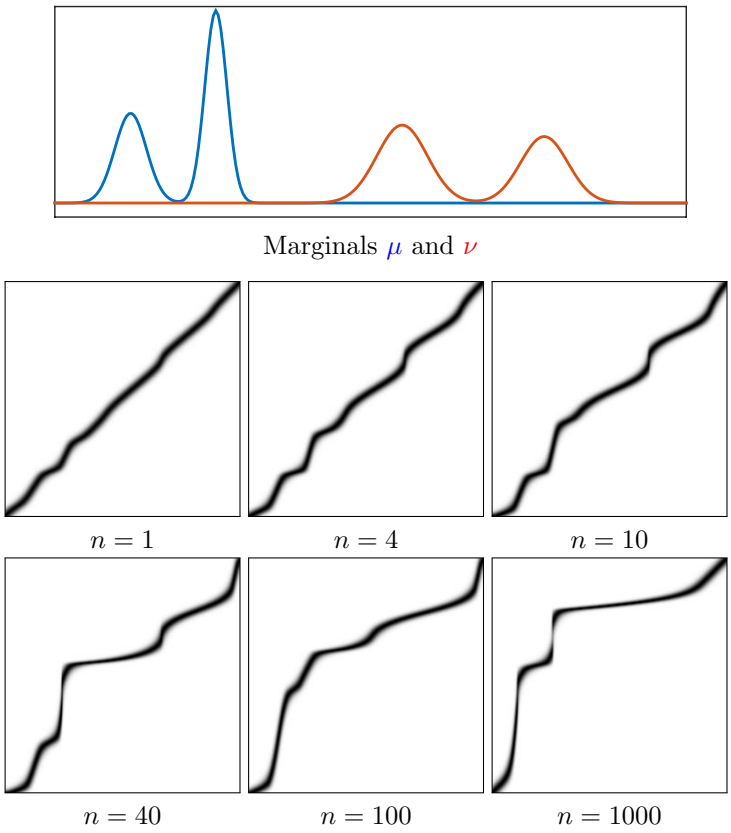

Figure 3.1: *Top: the input densities μ (blue curve) and ν (red curve). Bottom: evolution of the couplings $\gamma^{(n)}$ at iteration n of the Sinkhorn algorithm.*

In [104] Rüschendorf proves the convergence of the IPFP in a measure continuous framework. In the following Section we will give a convergence result

in the Hilbert metric and in finite dimension; anyway this kind of result can be easily extended to the infinite dimension case (see for instance [57, 17, 67]).

3.2.1 The Convergence of the IPFP in the Hilbert's metric

We now present a constructive proof of the convergence of the IPFP by using the Hilbert metric and the Birkhoff-Bushell theorem. The main idea of this approach lies on the fact that the solution of problem (3.4) can be seen as the fixed point of a contractive map in the Hilbert metric. Moreover, one obtains a geometric rate of convergence, and the rate factor can be estimated a priori. Let us firstly introduce the Hilbert's projective metric and the Birkhoff-Bushell theorem. Let p and q be elements of $\mathbb{R}^N_{++}$ (i.e. $p_i > 0$ for $i = 1, \cdots, N$), then

$$\mathrm{d_H}(p,q) := \log\left(\frac{\max_i(\frac{p_i}{q_i})}{\min_i(\frac{p_i}{q_i})}\right) = \log\left(\max_{i,j}\frac{p_i q_j}{q_i p_j}\right)$$

defines a projective metric on $\mathbb{R}^N_{++}$; the following properties hold for $p, q, z \in \mathbb{R}^N_+$

$$\mathrm{d_H}(p,q) = 0 \iff p = \alpha q \ \ for\ \alpha \in \mathbb{R}_+ \tag{3.10}$$

$$\mathrm{d_H}(p,q) = \mathrm{d_H}(q,p) \tag{3.11}$$

$$\mathrm{d_H}(p,z) \leqslant \mathrm{d_H}(p,q) + \mathrm{d_H}(q,z)\,. \tag{3.12}$$

We refer to $\mathrm{d_H}$ as the Hilbert's metric (see [25] for a survey of applications and remarks). Take a $m \times n$ matrix $A = (a_{ij})$ with positive entries which maps $\mathbb{R}^m_{++}$ into $\mathbb{R}^n_{++}$ (without loss of generality we take $m = n = N$) then we define the projective diameter as follows

$$\begin{aligned}\delta(A) &:= \sup\{\mathrm{d_H}(Ap, Aq) \mid p, q \in \mathbb{R}^N_+\} \\ &= \max\left\{\log\left(\frac{a_{ij}a_{kl}}{a_{il}a_{kj}}\right) \mid (i,j,k,l) \in \{1,\cdots,N\}^4\right\},\end{aligned}$$

and the contraction ratio as

$$\eta(A) := \sup\{\frac{\mathrm{d_H}(Ap, Aq)}{\mathrm{d_H}(p,q)} \mid p, q \in \mathbb{R}^N_{++}, p \neq \alpha q\ for\ \alpha \in \mathbb{R}^N_{++}\}.$$

Then the following theorem, due to Birkhoff [13], holds

Theorem 3.2.2 (Birkhoff-Bushell, [13] and [25])**.** *Let $A = (a_{ij}) \in \mathbb{R}^N_{++} \times \mathbb{R}^N_{++}$ such that $0 < \alpha \leqslant a_{ij} \leqslant \beta < +\infty\ \forall (i,j) \in \{1,\cdots,N\}^2$ then the equality*

$$\eta(A) = \frac{e^{\frac{1}{2}\delta(A)} - 1}{e^{\frac{1}{2}\delta(A)} + 1} = \tanh\left(\frac{1}{4}\delta(A)\right)$$

holds.

Remark 3.2.3. Actually, as $\tanh(x) < 1$, theorem 3.2.2 states that the operator A is a contraction.

Remark 3.2.4. The same result holds in infinite dimensions in which case A is a linear positive operator.

Let us briefly recall the iterates of the IPFP for the problem (3.4)

$$a^{(n)} = \frac{\mu}{\overline{\gamma} b^{(n)}} \text{ and } b^{(n+1)} = \frac{\nu}{\overline{\gamma}^T a^{(n)}},$$

where $b^{(0)} = \mathbf{1}$ and $\overline{\gamma} = e^{-C/\varepsilon}$. Then on can re-write them in the following way

$$a^{(n)} = \mathcal{I}_\mu(\mathcal{A}_{\overline{\gamma}}(b^{(n)})) \text{ and } b^{(n+1)} = \mathcal{I}_\nu(\mathcal{A}_{\overline{\gamma}^{\mathrm{T}}}(a^{(n)})),$$

where the operators $\mathcal{I}_\mu, \mathcal{A}_{\overline{\gamma}}, \mathcal{I}_\nu, \mathcal{A}_{\overline{\gamma}^{\mathrm{T}}}$ are defined as

$$\begin{aligned}
&\mathcal{I}_\mu : p \mapsto q = \frac{\mu}{p},\\
&\mathcal{I}_\nu : p \mapsto q = \frac{\nu}{p},\\
&\mathcal{A}_{\overline{\gamma}} : p \mapsto q = \overline{\gamma} p,\\
&\mathcal{A}_{\overline{\gamma}^{\mathrm{T}}} : p \mapsto q = \overline{\gamma}^T p.
\end{aligned}$$

It is clear that the iterates can be finally written as

$$b^{(n+1)} = \mathcal{D}(b^{(n)}),$$

where

$$\mathcal{D} := \mathcal{I}_\nu \circ \mathcal{A}_{\overline{\gamma}^{\mathrm{T}}} \circ \mathcal{I}_\mu \circ \mathcal{A}_{\overline{\gamma}}\,. \tag{3.13}$$

Then, the main result of this Section is

Theorem 3.2.5 (see also [56, 38])**.** *Given a positive matrix $\overline{\gamma} \in \mathbb{R}^N_{++} \times \mathbb{R}^N_{++}$, such that $0 < \alpha \leqslant a_{ij} \leqslant \beta < +\infty\ \forall (i,j) \in \{1, \cdots, N\}^2$, and two vectors $\mu, \nu \in \mathbb{R}^N_{++}$ then there exist two positive vectors $a^\star, b^\star$ solutions of the Schrödinger equations*

$$a^\star_i = \frac{\mu_i}{\sum_j \overline{\gamma}_{ij} b^\star_j} \quad \textit{and} \quad b^\star_j = \frac{\nu_j}{\sum_i \overline{\gamma}_{ij} a^\star_i}$$

and they are unique up to a multiplicative constant.

The proof of theorem 3.2.5 relies on the following lemma

Lemma 3.2.6 (see also [56, 38])**.** *Let $\overline{\gamma}, \mu, \nu$ as above. Then the map $\mathcal{D} : \mathbb{R}^N_+ \to \mathbb{R}^N_+$, defined in (3.13), is a contraction in the Hilbert's metric.*

Proof of Lemma 3.2.6. We firstly note the operators $\mathcal{I}_\mu$ and $\mathcal{I}_\nu$ are isometries in the Hilbert's metric since the inversion and element-wise scaling are both isometries: take two vectors $p, q \in \mathbb{R}^N_+$ then

$$\begin{aligned}
\mathrm{d_H}(p,q) &= \log\left(\max_{ij} \frac{p_i q_j}{q_i p_j}\right)\\
&= \log\left(\max_{ij} \frac{\frac{1}{p_j}\frac{1}{q_i}}{\frac{1}{q_j}\frac{1}{p_i}}\right) = \mathrm{d_H}\left(p^{-1}, q^{-1}\right),
\end{aligned}$$

and

$$\mathrm{d_H}(\mu \odot p, \mu \odot q) = \log\left(\max_{ij} \frac{(\mu_i p_i)(\mu_j q_j)}{(\mu_i q_i)(\mu_j p_j)}\right) = \mathrm{d_H}(p,q)\,,$$

where $\odot$ must be understood as an element-wise multiplication. Next we note that $\delta(\overline{\gamma})$ is finite and

$$\delta(\overline{\gamma}) = \delta(\overline{\gamma}^T),$$

so that we can reduce to study only the operator $\mathcal{A}_{\overline{\gamma}}$. $\mathcal{A}_{\overline{\gamma}}$ is a linear positive operator, thanks to the hypothesis on the matrix $\overline{\gamma}$ (which means we can apply theorem 3.2.2), we have that

$$\eta(\mathcal{A}_{\overline{\gamma}}) < 1.$$

Then

$$\eta(\mathcal{D}) = \eta(\mathcal{I}_\nu \circ \mathcal{A}_{\overline{\gamma}^{\mathrm{T}}} \circ \mathcal{I}_\mu \circ \mathcal{A}_{\overline{\gamma}}) = \eta(\mathcal{I}_\nu)\eta(\mathcal{A}_{\overline{\gamma}^{\mathrm{T}}})\eta(\mathcal{I}_\mu)\eta(\mathcal{A}_{\overline{\gamma}}) = \eta(\mathcal{A}_{\overline{\gamma}})^2 < 1,$$

and so the operator $\mathcal{D}$ is a contraction in the Hilbert's metric. □

Proof of theorem 3.2.5. [25] ensures that there exists a unique positive fixed point of the map $\mathcal{D}$ (and so we have the existence of vectors $a^\star$ and $b^\star$). □

3.3 Dykstra's Algorithm

In Section 3.1 we have introduced the Bregman's algorithm when the convex set $\mathcal{C}_\ell$ are affine subspaces. Indeed one can still use the iterative Bregman projections when $\mathcal{C}_\ell$ are not affine subspaces, but the sequence $x^{(n)}$ does not converge in general to the projection on the intersection, and so to the solution of problem (3.1.3). A way to avoid this issue is to use a generalization of Bregman projections proposed by Dykstra in [50]. Let us consider the same function f as in Section 3.1, and the induced Bregman distance D_f, M convex sets $\mathcal{C}_1, \cdots, \mathcal{C}_M$, M auxiliaries variables $z^{-(i-1)} := \mathbf{0}$ for $i = 1, \cdots, M$ and an initial point $x^{(0)} = \overline{x}$. The Dykstra's iterates are defined as follows

Definition 3.3.1 (Dykstra's iterates)**.**

$$x^{(n)} := (P^{(f)}_{\mathcal{C}_{[n]}} \circ \nabla f^*)(\nabla f(x^{(n-1)}) + z^{(n-M)}), \tag{3.14}$$

$$z^{(n)} := \nabla f(x^{(n-1)}) + z^{(n-M)} - \nabla f(x^{(n)}), \tag{3.15}$$

where $[\cdot]$ *denotes the mod* M *function with values in* $\{1, \cdots, M\}$ *and* f^* *is the Legendre transform of* f*, see Definition 3.3.2 .*

Definition 3.3.2 (Legendre transformation)**.** *Let* $f : \mathbb{R}^N \to \mathbb{R} \cup \{+\infty\}$ *be a convex function then the Legendre transform is a function* $f^* : R^N \to \mathbb{R} \cup \{+\infty\}$ *defined by*

$$f^*(x^*) := \sup_{x \in \mathbb{R}^N} \left(\langle x, x^* \rangle - f(x) \right),$$

where $\langle \cdot, \cdot \rangle$ *denotes the dot product.*

Then we have the following theorem (see [7] for a detailed proof)

Theorem 3.3.3 (Theorem 3.2, [7])**.** *Let* f *be a convex function of Legendre type. The sequence* $x^{(n)}$ *defined in (3.14) converges to* $P^{(f)}_{\mathcal{C}}(\overline{x})$*, where* $\mathcal{C} := \cap_{\ell=1}^{M} \mathcal{C}_\ell$*.*

We want now to re-write the iterates (3.14) by using Boltzmann/Shannon entropy $f(x) := x(\log x - 1)$, (we have already showed in Section 3.1 that problem (3.1.3) becomes the minimization of the Kullback-Leibler distance). Note that the Legendre transform of $f(x)$ is simply $f^*(x^*) = e^{x^*}$ and (3.14) become

$$x^{(n)} := P^{\mathrm{KL}}_{\mathcal{C}_{[n]}}(e^{\log(x^{(n-1)}) + z^{(n-M)}}), \tag{3.16}$$

$$z^{(n)} := \log(x^{(n-1)}) + z^{(n-M)} - \log(x^{(n)}). \tag{3.17}$$

If we define $q^{n-M} := \exp z^{n-M}$, the iterates (3.16) can be re-written in a more convenient form

$$x^{(n)} := P^{\mathrm{KL}}_{\mathcal{C}_{[n]}}(x^{(n-1)} \odot q^{(n-M)}),$$
$$q^{(n)} := q^{(n-M)} \odot \frac{x^{(n-1)}}{x^{(n)}},$$

where $\odot$ and $\frac{\cdot}{\cdot}$ denotes entry-wise multiplication and division, respectively. Finally, consider the following regularized transport problem

$$\min \left\{ \mathrm{KL}\left(\gamma | \overline{\gamma}\right) \mid \gamma \in \mathcal{C} \right\}, \tag{3.18}$$

where $\mathcal{C} := \cap_{\ell=1}^{M} \mathcal{C}_\ell$, for instance see Sections 4.3,4.4 and 5.1, then Dykstra's algorithm starts by initializing

$$\gamma^{(0)} := \overline{\gamma} \quad \text{and} \quad q^{(0)} = q^{(-1)} = \cdots = q^{-(M-1)} := \mathbf{1}.$$

and one iteratively defines

$$\gamma^{(n)} := P^{\mathrm{KL}}_{\mathcal{C}_n}(\gamma^{(n-1)} \odot q^{(n-L)}), \quad \text{and} \quad q^{(n)} := q^{(n-L)} \odot \frac{\gamma^{(n-1)}}{\gamma^{(n)}}. \tag{3.19}$$

Chapter 4

Applications

4.1 Optimal Transport Barycenters

We are given a set $\{\mu^k\}_{k=1}^K$ of input marginals $\mu^k \in \Sigma_N$ (we remind that $\Sigma_N := \{u \in \mathbb{R}^N \mid \sum_i u_i = 1\}$), and we wish to compute a weighted barycenter according to the Wasserstein metric. This problem finds many applications, as highlighted in [45] and [BCC+15].

Following [1], the general idea is to define the barycenter as a solution of a variational problem mimicking the definition of barycenters in Euclidean spaces. Given a set of normalized weights $\lambda \in \Sigma_K$, we consider the regularized Wasserstein barycenter problem studied in [45]

$$\min \left\{ \sum_{k=1}^K \lambda_k \mathcal{MK}_\varepsilon(\mu^k, \nu) \mid \nu \in \Sigma_N \right\}, \tag{4.1}$$

which as in [33] can be re-written as

$$\forall\, k = 1, \ldots, K, \quad \nu = {\gamma_k}^T \mathbf{1},$$

where the set of optimal couplings $\boldsymbol{\gamma} = \{\gamma^k\}_{k=1}^K \in (\mathbb{R}_+^{N \times N})^K$ solves

$$\min \left\{ \mathrm{KL}_\lambda\left(\boldsymbol{\gamma} | \overline{\boldsymbol{\gamma}}\right) := \sum_{k=1}^K \lambda_k \,\mathrm{KL}\left(\gamma^k | \overline{\gamma}^k\right) \;\middle|\; \boldsymbol{\gamma} \in \mathcal{C}_1 \cap \mathcal{C}_2 \right\} \tag{4.2}$$

$$\text{where} \quad \forall k, \quad \overline{\gamma}^k := \overline{\gamma} := e^{-\frac{C}{\varepsilon}},$$

and the constraint sets are defined by

$$\mathcal{C}_1 := \left\{ \boldsymbol{\gamma} = \{\gamma^k\}_k \in (\Sigma_N)^K \mid \forall\, k,\, \gamma^k \mathbf{1} = \mu^k \right\}$$
$$\text{and} \quad \mathcal{C}_2 := \left\{ \boldsymbol{\gamma} = \{\gamma^k\}_k \in (\Sigma_N)^K \mid \exists \nu \in \mathbb{R}^N, \forall\, k,\, {\gamma^k}^T \mathbf{1} = \nu \right\}.$$

It is easy to check that the Bregman iterative projection scheme can be applied to this setting by simply replacing KL by KL_λ.

The KL_λ projection on $\mathcal{C}_1$ is computed as detailed in Proposition 3.2.1, since it is equal to the KL projection of each $\overline{\gamma}^k = \overline{\gamma}$ on a constraint of fixed marginal μ^k. The KL_λ projection on $\mathcal{C}_2$ is computed as detailed in the following proposition.

Proposition 4.1.1 ([BCC+15]). *For $\bar{\boldsymbol{\gamma}} := \{\bar{\gamma}^k\}_k \in (\mathbb{R}_+^{N\times N})^K$, the projection $\boldsymbol{\gamma} := \{\gamma^k\}_{k=1}^K = P_{\mathcal{C}_2}^{\mathrm{KL}_\lambda}(\bar{\boldsymbol{\gamma}})$ satisfies*

$$\forall\, k, \quad \gamma^k = \operatorname{diag}\left(\frac{\nu}{\bar{\gamma}^k \mathbf{1}}\right)\bar{\gamma}^k \quad \textit{where} \quad \nu := \prod_{r=1}^K (\bar{\gamma}^r \mathbf{1})^{\lambda_r} \tag{4.3}$$

where $\prod$ and $(\cdot)^{\lambda_r}$ should be understood as entry-wise operators.

Proof. Introducing the variable ν such that for all k, $\gamma_k^T \mathbf{1} = \nu$, the first order conditions of the projection $P_{\mathcal{C}_2}^{\mathrm{KL}_\lambda}(\bar{\boldsymbol{\gamma}})$ states the existence of Lagrange multipliers $(u_k)_k$ such that

$$\forall\, k, \quad \lambda_k \log\left(\frac{\gamma^k}{\bar{\gamma}^k}\right) + u_k \mathbf{1}^T = 0 \quad \text{and} \quad \sum_r u_r = 0.$$

Denoting $a_k = e^{-u_k}$, one has $\prod_k a_k = \mathbf{1}$ and $\gamma^k = \operatorname{diag}(a_k^{1/\lambda_k})\bar{\gamma}^k$. Condition $\gamma_k^T \mathbf{1} = \nu$ thus implies that

$$a_k = \left(\frac{\nu}{\bar{\gamma}^k \mathbf{1}}\right)^{\lambda_k},$$

and condition $\prod_k a_k = \mathbf{1}$ gives the desired value (4.3) for p. □

Remark 4.1.2 (Special case). Note that when $K = 2$, $(\lambda_1, \lambda_2) = (0, 1)$, one retrieves exactly the IPFP/Sinkhorn algorithm to solve the entropic OT, as detailed in Section 3.2. Our novel scheme to compute barycenters should thus be understood as the natural generalization of this IPFP algorithm to barycenters.

Remark 4.1.3 (Memory efficient and parallel implementation,[BCC+15]). As we have showed in Section 3.2, one verifies that iterations (3.3) in the special case of problem (4.2) leads to iterates $\boldsymbol{\gamma}^{(n)} = \{\gamma^{k,(n)}\}_k$ which satisfy, for each k

$$\gamma^{k,(n)} = \operatorname{diag}(u_k^{(n)})\overline{\gamma}\operatorname{diag}(v_k^{(n)})$$

for two vectors $(u_k^{(n)}, v_k^{(n)}) \in \mathbb{R}^N \times \mathbb{R}^N$ initialized as $v_k^{(0)} = \mathbf{1}$ for all k, and computed with the iterations

$$u_k^{(n)} = \frac{\nu^{(n)}}{\overline{\gamma} v_k^{(n)}} \quad \text{and} \quad v_k^{(n+1)} = \frac{\mu^k}{\overline{\gamma}^T u_k^{(n)}}$$

where $\nu^{(n)}$ is the current estimate of the barycenter, computed as

$$\nu^{(n)} = \prod_{k=1}^N \left(u_k^{(n)} \odot (\overline{\gamma} v_k^{(n)})\right)^{\lambda_k}.$$

A nice feature of these iterations is that they can be computed in parallel for all k using multiplications between the matrix $\overline{\gamma}$ and matrices storing $(u_k^{(n)})_k$ and $(v_k^{(n)})_k$ as columns.

Figure 4.1 shows an example of barycenters computation for $K = 3$. The three vertices of the triangle show the input densities (p_1, p_2, p_3) which are

uniform on binary shapes (diamond, annulus and square). The other points in the triangle display the results for the following values of λ

$$
\begin{array}{ccccc}
 & & (0,0,1) & & \\
 & (1,\,0,\,3)/4 & & (0,\,1,\,3)/4 & \\
 & (1,0,1)/2 & (1,1,2)/4 & (0,1,1)/2 & \\
(3,0,1)/4 & & (2,1,1)/4 & (1,2,1)/4 & (0,3,1)/4 \\
(1,0,0) & (3,1,0)/4 & (1,1,0)/2 & (1,3,0)/4 & (0,1,0)
\end{array}
$$

The computation is performed on an uniform 2-D grid of $N = 256 \times 256$ points in $[0,1]^2$, and $\varepsilon = 2/N$.

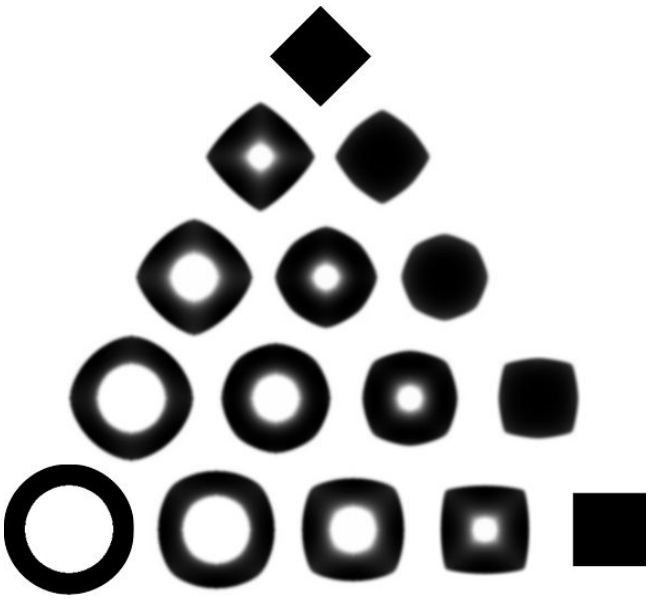

Figure 4.1: *Example of OT barycenters with entropic smoothing.*

We benchmark the performance of the Bregman iterative projection scheme to compute barycenters with the approaches proposed in [45] and [33]. We propose for this benchmark to compute the quadratic-Wasserstein barycenter of $K = 12$ probability histograms on the $N = 100 \times 100$ planar grid. These histograms are obtained as discretized and then renormalized truncated mixtures of Gaussians on the grid, as displayed in Figure 4.2. We consider for the $N \times N$ cost matrix C the matrix of squared Euclidean distances on the grid, normalized to have median 1.

We review briefly two competing methods for this task. The authors of [45] proposed to minimize directly Equation (4.1) with a regularizer $\varepsilon > 0$. That objective can be evaluated by running K Sinkhorn fixed-point iterations. That objective is differentiable and its gradient is equal to $\varepsilon \sum_k \lambda_k \log u_k$, where the u_k are the left optimal scalings obtained with the Sinkhorn subroutine, run in parallel. The cost of each iteration of the Sinkhorn algorithm is $2KN^2$, namely the cost associated to the updates of row and column scalings, each obtained by multiplying a $N \times N$ matrix (the kernel $\overline{\gamma}$) times a $N \times K$ matrix (a matrix of scalings). A weakness of that approach is that a precision threshold τ for

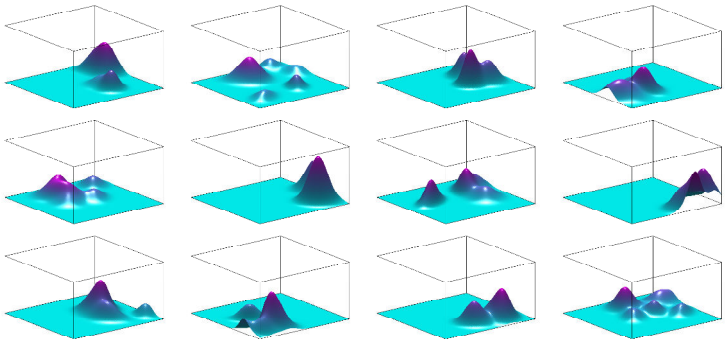

Figure 4.2: *Input measures considered in our experiment. They are formed by considering truncated mixtures of Gaussian densities on the planar square, which are then discretized on a regularly spaced* 100×100 *grid and normalized as histograms in* Σ_{10^4}.

each Sinkhorn fixed-point sub-iteration must be chosen. That precision can be measured by the difference in l_1 norm between the row and column marginals of $\mathrm{diag}(u_k)\overline{\gamma}\,\mathrm{diag}(v_k)$ and the target marginals. Setting that tolerance τ to a larger value ensures a faster convergence of the subroutine but results in noisier gradients. We experiment here with two thresholds $\tau \in \{0.01, 0.1\}$ and set a constant gradient stepsize t_0 to 1. The authors of [33] propose to solve directly the (non-differentiable) energy of Equation (4.1) when $\varepsilon = 0$. They study a dual formulation for that energy that involves splitting across dual variables and show that subgradients of the energy for each of these K dual variables can be computed in closed form by solving $K \times N$ nearest neighbor assignments (among N neighbors) on a shifted metric. They propose to use a L-BFGS method that exploits directly such subgradients, which we implement in practice using Matlab's `fmincon` function. At each step of their algorithm, iterates in the primal can be obtained by averaging all of the K subgradients.

Because our approach as well as that of [45] on the one hand, and that of [33] on the other hand, minimizes two different energies—the sum of K smoothed distances W_ε and the sum of K original Wasserstein distances W_0 respectively—comparing them on only one of these two energies does not make sense. We plot in Figure 4.3 the gap to optimality of each method with respect to smooth ($\varepsilon = 1/100$) and non smooth energies as a function of the number of iterations consumed by the algorithm. By gap to optimality we mean in the y axis the difference between the objective evaluated at the primal iterate and the optimal value for that problem, after x iterations in the x axis. We consider as a proxy for the optimal value the smallest value obtained across all methods after 10^5 iterations. This minimum across all methods is in fact attained much earlier by the Bregman alternated projections approach after only 771 iterations (we do not plot that point in our graph), which is set to terminate when the l_1 norm of two successive iterates is less than 10^{-8}. By one iteration, we mean an iteration whose cost is equal to N^2K elementary operations. The number N^2K corresponds to the K matrix-vector products of cost N^2 needed by both the Sinkhorn subroutine or the Bregman alternative projections, or $K \times N$ nearest-

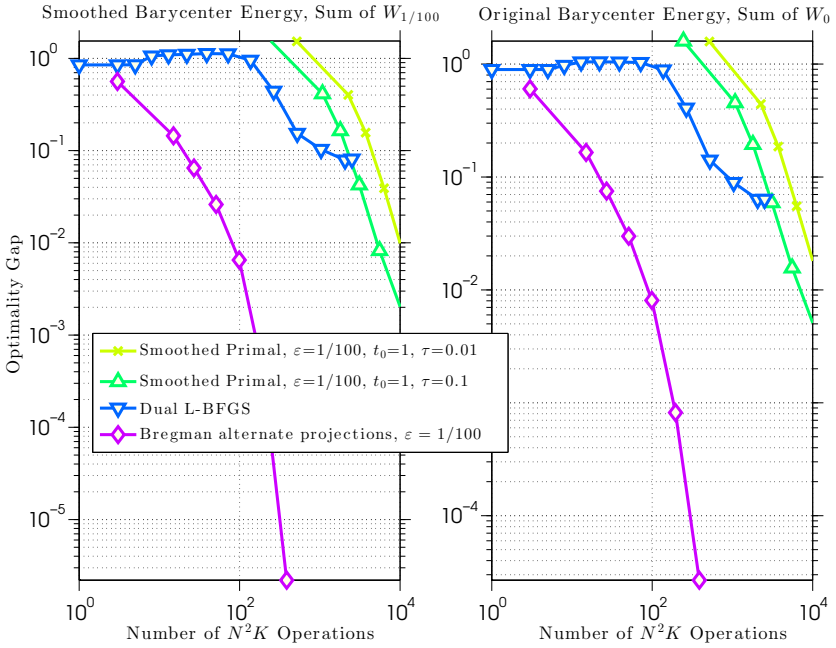

Figure 4.3: *Optimality gap as a function of the number of iterations (each consisting in N^2K operations) of the three considered methods with respect to both the smoothed Wasserstein energy that involves a sum of K smoothed distances $W_{1/100}$ terms, and the original Wasserstein barycenter energy involving sums of W_0 terms. The smoothed primal descent approach of [45] is considered here with two different tolerance parameters τ that control the convergence of the Sinkhorn subroutine used in that algorithm. We set the smoothing parameter ε to $1/100$, having renormalized the matrix of squared Euclidean distances between all nodes on the grid to have a median of 1. Notice that both x and y axis are displayed in logarithmic units. The Bregman alternative projection approach advocated in this paper converges orders of magnitude faster.*

neighbor assignments involving N candidates carried out in the dual descent. A perhaps surprising observations from these experiments is that the minimizer of the smoothed energy ends up providing, using either smoothed primal descent or Bregman iterations, a better minimizer of the non-smoothed energy as well. This is certainly due to the fact that we apply a relatively small smoothing $\varepsilon = 1/100$, and partly due to the tolerance and convergence criteria we have applied to the dual L-BFGS method. This reflects however the fundamental inability of the dual L-BFGS method to solve with a subgradient descent what is essentially a very large and degenerate linear program.

The barycenters we obtain for each of the three methods are displayed in Figure 4.4. We only report the barycenters as they appear after at most 10^4 iterations. The barycenter obtained after more than 10^5 iterations with the smoothed primal descent approach of [45] (not plotted here) is identical to that obtained with the Bregman iterative projection scheme, which should be expected since they minimize the same energy.

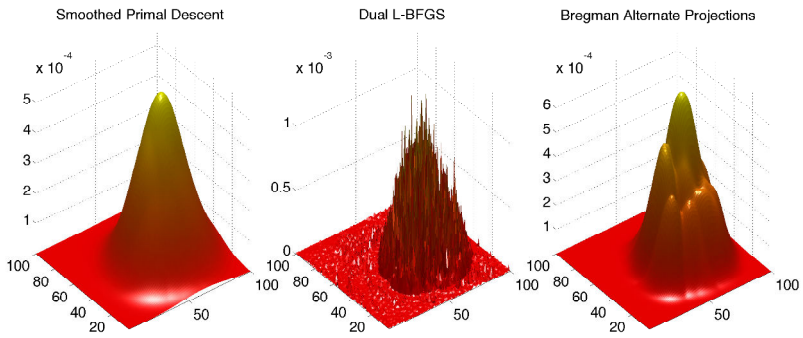

Figure 4.4: *Isobarycenters obtained with three different methods for the input measures displayed in Figure 4.2 after up to* 10^4 *iterations. The Bregman barycenter is obtained with a couple of hundred iterations.*

4.2 Matching for Teams

In this Section we present an application of the IPFP algorithm to *the matching for teams* problem which can be regarded as a generalization of the Wasserstein Barycenter. This model was introduced by Carlier and Ekeland in [32] and it deals with equilibrium of a market for a quality good. Indeed, producing a good requires gathering a team consisting of one buyer/consumer and a set of producers. In the following we will restrict ourselves to the finite setting and we introduce the model by the example of the *real estate market*. Thus, in the real estate market houses are the goods and they have a range of feasible qualities (location, surface, facilities, etc..) denoted by a set $Z := \{z_j\}_{j\in J}$, J is finite; the buyers buy one unit of good and they are characterized by the set $X_0 := \{x_i^0\}_{i\in I_0}$ and, finally, there are the producers $k \in \{1, \cdots, N\}$ (e.g. plumbers, electricians, etc...) characterized by $X_k := \{x_i^k\}_{i\in I_k}$. For each population $k \in K := \{0, \cdots, N\}$ we are given a cost function $c^k := \{c_{ij}^k\}_{i\in I_k, j\in J} \in \mathbb{R}^{I_k \times J}$ which can be interpreted as a cost for

an agent k with type x_i^k to work in a team that produces the good z_j. The distribution of type x_i^k is known and given by the probability $\mu^k \in \Sigma_k$ with

$$\Sigma_{I_k} := \{p \in \mathbb{R}^{I_k} \mid \sum_{i \in I_k} p_i = 1\}.$$

The goal is to find an equilibrium production line $\nu \in \Sigma_J$ which clears both the quality good and the market. Moreover, one looks for an equilibrium of monetary transfers: a system of transfers is a collection of vectors $\{\varphi^k\}_{k \in K} \in \mathbb{R}^J$ where φ_j^k is the amount paid to k by the other members of the team for producing the good j. It is clear that an equilibrium requires that the teams are self-financed

$$\sum_{k \in K} \varphi_j^k = 0 \quad \forall j \in J. \tag{4.4}$$

The c^k-transform of φ^k

$$\varphi^{c^k} := \{\varphi_i^{c^k}\}_{i \in I_k} = \min_{j \in J} c_{ij}^k - \varphi_j^k,$$

gives the net minimal cost for an agent from the population k with type $x_i^k \in X_k$. Then, it follows that $\varphi_j^k + \varphi_i^{c^k} \leqslant c_{ij}^k \ \forall (i,j) \in I_k \times J$ and the agents choose cost minimizing qualities $j \in J$ such that

$$\varphi_j^k + \varphi_i^{c^k} = c_{ij}^k. \tag{4.5}$$

The last unknown is a collection of transport plans $\{\gamma^k\}_{k \in K} \in \mathbb{R}^{I_k \times J}$ such that γ_{ij}^k is the probability that an agent k has a type x_i^k and belongs to the team which produces a quality j. It is obvious that at the equilibrium, we must have the following

$$\gamma^k \in \Pi(\mu^k, \nu) \quad \forall k \in K.$$

Thus, we have the following formal definition of equilibrium

Definition 4.2.1. *An equilibrium consists of a transfer system $\Phi = (\varphi^0, \cdots, \varphi^N)$, a collection probability measures $\boldsymbol{\gamma} = \{\gamma_k\}_{k \in K}$ and a probability measure $\nu \in \Sigma_J$ such that*

- *(4.4) holds,*
- *$\gamma^k \in \Pi(\mu^k, \nu)$ for $k \in K$,*
- *(4.5) holds on the support of γ^k for $k \in K$.*

If one knows the equilibrium ν then the two last conditions imply that the plan γ^k is optimal for the Monge-Kantorovich problem

$$\mathcal{MK}_{c^k}(\mu^k, \nu) = \inf_{\gamma^k \in \Pi(\mu^k, \nu)} \sum_{i,j \in I_k \times J} c_{ij}^k \gamma_{ij}^k.$$

Indeed, in [32] the equilibrium can be characterize by a variational approach, related to the following problem

$$\inf \left\{ \sum_{k \in K} \mathcal{MK}_{c^k}(\mu^k, \nu) \mid \nu \in \Sigma_J \right\}, \tag{4.6}$$

and its dual formulation

$$\sup\left\{\sum_{k\in K}\sum_{i\in I_k}\varphi_i^{c^k}\mu_i^k \mid \sum_{k\in K}\varphi^k = 0\right\}. \tag{4.7}$$

Thus, we have the following result

Theorem 4.2.2 ([32] Theorem 4)**.** $(\Phi, \boldsymbol{\gamma}, \nu)$ *is an equilibrium if and only if:*

1. ν *solves (4.6),*
2. Φ *solves (4.7),*
3. γ^k *solves* $\mathcal{MK}_{c^k}(\mu^k, \nu)$ *for* $k \in K$*.*

It is clear that the problem we have described so far, it is actually a generalization of the Wasserstein Barycenter problem. It follows that one can easily generalize the algorithm described in Section 4.1. We consider the regularized matching for teams problem which reads as

$$\min\left\{\sum_{k\in K}\lambda_k \mathcal{MK}_{c^k,\varepsilon}(\mu^k, \nu) \mid \nu \in \Sigma_J\right\}, \tag{4.8}$$

where $\lambda_k = \frac{1}{N+1}\ \forall k \in K$. The problem can be re-written as

$$\forall\, k = 1, \dots, K, \quad \nu = {\gamma^k}^T\mathbf{1},$$

where the set of optimal couplings $\boldsymbol{\gamma} = \{\gamma^k\}_{k=1}^K \in \times_{k\in K}(\mathbb{R}_+^{I_k \times J})$ solves

$$\min\left\{\mathrm{KL}_\lambda\left(\boldsymbol{\gamma}|\overline{\boldsymbol{\gamma}}\right) := \sum_{k=1}^K \lambda_k \,\mathrm{KL}\left(\gamma^k|\overline{\gamma}^k\right) \mid \boldsymbol{\gamma} \in \mathcal{C}_1 \cap \mathcal{C}_2\right\} \tag{4.9}$$

$$\text{where} \quad \forall k, \quad \overline{\gamma}^k := \overline{\gamma}^k := e^{-\frac{c^k}{\varepsilon}},$$

and the constraint sets are defined by

$$\begin{aligned} \mathcal{C}_1 &:= \left\{\boldsymbol{\gamma} = \{\gamma^k\}_k \in \otimes_{k\in K}\Sigma_{I_k} \mid \forall\, k,\ \gamma^k\mathbf{1} = \mu^k\right\} \\ \text{and} \quad \mathcal{C}_2 &:= \left\{\boldsymbol{\gamma} = \{\gamma^k\}_k \in \otimes_{k\in K}\Sigma_{I_k} \mid \exists \nu \in \mathbb{R}^J, \forall\, k,\ {\gamma^k}^T\mathbf{1} = \nu\right\}. \end{aligned}$$

It is easy to check that the Bregman iterative projection scheme can be applied to this setting by simply replacing KL by KL_λ.

The KL_λ projection on $\mathcal{C}_1$ is computed as detailed in Proposition 3.2.1, since it is equal to the KL projection of each $\overline{\gamma}^k = \overline{\gamma}$ on a constraint of fixed marginal μ^k. The KL_λ projection on $\mathcal{C}_2$ is computed as detailed in Proposition 4.1.1.

Remark 4.2.3 (Memory efficient and parallel implementation). Similarly as for Remark 4.1.3, one verifies that iterations (3.3) in the special case of problem (4.9) leads to iterates $\boldsymbol{\gamma}^{(n)} = \{\gamma^{k,(n)}\}_k$ which satisfy, for each k

$$\gamma^{k,(n)} = \mathrm{diag}(u_k^{(n)})\overline{\gamma}^k\,\mathrm{diag}(v_k^{(n)})$$

for two vectors $(u_k^{(n)}, v_k^{(n)}) \in \mathbb{R}^N \times \mathbb{R}^N$ initialized as $v_k^{(0)} = \mathbf{1}$ for all k, and computed with the iterations

$$u_k^{(n)} = \frac{\nu^{(n)}}{\overline{\gamma}^k v_k^{(n)}} \quad \text{and} \quad v_k^{(n+1)} = \frac{\mu^k}{\overline{\gamma}^{k^T} u_k^{(n)}}$$

where $\nu^{(n)}$ is the current estimate of the barycenter, computed as

$$\nu^{(n)} = \prod_{k=1}^{N} \left(u_k^{(n)} \odot (\overline{\gamma}^k v_k^{(n)}) \right)^{\lambda_k}.$$

For the numerical experiments we consider the same example as in [37]. $Z := \{(z_j^1, z_j^2)\}_{j \in J}$ and $X_0 := \{(x_i^0, y_i^0)\}_{i \in I_0}$ are a $M \times M$ discretization of $[0,1]^2$ and $[1,2]^2$ respectively, $X_1 := \{(x_i^1, y_i^1)\}_{i \in I_1}$ is a $M \times M$ discretization of $[1.25, 1.75] \times [1,2]$ and $X_2 := \{(x_i^2, y_i^2)\}_{i \in I_2}$ of $[1,2] \times [1.25, 1.75]$ with $M = 100$ and $\varepsilon = 0.05$. The given densities are

$$\begin{aligned} \mu^0 &= \chi_{[1,2]^2}, \\ \mu^1 &= \chi_{[1.25,1.75]\times[1,2]}, \\ \mu^2 &= \chi_{[1,2]\times[1.25,1.75]}, \end{aligned}$$

and corresponding cost functions are

$$\begin{aligned} c_{ij}^0 &= -5.5(x_i^0 z_j^1 + y_i^0 z_j^2) \\ c_{ij}^k &= (x_i^k + z_j^1)^2 + (y_i^k + z_j^2)^2 \; k = 1, 2. \end{aligned}$$

As displayed in Figure 4.5 the support of the optimal solution ν is mostly concentrated at the boundary and at the corners of the domain. If we compare it with the optimal one in [37], the effect of the regularization is clear.

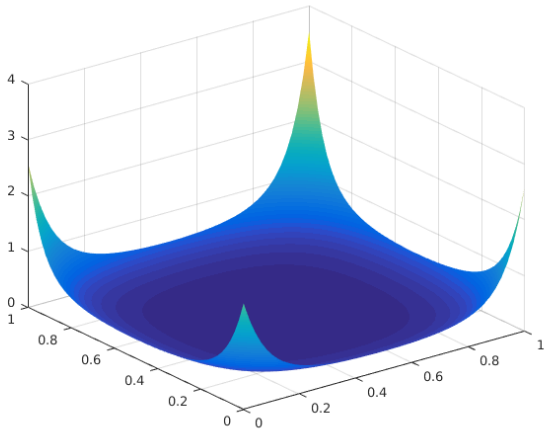

Figure 4.5: *Plot of the optimal solution ν.*

4.3 Partial Transport

In the partial transport problem, one is given two marginals $(\mu, \nu) \in (\mathbb{R}_+^N)^2$, not necessarily with the same total mass. We wish to transport only a given fraction of mass

$$m \in [0, \min(\mu^T \mathbf{1}, \nu^T \mathbf{1})],$$

minimizing the transportation cost $\langle C, \gamma \rangle$ where $C \in (\mathbb{R}_+)^{N \times N}$ is the ground cost.

The corresponding regularized problem reads

$$\min_{\gamma \in \mathbb{R}_+^{N \times N}} \left\{ \langle C, \gamma \rangle + \varepsilon \, \mathrm{H}(\gamma | \eta) \mid \gamma \mathbf{1} \leqslant \mu, \ \gamma^T \mathbf{1} \leqslant \nu, \mathbf{1}^T \gamma \mathbf{1} = m \right\} \tag{4.10}$$

where $\eta_{ij} = 1 \ \forall (i,j) \in \{1, \cdots, N\}^2$ and the inequalities should be understood component-wise.

Similarly to (3.4), this is equivalent to computing the projection of $\overline{\gamma} = e^{-\frac{C}{\varepsilon}}$ on the intersection $\mathcal{C}_1 \cap \mathcal{C}_2 \cap \mathcal{C}_3$ of $K = 3$ convex sets where

$$\mathcal{C}_1 := \{\gamma \mid \gamma \mathbf{1} \leqslant \mu\}, \quad \mathcal{C}_2 := \left\{\gamma \mid \gamma^T \mathbf{1} \leqslant \nu\right\}, \quad \mathcal{C}_3 := \left\{\gamma \mid \mathbf{1}^T \gamma \mathbf{1} = m\right\}. \tag{4.11}$$

The following proposition shows that the KL projection onto those three sets can be obtained in closed form.

Proposition 4.3.1 ([BCC+15]). *Let $\gamma \in \mathbb{R}_+^{N \times N}$. Denoting $\gamma^k := P_{\mathcal{C}_k}^{\mathrm{KL}}(\gamma)$ for $k \in \{1,2,3\}$ where $\mathcal{C}_k$ is defined by (4.11), one has*

$$\gamma^1 = \operatorname{diag}\left(\min\left(\frac{\mu}{\gamma \mathbf{1}}, \mathbf{1}\right)\right) \gamma,$$
$$\gamma^2 = \gamma \operatorname{diag}\left(\min\left(\frac{\nu}{\gamma^T \mathbf{1}}, \mathbf{1}\right)\right),$$
$$\gamma^3 = \gamma \frac{m}{\mathbf{1}^T \gamma \mathbf{1}},$$

where the minimum is component-wise.

Since the considered sets $\mathcal{C}_1$ and $\mathcal{C}_2$ are convex but not affine, one thus needs to use Dykstra iterations (3.19) which are ensured to converge to the solution of (4.10).

If $\gamma^\star$ is the optimal solution of (4.10) and

$$\mu_m := \gamma^\star \mathbf{1} \quad \text{and} \quad \nu_m := \gamma^{\star,T} \mathbf{1}$$

are its marginals, then we define the active source $\mathcal{S}_m$ and the active target $\mathcal{T}_m$ regions as follow

$$\mathcal{S}_m := \{x_i \mid (\nu_m)_i / m \geqslant \eta\},$$
$$\mathcal{T}_m := \{x_i \mid (\mu_m)_i / m \geqslant \eta\},$$

where $\eta > 0$ is a threshold we use to detect the region, namely the active region, where the transported mass is concentrated.

The continuous partial optimal transport problem has been studied in Caffarelli-McCann [27] and Figalli [54]. They show in particular that if there exists

an hyperplane separating the support of the two marginals then the "active region" is separated from the "inactive region" by a free boundary which can be parameterized as a semi concave graph over the separating hyperplane. This can be observed on the test case presented in Figure 4.6. The computation is performed on an uniform 2D-grid of $N = 256 \times 256$ points in $[0,1]^2$, $\varepsilon = 10^{-3}$ and $m = 0.7 \min(\langle \mu, \mathbf{1} \rangle, \langle \nu, \mathbf{1} \rangle)$.

Figure 4.6: *The red region is the active source $\mathcal{S}_m$, the green region is the active target $\mathcal{T}_m$ and the black ones are the inactive regions.*

4.4 Capacity Constrained Transport

Korman and McCann proposed and studied in [79, 80] a variant of the classical OT problem when there is an upper bound on the coupling weights so as to capture transport capacity constraints. The capacity is described by $\theta \in (\mathbb{R}_+)^{N \times N}$, where $\theta_{i,j}$ is the maximum possible mass that can be transferred from i to j. The corresponding regularized problem reads, for a ground cost $C \in (\mathbb{R}_+)^{N \times N}$ and marginals $(\mu, \nu) \in (\mathbb{R}_+^N)^2$,

$$\min_{\gamma \in \mathbb{R}_+^{N \times N}} \left\{ \langle C, \gamma \rangle + \varepsilon \, \mathrm{H}(\gamma | \eta) \mid \gamma \mathbf{1} = \mu, \ \gamma^T \mathbf{1} = \nu, \ \gamma \leqslant \theta \right\} \tag{4.12}$$

where $\eta_{ij} = \mu_i \otimes \nu_j$ for every $(i,j) \in \{1, \cdots, N\}^2$ and the inequalities should be understood component-wise. This problem is equivalent to a KL projection problem with $K = 3$ convex sets and

$$\mathcal{C}_1 := \{ \gamma \mid \gamma \mathbf{1} = \mu \}, \quad \mathcal{C}_2 := \left\{ \gamma \mid \gamma^T \mathbf{1} = \nu \right\}, \quad \mathcal{C}_3 := \{ \gamma \mid \gamma \leqslant \theta \}. \tag{4.13}$$

The projection on $\mathcal{C}_1$ and $\mathcal{C}_2$ is given by Proposition 3.2.1. The projection on $\mathcal{C}_3$ is simply

$$P_{\mathcal{C}_3}^{\mathrm{KL}}(\bar{\gamma}) = \min(\gamma, \bar{\gamma})$$

where the minimum is component-wise. Here we have to emphasize the difference between continuous and discrete notations for pointwise capacity constraints; in the continuous problem, one looks for an absolutely continuous with respect to Lebesgue's measure plan γ and the capacity constraint reads as $\gamma \leq \theta$ where γ represents a density and θ the capacity constraint. In the case of unidimensional marginals, if we think of the discrete weight $\gamma_{i,j}$ as the mass of a cell of area $1/N^2$, $\bar{\gamma}_{i,j}$ represents the integral of θ on this cell, hence $\bar{\gamma}_{i,j} \simeq \theta_{i,j}/N^2$.

Korman and McCann [80] established several interesting properties of minimizers in the continuous setting, in particular, they proved (theorem 3.3) that optimal plans must saturate the capacity constraint, that is optimal plans γ are of the form $\theta\, 1_W$, where 1_W is the characteristic function of a subset W of $\mathbb{R}^d \times \mathbb{R}^d$. For the quadratic transport cost, uniform marginals and a constant maximal capacity constraint θ, they also prove symmetry properties between minimizers $\gamma^\star$, $\tilde{\gamma}^\star$ with the same marginals but different capacity constraints θ and $\tilde{\theta}$ which are Hölder conjugate, i.e. $\frac{1}{\theta} + \frac{1}{\tilde{\theta}} = 1$. More precisely, assuming for simplicity that the marginals are symmetric with respect to 0, they show that

$$\gamma^\star = \theta\, 1_W \iff \tilde{\gamma}^\star = \tilde{\theta}\, 1_{R(\Omega \setminus W)} \tag{4.14}$$

where $R(x, y) = (x, -y)$ is the symmetry with respect to the second marginal axis and W the optimal support of the saturated constraint $\mathcal{C}_3$.

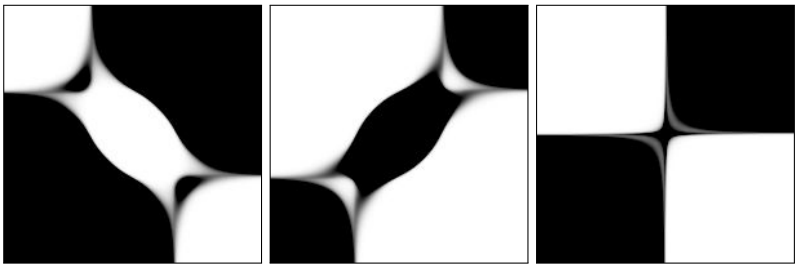

$\theta = 3/2$ $\theta = 3$ $\theta = 2$

Figure 4.7: *Comparison of optimal couplings $\gamma^\star$ for different values of θ. The saturated region W is represented in black.*

Korman and McCann [80] illustrated their theory with two 1-D numerical test cases (Figures 1 and 2 of [80]) computed by linear programming and a discretization of the problem on a cartesian grid. We tested our method on the same examples. The ground cost is the standard quadratic distance $c_{i,j} = \|x_i - x_j\|^2$, the marginals are discretization of the uniform distribution on $[-1/2, 1/2]$ using $N = 100$ points $(x_i)_i$. The simulation uses $\varepsilon = 10^{-3}$. We reproduce the expected symmetries (4.14) in Figure 4.7 in the 1-D test case for $\theta = \frac{3}{2}$ and $\tilde{\theta} = 3$ and also for the self dual Hölder conjugate $\theta = \tilde{\theta} = 2$.

We also computed the solutions of similar test cases but this time in 2-D, which would be computationally too expensive to solve with linear programming methods. The marginals (p, q) are discretization of the uniform distribution on the square $[-1/2, 1/2]^2$, discretized on a grid of $N = 50 \times 50$ points $(x_i)_i$. The simulation uses $\varepsilon = 10^{-3}$. Figure 4.8 shows some slices of the 4-D array representing the optimal transport plan $\gamma^\star$, $\tilde{\gamma}^\star$, illustrating the symmetries (4.14) in this setting.

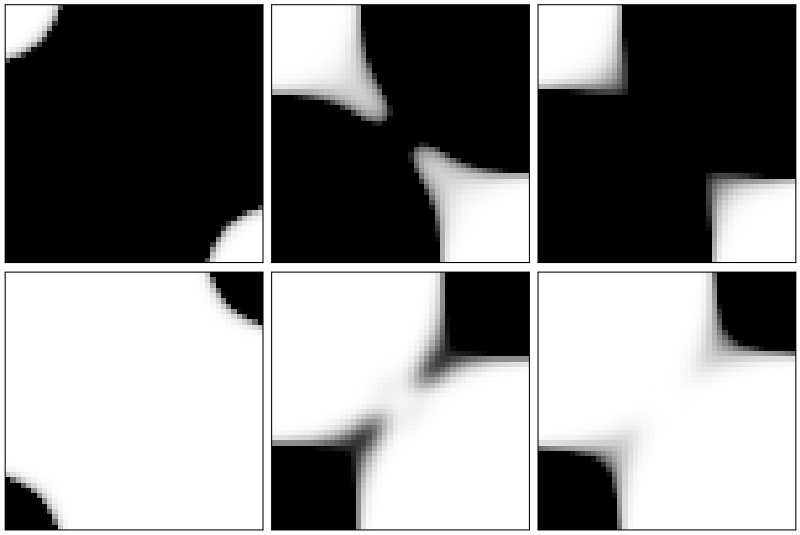

Figure 4.8: *2-D slices of the optimal coupling $\gamma^\star$ of the form $(\gamma^\star_{(i_1,i_2)(j_1,j_2)})_{i_1,j_1}$, each time for some fixed value of $(i_2, j_2) \in \{1, \dots, \sqrt{N}\}^2$, for $\theta = 3/2$ (top row) and $\theta = 3$ (bottom row).*

Chapter 5

Entropic Cournot-Nash equilibria

5.1 Cournot-Nash equilibria

We will restrict ourselves here to the following *finite* Cournot-Nash setting. Not only this will simplify the exposition and enable us to give a simple and self-contained exposition of the variational approach but this will also be consistent with our numerical scheme which anyway considers a finite number of agents' types and a finite number of strategies. We refer to [15] for the analysis of the continuum case. We consider a population of players, each of whom is characterized by a type which takes values in the type set $X := \{x_i\}_{i\in I}$ where I is finite. The frequencies of the players' type in the population is given by a probability $\mu := \{\mu_i\}_{i\in I}$ with $\mu_i \geq 0$ and $\sum_{i=1}^{N} \mu_i = 1$. Each agent has to choose a strategy y from the strategy set $Y := \{y_j\}_{j\in J}$ with J finite. The unknown of the problem is a matrix $\gamma := \{\gamma_{ij}\}_{i\in I,\, j\in J}$ where γ_{ij} is the probability that a player of type x_i chooses strategy y_j, there is an obvious feasibility constraint on this matrix, obviously it should have nonnegative entries and its first *marginal* should match the given distribution of players μ i.e.:

$$\sum_{j\in J} \gamma_{ij} = \mu_i,\ \forall i \in I. \tag{5.1}$$

The matrix γ induces a probability $\nu = \pi_2(\gamma) = \{\nu_j\}_{j\in J}$ (where $\pi_2 : \mathbb{R}^I \times \mathbb{R}^J \to \mathbb{R}^J$ is the canonical projection) on the set of strategies given by its *second marginal*:

$$\nu_j := \sum_{i\in I} \gamma_{ij},\ \forall j \in J. \tag{5.2}$$

Agents of type x_i who play strategy y_j incur a cost that not only depends on x_i and y_j but also on the whole probability $\nu := \{\nu_j\}_{j\in J}$ on the strategy space induced by the behavior of the whole population of players, and we denote this cost by $\Psi_{ij}[\nu]$. An equilibrium is then a probability matrix γ which is feasible and which is consistent with the cost minimizing behavior of players, which is summarized in the next definition:

Definition 5.1.1. *A Cournot-Nash equilibrium is a matrix* $\gamma = \{\gamma_{ij}\}_{i\in I,\, j\in J} \in \mathbb{R}_+^{I\times J}$ *which satisfies the feasibility constraint 5.1 and such that, defining the strategy marginal* $\nu = \pi_2(\gamma)$ *by 5.2, one has*

$$\gamma_{ij} > 0 \Rightarrow \Psi_{ij}[\nu] = \min_{k\in J} \Psi_{ik}[\nu].$$

Provided Ψ_{ij} depends continuously on ν, the existence of an equilibrium can easily be proven by Kakutanis' fixed-point theorem, but not much more can be said, at this level of generality. If one further specifies the form of the cost, as we shall do now, following [15], one may obtain equilibria by minimizing a certain cost functional.

5.2 A variational approach to Cournot-Nash equilibria

We now suppose that the cost $\Psi_{ij}[\nu]$ takes the following separable form

$$\Psi_{ij}[\nu] := c_{ij} + f_j(\nu_j) + \sum_{k\in J} \varphi_{kj}\nu_k$$

where $c := \{c_{ij}\}_{i\in I,\, j\in J} \in \mathbb{R}^{I\times J}$, each function f_j is nondecreasing and continuous, the matrix $\varphi := \{\varphi_{kj}\} \in \mathbb{R}^{J\times J}$ is symmetric, i.e. $\varphi_{kj} = \varphi_{jk}$,

A possible interpretation of this model is the following: the players represent a population of doctors, their type x represent their region of origin and their y strategy represent the location where they chose to dwell, the total cost of x_i-type doctors is the sum of

- a transport cost $c_{ij} = c(x_i, y_j)$,
- a congestion cost $f_j(\nu_j)$: if location y_j is very crowded i.e. if ν_j is large, the doctors settling at y_j will see their benefit decrease,
- an interaction cost with the rest of the population of doctors, one can think that φ_{kj} is an increasing function of some distance between y_k and y_j so that $\sum_{k\in J} \varphi_{kj}\nu_k$ represents the average distance to the rest of the population.

The variational approach of [15] relies on optimal transport, and we shall give a self-contained and simple presentation in the present discrete setting. Firstly it is useful to introduce the marginal maps:

$$\gamma \in \mathbb{R}^{I\times J} \mapsto \pi_1(\gamma) = \alpha \in \mathbb{R}^I,\ \alpha_i := \sum_{j\in J} \gamma_{ij},$$

and

$$\gamma \in \mathbb{R}^{I\times J} \mapsto \pi_2(\gamma) = \nu \in \mathbb{R}^J,\ \nu_j := \sum_{i\in I} \gamma_{ij},$$

as well as

$$\mathcal{C}_1 := \{\gamma = \{\gamma_{ij}\}_{i\in I,\, j\in J} \in \mathbb{R}_+^{I\times J} \ :\ \pi_1(\gamma) = \mu\}$$

which is the set of probabilities on $X \times Y$ having μ as first marginal (recall that μ is fixed). For $\nu = \{\nu_j\}_{j\in J} \in \mathbb{R}_+^J$ such that $\sum_{j\in J} \nu_j = 1$, let us also define

$$\mathcal{C}_2 := \{\gamma = \{\gamma_{ij}\}_{i\in I,\, j\in J} \in \mathbb{R}_+^{I\times J} \ : \ \pi_2(\gamma) = \nu\}$$

as the set of probabilities on $X \times Y$ having ν as second marginal. Let us then also define the set of transport plans between μ and ν as

$$\Pi(\mu, \nu) := \mathcal{C}_1 \cap \mathcal{C}_2. \tag{5.3}$$

Given ν a probability on Y, let us define

$$\mathcal{MK}(\nu) := \inf \Big\{ \sum_{i,j\in I\times J} c_{ij}\gamma_{ij} \mid \gamma \in \Pi(\mu, \nu) \Big\} \tag{5.4}$$

that is the value of the optimal transport problem between μ and ν for the cost c. Setting

$$\Sigma_J := \{\nu \in \mathbb{R}_+^J \ : \ \sum_{j\in J} \nu_j = 1\}$$

consider the optimization problem

$$\inf_{\nu\in\Sigma_J} \mathcal{MK}(\nu) + E(\nu) \tag{5.5}$$

where the energy E is given by

$$E(\nu) := \sum_{j\in J} F_j(\nu_j) + \frac{1}{2} \sum_{k,j\in J\times J} \varphi_{kj}\nu_k\nu_j \tag{5.6}$$

and F_j is a primitive of the congestion function f_j:

$$F_j(t) := \int_0^t f_j(s)\mathrm{d}s.$$

We then have

Theorem 5.2.1 ([BCN16b])**.** *Let ν solve (5.5) and $\gamma \in \Pi(\mu, \nu)$ be such that $\sum_{i,j\in I\times J} c_{ij}\gamma_{ij} = \mathcal{MK}(\nu)$, then γ is a Cournot-Nash equilibrium. This implies in particular that there exists Cournot-Nash equilibria.*

Proof. We have to prove that whenever $\gamma_{ij} > 0$ one has

$$c_{ij} + f_j(\nu_j) + \sum_{k\in J} \varphi_{kj}\nu_k = u_i \tag{5.7}$$

with

$$u_i := \min_{j\in J}\{c_{ij} + f_j(\nu_j) + \sum_{k\in j} \varphi_{kj}\nu_k\}.$$

First observe that E is of class C^1 and by construction

$$\frac{\partial E}{\partial \nu_j} = f_j(\nu_j) + \sum_{k\in j} \varphi_{kj}\nu_k. \tag{5.8}$$

To treat the transport term, $\mathcal{MK}$, we shall recall the classical Kantorovich duality (see [115, 105]) as follows. Firstly for $v \in \mathbb{R}^J$ let us define

$$\mathcal{K}(v) := -\sum_{i\in I} \min_{j\in J}(c_{ij} - v_j)\mu_i$$

note that $\mathcal{K}$ is a convex and Lipschitz function whose conjugate, thanks to Kantorovich duality, can be expressed as

$$K^*(\nu) = \overline{\mathrm{MK}}(\nu) := \begin{cases} \mathcal{MK}(\nu) \text{ if } \nu \in \Sigma_J, \\ +\infty \text{ otherwise.} \end{cases}$$

Since ν minimizes $\overline{\mathrm{MK}} + E$, one has $0 \in \partial\mathcal{MK}(\nu) + \nabla E(\nu)$, setting $v := -\nabla E(\nu)$, this can be rewritten as $\nu \in \partial\overline{\mathrm{MK}}^*(v) = \partial K(v)$ and since $\overline{\mathrm{MK}}(\nu) = \sum_{i,j\in I\times J} c_{ij}\gamma_{ij}$ this gives

$$\begin{aligned}\mathcal{MK}(\nu) = \sum_{i,j\in I\times J} c_{ij}\gamma_{ij} &= \sum_{j\in J} v_j\nu_j + \sum_{i\in I} \min_{j\in J}(c_{ij} - v_j)\mu_i \\ &= \sum_{j\in J} v_j\nu_j + \sum_{i\in I} u_i\mu_i = \sum_{i,j\in I\times J} (u_i + v_j)\gamma_{ij}.\end{aligned}$$

which, since $u_i + v_j \le c_{ij}$ implies that whenever $\gamma_{ij} > 0$, one has $c_{ij} - v_j = u_i$ which is exactly 5.7. This clearly implies the existence of Cournot-Nash equilibria since Σ_J is compact and both $\mathcal{MK}$ and E are continuous. □

Note that if E is convex then the optimality condition $0 \in \partial\overline{\mathrm{MK}}(\nu) + \nabla E(\nu)$ is necessary and sufficient and there is actually an equivalence between being an equilibrium and being a minimizer in this case.

5.3 Entropic regularization

Solving 5.5 in practice (even if E is convex) might be difficult because of the transport cost term $\mathcal{MK}$ for which it is expensive to compute a subgradient. There is however a simple regularization of $\mathcal{MK}$ which is much more convenient to handle: the entropic regularization (see chapter 2). Given a regularization parameter $\varepsilon > 0$, let us define for every $\nu \in \Sigma_J$:

$$\mathcal{MK}_\varepsilon(\nu) := \inf_{\gamma\in\Pi(\mu,\nu)} \Big\{ \sum_{i,j\in I\times J} c_{ij}\gamma_{ij} + \varepsilon \sum_{i,j\in I\times J} \gamma_{ij}(\ln(\gamma_{ij}) - 1) \Big\}.$$

We then consider the regularization of 5.5

$$\inf_{\nu\in\Sigma_J} \mathcal{MK}_\varepsilon(\nu) + E(\nu) \tag{5.9}$$

where E is again given by 5.6. Thanks to the entropic regularization term, 5.9 is a smooth minimization problem which consists in minimizing with respect to γ and ν the objective

$$\sum_{i,j\in I\times J} c_{ij}\gamma_{ij} + \varepsilon \sum_{i,j\in I\times J} \gamma_{ij}(\ln(\gamma_{ij}) - 1) + E(\nu)$$

subject to $\gamma_{ij} \geq 0$ (but because of the entropy, these non-negativity constraints are not binding) and the linear marginal constraints $\gamma \in \Pi(\mu, \nu)$. The first-order optimality conditions give the following Gibbs form for γ_{ij}:

$$\gamma_{ij} = a_i \exp\Big(-\frac{1}{\varepsilon}(c_{ij} + f_j(\nu_j) + \sum_{k \in J} \varphi_{kj}\nu_k)\Big) \tag{5.10}$$

for some $a_i > 0$ which has to fulfill the first marginal constraint i.e.

$$a_i = \frac{\mu_i}{\sum_{j \in J} \exp\Big(-\frac{1}{\varepsilon}(c_{ij} + f_j(\nu_j) + \sum_{k \in J} \varphi_{kj}\nu_k)\Big)}.$$

Note that these conditions can also be interpreted as a regularized form of a Cournot-Nash equilibrium since they mean that the conditional probabilities on the set of strategies given the players type $\{\frac{\gamma_{ij}}{\mu_i}\}_{j \in J}$ are proportional to $\exp(-\frac{\Psi_{ij}(\nu)}{\varepsilon})$ where $\Psi_{ij}[\nu] = c_{ij} + f_j(\nu_j) + \sum_{k \in J} \varphi_{kj}\nu_k$ is the total cost incurred by players x_i when choosing strategy y_j. Another equilibrium interpretation (which is customary in economics and econometrics in the framework of discrete choice models) is to consider that the total cost actually contains a random component that is of the form εX_{ij} where the X_{ij} are i.i.d. logistic random variables (see [61]).

Of course, again when E is convex, since $\overline{\mathrm{MK}}_\varepsilon$ is strictly convex, there is a unique minimizer and the first-order optimality condition for 5.9 is necessary and sufficient so that there is again equivalence between being a minimizer and a (regularized) Cournot-Nash equilibrium.

5.4 A proximal splitting algorithm

To solve 5.9, we shall use a proximal splitting scheme using the Kullback-Leibler divergence that was recently introduced by Peyré [100] in the context of entropic regularization of Wasserstein gradient flows. First, let us observe that 5.9 can be rewritten as a special instance of a Bregman proximal problem. To see this, let us first rewrite

$$\sum_{i,j \in I \times J} c_{ij}\gamma_{ij} + \varepsilon \sum_{i,j \in I \times J} \gamma_{ij}(\ln(\gamma_{ij}) - 1) = \varepsilon \sum_{i,j \in I \times J} \gamma_{ij}(\ln\Big(\frac{\gamma_{ij}}{e^{-\frac{c_{ij}}{\varepsilon}}}\Big) - 1)$$

which is the same as $\varepsilon\,\mathrm{KL}(\gamma|\overline{\gamma})$ where $\overline{\gamma}_{ij} = e^{-\frac{c_{ij}}{\varepsilon}}$ and KL is the Kullback-Leibler divergence

$$\mathrm{KL}(\gamma|\theta) := \sum_{i,j \in I \times J} \gamma_{ij}\Big(\ln\Big(\frac{\gamma_{ij}}{\theta_{ij}}\Big) - 1\Big),\ \gamma \in \mathbb{R}_+^{I \times J},\ \theta \in \mathbb{R}_+^{I \times J}.$$

Note that KL is the Bregman divergence associated to the entropy. Solving 5.9 then amounts to the proximal problem

$$\mathrm{prox}_G^{\mathrm{KL}}(\overline{\gamma}) = \mathrm{argmin}_{\gamma \in \mathbb{R}_+^{I \times J}} \Big\{ \mathrm{KL}(\gamma|\overline{\gamma}) + G(\gamma) \Big\} \tag{5.11}$$

with

$$G(\gamma) := \chi_{\{\pi_1(\gamma) = \mu\}} + \frac{1}{\varepsilon} E(\pi_2(\gamma)).$$

Computing directly $\mathrm{prox}_G^{\mathrm{KL}}(\overline{\gamma})$ may be an involved task, but the idea of Peyré's splitting algorithm is to express G as a sum of more elementary functionals:

$$G := \sum_{l=1}^{L} G_l$$

each of whom being simple in the sense that computing $\mathrm{prox}_{G_l}^{\mathrm{KL}}$ can be done easily (ideally in close form). The algorithm proposed by Peyré generalizes Dykstra's algorithm for KL projections on the intersection of convex sets and can be described as follows. First extend the sequence of functions $G_1, \cdots, G_L$ by periodicity:

$$G_{l+nL} = G_l,\ l = \{1, \cdots, L\},\ n \in \mathbb{N}$$

initialize the algorithm by setting the following values for the $I \times J$ matrices

$$\gamma^{(0)} = \overline{\gamma},\ z^{(0)} = z^{(-1)} = \cdots = z^{(-L+1)} = e,\ e_{ij} = 1,\ (i,j) \in I \times J,$$

and then iteratively define for $n \geq 1$

$$\gamma^{(n)} = \mathrm{prox}_{G_n}^{\mathrm{KL}}\Big(\gamma^{n-1} \odot z^{(n-L)}\Big) \tag{5.12}$$

and

$$z^{(n)} = z^{(n-1)} \odot \Big(\frac{\gamma^{(n-1)}}{\gamma^{(n)}}\Big) \tag{5.13}$$

where $\odot$ and $\div$ stand for entrywise multiplication/division operations:

We refer to [100] for the convergence of this algorithm under suitable assumptions (convexity of the functions G_l and a certain qualification condition), the idea being that at the level of the dual problem, which is smooth, this algorithm amounts to perform an alternate block minimization.

5.4.1 A class of convex problems

Note that the congestion term $\sum_{j\in J} F_j(\nu_j)$ is convex because f_j is non-decreasing, but the quadratic interaction energy $\nu \mapsto \sum_{j,k\in J\times J} \varphi_{kj}\nu_k\nu_j$ is in general not convex. However, using Cauchy-Schwarz inequality, it satisfies

$$\sum_{j,k\in J\times J} \varphi_{kj}\nu_k\nu_j \geq -\Big(\sum_{j,k\in J\times J} \varphi_{kj}^2\Big)\sum_{j\in J}\nu_j^2$$

so that if F_j is 1-strongly convex:

$$F_j(t) = \frac{1}{2}t^2 + H_j(t)$$

with H_j convex and

$$\sum_{j,k\in J\times J} \varphi_{kj}^2 < 1, \tag{5.14}$$

then E is convex as the sum $E = E_2 + E_3$ of the convex quadratic term

$$E_2(\nu) := \frac{1}{2}\sum_{j\in J}\nu_j^2 + \frac{1}{2}\sum_{k,j\in J\times J} \varphi_{kj}\nu_k\nu_j$$

and the remaining convex congestion term

$$E_3(\nu) := \sum_{j\in J} H_j(\nu_j).$$

In this setting one can write 5.9 as

$$\inf_{\gamma\in\mathbb{R}_+^{I\times J}} \Big\{ \mathrm{KL}(\gamma|\overline{\gamma}) + G_1(\gamma) + G_2(\gamma) + G_3(\gamma) \Big\}$$

where

$$G_1(\gamma) = \chi_{\{\pi_1(\gamma)=\mu\}} = \begin{cases} 0 \text{ if } \pi_1(\gamma) = \mu \\ +\infty \text{ otherwise} \end{cases}$$

and

$$G_2 = \frac{1}{\varepsilon} E_2 \circ \pi_2,\ G_3 = \frac{1}{\varepsilon} E_3 \circ \pi_2.$$

To implement the proximal splitting scheme 5.12-5.13 in this case, one has to be able to compute the three proximal maps $\mathrm{prox}_{G_l}^{\mathrm{KL}}$ with $l = 1, 2, 3$. The proximal map of G_1 corresponds to the fixed marginal constraint $\pi_1(\gamma) = \mu$, it is well-known and it is given in closed form as:

$$\Big(\mathrm{prox}_{G_1}^{\mathrm{KL}}(\theta)\Big)_{ij} = \frac{\mu_i \theta_{ij}}{\sum_{k\in J} \theta_{ik}}.$$

Given $\theta \in \mathbb{R}_+^{I\times J}$, $\gamma := \mathrm{prox}_{G_2}^{\mathrm{KL}}(\theta)$ is of the form

$$\gamma_{ij} = \theta_{ij} \exp\Big(- \frac{\nu_j + \sum_{k\in J} \varphi_{kj}\nu_k}{\varepsilon} \Big)$$

where ν denotes the second marginal of γ, so that summing over i, ν is obtained by solving the system:

$$\nu_j = \Big(\sum_{i\in I} \theta_{ij} \Big) \exp\Big(- \frac{\nu_j + \sum_{k\in J} \varphi_{kj}\nu_k}{\varepsilon} \Big)$$

which, when 5.14 holds, can be solved in practice in a few Newton's steps. The computation of $\gamma := \mathrm{prox}_{G_3}^{\mathrm{KL}}(\theta)$ is simpler, setting $h_j := H_j'$ the first-order equation first leads to

$$\gamma_{ij} = \theta_{ij} \exp\Big(- \frac{h_j(\nu_j)}{\varepsilon} \Big)$$

and the ν_j's are obtained by solving

$$\nu_j = \Big(\sum_{i\in I} \theta_{ij} \Big) \exp\Big(- \frac{h_j(\nu_j)}{\varepsilon} \Big) \tag{5.15}$$

which is a separable system of monotone equations, which we shall again solve by Newton's method.

5.4.2 A semi-implicit scheme for more general nonconvex cases

We now go back to the general case where E is not necessarily convex because of the interaction term given by the symmetric matrix φ_{kj}. Eventhough there is no theoretical convergence guarantee (but if the folllowing scheme converges, it converges to an equilibrium), the semi-implicit scheme which we now describe gives good results in practice. The idea is simple and consists in replacing the nonconvex interaction term by its linearization. More precisely, we will approximate our initial problem 5.9:

$$\inf_{\nu\in\Sigma_J} \mathcal{MK}_\varepsilon(\nu) + E(\nu) \tag{5.16}$$

where E is the sum of the convex congestion cost and the nonconvex quadratic interaction cost, by a succession of convex problems, starting from $\nu^0 \in \Sigma_J$, iteratively solve for $n \geq 1$

$$\nu^{(n+1)} = \text{argmin}_{\nu\in\Sigma_J}\, \mathcal{MK}_\varepsilon(\nu) + E^{(n)}(\nu) \tag{5.17}$$

where in $E^{(n)}$ we have linearized the interaction term:

$$E^{(n)}(\nu) = \sum_{j\in J} F_j(\nu_j) + \sum_{j\in J} V_j^{(n)}\nu_j,\ V_j^{(n)} := \sum_{k\in J} \varphi_{kj}\nu_k^{(n)}.$$

Of course, we can solve 5.17 by the Dykstra proximal-splitting scheme described in the previous paragraph. More precisely, the linear term can be absorbed by the KL term so that we only have two proximal steps: one corresponding to the (explicit) projection fixed marginal constraint and one corresponding to the congestion cost (corresponding to 5.15 using f_j instead of h_j).

5.5 Numerical results

We now present some numerical results in dimension $d = 1$ and $d = 2$. As we have pointed out in section 5.3, the strength of the entropic regularization, and consequently of the Dykstra's algorithm, lies in the fact that we can treat optimal transportation problems with any transport cost, in particular both concave and convex cost functions can be considered. Thus, if we consider the cost $c_{ij} = |x_i - y_j|^p$ with $p > 0$ (convex cost if $p > 1$ and concave otherwise), then the idea is to analyze how the shape of the unknown marginal ν changes by varying the exponent p. Before showing the results, we want to focus on an other aspect of the entropic regularization, namely diffusion. Indeed, once we add the entropic term to the optimal transport term, then this regularization spreads the support of the plan γ and defines a strongly convex problem with a unique solution. So it is interesting to see how the support of the optimal γ varies by decreasing the parameter ε. Let us consider the standard quadratic cost $c_{ij} = |x_i - y_j|^2$ and the following energy $E(\nu)$

$$E(\nu) = \sum_{j\in J} \nu_j^8 + \frac{1}{2}\sum_{k,j\in J\times J} \varphi_{kj}\nu_k\nu_j + \sum |y_j - 9|^4, \tag{5.18}$$

where $\varphi_{kj} = 10^{-4}|y_k - y_j|^2$ and the third term is a confinement potential. We notice that there is no need to compute a proximal step for the potential, indeed

it can be absorbed by the KL term. We know that in this case the optimal γ (for instance see [15]) is a pure Cournot-Nash equilibrium, which actually means that γ has the form $\gamma_T = (\mathrm{id}, T)_{\#}\mu$ where T is the optimal map. In Figure 5.1 we plot the support of the optimal γ and its marginal ν for different values of ε. As expected the support of the regularized γ concentrates on the graph of T as ε decreases.

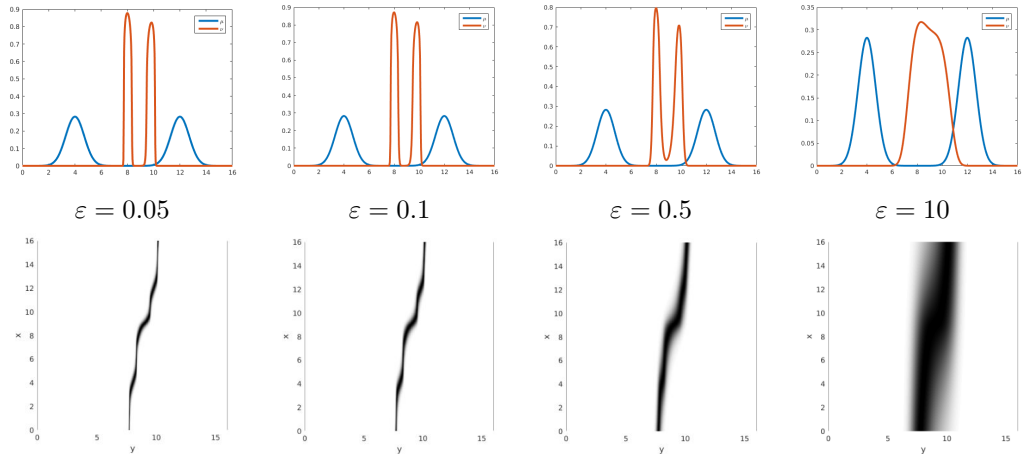

Figure 5.1: *Top: The initial distribution μ (blue solid line) and the solution ν (red solid line) for $\varepsilon \in \{0.05, 0.1, , 0.5, 10\}$. Bottom: The support of γ for $\varepsilon \in \{0.05, 0.1, , 0.5, 10\}$.*

In Section 5.4.2, we have pointed out that a semi-implicit approach can be applied in order to treat an energy E which is not convex. We want, now, to compare the performances of the implicit and the semi-implicit approach in terms of *CPU time* and *number of iterations* when ε varies. By looking at the Figure 5.2 we notice the number of iterations, as well as the CPU time, of the semi-implicit approach is smaller than the ones for the implicit approach. This is quite obvious as in the semi-implicit scheme, the interaction term can be absorbed by the KL term so that one has to compute only two proximal steps instead of three.

5.5.1 Dimension one

Let us first consider the one-dimensional case. One of the main advantages of the scheme we have proposed is that we can consider any kind of cost function. Thus, take $c_{ij} = |x_i - y_j|^p$ and the energy E given by (5.18), then we want to visualize the optimal ν as $p \in (0, M]$ with M large. For the simulations in Figure 5.3, we have used a $N = 500$ grid points discretization of $[0, 16]$ and we have treated the interaction term with a semi-implicit approach. Then, we have chosen the smallest ε possible for each cost function tested. As one can notice for $p \leqslant 1$ the optimal ν has a connected support where as for $p > 1$, the support of ν is closer to the one of μ. Finally, we obtain an optimal ν which tends to be concentrated near $y = 9$ due to the external potential, except for large p where

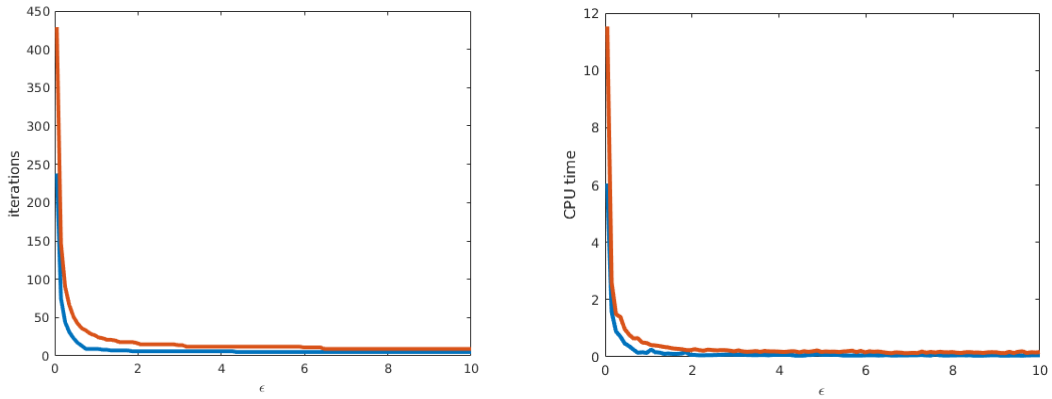

iterations CPU time in seconds

Figure 5.2: *Left: the number of iterations for the semi-implict (blue) and for the implicit (red). Right: CPU time for the semi-implict (blue) and for the implicit (red).*

the optimal transport term becomes *dominant* so that the second marginal ν tends to be *close* to the initial distribution μ.

Let us now consider an energy E given by

$$E(\nu) = \sum_{j\in J} \ln(\nu_j) + \sum_{k,j\in J\times J} \varphi_{kj}\nu_k\nu_j + \sum_{j\in J}(y_j - 5)^3 \tag{5.19}$$

where φ_{kj} is a cubic interaction $\varphi_{kj} = 10^{-4}|x_i - y_j|^3$. The simulations are presented in Figures 5.4 and 5.5 for different initial distribution: a uniform density on $[0, 1]$ and the sum of two translated gaussians, respectively. For both the numerical experiments we have used $N = 500$ grid points discretization of $[0, 10]$ and treated the interaction term with a semi-implicit approach. One can observe, as in the previous case, that the structure of the optimal ν becomes close to the one of the initial ditribution as p increases.

5.5.2 Dimension two

For the $2d$ case, we always take a cost $c(x, y) = \|x-y\|^p$ and then a congestion $F_j(\nu_j) = \nu_j^8$, an interaction $\varphi_{kj} = 10^{-4}\|y_k - y_j\|^2$ and a potential $v_j = \|y_j - 3\|^4$. The simulations in Figure 5.6 are obtained by using a $N \times N$, with $N = 80$, discretization of $[0, 5]^2$ and by treating the interaction term with a semi-implicit approach. As in the $1-$dimensional case, we notice the same effect on the support of ν when we make p vary.

5.6 Extension to several populations

5.6.1 A class of two-populations models

We end the paper by briefly explaining how our approach can easily be extended to the case of several populations of players. For the sake of simplicity, we take the two-populations case and assume that these two populations interact through a congestion term. More precisely, we are given two finite type spaces

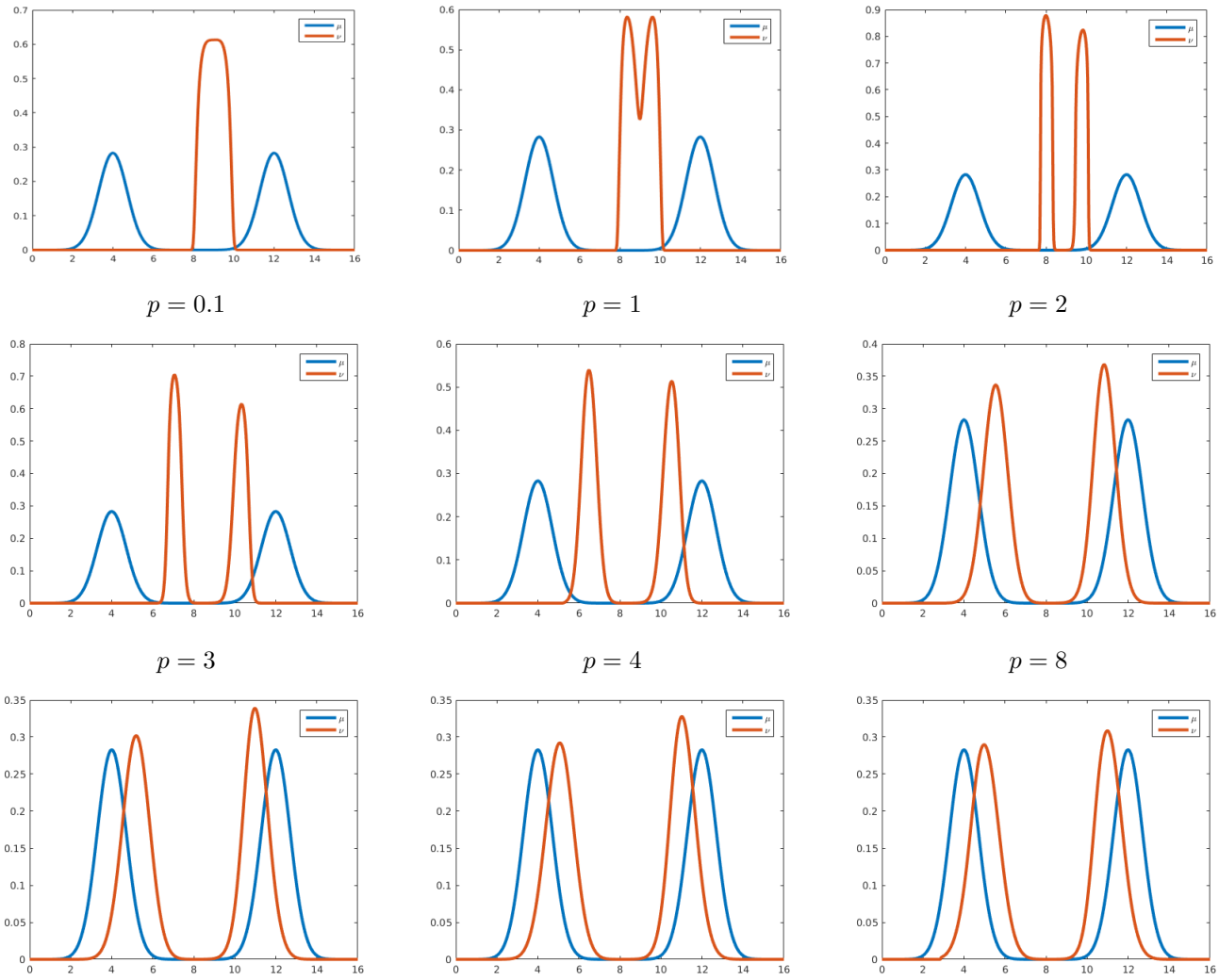

$p = 0.1$ $p = 1$ $p = 2$

$p = 3$ $p = 4$ $p = 8$

$p = 16$ $p = 32$ $p = 64$

Figure 5.3: *The initial distribution μ, a sum of two translated gaussian, (blue solid line) and the solution ν (red solid line) for $p \in \{0.1, 1, 2, 3, 4, 8, 16, 32, 64\}$.*

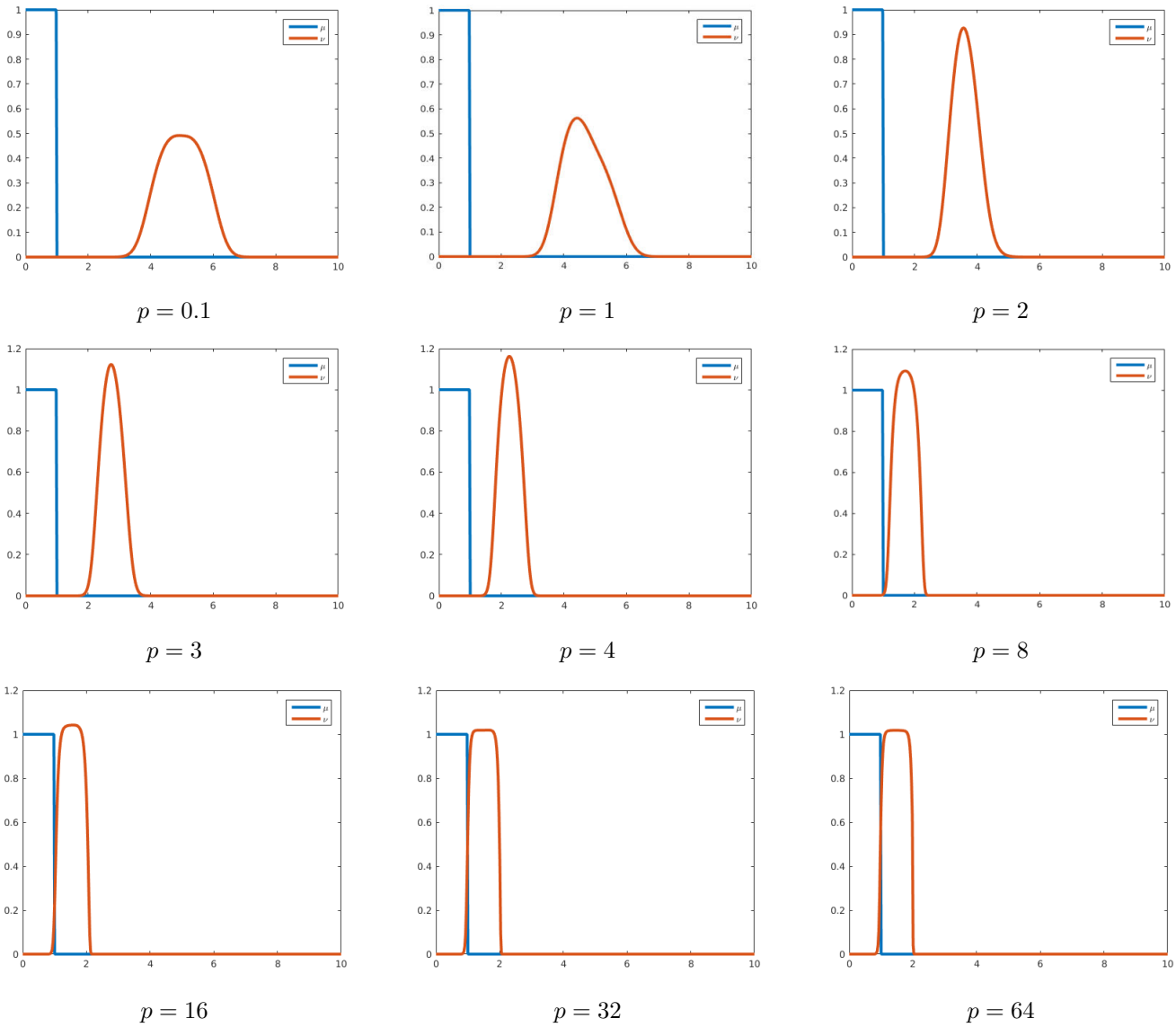

Figure 5.4: *The initial distribution μ, a uniform density on $[0, 1]$, (blue solid line) and the solution ν (red solid line) for $p \in \{0.1, 1, 2, 3, 4, 8, 16, 32, 64\}$.*

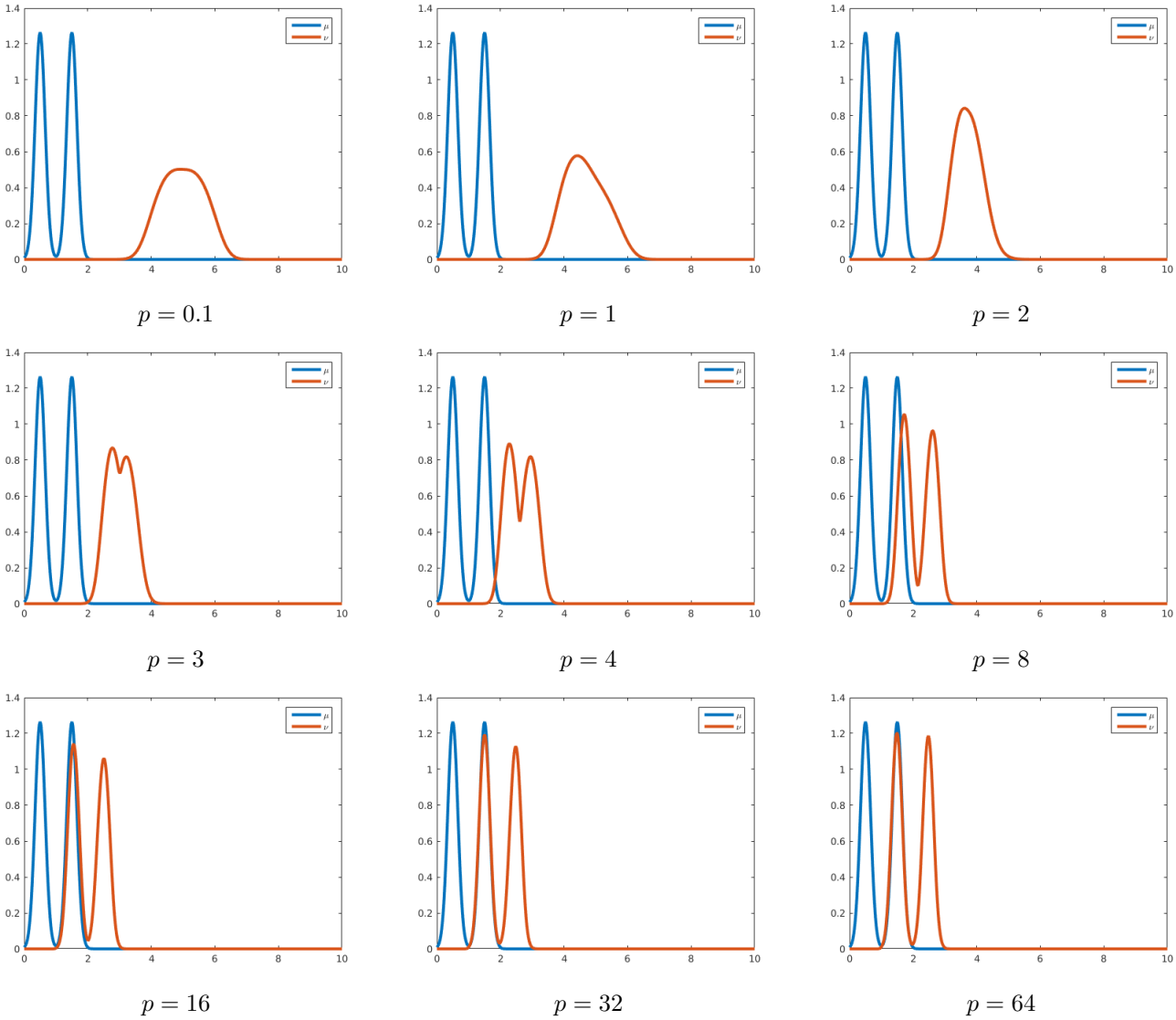

$p = 0.1$ $p = 1$ $p = 2$

$p = 3$ $p = 4$ $p = 8$

$p = 16$ $p = 32$ $p = 64$

Figure 5.5: *The initial distribution μ, a sum of two translated gaussians, (blue solid line) and the solution ν (red solid line) for $p \in \{0.1, 1, 2, 3, 4, 8, 16, 32, 64\}$.*

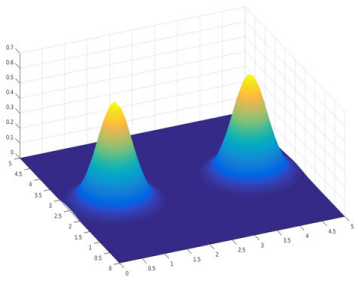

surface plot of μ

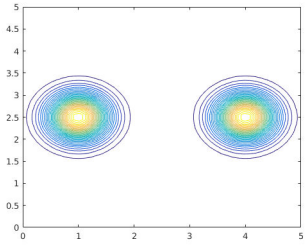

support of μ

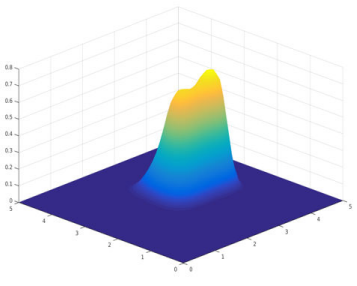

surface plot of ν for $p = 0.5$

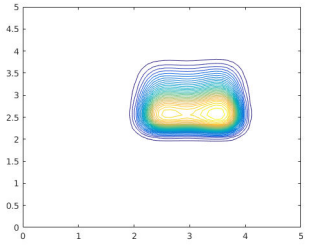

support of ν for $p = 0.5$

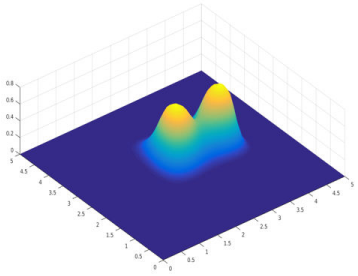

surface plot of ν for $p = 1$

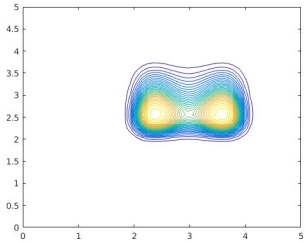

support of ν for $p = 1$

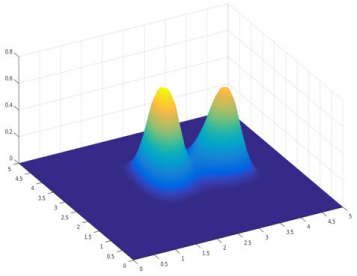

surface plot of ν for $p = 2$

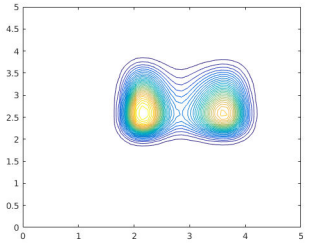

support of ν for $p = 2$

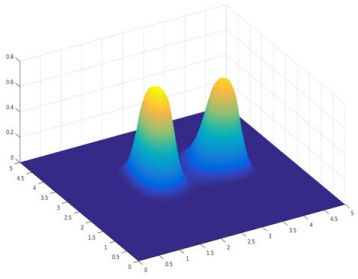

surface plot of ν for $p = 4$

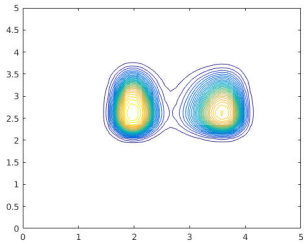

support of ν for $p = 4$

Figure 5.6: *The initial distribution μ, a sum of two translated gaussian, and the solution ν for different values of p.*

$X_1 = \{x_i^1\}_{i\in I_1}$ and $X_2 = \{x_i^2\}_{i\in I_2}$, a common strategy space $Y = \{y_j\}_{j\in J}$, given distributions of the players types $\mu^1 \in \Sigma_{I_1}$, $\mu^2 \in \Sigma_{I_2}$, two transport cost matrices $c^1 \in \mathbb{R}^{I_1\times J}$, $c^2 \in \mathbb{R}^{I_2\times J}$, and consider the minimization problem:

$$\inf_{(\nu^1,\nu^2)\in\Sigma_J\times\Sigma_J} \Big\{\mathcal{MK}^1_{\varepsilon_1}(\nu^1)+\mathcal{MK}^2_{\varepsilon_2}(\nu^2)+E_1(\nu^1)+E_2(\nu^2)+F(\nu^1+\nu^2)\Big\} \quad (5.20)$$

where for $l = 1, 2$, $\varepsilon_l > 0$ is a regularization (or noise) parameter, $\mathcal{MK}^l_{\varepsilon_l}(\nu^l)$ represents the regularized transport cost:

$$\mathcal{MK}^l_{\varepsilon_l}(\nu^l) := \inf_{\gamma\in\Pi(\mu^l,\nu^l)} \Big\{ \sum_{i,j\in I_l\times J} c^l_{ij}\gamma_{ij} + \varepsilon_l \sum_{i,j\in I_l\times J} \gamma_{ij}(\ln(\gamma_{ij}) - 1)\Big\},$$

$E_l(\nu^l)$ represents an individual cost for population k, for instance, an interaction cost:

$$E_l(\nu^l) := \sum_{j,k\in J\times J} \varphi^l_{kj}\nu^l_j\nu^l_k$$

and F is a total congestion cost

$$F(\nu^1 + \nu^2) := \sum_{j\in J} F_j(\nu^1_j + \nu^2_j)$$

where F_j is convex.

Remark 5.6.1. The proximal step related to F can be computed as in (5.15) by taking $\nu_j = \nu^1_j + \nu^2_j$.

Numerical Results

For the two populations case, we take the following energies E_l

$$E_l(\nu^l) = \sum_{j\in J}(\nu^l_j)^8 + \sum_{k,j\in J\times J} \varphi^l_{kj}\nu^l_j\nu^l_k + \sum_{j\in J} |y_j - 10|^4,$$

where $\varphi^l_{kj} = 10^{-4}|y_k - y_j|^2$ and the total congestion F_j is given by

$$F_j(\nu^1_j + \nu^2_j) = (\nu^1_j + \nu^2_j)^4.$$

As usual, we consider cost functions of the form $c_{ij} = |x_i - y_j|^p$ and we want to analyze the support of ν^l as p varies. For the simulations in Figure 5.7 we have used $N = 500$ grid points discretization of $[0, 16]$ and treated the interaction term with a semi-implicit approach. As we can notice in Figure 5.7 there is a *competition* between the confinement potential and the total congestion: the two populations tend to concentrated near $y = 10$ by the potential, but the effect of the congestion term makes it costly. This becomes clear if we compare (for instance, the case with $p = 2$) ν^1 with the optimal one in Figure 5.3; even if the energies are the same, the effect of congestion makes the support of the optimal solutions quite different.

Thus, let us now consider the following case: let E_l be as above and $p = 2$, then we take the total congestion given by

$$F_j(\nu^1_j + \nu^2_j) = (\nu^1_j + \nu^2_j)^r$$

and we compute the optimal ν^l for different values of r. In Figure 5.8 we can see that the congestion term becomes more dominant as r increases so that the two populations try to be as far as possible, despite the effect of the confinement potential which is minimal at $y = 10$.

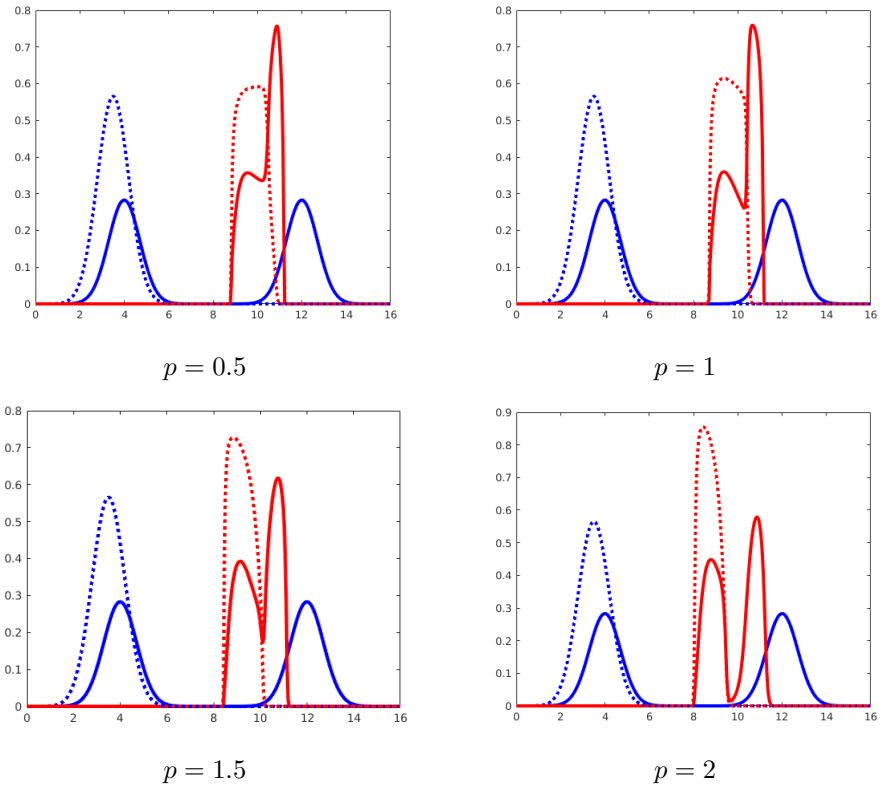

Figure 5.7: *The initial distributions μ^1 and μ^2 (blue solid line and blue dotted line) and the solutions ν^1 and ν^2 (red solid line and red dotted line) for different values of p.*

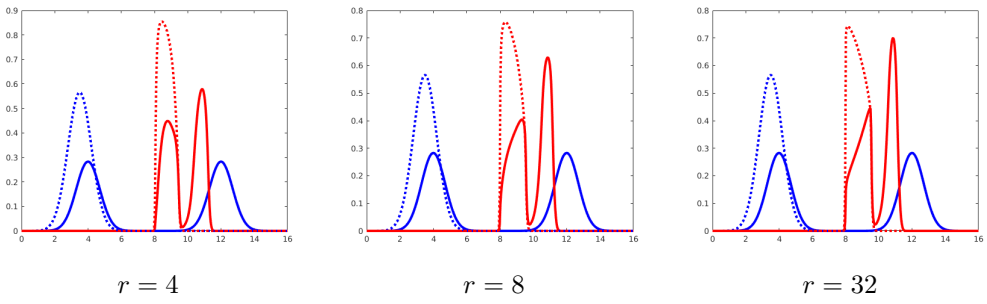

Figure 5.8: *The initial distributions μ^1 and μ^2 (blue solid line and blue dotted line) and the solutions ν^1 and ν^2 (red solid line and red dotted line) for different values of r.*

Part II

Multi-Marginal Optimal Transportation

Résumé

Dans cette Partie nous présentons le problème du transport optimal multi-marges (TOMM) et sa version régularisée. On montre que le problème (TOMM) apparaît d'une façon assez naturelle dans le cadre des solutions généralisées, au sens de Brenier, des équations d'Euler pour les fluides incompressibles. D'ailleurs, nous montrons que, en se basant sur le principe variationnel de Brenier, on retrouve un problème de transport multi-marges. Ensuite nous présentons le problème (TOMM) avec le coût quadratique, qui a été introduit par Gangbo et Swiech dans leur article fondateur [66]. De plus, d'autres types de problèmes comme le barycentre dans l'espace de Wasserstein et le matching for teams peuvent être reformulés dans la cadre du (TOMM). Nous étendons la méthode numérique présentée dans la partie I afin de les traiter numériquement. Enfin nous exposons une classe particulière de problèmes du transport optimal multi-marges, connue sous le nom de transport optimal répulsif. Cette partie est basée sur des travaux en commun avec Jean-David Benamou, Marco Cuturi, Guillaume Carlier, Simone Di Marino, Augusto Gerolin et Gabriel Peyré: [BCC$^+$15], [BCN15], [DMGN15] and [BCN16a].

Abstract

In this Part we introduce the multi-marginal optimal transportation (MMOT) and its entropic counterpart. We show that a (MMOT) problem naturally arises in the framework of generalized solutions of incompressible Euler equations. Indeed, we will show that starting from the Brenier's variational principle, we retrieve a multi-marginal optimal transport problem. Then we present the quadratic MMOT, firstly introduced by Gangbo and Swiech in their seminal work [66]. Moreover, some problems such as the Wasserstein Barycenter or the Matching for teams can be easily re-cast in multi-marginal transportation term. We provide an extension of the numerical method described in Part I. Finally, we introduce a particular class of (MMOT) problems, known as repulsive optimal transport problems. This part is based on joint works with Jean-David Benamou, Marco Cuturi, Guillaume Carlier, Simone Di Marino, Augusto Gerolin et Gabriel Peyré: [BCC$^+$15], [BCN15], [DMGN15] and [BCN16a].

Chapter 6

From Euler equations to Multi-Marginal optimal transport

In this Chapter, we wish to introduce the incompressible Euler equations and Brenier's variational principle. Indeed we will show that the principle introduced by Brenier in several works [20, 19, 22, 23] can be considered as the forerunner of the so-called Multi-Marginal optimal transport. We will also point out that as we add the relative entropy to the Brenier's problem in order to regularize it and derive a suitable numerical method , as we have explained in Chapter 2 and 3, we recover a new interesting problem which can be seen as a variational principle for a stochastic Navier-Stokes system (see [4, 5]).
Sections 6.1 and 6.2 present the variational models introduced by Arnold [6] and Brenier [20]; this brief review follows very closely the survey of Daneri and Figalli [47].

6.1 Incompressible Euler Equations and Arnold's Principle

In 1755 Euler (we refer the interested reader to Euler's seminal work [52]) introduced a set of equations governing the motion of incompressible fluids inside a bounded Lipschitz domain $\mathcal{D} \subseteq \mathbb{R}^d$ without the action of external forces. Let $u : [0,T] \times \mathcal{D} \to \mathbb{R}^d$ denote the velocity field and $p : [0,T] \times \mathcal{D} \to \mathbb{R}$ the pressure field, then the Incompressible Euler Equations read as

$$\begin{cases} \partial_t u + (u \cdot \nabla)u + \nabla p = 0 & \text{in } [0,T] \times \mathcal{D} \\ \operatorname{div}(u) = 0 & \text{in } [0,T] \times \mathcal{D} \\ u \cdot n = 0 & \text{on } [0,T] \times \partial\mathcal{D}, \end{cases} \tag{6.1}$$

where n is the unit external normal to $\partial\mathcal{D}$. The motion of an incompressible fluid inside $\mathcal{D}$ can be described also by a Lagrangian point of view: one can look at the motion of the particles of the fluid with respect to their initial position. Thus, let us assume that the velocity field u is a smooth solution of the system

(6.1) and let $g : [0,T] \times \mathcal{D} \to \mathbb{R}^d$ denote the flow map solution of

$$\begin{cases} \partial_t g(t,x) = u(t, g(t,x)) & (t,x) \in [0,T] \times \mathcal{D} \\ g(0,x) = x & x \in \mathcal{D}. \end{cases} \tag{6.2}$$

One can notice that due to the boundary condition in (6.1) we have that $g(t,\mathcal{D}) = \mathcal{D}\ \forall t \in [0,T]$. By differentiating (6.2) and using the identity

$$\frac{d}{d\lambda} \det(A + \lambda BA)|_{\lambda=0} = \mathrm{Tr}(B) \det(A)$$

we obtain

$$\partial_t(\det(\nabla g(t,x))) = \mathrm{div}(u(t,x)) \det(\nabla g(t,x)), \tag{6.3}$$

where we have used the fact that $\mathrm{Tr}(\nabla u(t,x)) = \mathrm{div}(u(t,x))$. Then, (6.3) and the incompressibility constraint in (6.1) imply

$$\det(\nabla g(t,x)) = 1, \tag{6.4}$$

which means that the map $g(t) := g(t,\cdot)$ belongs to the space $\mathbb{S}\mathrm{Diff}(\mathcal{D})$ of orientations and measure-preserving diffeomorphisms of $\mathcal{D}$. Let us now differentiate (6.2) with respect to t and use the equations (6.1), then we obtain that the map $t \mapsto g(t)$ satisfies the following ODE

$$\partial_{tt} g(t,x) = -\nabla p(t, g(t,x)) \quad \text{in } [0,T] \times \mathcal{D} \tag{6.5}$$

under the constraint

$$g(t) \in \mathbb{S}\mathrm{Diff}(\mathcal{D}) \quad \forall t \in [0,T].$$

Thus one can show that the following is true: in the smooth case, $u : [0,T] \times \mathcal{D} \to \mathbb{R}^d$ solves (6.1) with the initial condition $u(0,x) = u_0(x)$ if and only if its flow map g satisfies (6.5) with the initial conditions $\partial_t g(0,x) = u_0(x)$ and $g(0) = \mathrm{Id}_{\mathcal{D}}$, where $\mathrm{Id}_{\mathcal{D}} : \mathcal{D} \to \mathcal{D}$ denotes as usual the identity map.
In [6], Arnold interprets the ODE (6.5) as the geodesic equation on $\mathbb{S}\mathrm{Diff}(\mathcal{D})$, seen formally as an infinite-dimensional submanifold of $\mathrm{L}^2(\mathcal{D};\mathbb{R}^d)$ with respect to the induced metric. Thus, in analogy with the finite dimensional Riemannian setting one has the following problem

Problem 6.1.1. *Given $g_\star, g^\star \in \mathbb{S}\mathrm{Diff}(\mathcal{D})$, then solve*

$$(\mathcal{A}) \quad \inf\left\{\mathcal{A}(g) \mid t \mapsto g(t) \in \mathscr{S}(g_\star, g^\star)\right\}, \tag{6.6}$$

where $\mathcal{A}(g) = T\int_0^T \frac{1}{2}\|\partial_t g(t,x)\|^2_{\mathrm{L}^2(\mathcal{D};\mathbb{R}^d)} dt$ and

$$\mathscr{S}(g_\star, g^\star) := \{t \mapsto g(t) \in \mathbb{S}\mathrm{Diff}(\mathcal{D}) \mid g(0) = g_\star,\ g(T) = g^\star\}.$$

Observe that the functional $\mathcal{A}(g)$ is invariant with respect to the right composition on $\mathbb{S}\mathrm{Diff}(\mathcal{D})$, which means that by composing any curve connecting $g_\star$ to $g^\star$ with the map $g_\star^{-1}$, the problem (6.6) is equivalent to connect the identity map $\mathrm{Id}_{\mathcal{D}}$ to $g^\star$. Hence, without loss of generality we will always take $g_\star = \mathrm{Id}_{\mathcal{D}}$. Moreover, up to rescaling time we can also assume that $T = 1$.

Remark 6.1.2. Let us notice that the functional in (6.6) does not penalize the spatial derivatives of g which actually appear in the unit Jacobian constraint defining $\mathbb{S}\mathrm{Diff}(\mathcal{D})$. Thus, one can try to relax (6.6) by replacing $\mathbb{S}\mathrm{Diff}$ with $\mathbb{S} \subset \mathrm{L}^2(\mathcal{D};\mathbb{R}^d)$ where $\mathbb{S}$ stands for the space of maps preserving the Lebesgue measure on $\mathcal{D}$

$$\mathbb{S} := \{f : \mathcal{D} \to \mathcal{D} \mid f_\sharp \mathcal{L}_\mathcal{D} = \mathcal{L}_\sharp \mathcal{D}\}.$$

Notice that in the case in which $d \geqslant 3$ $\mathbb{S}$ is the L^2-closure of $\mathbb{S}\mathrm{Diff}$. Despite this, problem 6.6 may not have minimizers as we will see below. In some way we can highlight an *analogy* between the problem introduced by Arnold and the Monge problem. Both of them are difficult to treat due to the high non linearity of the constraint and a solution does not necessarily exist, as we will see below.

The first result about the existence of solutions for problem (6.6) has been established by Ebin and Marsden in [51].

Theorem 6.1.3 (Theorem 3.1, [51])**.** *If $\mathcal{D}$ is a smooth compact manifold with no boundary and $\|g^\star - \mathrm{Id}_\mathcal{D}\|_{\mathrm{H}^s(\mathcal{D};\mathbb{R}^d)} \ll 1$ for some $s > [\frac{d}{2}]+1$, then there exists a unique minimizer for (6.6).*

Notice that the main hypothesis of theorem 6.1.3 concerns the fact that the initial and final data must be *very close* in a strong topology, indeed there is no general existence result for arbitrary data.
The existence of connecting curves of finite energy on the $d-$dimensional unit cube $\mathcal{D} = [0,1]^d$ with $d \geqslant 3$ was proved by Shnirelman in [112].

Theorem 6.1.4 ([112])**.** *If $\mathcal{D} = [0,1]^d$ and $d \geqslant 3$, then for all $g^\star \in \mathbb{S}\mathrm{Diff}(\mathcal{D})$ there exists a curve $t \mapsto g(t) \in \mathbb{S}\mathrm{Diff}(\mathcal{D})$, with $\mathcal{A}(g) < \infty$, connecting $\mathrm{Id}_\mathcal{D}$ to $g^\star$.*

Unfortunately, Shnirelman also found two counterexamples to the existence of minimizers (for more details see [112, 111]).

Theorem 6.1.5 (Theorem 1.1, [112])**.** *If $\mathcal{D} = [0,1]^d$ and $d \geqslant 3$, there exists $g^\star \in \mathbb{S}\mathrm{Diff}(\mathcal{D})$ for which the infimum in (6.6) is not achieved.*

Theorem 6.1.6 (Corollary in Section 2.3, [111])**.** *If $\mathcal{D} = [0,1]^2$, there exists $g^\star \in \mathbb{S}\mathrm{Diff}(\mathcal{D})$ for which there is no curve $t \mapsto g(t) \in \mathbb{S}\mathrm{Diff}(\mathcal{D})$ satisfying $g(0) = \mathrm{Id}_\mathcal{D}$, $g(T) = g^\star$ and $\mathcal{A}(g) < \infty$.*

Here we report a simplified and pedagogical proof of theorem 6.1.5 given by Brenier in [22].

proof of theorem 6.1.5. Consider the following velocity field

$$u(t,x) = (u_1(t,x_1,x_2), u_2(t,x_1,x_2), 0)$$

and the induced path $g_u(t,x)$. It is clear that $h(x_1,x_2,x_3) = g_u(T,x_1,x_2,x_3)$ must have the form $h(x_1,x_2,x_3) = (H(x_1,x_2),x_3)$, so we can introduce the subset $\mathscr{S}_2$ of $\mathbb{S}\mathrm{Diff}([0,1]^3)$ defined as following

$$\mathscr{S}_2 := \{h \in \mathbb{S}\mathrm{Diff}([0,1]^3) \mid h(x_1,x_2,x_3) = (H(x_1,x_2),x_3) \text{ with } H \in \mathbb{S}\mathrm{Diff}([0,1]^2)\}.$$

Then, define

$$I_2(h) := \inf\{\mathcal{A}(g) \mid g(t) \in \mathscr{S}_2,\ g(0) = \mathrm{Id}_\mathcal{D},\ g(T) = h\},$$
$$I_3(h) := \inf\{\mathcal{A}(g) \mid g(t) \in \mathbb{S}\mathrm{Diff}([0,1]^3),\ g(0) = \mathrm{Id}_\mathcal{D},\ g(T) = h\}.$$

It follows that $I_2 \geqslant I_3$. By theorems 6.1.4 and 6.1.6, we can choose $\tilde{h} \in \mathscr{S}_2$ such that $I_2(\tilde{h}) > I_3(\tilde{h})$ (for instance, $\tilde{h}(x_1, x_2, x_3) = (H(x_1, x_2), x_3)$ with H as in theorem 6.1.6). Take now a map $t \mapsto g(t) \in \mathbb{S}\mathrm{Diff}([0,1]^3)$ such that $\mathcal{A}(g) < I_2(\tilde{h})$, then if we look at the associated velocity field $u = \partial_t g \circ g^{-1}$, we have that the third component of $u = (u_1(t,x), u_2(t,x), u_3(t,x))$ cannot be identically equal to 0, otherwise $\partial_t g_3(t) = 0$ and $g(t)$ would belong to $\mathscr{S}_2$. This would mean that $\mathcal{A}(g) \geqslant I_2(\tilde{h})$. We can rescale u by setting $\eta(x_3) = a(x_3 \mod 1)$, where $a \in \mathbb{N}$ and obtain $\tilde{u} = (\tilde{u}_1, \tilde{u}_2, \tilde{u}_3)$ defined as follows

$$\begin{aligned}
\tilde{u}_1(t, x_1, x_2, x_3) &= u_1(t, x_1, x_2, \eta(x_3)),\\
\tilde{u}_2(t, x_1, x_2, x_3) &= u_2(t, x_1, x_2, \eta(x_3)),\\
\tilde{u}_3(t, x_1, x_2, x_3) &= \frac{1}{a} u_3(t, x_1, x_2, \eta(x_3)).
\end{aligned}$$

$\tilde{u}$ induces a path $\tilde{g}$ which still belongs to $\mathbb{S}\mathrm{Diff}([0,1]^3)$ and such that it connects $\mathrm{Id}_{\mathcal{D}}$ to $\tilde{h}$, but the energy $\mathcal{A}(\tilde{g})$ is strictly smaller than $\mathcal{A}(g)$. Indeed one has

$$\mathcal{A}(\tilde{g}) = T \int_{\mathcal{D}} \int_0^1 \left(\partial_t g_1^2 + \partial_t g_2^2 + \frac{1}{a^2} \partial_t g_3^2 \right) dt dx.$$

Thus, if g is assumed to be minimal, this lead to a contradiction. □

In remark 6.1.2 we have pointed out that the problem posed by Arnold is actually difficult to treat by the direct method of calculus of variations. These considerations led Brenier [20] to introduce a relaxed formulation of problem (6.6), and the concept of generalized solution, as we will see in the next section.

6.2 Brenier's Principle and Generalized Solutions

6.2.1 Generalized incompressible flows

Let us consider $T = 1$ and $\Omega(\mathcal{D})$ the space of continuous paths

$$\Omega(\mathcal{D}) := C([0,1]; \mathcal{D}),$$

whose elements are denoted by $\omega(t) : [0,1] \to \mathcal{D}$ and denote by $\mathcal{P}(\Omega(\mathcal{D}))$ the space of probability measures on $\Omega(\mathcal{D})$. $\Omega(\mathcal{D})$ is a separable Banach space with respect to the supremum norm. We refer to an element γ of $\mathcal{P}(\Omega(\mathcal{D}))$ as a *generalized flow*. Define for a finite subset of times $\{t_1, \cdots, t_k\} \subset [0,1]$, the evaluation map

$$\{e_{t_i}\}_{i=1}^K : \mathcal{D}^{[0,1]} \to \mathcal{D}^K, \ \{e_{t_i}\}_{i=1}^K(\omega) := \{\omega(t_i)\}_{i=1}^k,$$

where $\mathcal{D}^{[0,1]} = \otimes_{t \in [0,1]} \mathcal{D}$ (note that $\mathcal{D}^{[0,1]}$ is the space of all paths $t \in [0,1] \mapsto \omega(t) \in \mathcal{D}$) and $\mathcal{D}^k = \otimes_{i=1}^k \mathcal{D}$, then the marginal of $\gamma \in \mathcal{P}(\Omega(\mathcal{D}))$ at times $\{t_1, \cdots, t_k\}$ is

$$\gamma_{t_1, \cdots, t_k} := (\{e_{t_i}\}_{i=1}^k)_\sharp \gamma.$$

Then every smooth family of diffeomorphisms $g(t)$ induces a generalized flow γ_g setting

$$\gamma_g := \Phi_{g,\sharp} \mathcal{L}_{\mathcal{D}}, \ \ \Phi_g(x) := g(\cdot, x) : \mathcal{D} \to \Omega(\mathcal{D}), \tag{6.7}$$

where $\mathcal{L}_{\mathcal{D}}$ denotes the (renormalized) Lebesgue measure on $\mathcal{D}$. If $g(0) = \mathrm{Id}_{\mathcal{D}}$, one can reconstruct g from γ_g via the disintegration formula

$$(e_0, e_t)_\sharp \gamma_g = (\mathrm{Id}_{\mathcal{D}}, g(t,\cdot))_\sharp \mathcal{L}_{\mathcal{D}}. \tag{6.8}$$

Given two diffeomorphisms $g_0, g_1 : \mathcal{D} \to \mathcal{D}$, such that $g_0 \in \mathbb{S}\mathrm{Diff}(\mathcal{D})$, then we say that g *connects* g_0 to g_1 if

$$\gamma_{0,1} := (e_0, e_1)_\sharp \gamma = (g_0, g_1)_\sharp \mathcal{L}_{\mathcal{D}} = (\mathrm{Id}_{\mathcal{D}}, g_1 \circ g_0^{-1})_\sharp \mathcal{L}_{\mathcal{D}}.$$

Remark 6.2.1. We say that a curve of plans $\gamma_{0,t}$ is *deterministic* if $\forall t \in [0,1]$ the plan $\gamma_{0,t}$ is concentrated on the graph of a function, namely $\gamma_{0,t} = (h_0, h_t)_\sharp \mathcal{L}_{\mathcal{D}}$ with $h_0, h_t : \mathcal{D} \to \mathcal{D}$. Notice that if $\gamma_{0,1}$ is deterministic, the curve $\gamma_{0,t}$ may not be deterministic in between.

Definition 6.2.2 (Incompressible generalized flow)**.** *A generalized flow $\gamma \in \mathcal{P}(\Omega(\mathcal{D}))$ is incompressible if*

$$(e_t)_\sharp \gamma = \gamma_t = \mathcal{L}_{\mathcal{D}}, \quad \forall t \in [0,1], \tag{6.9}$$

Remark 6.2.3. Notice that constraint 6.9 can be phrased in term of test functions:

$$\int_\Omega \varphi(\omega(t)) d\gamma(\omega) = \int_{\mathcal{D}} \varphi(x) dx, \quad \forall \varphi \in \mathcal{C}(\Omega).$$

Remark 6.2.4. The flow γ_g defined in (6.7) is incompressible if and only if $(e_t)_\sharp \gamma_g = (g(t))_\sharp \mathcal{L}_{\mathcal{D}} = \mathcal{L}_{\mathcal{D}}$ $\forall t \in [0,1]$, that is, if and only if $g(t)$ is a measure preserving map (we remind that a function $f : \mathcal{D} \to \mathcal{D}$ is a measure preserving map if and only if $f_\sharp \mathcal{L}_{\mathcal{D}} = \mathcal{L}_D$).

Remark 6.2.5. We remark that if γ is incompressible then the curve $\gamma_{0,t}$ is a curve of measure preserving plans

$$t \mapsto \gamma_{0,t} \in \Gamma(\mathcal{D}) \text{ for } t \in [0,1],$$

where $\Gamma(\mathcal{D}) := \{\gamma \in \mathcal{P}(\mathcal{D} \times \mathcal{D}) \mid \pi_1(\gamma) = \mathcal{L}_{\mathcal{D}},\ \pi_2(\gamma) = \mathcal{L}_{\mathcal{D}},\}$ and $\pi_1, \pi_2 : \mathcal{D} \times \mathcal{D} \to \mathcal{D}$ are the canonical projections. We refer also to $\Gamma(\mathcal{D})$ as the set of *doubly stochastic measures*. Moreover, if $\gamma_{0,t}$ is deterministic, i.e. $\gamma_{0,t} = (\mathrm{Id}_{\mathcal{D}}, h_t)_\sharp \mathcal{L}_{\mathcal{D}}$ for a function $h_t : \mathcal{D} \to \mathcal{D}$, then h_t is a measure preserving map.

We are now ready to introduce the Brenier's variational principle

Problem 6.2.6. *Given an initial and a final configuration $g_\star, g^\star \in \mathbb{S}\mathrm{Diff}(\mathcal{D})$, solve*

$$(\mathcal{B}) \quad \inf \left\{ \mathcal{E}(\gamma) \mid \gamma \in \Pi^\Omega(\Omega; \tilde{\gamma}, \mathcal{L}_{\mathcal{D}}) \right\}, \tag{6.10}$$

where

$$\mathcal{E}(\gamma) := \int_{\Omega(\mathcal{D})} \int_0^1 \frac{1}{2} |\dot{\omega}(t)|^2 dt d\gamma(\omega)$$

and $\Pi^\Omega(\Omega; \tilde{\gamma}, \mathcal{L}_{\mathcal{D}})$ is defined as

$$\Pi^\Omega(\Omega; \tilde{\gamma}, \mathcal{L}_{\mathcal{D}}) := \{\gamma \in \mathcal{P}(\Omega(\mathcal{D})) \mid (e_t)_\sharp \gamma = \mathcal{L}_{\mathcal{D}},\ \ \forall t \in [0,1] \text{ and } \gamma_{0,1} = \tilde{\gamma}\},$$

where $\tilde{\gamma} := (g_\star, g^\star)_\sharp \mathcal{L}_{\mathcal{D}}$.

Remark 6.2.7. Notice that $\tilde{\gamma}$ belongs to $\Gamma(\mathcal{D})$. Using the terminology introduced by Brenier, we refer to the elements of $\Pi^{\Omega}(\Omega; \tilde{\gamma}, \mathcal{L}_{\mathcal{D}})$ as the incompressible flows *compatibles* with $\tilde{\gamma}$.

Remark 6.2.8. If the generalized incompressible flow γ is induced by a smooth family of diffeomorphism $t \mapsto g(t)$, namely $\gamma = \gamma_g$, then $\mathcal{E}(\gamma_g) = \mathcal{A}(g)$.

Remark 6.2.9. In remark 6.1.2 we have pointed out an analogy between Arnold's problem and the Monge's one. In the same way we can state that the Brenier's model is a Monge-Kantorovich problem with an infinite number of marginals. Indeed if we look closer at (6.10), it is clear that this kind of relaxation allow the *splitting of mass*: the fluid particles are allowed to split/cross at intermediate times. Even if this might look unphysical, in [23] Brenier shows that these generalized solutions are quite conventional, in the sense that they obey a variant of the Euler equations for which the vertical acceleration is neglected, according to the *hydrostatic approximation* of Euler equations (see 6.2.2).

6.2.2 The hydrostatic approximation

In section 6.1 we have introduced the Arnold's principle and then we have given both existence and non-existence results due to Shnirelman, see theorems 6.1.4 and 6.1.5 , 6.1.6. Thus, consider the unit cube $\mathcal{D} = [0,1]^3$ and the special data $g^\star = h$ (we will refer to them as *Shnirelman's data*) which have the form

$$h(x_1, x_2, x_3) = (H(x_1, x_2), x_3),$$

where H belongs to $\mathbb{S}\mathrm{Diff}([0,1]^2)$ and x_i are the components of $x \in [0,1]^3$. In the proof of theorem 6.1.5 we have shown that due to the degeneracy of the data in the vertical coordinate, we cannot get a solution to problem (6.6). We will show that a new kind of solution can be introduced. Let us firstly consider the functional $\mathcal{A}(g)$ dropping the vertical component of the flow map g so that the minimization problem (6.6) becomes

$$(\mathcal{A}_2) \quad \min\left\{\mathcal{A}_2(g) \mid t \mapsto g(t) \in \mathscr{S}(\mathrm{Id}_{\mathcal{D}}, h)\right\}, \tag{6.11}$$

where

$$\mathcal{A}_2(g) = \int_0^1 \left(\frac{1}{2} \int_{\mathcal{D}} \partial_t g_1(t,x)^2 + \partial_t g_2(t,x)^2 dx \right) dt$$

$\mathscr{S}(\mathrm{Id}_{\mathcal{D}}, h)$ is as in (6.6) and $t \mapsto g(t)$ is still valued in $\mathbb{S}\mathrm{Diff}(\mathcal{D})$ with $\mathcal{D} = [0,1]^3$. Then the corresponding Lagrangian becomes

$$\mathcal{L}(g,p) = \int_0^1 \int_{\mathcal{D}} \left[\frac{1}{2} \left(\partial_t g_1(t,x)^2 + \partial_t g_2(t,x)^2 \right) - p(t, g(t,x)) + p(t,x) \right] dx dt,$$

where the pressure $p(t,x)$ plays the role of the Lagrangian multiplier associated to the incompressibility constraint and the optimality equations

$$\partial_{tt} g_i(t,x) + \partial_i p(t, g(t,x)) = 0, \quad i = 1,2, \tag{6.12}$$

$$\partial_3 p(t, g(t,x)) = 0, \tag{6.13}$$

$$\det(\nabla_x g(t,x)) = 1. \tag{6.14}$$

If we rewrite (6.12), (6.13) and (6.14) in Eulerian coordinates by using the velocity field $u(t,x)$ given by (6.2) we obtain

$$\partial_t u_i + (u\cdot\nabla)u_i + \partial_i p = 0, \quad i = 1,2, \tag{6.15}$$

$$\partial_3 p = 0, \tag{6.16}$$

$$\mathrm{div}(u) = 0, \tag{6.17}$$

which are the Euler equations where the vertical acceleration is neglected under the hydrostatic approximation (see that the pressure does not depend on the vertical coordinate). Even if the system of equations (6.12), (6.13) and (6.14) is fully 3 dimensional, we can ignore the component g_3 and find a set of equations still consistent for p and $\tilde{g} := (g_1, g_2)$. Consider the following initial and final condition

$$\begin{aligned} &\tilde{g}(0,x_1,x_2,x_3) = g_\star = (x_1,x_2) \quad \forall (x_1,x_2)\in[0,1]^2,\\ &\tilde{g}(1,x_1,x_2,x_3) = g^\star = H(x_1,x_2) \quad \forall (x_1,x_2)\in[0,1]^2, \end{aligned} \tag{6.18}$$

then it is clear that the component x_3 is now just an extra parameter without a geometric meaning and we can rename it as $\tilde{x}$. Thus, the horizontal component of the 3D flow obtained through the hydrostatic approximation can be seen as a 2D flow. Notice that the flow $t \mapsto \tilde{g}(t,x,\tilde{x}) \in [0,1]^2$ is not conventional at all as the fluid particle initially located at $x \in \mathcal{D}_2 := [0,1]^2$ can now split and follow different paths (allowed to cross each other) labeled by $\tilde{x}$. Indeed we can see the 2D flow $\tilde{g}$ as the horizontal projection of a conventional 3D incompressible flow: each fluid particle initially located at $\overline{x} \in \mathcal{D}$ corresponds to an entire vertical column of $3D$ fluid particles (see figure 6.1 left), which ends up at $t = 1$ as the vertical column above $H(\overline{x})$. However, at each time $0 < t < 1$, the fluid 3D particles, initially located at $\overline{x}$ do not necessarily form a vertical column, but rather a curve in $[0,1]^3$ (see 6.1 center) with horizontal projection given by $\tilde{x} \mapsto \tilde{g}(t,\overline{x},\tilde{x})$. Thus, this generalized 2D flow arises as a projection from 3 to 2 dimensions.

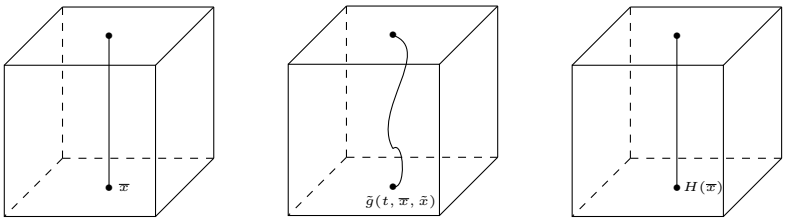

(a) *t=0* **(b)** $0 < t < 1$ **(c)** *t=1*

Figure 6.1: *Display the 3D euler flow particles in the unit cube at time* $t = 0$, $0 < t < 1$ *and* $t = 1$ *for fixed position* $\overline{x}$.

Now we have to minimize the action

$$\mathcal{A}(\tilde{g}) = \frac{1}{2}\int_0^1 dt \int_{\mathcal{D}_2\times[0,1]} |\partial_t \tilde{g}(t,x,\tilde{x})|^2 dx d\tilde{x},$$

over all the $\tilde{g}$ which satisfy the boundary conditions (6.18) and the incompressibility constraint

$$\int_{\mathcal{D}_2\times[0,1]} f(\tilde{g}(t,x,\tilde{x}))dxd\tilde{x} = \int_{\mathcal{D}_2} f(x)dx, \quad \forall f \in \mathcal{C}(\mathcal{D}_2).$$

If we define a probability measure $\gamma = \omega^{x,\tilde{x}}_{\sharp}(\mathcal{L}_{\mathcal{D}_2} \otimes \mathcal{L}_{[0,1]})$ where $\omega^{x,\tilde{x}}(t) := \tilde{g}(t, \overline{x}, \tilde{x})$, the action $\mathcal{A}(\tilde{g})$ reads as

$$\frac{1}{2}\int_0^1 dt \int_{\Omega([0,1]^3)} |\dot{\omega}(t)|^2 d\gamma,$$

and we exactly recover the functional $\mathcal{E}(\gamma)$ which appears in (6.10).

Remark 6.2.10 (An exact unique generalized solution). In [20] Brenier manages to compute an exact generalized solution for a $1-$dimensional example. Take $h(x) = 1 - x$ and $\mathcal{D} = [0, 1]$ then the map $\tilde{g}$ is given by

$$\tilde{g}(t, x, \tilde{x}) = \frac{1}{2} + (x - \frac{1}{2})\cos(\pi t) + v(x, \tilde{x})\sin(\pi t),$$

where

$$v(x, \tilde{x}) = \sqrt{\frac{x(1-x)}{2}}\cos(\pi\tilde{x}),$$

for $t, x, \tilde{x} \in [0, 1]$.

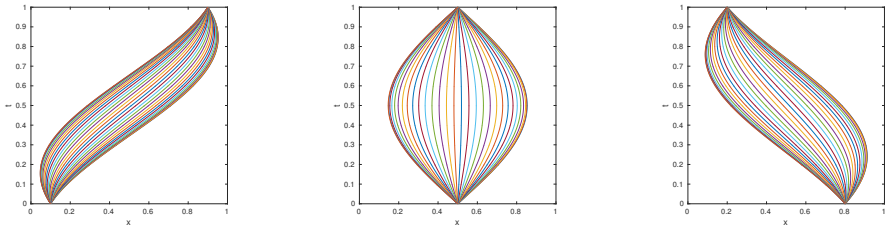

$x = 0.1$ $x = 0.5$ $x = 0.8$

Figure 6.2: *Display the $\tilde{g}(t, x, \tilde{x})$ for three particles initially located at $x = 0.1$, $x = 0.5$ and $x = 0.8$. Each path $\tilde{x}$ has a different color.*

6.2.3 Existence and Consistency with classical solutions

We discuss now the main results concerning the existence of minimizers of (6.10) and the consistency of the generalized solutions with the classical ones. If we consider a compact $\mathcal{D}$, then the existence of generalized incompressible flows in $\Pi^{\Omega}(\Omega; \tilde{\gamma}, \mathcal{L}_{\mathcal{D}})$, guarantees, by standard compactness and lower semicontinuity arguments, the existence of a minimizer. Let us consider a preliminary result given by Brenier in [19]

Proposition 6.2.11 (Proposition 8.1, [19]). *For all $R > 0$, the set*

$$\mathcal{P}_R(\Omega) := \{\gamma \in \mathcal{P}(\Omega(\mathcal{D})) \mid \mathcal{E}(\gamma) \leqslant R\}$$

is sequentially weak-compact in $\mathcal{P}(\Omega(\mathcal{D}))$.*

Then one can prove the following

Proposition 6.2.12 (Proposition 3.3, [20]). *Let $\mathcal{D} \subset \mathbb{R}^d$ be a compact set. Then, for all $\gamma \in \Pi^{\Omega}(\Omega; \tilde{\gamma}, \mathcal{L}_{\mathcal{D}})$ for which problem $\mathcal{E}(\gamma)$ is finite, problem (6.10) has a solution.*

In the case in which $\mathcal{D}$ is the $d-$dimensional torus, with, $d \geqslant 2$, the following theorem holds

Theorem 6.2.13 (Proposition 4.3, [20]). *Let $\mathcal{D} = \mathbb{T}^d$, $d \geqslant 2$. Then for any $\tilde{g} \in \Gamma(\mathcal{D})$ there exists a generalized incompressible flow $\gamma^\star \in \Pi^\Omega(\Omega; \tilde{\gamma}, \mathcal{L}_\mathcal{D})$ such that $\mathcal{E}(\gamma^\star) \leqslant 2d$.*

Remark 6.2.14. Notice that the previous theorem holds if $\mathcal{D} = \mathbb{T}^d$. Indeed, Ambrosio and Figalli managed in [2], see theorem 3.3, to extend it to any domain $\mathcal{D}$ for which there exists a Lipschitz measure preserving map Ψ from $[0,1]^d$ to $\mathcal{D}$.

A question which may naturally arise is whether the notion of generalized incompressible flow is consistent with the one of classical solution of the Cauchy problem (6.2). In [20], Brenier provides an answer which states that whenever a generalized incompressible flow is concentrated on solutions of (6.2) for a sufficiently regular pressure field p, then it is a minimizer of (6.10) for small times. This is summarized in the following theorem

Theorem 6.2.15 (Theorem 5.1, [20]). *Let $\gamma \in \Pi^\Omega(\Omega; \tilde{\gamma}, \mathcal{L}_\mathcal{D})$ be a generalized incompressible flow such that*

$$\ddot{\omega}(t) = -\nabla p(t, \omega(t)), \quad \text{for } \gamma - a.e.\ \omega \in \Omega(\mathcal{D}), \tag{6.19}$$

where $p : [0,T] \times \mathcal{D} \to \mathbb{R}$ is continuously differentiable with respect to x and satisfies

$$\sup_{(t,x)\in(0,T)\times\mathcal{D}} \nabla_x^2 p(t,x) \leqslant (\frac{\pi^2}{T^2})\,\mathrm{Id} \tag{6.20}$$

in the sense of distributions and symmetric matrices. Then γ solves problem (6.10) among all incompressible flows in $\Pi^\Omega(\Omega; \tilde{\gamma}, \mathcal{L}_\mathcal{D})$. Moreover, if the inequality (6.20) is strict, then γ is the unique minimizer and has the following deterministic property: $\gamma-$almost surely, two paths ω and ω' satisfying both $\omega(0) = \omega'(0)$ and $\omega(T) = \omega'(T)$ are equal.

Then, a direct consequence of the above theorem is the following corollary which treats the case of deterministic generalized flows induced by a map $g \in \mathbb{S}\mathrm{Diff}(\mathcal{D})$.

Corollary 6.2.16 (Corollary 1.35, [47]). *Let $t \mapsto g(t) \in \mathbb{S}\mathrm{Diff}(\mathcal{D})$ for $t \in [0,T]$ be a smooth flow whose trajectories $t \mapsto g(t,x)$ satisfy (6.5) for $\mathcal{L}_\mathcal{D}-a.e.\ x \in \mathcal{D}$, with the pressure field $p : [0,T] \times \mathcal{D} \to \mathbb{R}$ which is continuously differentiable with respect to x and satisfies (6.20). Then γ_g is a minimizer of (6.10) among all the possible generalized incompressible flows in $\Pi^\Omega(\Omega; \tilde{\gamma}, \mathcal{L}_\mathcal{D})$. Moreover, if the inequality (6.20) is strict, then γ_g is the unique minimizer.*

Remark 6.2.17. The inequality (6.20) is sharp. In 7.5.6 we will show an example (supported both by theory and numerics) on the unit disk in $\mathbb{R}^2$ such that there are several (both classical and non-deterministic) minimizers at the time T for which the equality in (6.20) holds.

6.3 Brenier's principle and Multi-Marginal Optimal Transport

We want now to show that a new kind of optimal transport problem (namely the multi-marginal optimal problem) arises when one tries to discretize in time (6.10). Notice that in [19] Brenier had already remarked that the time discretization of (6.10) yielded to a "multidimensional" Monge-Kantorovich problem, so this is the reason why we can consider the Brenier's principle a sort of forerunner of the multi-marginal transportation.

We take $\mathcal{D} = \mathbb{T}^d$, where $\mathbb{T}^d$ is the $d-$dimensional torus, $K = 2^l$ with $l > 0$, $t_i = \frac{i}{K}$ and we denote by $E_K : \Omega \to \mathbb{R}_+ \cup \{+\infty\}$ the discrete (in time) energy defined as

$$E_K(\omega) = \sum_{i=1}^{K} \frac{K}{2} |\omega(t_i) - \omega(t_{i-1})|^2,$$

and by $E : \Omega \to \mathbb{R}_+ \cup \{+\infty\}$ the continuous energy

$$E(\omega) = \begin{cases} \int_0^1 |\dot{\omega}(t)|^2 dt, & \text{if } \omega \in \mathrm{H}^1([0,1];\mathcal{D}) \\ +\infty \quad \text{otherwise.} \end{cases}$$

By using the Cauchy-Schwarz inequality and the mean value theorem one has

$$E_K(\omega) \leqslant E_{2K}(\omega) \leqslant E(\omega) \quad \forall K = 2^l,$$

and consequently

$$\mathcal{E}_K(\gamma) \leqslant \mathcal{E}_{2K}(\gamma) \leqslant \mathcal{E}(\gamma) \quad \forall \gamma \in \mathcal{P}(\Omega). \tag{6.21}$$

Moreover, if we consider paths with finite energy $E(\omega) < \infty$, namely $\omega \in \mathrm{H}^1([0,1];\mathcal{D})$, then E_K is a non-increasing bounded sequence and $E(\omega) = \sup_K E_K$. Denote by $\Pi_K^{\Omega}(\Omega; \tilde{\gamma}, \mathcal{L}_{\mathcal{D}})$ the set

$$\Pi_K^{\Omega}(\Omega; \tilde{\gamma}, \mathcal{L}_{\mathcal{D}}) := \{\gamma \in \mathcal{P}(\Omega) \mid \gamma_{0,1} = \tilde{\gamma},\ \gamma_{t_i} = \mathcal{L}_D\ i = 0, \cdots, K\}. \tag{6.22}$$

If we define the set of piecewise linear paths, for $\{t_0, \cdots, t_K\}$, $\mathcal{G} := \bigcup_{(x_0,\cdots,x_K) \in \mathcal{D}^{K+1}} \mathcal{G}_{x_0,\cdots,x_K}$, where

$$\mathcal{G}_{x_0,\cdots,x_K} := \{\omega \in \Omega \mid \omega(t_i) = x_i\ i = 0, \cdots, K,\ E(\omega) = E_K(\omega)\}.,$$

and we denote by $G : \mathcal{D}^{K+1} \to \mathcal{G}$ the map which associates a point $(x_0, \cdots, x_K) \in \mathcal{D}^{K+1}$ with a path in $\mathcal{G}$. Given a measure $\lambda \in \mathcal{P}(\mathcal{D}^{K+1})$, we can define the image measure $\gamma \in \mathcal{P}(\Omega(\mathcal{D}))$ through the map G as

$$\langle \gamma, \varphi \rangle = \int_{\mathcal{D}^{K+1}} \varphi(G(x_0, \cdots, x_K)) \lambda(x_0, \cdots, x_K) \quad \forall \varphi \in \mathcal{C}(\Omega).$$

Moreover, such a γ belongs to $\Pi_K^{\Omega}(\Omega; \tilde{\gamma}, \mathcal{L}_{\mathcal{D}})$ and satisfies

$$\mathcal{E}_K(\gamma) = \int_{\Omega} E_K(\omega) d\gamma(\omega) = \int_{\mathcal{D}^{K+1}} \sum_{i=1}^{K} \frac{K}{2} |x_i - x_{i-1}|^2 d\lambda(x_0, \cdots, x_K) =$$

$$\int_{\mathcal{D}^{K+1}} E(G(x_0, \cdots, x_K)) d\lambda(x_0, \cdots, x_K) = \mathcal{E}(\gamma).$$

By fixing the number K of marginals, we can define a discretized, in time, version of the problem (6.10) which reads as

$$(\mathcal{B}_K) \quad \inf\left\{\mathcal{E}_K(\gamma) \mid \gamma \in \Pi_K^{\Omega}(\Omega;\tilde{\gamma},\mathcal{L}_{\mathcal{D}})\right\}, \tag{6.23}$$

moreover we have

$$\begin{aligned}\inf(\mathcal{B}_K) = \inf\{ \int_{\mathcal{D}^{K+1}} \sum_{i=1}^{K} \frac{K}{2}|x_i - x_{i-1}|^2 d\lambda(x_0,\cdots,x_K) \mid \lambda \in \mathcal{P}(\mathcal{D}^{K+1}),\\ \pi_{0,1}(\lambda) = \tilde{\gamma},\ \pi_i(\lambda) = \mathcal{L}_{\mathcal{D}}\ i = 0,\cdots,K\}.\end{aligned} \tag{6.24}$$

Problem (6.23) looks like a standard optimal transport problem with $K > 2$ marginals: indeed if we look at (7.1) in section 7.1, this is exactly the same problem with an extra constraint on the initial and final position.

Remark 6.3.1. If we assume that a measure $\gamma \in \Pi^{\Omega}(\Omega;\tilde{\gamma},\mathcal{L}_{\mathcal{D}})$ has finite energy $\mathcal{E}(\gamma)$, then it follows that

$$\inf(\mathcal{B}_K) \leqslant \inf(\mathcal{B}_{2K}) \leqslant \cdots \leqslant \inf(\mathcal{B}) < +\infty,$$

since the inequality (6.21) holds and $\Pi^{\Omega}(\Omega;\tilde{\gamma},\mathcal{L}_{\mathcal{D}}) \subset \Pi_K^{\Omega}(\Omega;\tilde{\gamma},\mathcal{L}_{\mathcal{D}})$.

We end the section by summarizing in the following theorem the results of section 6 in [19].

Theorem 6.3.2 ($\Gamma-$convergence)**.** *Given the following functionals*

$$\mathcal{F}_K(\gamma) = \begin{cases} \int_{\Omega} E_K(\omega) d\gamma(\omega) & \gamma \in \Pi_K^{\Omega}(\Omega;\tilde{\gamma},\mathcal{L}_{\mathcal{D}}) \\ +\infty & \textit{otherwise,} \end{cases} \tag{6.25}$$

and

$$\mathcal{F}(\gamma) = \begin{cases} \int_{\Omega} E(\omega) d\gamma(\omega) & \gamma \in \Pi^{\Omega}(\Omega;\tilde{\gamma},\mathcal{L}_{\mathcal{D}}) \\ +\infty & \textit{otherwise,} \end{cases} \tag{6.26}$$

where $E_K(\gamma)$ and $E(\gamma)$ have been defined above. Then, $\mathcal{F}_K$ $\Gamma-$converges to $\mathcal{F}$ w.r.t. the weak topology on $\mathcal{P}(\Omega(\mathcal{D}))$.*

Before giving the proof of theorem 6.3.2, we recall the definition of $\Gamma-$convergence.

Definition 6.3.3 ($\Gamma-$convergence)**.** *Let X be a metric space and $F_k : X \to \mathbb{R} \cup \{\infty\}$ be a sequence of functionals on X. Then F_k is said to $\Gamma-$converge to the $\Gamma-$limit $F : X \to \mathbb{R} \cup \{\infty\}$ if the following conditions hold*

- *For every sequence $x_k \in X$ such that $x_k \to x$ as $k \to +\infty$,*

$$F(x) \leqslant \liminf_{k\to+\infty} F_k(x_k). \tag{6.27}$$

- *For every $x \in X$, there is a sequence x_k converging to x such that*

$$F(x) \geqslant \limsup_{k\to+\infty} F_k(x_k). \tag{6.28}$$

Proof. We can skip the case $\gamma \notin \Pi_K^{\Omega}(\Omega;\tilde{\gamma},\mathcal{L}_{\mathcal{D}})$ as the conditions (6.27) and (6.28) trivially hold. We begin by proving the lim inf inequality: for a sequence $\gamma_K \in \Pi_K^{\Omega}(\Omega;\tilde{\gamma},\mathcal{L}_{\mathcal{D}})$ such that $\gamma_K \rightharpoonup \gamma$ we have to prove

$$\mathcal{F}(\gamma) \leqslant \liminf_{K\to+\infty} \mathcal{F}_K(\gamma_K), \tag{6.29}$$

$$\gamma \in \Pi^{\Omega}(\Omega;\tilde{\gamma},\mathcal{L}_{\mathcal{D}}). \tag{6.30}$$

We denote by $I_K : \omega \mapsto \omega_K$ the map from the a.c. path to the piecewise linear path such that $\omega_K(t_i) = \omega(t_i)$ for every $i = 0,\cdots,K$. Then, it is clear that we have the equalities

$$\int_{\Omega} E_K(\omega)d\gamma(\omega) = \int_{\Omega} (E\circ I_K)(\omega)d\gamma(\omega) = \int_{\Omega} E(\omega)d\overline{\gamma}, \tag{6.31}$$

where $\overline{\gamma}_K := (I_K)_\sharp\gamma$, notice that I_K converges to the identity as $K\to\infty$. We can restrict ourselves to the paths $\omega \in \mathrm{H}^1([0,1];\mathcal{D})$ with finite energy $E(\omega) < \infty$ otherwise the inequality trivially holds. Thus, we can consider probability measures $\gamma_K \in \mathcal{P}_\alpha(\Omega(\mathcal{D}))$, where

$$\mathcal{P}_\alpha(\Omega(\mathcal{D})) := \{\eta \in \mathcal{P}(\Omega(\mathcal{D})) \mid \mathcal{E}(\eta) < \alpha,\ \alpha > 0\},$$

and since for all $\alpha > 0$ $\mathcal{P}_\alpha(\Omega(\mathcal{D}))$ is sequentially weak*-compact in $\mathcal{P}(\Omega(\mathcal{D}))$ (see proposition 6.2.11) we have that for every sequence $\gamma_K \in \mathcal{P}_\alpha(\Omega(\mathcal{D}))$ there exists a subsequence $(\gamma_k)_k$ which converges to $\gamma \in \mathcal{P}_\alpha(\Omega(\mathcal{D}))$. Take a sequence $\gamma_k \rightharpoonup \gamma$ such that $\gamma_K \in \mathcal{P}_\alpha(\Omega(\mathcal{D})) \cap \Pi_K^{\Omega}(\Omega;\tilde{\gamma},\mathcal{L}_{\mathcal{D}})$ and by compactness of $\mathcal{P}_\alpha(\Omega(\mathcal{D}))$ we have that $\gamma \in \mathcal{P}_\alpha(\Omega(\mathcal{D}))$. Then, by (6.31), take the image measure $\tilde{\gamma}_K = (I_K)_\sharp\gamma_K)$, and the l.s.c. of $\mathcal{E}(\gamma)$ we have that (6.29) holds. In order to prove (6.30) we have to verify that

(i) $\int_\Omega \varphi(\omega(0),\omega(1))d\gamma(\omega) = \int_{\mathcal{D}^2} \varphi(x,y)d\tilde{\gamma}(x,y)\ \forall\varphi \in \mathcal{C}(\mathcal{D}^2)$,

(ii) $\int_\Omega \varphi(\omega(t))d\gamma(\omega) = \int_{\mathcal{D}} \varphi(x)dx\ \forall t \in [0,1]$ and $\forall\varphi \in \mathcal{C}(\mathcal{D})$.

(i) trivially holds so we have only to verify (ii). Notice that if t is dyadic then the property (ii) is true since K is of the form 2^l. It is enough if we check (ii) when φ is Lipschitz continuous (denote by M_φ the Lipschitz constant), so for every t_i with $i = 0,\cdots,K$ we have:

$$\begin{aligned}
&\left|\int_{\mathcal{D}} \varphi(\omega(t))d\gamma_K(\omega) - \int_{\mathcal{D}} \varphi(x)dx\right| \\
&= \left|\int_{\mathcal{D}} \left(\varphi(\omega(t)) - \varphi(\omega(t_i))\right) d\gamma_K(\omega)\right| \\
&\leqslant \int_{\mathcal{D}} \left|\varphi(\omega(t)) - \varphi(\omega(t_i))\right| d\gamma_K(\omega) \\
&\leqslant M_\varphi \int_{\mathcal{D}} \left|\omega(t) - \omega(t_i)\right| d\gamma_K(\omega) \\
&\leqslant M|t-t_i|^{1/2},
\end{aligned} \tag{6.32}$$

where $M = 2M_\varphi\sqrt{\mathcal{E}(\gamma_K)} < \infty$ as $\gamma_K \in \mathcal{P}_\alpha(\Omega(\mathcal{D}))$, then (ii) follows.
We now prove the lim sup inequality. Again we can restrict ourselves to probability measures in $\mathcal{P}_\alpha(\Omega(\mathcal{D}))$. Choose $\gamma \in \mathcal{P}_\alpha(\Omega(\mathcal{D}))\cap\Pi^{\Omega}(\Omega;\tilde{\gamma},\mathcal{L}_{\mathcal{D}})$, then it is clear

that γ belongs to $\Pi_K^\Omega(\Omega;\tilde{\gamma},\mathcal{L}_\mathcal{D})$ for every K. Moreover, as $E(\omega)=\sup_K E_K(\omega)$ then by monotone convergence we have $\mathcal{F}_K(\gamma)\to\mathcal{F}(\gamma)$ and the lim sup inequality holds.

□

Remark 6.3.4 (Convergence of the minimizers). As a consequence of the $\Gamma-$convergence of $\mathcal{F}_K$ to $\mathcal{F}$ and proposition 6.2.11, we have that the minimizers of $\inf(\mathcal{B}_K)$ converge to the minimizers of $\inf(\mathcal{B})$.

6.4 A Brenier's principle with viscosity

In section 2.1 we have proposed a regularization of the standard optimal transport by adding an entropy term. Moreover, we have showed that in the case in which the cost function is the square distance, then the regularized optimal transport problem coincides with the Schrödinger problem which can be seen as a viscous version of Monge-Kantorovich. Thus, following section 2.1 we present a Schrödinger problem, with an infinite number of marginals and prescribed initial and final configuration, which can be seen as a Brenier's principle for viscid fluids (see [4, 5]). Let us consider the following extension of the dynamic Schrödinger problem (2.7)

$$(\mathscr{S}_\infty)\quad \inf\left\{\mathrm{H}(P|R)\mid P\in\mathcal{P}(\Omega),\ (e_t)_\sharp P=\mathcal{L}_\mathcal{D},\ (e_0,e_1)_\sharp P=\tilde{P}\right\},\qquad(6.33)$$

where $\tilde{P}\in\Gamma(\mathcal{D})$ links the initial and the final configuration, for instance one can take $\tilde{P}=(\mathrm{Id}_\mathcal{D},g^\star)_\sharp\mathcal{L}_\mathcal{D}$ as for the Brenier's principle, and $R(\cdot)=\int_\mathcal{D}\mathcal{W}_x(\cdot)dx$ is a reference measure with $\mathcal{W}_x$ which is the Wiener measure induced by a Brownian motion B_t^x which starts at x. Notice that one usually considers a standard Brownian motion B_t starting at 0 and, since B_t is invariant by translation , the Brownian motion starting at x is given by $B_t^x=B_t+x$. Let us now give the following definition of the Wiener measure.

Definition 6.4.1. *Consider the space Ω and the Brownian motion B_t starting at 0. Then, B_t induces a distribution measure $\mathcal{W}_0$ on Ω called the Wiener measure. That is, $\mathcal{W}_0$ is the unique probability measure on Ω such that for any finite sequence of times $0<t_1<\cdots<t_K$ and Borel sets $A_1,\cdots,A_K$*

$$\mathcal{W}_0(\{\omega\mid\omega(t_1)\in A_1,\cdots,\omega(t_K)\in A_K\})=$$
$$\int_{A_1}\cdots\int_{A_K}p(t_1,0,x_1)p(t_2-t_1,x_1,x_2)\cdots p(t_K-t_{K-1},x_{K-1},x_K)dx_1,\cdots dx_K,\qquad(6.34)$$

where

$$p(t,x,y)=\frac{1}{(2\pi t)^{d/2}}\exp\left(-\frac{|x-y|^2}{2t}\right),$$

defined for any $x,y\in\mathcal{D}$ and $t\in[0,1]$.

Let us now fix the number $K=2^l$ $l>0$ of marginals, as we have done in section 6.3, such that $t_i=i/K$ for $i=0,\cdots,K$, then the discretization in time of problem (6.33) can be written as follows

$$(\mathscr{S}_{dyn,K})\quad \inf\left\{\mathrm{H}(P|R)\mid P\in\Pi_K^\Omega(\Omega;\tilde{\gamma},\mathcal{L}_\mathcal{D})\right\},\qquad(6.35)$$

where $\Pi_K^{\Omega}(\Omega;\tilde{\gamma},\mathcal{L}_{\mathcal{D}})$ is defined as in (6.22). Notice that $\inf(\mathscr{S}_{dyn,K}) \leqslant \inf(\mathscr{S}_{\infty})$ as we are minimizing over a larger set. Moreover, we can now define also a static formulation of $(\mathscr{S}_{dyn,K})$ which reads as

$$(\mathscr{S}_{static,K}) \quad \inf\left\{\mathrm{H}(\gamma|\eta) \mid \gamma \in \Pi_K(\mathcal{D}^{K+1};\tilde{\gamma},\mathcal{L}_{\mathcal{D}})\right\}, \tag{6.36}$$

where

$$\Pi_K(\mathcal{D}^{K+1};\tilde{\gamma},\mathcal{L}_{\mathcal{D}}) := \{\gamma \in \mathcal{P}(\mathcal{D}^{K+1}) \mid \pi_{0,1}(\gamma) = \tilde{P},\ \pi_i(\gamma) = \mathcal{L}_D, 1 = 0,\cdots,K\}$$

and $\eta = (e_{t_0},\cdots,e_{t_K})_\sharp R$.

Notice that if $R(\cdot) = \int_{\mathcal{D}} \mathcal{W}_x(\cdot)dx$ is the Wiener probability measure with initial marginal δ_x then thanks to definition 6.4.1 one can deduce that η is absolutely continuous with respect the Lebesgue measure and its density $\tilde{\eta}$ is given by

$$\tilde{\eta} := \prod_{i=1}^{K} p(t_i - t_{i-1}, x_{i-1}, x_i), \tag{6.37}$$

where $t_i - t_{i-1} = \frac{1}{K}\ \forall i$, $x_i := \omega(t_i)$ and we have considered a Wiener measure induced by a Brownian motion which starts at x_0. Then, $\tilde{\eta}$ can be rewritten as

$$\tilde{\eta} = \frac{1}{(2\pi/K)^{dK/2}} \exp\left(-\frac{K}{2}\sum_{i=1}^{K}|x_i - x_{i-1}|^2\right). \tag{6.38}$$

Take now the relative entropy

$$\mathrm{H}(\gamma|\eta) = \int_{\mathcal{D}^{K+1}} \big(\log(\frac{d\gamma}{d\eta}) - 1\big)d\gamma + 1,$$

then thanks to the special form of η we can rewrite $\mathrm{H}(\gamma|\eta)$ as

$$\mathrm{H}(\gamma|\eta) = \int_{\mathcal{D}^{K+1}} \big(\log(\frac{\gamma}{\tilde{\eta}}) - 1\big)\gamma dx + 1,$$

where now γ denotes the density of γ (notice that γ must be absolutely continuous with respect to η) and by using the property of the logarithm one obtains

$$\begin{aligned}\mathrm{H}(\gamma|\eta) = &\mathrm{H}(\gamma|\mathcal{L}) - \int_{\mathcal{D}^{K+1}} \log(\tilde{\eta})\gamma dx = \\ &\mathrm{H}(\gamma|\mathcal{L}) + \frac{K}{2}\int_{\mathcal{D}^{K+1}}\sum_{i=1}^{K}|x_i - x_{i-1}|^2\gamma dx + \log(\frac{1}{(2\pi/K)^{dK/2}}) = \\ &\mathrm{H}(\gamma|\mathcal{L}) + \frac{1}{(2\pi/K)^{dK/2}}\mathcal{E}_K(\gamma) + C,\end{aligned} \tag{6.39}$$

which corresponds to the entropic regularization of the discrete problem (6.23). Notice that $C = \log(\frac{1}{(2\pi/K)^{dK/2}})$ is a constant and we can neglect it when we consider $\inf \mathrm{H}(\gamma|\eta)$.

Remark 6.4.2 (The regularized problem). As we have done in section 2.1.1 we can define a reference measure R^ε which depends on a parameter ε and we recover

$$\tilde{\eta}_\varepsilon = \frac{1}{(2\pi\varepsilon/K)^{dK/2}} \exp\left(-\frac{K}{2\varepsilon}\sum_{i=1}^{K}|x_i - x_{i-1}|^2\right),$$

then

$$(\mathscr{S}^{\varepsilon}_{static,K}) \quad \inf\left\{\mathrm{H}(\gamma|\eta_\varepsilon) \mid \gamma \in \Pi_K(\mathcal{D}^{K+1}; \tilde{\gamma}, \mathcal{L}_{\mathcal{D}})\right\}$$

is, indeed, the entropic regularization of

$$\inf\left\{\mathcal{E}_K(\gamma) \mid \gamma \in \Pi_K(\mathcal{D}^{K+1}; \tilde{\gamma}, \mathcal{L}_{\mathcal{D}})\right\}$$

where ε is the regularization parameter. In section 7.4 we will show an extension of the IPFP (sinkhorn) algorithm to this *multi-marginal* case which actually leads to solve the discrete, in space, version of $(\mathscr{S}^{\varepsilon}_{static,K})$.

The optimization problems $(\mathscr{S}_{dyn,K})$ and $(\mathscr{S}_{static,K})$ are strictly connected; in the two marginals case we have seen that the solution of the dynamic and the static Schrödinger problems are closely related (this is proven in [55]). In this case we want to extend the Föllmer's result to the $K-$marginals case.

Proposition 6.4.3 ([BCN16a])**.** *The problems (6.35) and (6.36) admit respectively at most one solution $P^\star \in \mathcal{P}(\Omega)$ and $\gamma^\star \in \mathcal{P}(\mathcal{D}^{K+1})$. If (6.35) admits a solution $P^\star$, then $\gamma^\star = P^\star_{0,\cdots,K} := (e_0, \cdots, e_K)_\sharp P^\star$ is the solution of (6.36). Conversely, if $\gamma^\star$ solves (6.36), then (6.35) admits the solution*

$$P^\star(\cdot) = \int_{\mathcal{D}^{K+1}} R^{x_0\cdots x_K} d\gamma^\star(x_0 \cdots x_K) \in \mathcal{P}(\Omega) \tag{6.40}$$

which means that $P^\star_{0,\cdots,K} = \gamma^\star$ and

$$P^{\star,x_0\cdots x_K} = R^{x_0\cdots x_K} \quad \forall (x_0 \cdots x_K)\ \gamma^\star - a.e.$$

Remark 6.4.4 (Disintegration formula). As we have showed in section 2.1.1, a measure $P \in \mathcal{P}(\Omega)$ disintegrates as follows

$$P(\cdot) = \int_{\mathcal{D}^{K+1}} P^{x_0\cdots x_K}(\cdot) dP_{0\cdots K}(x_0, \cdots, x_K), \tag{6.41}$$

where $P_{0\cdots K} = (e_0, \cdots, e_K)_\sharp P$, $P^{x_0\cdots x_K} \in \mathcal{P}(\Omega^{x_0\cdots x_K})$ with $(e_i)_\sharp P^{x_0\cdots x_K} = \delta_{x_i}$ for $i = 0, \cdots, K$ and

$$\Omega^{x_0\cdots x_K} := \{\omega \in \Omega \mid \omega(t_i) = x_i\}$$

is the space of continuous paths such that $\omega(t_i) = x_i$ for $i = 0, \cdots, K$.

Remark 6.4.5. Notice that $P^{\star,x_0\cdots x_K}$ is the *bridge* of $P^\star$.

Proof. Being strictly convex problems, (6.35) and (6.36) admit respectively at most one solution. Given a function $\varphi : \Omega \to \mathcal{D}^{K+1}$ such that $\varphi = (e_0, \cdots, e_K)$ then the following property formula of the entropy holds

$$\begin{aligned}\mathrm{H}(P|R) =& \mathrm{H}(\varphi_\sharp P|\varphi_\sharp R) + \int_{\mathcal{D}^{K+1}} \mathrm{H}(P^{x_0\cdots x_K}|R^{x_0\cdots x_K}) d\varphi_\sharp P(x_0 \cdots x_K) = \\ & \mathrm{H}(P_{0,\cdots,K}|R_{0,\cdots,K}) + \int_{\mathcal{D}^{K+1}} \mathrm{H}(P^{x_0\cdots x_K}|R^{x_0\cdots x_K}) dP_{0,\cdots,K}(x_0 \cdots x_K).\end{aligned} \tag{6.42}$$

Now, we can rewrite the constraint in (6.35) as follows:

$$P \in \Pi^\Omega_K(\Omega; \tilde{\gamma}, \mathcal{L}_{\mathcal{D}}) \iff P \in \{P \in \mathcal{P}(\Omega) \mid (e_0, \cdots, e_K)_\sharp P = \gamma, \text{ with } \gamma \in \Pi_K(\mathcal{D}^{K+1}; \tilde{\gamma}, \mathcal{L}_{\mathcal{D}})\}.$$

Thus, the minimization problem can be recast as

$$\begin{aligned}&\inf\left\{\mathrm{H}(P|R) \mid P \in \Pi_K^{\Omega}(\Omega;\tilde{\gamma},\mathcal{L}_{\mathcal{D}})\right\} = \\ &\inf\left\{\inf\left\{\mathrm{H}(P|R) \mid P \in \mathcal{P}(\Omega)\ P_{0,\cdots,K} = \gamma\right\} \mid \gamma \in \Pi_K(\mathcal{D}^{K+1};\tilde{\gamma},\mathcal{L}_{\mathcal{D}})\right\}.\end{aligned} \tag{6.43}$$

Considering the additive formula (6.42), the inner minimization becomes

$$\begin{aligned}&\inf\left\{\mathrm{H}(P|R) \mid P \in \mathcal{P}(\Omega)\ P_{0,\cdots,K} = \gamma\right\} = \\ &\mathrm{H}(\gamma|R_{0,\cdots,K}) + \inf\left\{\int_{\mathcal{D}^{K+1}} \mathrm{H}(P^{x_0\cdots x_K}|R^{x_0\cdots x_K})d\gamma(x_0\cdots x_K) \mid P \in \mathcal{P}(\Omega)\ P_{0,\cdots,K} = \gamma\right\} = \\ &\mathrm{H}(\gamma|\eta),\end{aligned}$$

where inf is uniquely attained when $P^{x_0\cdots x_K} = R^{x_0\cdots x_K}$ for $\gamma-$almost every $(x_0\cdots x_K) \in \mathcal{D}^{K+1}$ since $\mathrm{H}(P^{x_0\cdots x_K}|R^{x_0\cdots x_K}) = 0$ is the minimal value of the relative entropy. Moreover, for each $\gamma \in \Pi_K(\mathcal{D}^{K+1};\tilde{\gamma},\mathcal{L}_{\mathcal{D}})$ we have

$$\inf\left\{\mathrm{H}(P|R) \mid P \in \mathcal{P}(\Omega)\ P_{0,\cdots,K} = \gamma\right\} = \mathrm{H}(R^{\gamma}|R_{x_0\cdots x_K}) = \mathrm{H}(\gamma|\eta),$$

where

$$R^{\gamma}(\cdot) = \int_{\mathcal{D}^{K+1}} R^{x_0\cdots x_K}(\cdot)d\gamma(x_0\cdots x_K),$$

and the solution of (6.35) is

$$P^{\star} = R^{\gamma^{\star}}$$

where $\gamma^{\star}$ is the unique solution of (6.36). □

We end this section by listing all the models for both inviscid and viscous flows. In section 7.5.3 we propose a numerical algorithm based on the entropic regularization and we show some numerical results in $d = 1$ and $d = 2$.

Arnold's Principle

$$\inf\left\{\mathcal{A}(g) \mid t \mapsto g(t) \in \mathscr{S}(\mathrm{Id}_{\mathcal{D}}, g^\star)\right\},$$

where

$$\mathcal{A}(g) = \int_0^1 \frac{1}{2}\|\partial_t g(t,x)\|^2_{\mathrm{L}^2(\mathcal{D};\mathbb{R}^d)} dt.$$

Brenier's Principle

$$\inf\left\{\mathcal{E}(\gamma) \mid \gamma \in \Pi^{\Omega}(\Omega; \tilde{\gamma}, \mathcal{L}_{\mathcal{D}})\right\},$$

where

$$\mathcal{E}(\gamma) := \int_{\Omega(\mathcal{D})} \int_0^1 \frac{1}{2}|\dot{\omega}(t)|^2 dt d\gamma(\omega)$$

and $\tilde{\gamma} = (\mathrm{Id}, g^\star)_\sharp \mathcal{L}_{\mathcal{D}}$.

Discrete Brenier's Principle

$$\inf\left\{\mathcal{E}_K(\gamma) \mid \eta \in \Pi_K^{\Omega}(\Omega; \tilde{\gamma}, \mathcal{L}_{\mathcal{D}})\right\},$$

where $\mathcal{E}_K(\gamma) = \int_\Omega E_K(\omega) d\gamma(\omega)$ and $E_K(\omega) = \sum_{i=1}^K \frac{K}{2}|\omega(t_i) - \omega(t_{i-1})|^2$.

Viscous Brenier's Principle

$$\inf\left\{\mathrm{H}(P|R_\varepsilon) \mid P \in \mathcal{P}(\Omega),\ (e_t)_\sharp P = \mathcal{L}_{\mathcal{D}},\ (e_0, e_1)_\sharp P = \tilde{P}\right\},$$

where $\mathrm{H}(P|R_\varepsilon)$ is the relative entropy, $\tilde{P} = \tilde{\gamma}$, R_ε a Brownian motion with variance ε and ε can be interpreted as a viscosity parameter.

Discrete Viscous Brenier's Principle

$$\inf\left\{\mathrm{H}(P|R_\varepsilon) \mid P \in \Pi_K^{\Omega}(\Omega; \tilde{\gamma}, \mathcal{L}_{\mathcal{D}})\right\} = \inf\left\{\mathrm{H}(\gamma|\eta_\varepsilon) \mid \gamma \in \Pi_K(\mathcal{D}^{K+1}; \tilde{\gamma}, \mathcal{L}_{\mathcal{D}})\right\},$$

where

$$\eta_\varepsilon = \frac{1}{(2\pi\varepsilon/K)^{dK/2}} \exp\left(-\frac{K}{2\varepsilon}\sum_{i=1}^K |x_i - x_{i-1}|^2\right) dx_0 \cdots dx_K.$$

Chapter 7

A Review on Multi-Marginal Optimal Transportation

7.1 The Multi-Marginal OT problem: the continuous setting

We denote by K the number of marginals, d the dimension of the space and $\mathcal{I} = \{1, \dots, K\}$ an index set. Then the multi-marginal Monge-Kantorovich problem becomes

Problem 7.1.1. *Given K marginals $\mu_i \in \mathcal{P}(\mathbb{R}^d)$ $\forall i \in \mathcal{I}$ and $c : \mathbb{R}^{dK} \to \mathbb{R}$, a lower semi-continuous cost function $c(x_1, \cdots, x_K) : \mathbb{R}^{dK} \to \mathbb{R}^d$, solve*

$$(\mathcal{MK}_K) \quad \inf \left\{ \int_{\mathbb{R}^{dK}} c(x_1, \dots, x_K) d\gamma(x_1, \dots, x_K) \mid \gamma \in \Pi(\mathbb{R}^{dK}; \mu_1, \cdots, \mu_K) \right\}, \tag{7.1}$$

where $\Pi(\mathbb{R}^{dK}; \mu_1, \cdots, \mu_K)$ denotes the set of couplings $\gamma(x_1, \dots, x_K)$ having μ_i as marginals, for all $i \in \mathcal{I}$,

$$\Pi(\mathbb{R}^{dK}; \mu_1, \cdots, \mu_K) := \{\gamma \in \mathcal{P}(\mathbb{R}^{dK}) \mid \pi_i(\gamma) = \mu_i \ \forall i \in \mathcal{I}\},$$

where $\pi_i : \mathbb{R}^{dK} \to \mathbb{R}^d$ is the canonical projection.

Notice that the existence of a minimum for (7.1) is quite standard in Optimal Transport Theory. Indeed, $\Pi(\mathbb{R}^{dK}; \mu_1, \cdots, \mu_K)$ *is trivially non empty*, since the independent coupling $\otimes_{i \in \mathcal{I}} \mu_i$ belongs to $\Pi(\mathbb{R}^{dK}; \mu_1, \cdots, \mu_K)$; the set $\Pi(\mathbb{R}^{dK}; \mu_1, \cdots, \mu_K)$ is convex and compact for the weak*-topology thanks to the imposed marginals; and moreover the quantity to be minimized $\gamma \mapsto \int c \, d\gamma$ is linear with respect to γ. Hence, we can guarantee the existence of a minimum for (7.1) by imposing a very weak hypothesis on the cost function, such as lower-semicontinuity.

We are interested in characterizing some class of optimal transport plans or, at least, understand when that optimal coupling is *deterministic*, namely when the transport plan has the form $\gamma = (T_1, \cdots T_K)$, where $T_i : \mathbb{R}^d \to \mathbb{R}^d$ are the

transport maps and $T_1 = \mathrm{Id}$. Thus, as in the 2 marginal case one can define the multi-marginal Monge problem

Problem 7.1.2. *Given K marginals $\mu_i \in \mathcal{P}(\mathbb{R}^d)$ $\forall i \in \mathbb{I}$ and $c : \mathbb{R}^{dK} \to \mathbb{R}$, a lower semi-continuous cost function $c(x_1, \cdots, x_K) : \mathbb{R}^{dK} \to \mathbb{R}^d$, solve*

$$(\mathcal{M}_K) \quad \inf \left\{ \int_{\mathbb{R}^{dK}} c(x, T_2(x), \cdots, T_K(x)) d\mu_1(x) \mid T = \{T_i\}_{i \in \mathcal{I}} \in \mathcal{T}_K \right\}, \quad (7.2)$$

where

$$\mathcal{T}_K := \{T = \{T_i\}_{i \in \mathcal{I}} \mid T_i : \mathbb{R}^d \to \mathbb{R}^d \ (T_i)_\sharp \mu_1 = \mu_i, \forall i \in \mathcal{I} \text{ and } T_1 = \mathrm{Id}\}.$$

Remark 7.1.3. When $K = 2$ in (7.1) and (7.2), we exactly retrieve the standard Monge-Kantorovich and Monge problem, respectively.

As usual, it is easy to see that the set of *admissible plans in* (7.1) *"contains" the set of Monge transport maps in* (7.2): in fact, given a transport map $T = (\mathrm{Id}, T_2, \ldots, T_K)$, we can consider a measure γ_T on $\mathbb{R}^{dK}$ defined by $\gamma_T = (\mathrm{Id}, T_2, \cdots, T_K)_\sharp \mu_1$. Let $h : \mathbb{R}^{dK} \to \mathbb{R}$ be a γ_T-measurable function, then

$$\int_{\mathbb{R}^{dK}} h(x_1, \ldots, x_K) d\gamma_T(x_1 \ldots, x_K) = \int_{\mathbb{R}^d} h(x_1, T_2(x_1), \ldots, T_K(x_1)) d\mu_1(x_1);$$

and if we have γ_T-measurable function $f : \mathbb{R}^d \to [0, \infty]$

$$\forall i \in \mathcal{I}, \quad \int_{\mathbb{R}^{dK}} f(x_i) d\gamma_T(x_1, \ldots, x_K) = \int_{\mathbb{R}^d} f(x_i) d\mu_i(x_i),$$

and so, γ_T is a transport plan. In particular, the value of the minimization over all the feasible couplings in $\Pi(\mathbb{R}^{dK}; \mu_1, \cdots, \mu_K)$ is smaller than or equal to the value of the minimization over the deterministic couplings

$$\min(\mathcal{MK}_K) \leqslant \inf(\mathcal{M}_K).$$

Contrary to (7.1), the existence of transport maps in (7.2) is not obvious and the difficulties lie both on the "multi-marginality" of the problem (see for instance the fractal map in theorem 8.1.6 which appears in the three marginals case, but not in the 2 marginals one) and on the high non-linearity of the constraints as for the 2 marginal case. Moreover, as we will show later (see for instance chapter 8 and 9) the multi-marginal problem presents a high sensitivity to the cost function which is largely absent from two marginal problems: we will exhibit cost functions for which optimizers of (7.1) have a Monge form (namely the optimal plan γ is induced by an optimal map $T = (\mathrm{Id}, T_2, \cdots, T_K)$) and are unique, as well as some for which these properties fail.

An important disadvantage in using the relaxed approach (7.1) in the multi-marginal OT is that the set of optimal transportation plans could be very large and we could need to select some special classes of transportation plans.

In the 2-marginal setting, the two formulations (7.1) and (7.2) are proved to have the same value for general Polish Spaces, in particular we have the following result established by Pratelli in [101].

Theorem 7.1.4 (Monge equals Monge-Kantorovich in the 2-marginals case, [101])**.** *Let $(X,\mu),(Y,\nu)$ be Polish spaces, where $\mu\in\mathcal{P}(X)$ and $\nu\in\mathcal{P}(Y)$ are non-atomic probability measures. If $c: X\times Y\to\mathbb{R}\cup\{\infty\}$ is a continuous cost, then*

$$\inf\left\{\int_{X\times Y} c(x,y)d\gamma(x,y)\ :\ \gamma\in\Pi(\mathbb{R}^d;\mu,\nu)\right\}= \tag{7.3}$$

$$=\inf\left\{\int_X c(x,T(x))d\mu(x),\ :\ \begin{array}{l} T_\sharp\mu=\nu,\\ T: X\to Y \text{ Borel}\end{array}\right\} \tag{7.4}$$

where $\Pi(\mathbb{R}^d;\mu,\nu)$ denotes, as usual, the set of transport plans $\gamma\in\mathcal{P}(X\times Y)$ having μ and ν as marginals.

In the case of the multi-marginal OT problems, (7.2) and (7.1), whith K marginals to μ_i, we can apply the previous theorem (7.1.4) on the Polish spaces $X=\mathbb{R}^d, Y=(\mathbb{R}^d)^{K-1}$ with measures $\mu=\mu_1$ and $\nu=(\pi_2,\cdots,\pi_K)_\sharp\gamma$, for every $\gamma\in\Pi(\mathbb{R}^{dK};\mu_1,\cdots,\mu_K)$, and obtain the following corollary

Corollary 7.1.5. *Let $\mu_1,\cdots,\mu_K$ be probability measures on $\mathbb{R}^d$ and $c:\mathbb{R}^{dK}\to\mathbb{R}$ be a continuous cost function. Then,*

$$\min(\mathcal{MK}_K)=\inf(\mathcal{M}_K).$$

Notice that, in general, the equivalence between (7.1) and (7.2) is not an immediate consequence of the theorem 7.1.4. In particular, remark that the image measure of $Y=\mathbb{R}^{d(K-1)}$ is not prescribed, but only its marginals.

7.1.1 The Dual problem

As in the two marginal case we can derive the following dual formulation of (7.1)

Problem 7.1.6. *Given K marginals $\mu_i\in\mathcal{P}(\mathbb{R}^d)$ solve*

$$\begin{aligned}(\mathcal{K}_K)\quad \sup\Bigg\{&\int_{\mathbb{R}^d}\sum_{i\in\mathcal{I}}u_i(x_i)d\mu_i(x_i)\mid u_i\in \mathrm{L}^1(\mathbb{R}^d,\mu_i)\ \forall i\in\mathcal{I},\\ &\sum_{i\in\mathcal{I}}u_i(x_i)\leqslant c(x_1,\cdots,x_K),\ \forall(x_1,\cdots,x_K)\in\mathbb{R}^{dK}\Bigg\},\end{aligned} \tag{7.5}$$

where u_i are called Kantorovich potentials and are upper semicontinuous for all $i\in\mathcal{I}$.

Remark 7.1.7. Notice that, when all marginals are equal $\mu_i=\rho(x)\mathcal{L}^d\ \forall i\in\mathcal{I}$ and the cost is symmetric (i.e. the quadratic cost $\sum_{i\neq j}|x_i-x_j|^2$), we can assume the Kantorovich potentials $u_i(x_i)$ are all the same $u(x_i)$, and we can rewrite the constraint in (7.5) as

$$\sum_{i=1}^K u(x_i)\leqslant c(x_1,\ldots,x_K).$$

Among all Kantorovich potentials, a particular class is of special interest.

Definition 7.1.8 (c-conjugate function)**.** *Let $c : \mathbb{R}^{dK} \to \mathbb{R} \cup \{\infty\}$ a Borel function. We say that the K-tuple of functions $(u_1, \dots, u_K)$ is a c-conjugate function for c, if*

$$u_i(x_i) = \inf \left\{ c(x_1, \dots, x_K) - \sum_{j=1, j\neq i}^{K} u_j(x_j) : x_j \in X_j \ , \ j \neq i \right\}, \quad \forall i = 1, \dots, K.$$

As we will see in the next theorem 7.1.9, the optimal potentials $u_1, \dots, u_K$ in $(\mathcal{K}_K)$ are c-conjugates, and therefore semi-concave. So, they admit super-differentials $\overline{\partial} u_i(x_i)$ at each point $x_i \in \mathbb{R}^d$ and then, at least in the compact case, we can expect that for each $x_i \in \mathbb{R}^d$, there exists $\{x_j\}_{j\neq i} \in \mathbb{R}^{d(K-1)}$, such that

$$u_i(x_i) = c(x_1, \dots, x_K) - \sum_{j\neq i} u_j(x_j).$$

Moreover, if $c : \mathbb{R}^{dK} \to \mathbb{R}$ is differentiable and $|u_i(x_i)| < \infty$, for some $x_i \in \mathbb{R}^d$, u_i is locally Lipschitz. The well-known general result linking both (7.1) and (7.5) has been proven by Kellerer in 1984.

Theorem 7.1.9 (Kellerer, [76])**.** *Let $(X_1, \mu_1), \cdots, (X_K, \mu_K)$ be Polish spaces equipped with Borel probability measures $\mu_1, \dots, \mu_K$. Consider $c : X_1 \dots X_K \to \mathbb{R}$ a Borel cost function and assume that $\overline{c} = sup_X c < \infty$ and $\underline{c} = \inf_X c > -\infty$. Then,*

(i) There exists a solution γ of the Monge-Kantorovich problem (7.1) *and a c-conjugate solution $(u_1, u_2, ..., u_K)$ of the dual problem (7.5).*

(ii) "Duality holds",

$$\inf \left\{ \int_{X_1 \dots X_K} c d\gamma \ : \ \gamma \in \Pi(\mu_1, \dots, \mu_K) \right\} = \sup \left\{ \sum_{i=1}^{K} \int_{X_i} u_i(x_i) d\mu_i : u_i \in \mathcal{D} \right\}, \tag{7.6}$$

where $\mathcal{D}$ is the set of functions $u_i : \mathbb{R}^d \to \mathbb{R}$, $i = 1, \dots, K$, such that

$$\sum_{i=1}^{K} u_i(x_i) \leqslant c(x_1, \dots, x_K), \quad \text{and} \quad \frac{1}{K}\overline{c} - (\overline{c} - \underline{c}) \leqslant \sum_{i=1}^{K} u_i(x_i) \leqslant \frac{1}{K}\overline{c}.$$

(iii) For any solution γ of (7.1)*, any conjugate solution of* (7.5) *and γ a.e. $(x_1, \dots, x_K)$, we have*

$$\sum_{i=1}^{K} u_i(x_i) = c(x_1, \dots, x_K).$$

Remark 7.1.10. We remark that despite its generality, Kellerer's theorem can not be applied directly to some interesting costs as Coulomb-type ones

$$c(x_1, \cdots, x_K) = \sum_{i\neq j}^{K} \frac{1}{|x_i - x_j|^s},$$

since they do not satisfy the boundedness hypothesis $\overline{c} = sup_X c < \infty$ and can not be bounded by functions in $\mathrm{L}^1(\mathbb{R}^d, \rho\mathcal{L}^d)$. A generalization of Kellerer's theorem due to M. Beiglboeck, C. Léonard and W. Schachermayer [9], extends this duality for more general costs, but only a recent result by De Pascale [48] extended the proof of duality to Coulomb-type costs, see Theorem 9.5.1. In fact, suppose $\mu = \rho(x)dx$ is a probability measure on $\mathbb{R}^d$ which does not give mass to sets of cardinality less than or equal to $d-1$, then

$$\min_{\gamma\in\Pi_K(\mu)} \int_{\mathbb{R}^{dK}} \sum_{i=1}^{K}\sum_{j=i+1}^{K} \frac{1}{|x_i - x_j|} d\gamma = \max_{u\in\tilde{\mathcal{D}}} \int_{\mathbb{R}^d} Ku(x)\rho(x)dx \tag{7.7}$$

where $\tilde{\mathcal{D}}$ is the set of potentials $u \in L^1(\mathbb{R}^d, \mu)$ such that

$$\sum_{i=1}^{K} u(x_i) \leqslant \sum_{i=1}^{K}\sum_{j=i+1}^{K} \frac{1}{|x_j - x_i|}, \quad \otimes_{i=1}^{K}\rho - \textit{ almost everywhere.} \tag{7.8}$$

Moreover, we get the conclusions (i) and (iii) of the theorem 7.1.9.

More generally, the main theorem in [48] shows that the Kantorovich duality holds, for instance, for costs of form

$$\sum_{i=1}^{K}\sum_{j=i+1}^{K} \frac{1}{|x_j - x_i|^s}, \quad s \geqslant 1.$$

7.1.2 Geometry of the Optimal Transport sets

We now present the relation between the support of a coupling γ and optimality in the Monge-Kantorovich problem (7.1). In the following, we will just summarize some key results necessary to discuss recent developments of optimal transportation with Coulomb and repulsive harmonic-type costs (see chapters 8 and 9).

Roughly speaking, it is well-known in optimal transport theory with 2-marginals that, for a wide class of costs c, a coupling γ is optimal if, and only if, the support of γ is concentrated in a c-cyclically monotone set [3, 102, 106]:

Definition 7.1.11 (c-cyclically monotone, 2-marginal case)**.** *Let X, Y be Polish spaces, $c : X \times Y \to \mathbb{R}\cup\{\infty\}$ be a cost function, Γ be subset of the product space $X \times Y$ and σ a permutation of $\{1, \cdots, M\}$. We say that Γ is a c-cyclically monotone set if, for any finite couples of points $\{(x_i, y_i)\}_{i=1}^{M} \subset \Gamma$,*

$$\sum_{i=1}^{M} c(x_i, y_i) \leqslant \sum_{i=1}^{M} c(x_i, y_{\sigma(i)}).$$

In [97], Pass suggested a possible extension of the concept of c-cyclically monotone sets for the multi-marginal case. Here, it is enough to consider this notion in $\mathbb{R}^d$.

Definition 7.1.12 (c-cyclically monotone set)**.** *Let $c : \mathbb{R}^{dK} \to \mathbb{R}$ be a cost function. A subset $\Gamma \subset \mathbb{R}^{dK}$ is said to be c-monotone with respect to a partition $(p, p^c), p \subset I$, if, for all $x = (x_1, \dots, x_K), y = (y_1, \dots, y_K) \in \Gamma$*

$$c(x) + c(y) \leqslant c(X(x, y, p)) + c(Y(x, y, p)),$$

where $X(x, y, p), Y(x, y, p) \in \mathbb{R}^K$ are functions obtained from x and y by exchanging their coordinates on the complement of p, namely

$$X_i(x, y, p) = \begin{cases} x_i, & \text{if } i \in p \\ y_i, & \text{if } i \in p^c \end{cases} \quad \text{and} \quad Y_i(x, y, p) = \begin{cases} y_i, & \text{if } i \in p \\ x_i, & \text{if } i \in p^c \end{cases} \quad \forall i \in I$$

We say that $\Gamma \subset \mathbb{R}^{dK}$ is c-cyclically monotone, if it is c-monotone with respect to any partition (p, p^c), $p \subset I$.

The notion of c-cyclical monotonicity in the multi-marginal setting was studied by Ghoussoub, Moameni, Maurey, Pass [68, 69, 97, 98] and successfully applied in the study of decoupling PDE systems [70]. In [49] the authors have used it in order to characterize the optimal transport maps in the one-dimensional case for the Coulomb cost.

More recently, Beiglboeck and Griessler [8], presented a new notion called *finistic optimality* inspired by the martingale optimal transport, which is equivalent, in the 2-marginals case, to the definition 7.1.11.

The next proposition gives a necessary condition on the support for an optimal transport plan γ. For the proof, which is based on the 2-marginal result [114], we refer the reader to Lemma 3.1.2 of [97].

Proposition 7.1.13 (Support of transport plan are c-cyclically monotonic)**.** *Let $c : \mathbb{R}^{dK} \to [0, \infty]$ be a continuous cost and $\mu_1, \dots, \mu_K$ absolutely continuous probability measures on $\mathbb{R}^d$. Suppose that $\gamma \in \Pi(\mathbb{R}^{dK}; \mu_1, \cdots, \mu_K)$ is an optimal transport plan for the multi-marginal Monge-Kantorovich Problem (7.1) and assume $(\mathcal{MK}) < \infty$. Then γ is concentrated in a c-cyclically monotone set.*

7.1.3 Some symmetric cases

The radial symmetry

An interesting class of examples is those for which the cost function is radially symmetric.

Definition 7.1.14 (Radially symmetric cost)**.** *A cost $c : \mathbb{R}^{dK} \to \mathbb{R}$ is said radially symmetric if*

$$c(Ax_1, \cdots, Ax_K) = c(x_1, \cdots, x_K),$$

for all rotations $A \in SO(\mathbb{R}^d)$.

This class includes the Gangbo-Swiech cost $\sum_{i \neq j} |x_i - x_j|^2$ (aka the quadratic cost for the multi-marginal case) [66], the determinant cost $-\det(x_1, \cdots, x_K)$, with $K = d$ so that $(x_1, \cdots, x_K)$ is a square matrix, introduced by Carlier and Nazaret in [36] (see also section 8.3 for a detailed description) and the Coulomb cost $\sum_{i \neq j} \dfrac{1}{|x_i - x_j|}$ (see chapter 9). We define a radially symmetric measure as follows

Definition 7.1.15 (Radially symmetric probability measures)**.** *A probability measure $\mu \in \mathcal{P}(\mathbb{R}^d)$ is radially symmetric if*

$$(A)_\sharp \mu = \mu \quad \forall A \in SO(\mathbb{R}^d).$$

$\gamma \in \mathcal{P}(\mathbb{R}^{dK})$ is radially symmetric if

$$(A, \cdots, A)_\sharp \gamma = \gamma \quad \forall A \in SO(\mathbb{R}^d).$$

Then we have the following result, firstly proven in [36] and then extended to the general case by Pass in [99]

Theorem 7.1.16. *Assume c and each μ_i is radially symmetric then there is an optimal γ for (7.1) such that*

- *γ is radially symmetric.*
- *For each $(x_1, \cdots, x_K) \in \operatorname{supp}(\gamma)$ we have*

$$(x_1, \cdots, x_K) \in \operatorname{argmin}_{|y_i|=r_i, i\in\mathcal{I}} c(y_1, \cdots, y_K), \tag{7.9}$$

where $r_i = |x_i|$.

Even more interesting is a corollary of the previous theorem which states that for some cost functions the optimal plan is not of Monge type, but it is supported on sets of Hausdorff dimension equal or bigger then $2K-2$

Corollary 7.1.17 (Pass, [99])**.** *Let $c : \mathbb{R}^{dK} \to \mathbb{R}$ be a symmetric cost (see definition 7.1.14) and $\{\mu_i\}_{i\in\mathcal{I}}$ be radially symmetric and absolutely continuous with respect to Lebesgue measure in $\mathbb{R}^d$. Suppose that for every radii $(r_1, ...r_K)$ the minimizers*

$$(x_1, \ldots, x_K) \in \operatorname{argmin}_{|y_i|=r_i} c(y_1, y_2, \ldots y_K) \quad \textit{are not all co-linear.}$$

Then, there exists solutions γ whose support is at least $(2K-2)$-dimensional.

We, finally, remark that if $c(y_1, y_2, \ldots y_K)$ and each μ_i is radially symmetric then problem (7.1) can be reduced to a $1-$dimensional problem. The following lemma holds

Lemma 7.1.18 ([BCN15])**.** *Let $\mu_i \in \mathcal{P}(\mathbb{R}^d)$ be K radially symmetric measures. In particular each μ_i is determined by $\mu_r^i = |\cdot|_\sharp \mu$. Consider the following $1-$dimensional problem*

$$(\mathcal{MK}_K^r) \quad \min\left\{\int_{\mathbb{R}^K} \tilde{c}(r_1, \ldots, r_K) d\gamma_r \mid \gamma_r \in \Pi_K(\mu_r^1, \cdots, \mu_r^K)\right\}, \tag{7.10}$$

where $\tilde{c}$ is the reduced cost

$$\tilde{c}(r_1, \ldots, r_K) = \min\left\{c(x_1, \cdots, x_N) \mid |x_i| = r_i \ \forall i = 1, \ldots, K\right\}.$$

Then,

$$\min(\mathcal{MK}_K) = \inf(\mathcal{MK}_K^r).$$

Proof. We first prove that $\min(\mathcal{MK}_K) \geqslant \inf(\mathcal{MK}_K^r)$. This is quite easy: indeed for an optimal $\gamma \in \Pi(\mathbb{R}^{dK}; \mu_1, \cdots, \mu_K)$ we can define its radial component as $\gamma_r = R_\sharp \gamma$, where $R : (x_1, \ldots, x_K) \mapsto (|x_1|, \ldots, |x_K|)$. It is clear that $\gamma_r \in \Pi_K(\mu_r^1, \cdots, \mu_r^K)$ and since $c \geqslant \tilde{c}$ the inequality $\min(\mathcal{MK}_K) \geqslant \inf(\mathcal{MK}_K^r)$ follows. In order to prove the converse inequality, we use duality. Indeed, by standard convex duality, we have

$$(\mathcal{MK}_K) = \sup_{u_i} \Big\{ \sum_{i=1}^K \int_{\mathbb{R}^d} u_i(x) d\mu_i(x) \mid \sum_{i=1}^N u_i(x_i) \leq c(x_1, \cdots, x_K) \Big\} \tag{7.11}$$

and similarly

$$(\mathcal{MK}_K^r) = \sup_{v_i} \Big\{ \sum_{i=1}^K \int_{\mathbb{R}_+} v_i(r) d\mu_r^i(r) \mid \sum_{i=1}^N v_i(r_i) \leq \tilde{c}(r_1, \cdots, r_N) \Big\}. \tag{7.12}$$

Now since μ_i are radially symmetric and the constraint of (7.11) is invariant by changing u_i by $u_i \circ A$ with A a rotation, there is no loss of generality in restricting the maximization in (7.11) to potentials of the form $u_i(|x_i|) = v_i(r_i)$. Thus, take for example v_i optimal for (7.12), then the constraint of (7.11) are automatically satisfied, but v_i could not be the optimal solutions to (7.11) and so we have $\min(\mathcal{MK}_K) \leq \inf(\mathcal{MK}_K^r)$. □

The indistinguishability symmetry

Consider now the case in which *all the marginals are equal* $\mu_i = \mu$ $i = 1, ..., K$, in other words the marginals are indistinguishable, and the cost is *symmetric in the marginals* (with an abuse of notation we will refer to this kind of cost as *indistinguishability or cyclically symmetric cost*) which means the following

$$c(x_1, \cdots, x_K) = c(\overline{\sigma}(x_1, x_2, \ldots, x_K))$$

for all cyclical permutations $\overline{\sigma}$. Then, we can reduce our study of the Monge-Kantorovich (7.1) and the Monge problems (7.2) to a suitable class of transport plans (symmetric plans) and transport maps (called cyclic maps), respectively.

Remark 7.1.19. Notice that radial symmetry and indistinguishability symmetry are quite different. For instance, the cost $c(x_1, x_2, x_3) = |x_1 - x_2|^2$ is radially symmetric, but not indistinguishability symmetric. And the cost $c(x_1, \cdots, x_K) = \sum_{i<j} |x_i - x_j|_\infty$ is indistinguishability symmetric, but not radially.

Definition 7.1.20 (Cyclically symmetric probability measures)**.** *A probability measure $\gamma \in \mathcal{P}(\mathbb{R}^{dK})$ is cyclically symmetric if*

$$\int_{\mathbb{R}^{dK}} f(x_1, \ldots, x_K) d\gamma = \int_{\mathbb{R}^{dK}} f(\overline{\sigma}(x_1, \ldots, x_K)) d\gamma, \ \forall f \in \mathcal{C}(\mathbb{R}^{dK})$$

where $\overline{\sigma}$ is the cyclical permutation

$$\overline{\sigma}(x_1, x_2, \ldots, x_K) = (x_2, x_3, \ldots, x_K, x_1).$$

We will denote by $\Pi_K^{sym}(\mathbb{R}^{dK}; \mu)$, the space of all cyclically symmetric probability measures on $\mathbb{R}^{dK}$ having all the marginals equal to μ.

As previously, we can define the multi-marginal symmetric Monge-Kantorovich problem as follows

Problem 7.1.21 (Symmetric Monge-Kantorovich problem)**.** *Solve*

$$(\mathcal{MK}_{sym}) \quad \inf\left\{ \int_{\mathbb{R}^{dK}} c(x_1,\dots,x_K)d\gamma(x_1,\dots,x_K) \mid \gamma \in \Pi_K^{sym}(\mathbb{R}^{dK};\mu) \right\}, \tag{7.13}$$

and the associated multi marginal cyclically Monge Problem

Problem 7.1.22 (Cyclically Monge Problem)**.** *Solve*

$$\begin{aligned}(\mathcal{M}_{cycl}) \quad \inf\Bigg\{ &\int_{\mathbb{R}^d} c(x,T^{(1)}(x),T^{(2)}(x),\dots,T^{(K-1)}(x))d\mu_1(x) \mid \\ &T:\mathbb{R}^d\to\mathbb{R}^d,\ T_\sharp\mu=\mu,\ T^{(K)}=\mathrm{Id} \Bigg\},\end{aligned} \tag{7.14}$$

where $T^{(i)}$ stands for the $i-$th composition of T with itself.

Remark 7.1.23. $(\mathcal{M}_{cycl})$ is related to $(\mathcal{M})$ by choosing $T_\sharp\mu = \mu$, $T_{i+1}(x) = T^{(i)}(x)$ for every $i \in \{1,\dots,K-1\}, T^{(K)} = \mathrm{Id}$.

Proposition 7.1.24. *Suppose $\mu_1 = \cdots = \mu_K = \mu \in \mathcal{P}(\mathbb{R}^d)$ is an absolutely continuous probability measure with respect to the Lebesgue measure and $c : \mathbb{R}^{dK} \to \mathbb{R}$ is a continuous cyclically symmetric cost. Then,*

$$\inf(\mathcal{MK}) = \inf(\mathcal{MK}_{sym}).$$

Proof. The fact that the infimum of (7.1) is smaller than or equal to (7.13) is obvious. Now, we need to show that for every transport plan $\gamma \in \Pi_K(\mu)$ we can associate a symmetric plan in $\Pi_K^{sym}(\mathbb{R}^{dK};\mu)$. Indeed, given $\gamma \in \Pi_K(\mathbb{R}^{dK};\mu)$ (where $\Pi_K(\mathbb{R}^{dK};\mu)$ is the set of plans γ having all marginals equal to μ), we define

$$\overline{\gamma} = \frac{1}{K!}\sum_{\sigma\in\mathscr{S}_K} \sigma_\sharp\gamma,$$

and finally we notice that $\overline{\gamma}$ has the same cost as γ. □

We remark that proving $\inf(\mathcal{M}_{cycl}) \leqslant \inf(\mathcal{M}_K)$ is not obvious . However, we can avoid this problem in order to prove the equivalence between the Multi-marginal cyclic problem and Multi-marginal OT problem, by noticing that $\inf(\mathcal{M}_{sym}) \leqslant \inf(\mathcal{M}_{cycl})$. The last part was proved by M. Colombo and S. Di Marino [40]. We give the precise statement of this theorem.

Theorem 7.1.25 (M. Colombo and S. Di Marino, [40])**.** *Let $c : \mathbb{R}^{dK} \to \mathbb{R}$ be a symmetric continuous function and bounded from below. If μ has no atoms, then*

$$\inf(\mathcal{MK}_{sym}) = \inf(\mathcal{M}_{cycl}).$$

Finally, we have the equality between the multi-marginal cyclic problem and multi-marginal OT problem.

Corollary 7.1.26. *If μ has no atoms and $c : \mathbb{R}^{dK} \to \mathbb{R}$ is a cyclically symmetric continuous function and bounded from below, then*

$$\inf(\mathcal{MK}_{sym}) = \inf(\mathcal{MK}) = \inf(\mathcal{M}_K) = \inf(\mathcal{M}_{cycl}).$$

Remark 7.1.27 (N-cyclically vector fields). We remark that in the literature (see [68, 69, 62]) we can find example of symmetric Monge-Kantorovich problem like (7.13) for which the existence of Monge solutions (namely transport optimal supported on the graph of cyclical maps) has been established ([69]). The idea is to consider cost of the form

$$c(x_1, \cdots, x_K) = \sum_{i=1}^{K-1} \langle u_i(x_1), x_{i+1} \rangle,$$

where the u_is are a family of jointly $K-$monotone vector fields, namely for every cycle $x_1, \cdots, x_K$ of points such that $x_{K+l} = x_1$ we have that

$$\sum_{i=1}^{K} \sum_{l=1}^{K-1} \langle u_l(x_i), x_i - x_{i+l} \rangle \geqslant 0.$$

Notice that if we take two marginals and $u(x) = -x$ we retrieve the classic quadratic cost and the Brenier's transport map, see [68].

7.1.4 The Gangbo-Swiech cost

We want to conclude this section about the *continuous* multi-marginal problem by presenting the MM-OT with the so-called Gangbo-Swiech cost, after the seminal work by Gangbo and Swiech [66], which can be regarded as an extension of the classical quadratic cost we have introduced in chapter 1.

Let us consider K marginals $\mu_i \in \mathcal{P}(\mathbb{R}^d)$ then the multi-marginal Monge problem with the Gangbo-Swiech cost is

$$\inf \left\{ \int_{\mathbb{R}^d} \sum_{i=1}^{K} \sum_{j=i+1}^{K} \frac{|T_i(x) - T_j(x)|^2}{2} d\mu_1(x) \mid T = \{T_i\}_{i \in \mathcal{I}} \in \mathcal{T}_K \right\}, \tag{7.15}$$

where $\mathcal{T}_K := \{T = \{T_i\}_{i \in \mathcal{I}} \mid T_i : \mathbb{R}^d \to \mathbb{R}^d \ (T_i)_\sharp \mu_1 = \mu_i \ T_1 = \mathrm{Id}\}$ and the Monge-Kantorovich problem becomes

$$\inf \left\{ \int_{\mathbb{R}^{dK}} \sum_{i=1}^{K} \sum_{j=i+1}^{K} \frac{|x_i - x_j|^2}{2} d\gamma(x_1, \cdots, x_K) \mid \gamma \in \Pi(\mathbb{R}^{dK}; \mu_1, \cdots, \mu_K) \right\}. \tag{7.16}$$

Remark 7.1.28. If we assume that the marginals μ_i have finite second moment then, as in the two marginal case, problem (7.16) can be rewritten in the following form

$$\sup \left\{ \int_{\mathbb{R}^{dK}} \sum_{i=1}^{K} \sum_{j=i+1}^{K} \langle x_i, x_j \rangle d\gamma(x_1, \cdots, x_K) \mid \gamma \in \Pi(\mathbb{R}^{dK}; \mu_1, \cdots, \mu_K) \right\}, \tag{7.17}$$

where $\langle \cdot, \cdot \rangle$ denotes the usual dot product in $\mathbb{R}^d$.

One can easily derive the dual formulation of (7.16)

$$\sup\Bigg\{ \sum_{i}^{K} \int_{\mathbb{R}^d} u_i d\mu_i \mid u_i \in \mathrm{L}^1(\mathbb{R}^d, \mu_i)\ u_i \text{ are upper semicontinuous and } \sum_{i=1}^{K} u_i(x_i) \leqslant \sum_{i=1}^{K} \sum_{j=i+1}^{K} \frac{|x_i - x_j|^2}{2} \forall (x_1, \cdots, x_K) \in \mathbb{R}^{dK} \Bigg\}. \tag{7.18}$$

Then, Gangbo and Swiech proved the following theorem which yields the existence of optimal maps

Theorem 7.1.29 (Gangbo-Swiech [66])**.** *Assume that $\mu_1 \cdots, \mu_K$ probability measure vanishing on $(d-1)-$rectifiable sets and having finite second moments (i.e. $\int_{\mathbb{R}^d} |x|^2 d\mu_i(x) < +\infty$). Then,*

(1). Problem (7.18) admits a maximizer $u = \{u_i\}_{i \in \mathcal{I}}$.

(2). There is a minimizer $T \in \mathcal{T}_K$ for (7.15). The T_i are one-to-one μ_i-a.e., are uniquely determined, and have the form

$$T_i(x) = \mathrm{D}\, f_i^*(\mathrm{D}\, f_1(x)) \quad \text{where} \quad f_i(x) = \frac{|x|^2}{2} + \varphi_i(x), \tag{7.19}$$

the φ_i are convex functions, and $f_i^* \in \mathcal{C}^1(\mathbb{R}^d)$.

(3). Duality holds: the optimal values in problems (7.15) and (7.18) coincide.

(4). If $\overline{u}$ is another maximizer for problem (7.18) we can modify the $\overline{u}_i$'s on sets of zero μ_i measure to obtain a maximizer, still denoted $\overline{u}$, such that $\overline{u}_i$ is differentiable μ_i-a.e.. Furthermore,

$$\mathrm{D}\, u_i = \mathrm{D}\, \overline{u}_i \ \mu_i\text{-a.e.}$$

(5.) Problem (7.16) admits a unique minimizer $\gamma \in \Pi(\mathbb{R}^{dK}; \mu_1, \cdots, \mu_K)$.

Remark 7.1.30. Theorem 7.1.29 provides a geometrical characterization of the optimal measure for problem 7.16.

Remark 7.1.31 (Connection with the Wasserstein barycenter). In section 7.3.1 we will show that the Wasserstein barycenter problem is indeed a multi-marginal problem and that theorem 7.1.29 can provide a geometrical characterization of the barycenter.

Remark 7.1.32 (Connection with the standard OT problem with the quadratic cost). Notice that if $K = 2$ then we exactly retrieve the Brenier's theorem for the standard quadratic cost; indeed *(2)* returns the Brenier's map.

Remark 7.1.33. *(4)* states that as in the two marginal case the Kantorovich potential are unique up to an additive constant.

Remark 7.1.34 (Monge-Ampère system). As we have seen in section 1.1 the constraint of the Monge problem with can be rewritten as the Monge-Ampère equation. In this case we actually have a system of Monge-Ampère equations. Assume that the measures μ_i are absolutely continuous with respect the Lebesgue measure $\mu_i = \rho_i \mathcal{L}^d$ then formally the f_i's satisfy the following set of equations

$$\rho_i(\mathrm{D}\, f_i^*(x)) \det(\mathrm{D}^2\, f_i^*(x)) = \rho_1(\mathrm{D}\, f_1^*(x)) \det(\mathrm{D}^2\, f_1^*(x)) = \rho(x), \tag{7.20}$$

where the function $\rho(x)$ is unknown.

7.2 The Multi-Marginal OT problem: the discrete setting

In this section we introduce the discrete version of the Multi-Marginal Monge-Kantorovich

$$(\mathcal{MK}_K)\ \min\left\{\int_{(\mathbb{R}^d)^K} c(x_1,\cdots,x_K)d\gamma(x_1,\cdots,x_K)\mid \gamma\in\Pi(\mathbb{R}^{dK};\mu_1,\cdots,\mu_K)\right\}, \tag{7.21}$$

where K is the number of marginals , $c(x_1,...,x_K)$ is the cost function, γ the transport plan and $\Pi(\mathbb{R}^{dK};\mu_1,\cdots,\mu_K):=\{\gamma\in\mathcal{P}(\mathbb{R}^{dK})\mid \pi_i(\gamma)=\mu_i\}$ with $\pi_i:\mathbb{R}^{dK}\to\mathbb{R}^d$ the canonical projection. From now on, we assume (with an abuse of notation) that $\mu_i=\mu_i(x_i)\mathcal{L}^d$ where $\mu_i:\mathbb{R}^d\to\mathbb{R}$. Then we use a discretization with N points of the support of the kth density as $\{x_{j_k}\}_{j_k=1,\cdots,N}$. If the densities μ_k are approximated by $\sum_{j_k}\mu_{j_k}\delta_{x_{j_k}}$, we get the following discrete problem

Problem 7.2.1. *Given K marginals $\mu_k\in\Sigma_N:=\{\mu_k\in\mathbb{R}^N\mid\sum_{j_k=1}^N\mu_{j_k}=1\}$, solve*

$$\min\left\{\sum_{j_1,\cdots j_K}c_{j_1,\cdots,j_K}\gamma_{j_1,\cdots,j_K}\mid\gamma\in\Pi_N^K(\mathbb{R}^{dKN};\mu_1,\cdots,\mu_K)\right\}, \tag{7.22}$$

where $c_{j_1,\cdots,j_K}=c(x_{j_1},\cdots,x_{j_K})$ is a matrix in $\otimes_{i=1}^K\mathbb{R}^N$, the transport plan support for each coordinate is restricted to the points $\{x_{j_k}\}_k=1,\cdots,N$ thus becoming a $(N)^K$ matrix with non-negative entries again denoted γ with elements $\gamma_{j_1,\cdots,j_K}$ and the set $\Pi_N^K(\mathbb{R}^{dKN};\mu_1,\cdots,\mu_K)$ is defined as

$$\Pi_N^K(\mathbb{R}^{dKN};\mu_1,\cdots,\mu_K):=\{\gamma\in\mathbb{R}_+^{(N)^K}\mid S_k(\gamma)=\mu_k,\ \forall k=1,\cdots,K\}. \tag{7.23}$$

where the push-forward $S_k(\gamma)\in\mathbb{R}^N$ of such a γ along dimension k is computed as

$$\forall\, i\in\{1,\dots,N\},\quad S_k(\gamma)_i:=\sum_{j_1,j_2,\dots,j_{k-1},j_{k+1},..,j_K}\gamma_{j_1,j_2,\dots,j_{k-1},i,j_{k+1},..,j_K}. \tag{7.24}$$

The discrete optimal transport problem (7.22) is a linear program problem and its dual can be written as follows

$$\max\{\sum_{i=1}^K\sum_{j_i=1}^M u_{j_i}^i\mu_{j_i}^i\quad\mid\quad\sum_{k=1}^K u_{j_k}^k\leqslant c_{j_1,\dots,j_K}\quad\forall(j_1,\cdots,j_K)\in\{1,\cdots,M\}^K\}. \tag{7.25}$$

where $u_{j_i}^i=u^i(x_{j_i})$.

Remark 7.2.2. Notice that the primal (7.22) has $(N)^K$ unknowns and $N\times K$ linear constraints and the dual (7.25) $N\times K$ unknowns but still $(N)^K$ constraints. This makes them computationally not solvable with standard linear programming methods even for small cases.

7.3 Hidden multi-marginal optimal transport problems

7.3.1 The multi-marginal Wasserstein Barycenter

In section 4.1 we have introduced the discrete formulation of the Wasserstein barycenter and then we have used the IPFP algorithm in order to compute the barycenter. Here, we would like to underline that the formulation of the Wasserstein barycenter given by Agueh and Carlier in [1] is indeed equivalent to solve a multi-marginal optimal problem with a Gangbo-Swiech type cost Let us consider, as usual, K marginals $\mu_i \in \mathcal{P}(\mathbb{R}^d)$, having finite second moment, and K weights $\lambda = \{\lambda_i\}_{i=1}^K$ such that $\lambda \in \Sigma_K$, then the minimization problem is

Problem 7.3.1 (Wasserstein barycenter)**.** *Solve*

$$\inf\left\{\sum_{i=1}^K \lambda_i \mathcal{MK}(\mu_i,\nu) \mid \nu \in \mathcal{P}(\mathbb{R}^d)\right\}, \tag{7.26}$$

where the measure ν is the barycenter and $\mathcal{MK}$ is the 2-Wasserstein distance, namely the optimal transport problem with the quadratic cost.

Define now for every $x = (x_1, \cdots, x_K) \in \mathbb{R}^{dK}$ the Euclidean barycenter $\mathcal{B}(x) := \sum_{i=1}^K \lambda_i x_i$, then consider the following multi-marginal problem

$$\inf\left\{c(x_1,\cdots,x_K)d\gamma(x_1,\cdots,x_K) \mid \gamma \in \Pi(\mathbb{R}^{dK};\mu_1,\cdots,\mu_K)\right\}, \tag{7.27}$$

where the cost function is

$$c(x_1,\cdots,x_K) := \sum_{i=1}^K \frac{\lambda_i}{2}|x_i - \mathcal{B}(x)|^2. \tag{7.28}$$

If we now develop the square in (7.28) we immediately notice that problem (7.27) is equivalent to

$$\sup\left\{\sum_{i=1}^K\sum_{j=i+1}^K \lambda_i\lambda_j\langle x_i,x_j\rangle d\gamma(x_1,\cdots,x_K) \mid \gamma \in \Pi(\mathbb{R}^{dK};\mu_1,\cdots,\mu_K)\right\}, \tag{7.29}$$

which is actually the problem (7.17) solved by Gangbo and Swiech. Thus, we can apply theorem 7.1.29 noticing that due to the weights λ_i, the f_i must be rewritten as

$$f_i(x) = \frac{\lambda_i}{2}|x|^2 + \varphi_i(x).$$

Then, Agueh and Carlier established the following relation between problems (7.26) and (7.27)

Proposition 7.3.2 (Proposition 4.2 in [1])**.** *Assume the same hypothesis as in theorem 7.1.29. Then the solution of (7.26) is given by $\nu = \mathcal{B}_\sharp\gamma$, where γ is the solution of (7.27).*

Remark 7.3.3. It is not surprising that since the optimal measure γ is induced by maps T_i (see *(2)* in theorem 7.1.29), then the barycenter ν can be characterized as follows

$$\nu := (\sum_{i=1}^{K} \lambda_i T_i)_\sharp \mu_1.$$

We refer the reader to section 7.5.1 for the numerical experiments by using the multi-marginal formulation of the Wasserstein barycenter.

7.3.2 The multi-marginal Matching for teams problem

We conclude this section by pointing out that another problem, namely the Matching for teams problem, can be recast as a multi-marginal problem. Again, consider K marginals $\mu_i \in \mathcal{P}(\mathbb{R}^d)$ and cost functions $c^k : \mathbb{R}^{2d} \to \mathbb{R}$ then the matching for teams problem introduced by Carlier and Ekeland in [32] is

$$\inf \left\{ \sum_{i=1}^{K} \mathcal{MK}_{c_i}(\mu_i, \nu) \mid \nu \in \mathcal{P}(\mathbb{R}^d) \right\}, \tag{7.30}$$

ν is the equilibrium and $\mathcal{MK}_{c_i}$ are the optimal transport problems with cost c_i. Then Carlier and Ekeland showed that problem (7.30) is indeed equivalent to the following multi-marginal problem

$$\inf \left\{ c(x_1, \cdots, x_K) d\gamma(x_1, \cdots, x_K) \mid \gamma \in \Pi(\mathbb{R}^{dK}; \mu_1, \cdots, \mu_K) \right\}, \tag{7.31}$$

where the cost function $c(x_1, \cdots, x_K)$ is given by

$$c(x_1, \cdots, x_K) := \inf \left\{ \sum_{i=1}^{K} c_i(x_i, y) \mid y \in \mathbb{R}^d \right\}. \tag{7.32}$$

Assume now that the infimum in (7.32) is uniquely attained for every $x = (x_1, \cdots, x_K) \in \mathbb{R}^{dK}$ at some point $\overline{y}(x)$, then the connection between problems (7.30) and (7.31) is established by the following proposition

Proposition 7.3.4 (Proposition 3 in [32])**.** *Under the previous assumptions, one has*

(1). Problems (7.30) and (7.31) have the same value.

(2). If γ is solution to (7.31), then $\nu := \overline{y}_\sharp \gamma$ is solution to (7.30).

(3). If ν solves (7.30), then there exists a solution to (7.31) such that $\nu = \overline{y}_\sharp \gamma$.

7.4 Regularized Multi-Marginal OT and generalization of the IPFP

Let us now consider the discrete formulation of the multi-marginal problem that we have discussed in section 7.2. We would like to introduce its regularized counterpart as we have done for the standard optimal transport problem. Thus, we are given K marginals $(\mu_k)_{k=1}^K$. We denote by $\gamma \in \mathbb{R}_+^{N^K}$ a K-dimensional

array, indexed as γ_j for $j = (j_1, \dots, j_K) \in \{1 \dots, N\}^K$ where $N$is the number of gridpoints used to discretize $\mathbb{R}^d_+$ and by $S_k(\gamma) \in \mathbb{R}^N$ the push-forward defined in (7.24). In order to simplify the notation, take $j := (j_1, \cdots, j_K) \in \mathcal{K}$ where $\mathcal{K} := \{1, \cdots, N\}^K$ Then, the regularized OT problem (2.15) can be generalized to the multi-marginal setting as

Problem 7.4.1. *Given K marginals $(\mu_k)_{k=1}^K$ and a cost matrix $C \in \mathbb{R}_+^{NK}$ such that $(C)_{j_1,\cdots,j_K} = c_{j_1,\cdots,j_K}$, solve*

$$\min \left\{ \sum_{j \in \mathcal{K}} c_j \gamma_j + \varepsilon \, \mathrm{H}(\gamma|\eta) \mid \gamma \in \Pi_N^K(\mathbb{R}^{dKN}; \mu_1, \cdots, \mu_K) \right\} \tag{7.33}$$

where $\eta = \otimes_{i=1}^K \mu_i$ and $\mathrm{H}(\cdot|\cdot)$ is the relative entropy defined as follows

$$\mathrm{H}(\gamma|\eta) := \sum_{j \in \mathcal{K}} \gamma_j (\log(\frac{\gamma_j}{\eta_j}) - 1) \forall \gamma, \eta \in \mathbb{R}_{++}^{N^K}.$$

Similarly as (2.15), this problem can be re-cast as a KL projection (we remind that $\mathrm{KL}(\gamma|\eta) = \mathrm{H}(\gamma|\eta)$)

$$\min \{ \mathrm{KL}(\gamma|\overline{\gamma}) \mid \gamma \in \mathcal{C}_1 \cap \mathcal{C}_2 \cap \ldots \cap \mathcal{C}_K \} \quad \text{where} \quad \overline{\gamma}_j := \exp(-\frac{c_j}{\varepsilon}) \tag{7.34}$$

where the exponentiation is exponent-wise, and where

$$\mathcal{C}_k := \left\{ \gamma \in \mathbb{R}_{++}^{N^K} \mid S_k(\gamma) = \mu_k \right\}.$$

The Bregman projection on each of the convex $\mathcal{C}_k$ are again given by a simple normalization as detailed in the following proposition.

Proposition 7.4.2 (KL projection for the multi-marginal problem, [BCC+15])**.** *For any k, denoting $\gamma = P_{\mathcal{C}_k}^{\mathrm{KL}}(\bar{\gamma})$, one has*

$$\forall \, j = (j_1, \dots, j_K), \quad \gamma_j = \frac{(\mu_k)_{j_k}}{S_k(\bar{\gamma})_{j_k}} \bar{\gamma}_j$$

Proof. Introducing Lagrange multipliers λ_{j_k} associated to the constraint associated to $\mathcal{C}_k$

$$S_k(\gamma_j)_{j_k} = (\mu_k)_{j_k} \tag{7.35}$$

the KL projection is given by the optimality condition :

$$\log\left(\frac{\gamma_j}{\bar{\gamma}_j}\right) - \lambda_{j_k} = 0 \tag{7.36}$$

so that

$$\gamma_j = a_{j_k} \bar{\gamma}_j, \tag{7.37}$$

where $a_{j_k} = \exp(\lambda_{j_k})$. By using both equation (7.37) and (7.35), we get

$$a_{j_k} = \frac{(\mu_k)_{j_k}}{S_k(\bar{\gamma})_{j_k}},$$
$$\gamma_j = \frac{(\mu_k)_{j_k}}{S_k(\bar{\gamma})_{j_k}} \bar{\gamma}_j,$$

which end the proof. □

It is thus possible to use the Bregman iterative projection detailed in Section 3.1 to compute the projection (7.34).

Remark 7.4.3. Here, we have assumed that the sets $\mathcal{C}_k$ are all affine subspaces of $\mathbb{R}^{NK}_{++}$ which thanks to theorem 3.1.4 assures the convergence of the alternate projections algorithm. If $\mathcal{C}_k$ are not affine, see for instance section 7.5.2, then one must apply the Dykstra's iterates as we have explained in section 3.3.

As we have already noticed for the two marginals case, problem (7.34) is a strictly convex problem. Moreover, one can generalize proposition 2.2.5 to the multi-marginal case and obtain the following result

Proposition 7.4.4. *Assume that all the sets $\mathcal{C}_k$ are affine subspaces of $\mathbb{R}^{NK}_{++}$, then problem (7.34) admits a unique solution. Furthermore, there exist K non-negative vectors $a^k \in \mathbb{R}^N_+$, uniquely determined, up to a multiplicative constant, such that the solution $\gamma^{\varepsilon,\star}$ to (7.34) has the form*

$$\gamma^{\varepsilon,\star}_j = \overline{\gamma}_j \prod_{k=1}^{K} a^k_{j_k}.$$

Remark 7.4.5. As for the 2-marginal case the vectors a^k play the role of the dual variable of problem (7.34).

Remark 7.4.6. The a^k are uniquely determined, up to a multiplicative constant, by the constraints over the marginals of γ

$$a^k_{j_k} = \frac{(\mu_k)_{j_k}}{S_k(\tilde{g})_{j_k}}, \tag{7.38}$$

where $\tilde{g} \in \mathbb{R}^{NK}_{++}$ defined as

$$(\tilde{g})_j := \bar{\gamma}_j \prod_{\ell \neq k} a^\ell_{j_\ell}.$$

Thanks to proposition 7.4.4 and remark 7.4.6 we can now define the IPFP procedure (aka the Sinkhorn algorithm) for K marginals as

$$a^{k,(n)}_{j_k} = \frac{(\mu_k)_{j_k}}{S_k(\tilde{g}^{k,(n)})_{j_k}}, \tag{7.39}$$

where $\tilde{g}^{k,(n)}$ is defined as

$$(\tilde{g}^{k,(n)})_j := \bar{\gamma}_j (\prod_{\ell<k} a^{\ell,(n)}_{j_\ell})(\prod_{\ell>k} a^{\ell,(n-1)}_{j_\ell}).$$

7.5 Applications

7.5.1 Wasserstein Barycenter

As shown in Section 7.3.1, the computation of barycenters of measures can be computed by solving a multi-marginal transport problem.

Let us suppose that the input measures $\{\mu^k\}_{k=1}^K$ defined on $\mathbb{R}^d$ are of the form $\mu^k = \sum_{i=1}^N \mu_{k,i}\delta_{x_i}$, where $\mu^k = \{\mu^k_i\}_{i=1}^N \in \Sigma_N$, where $\{x_i\}_i \subset \mathbb{R}^d$ and δ_x is

the Dirac measure at location $x \in \mathbb{R}^d$. In section 7.3.1 we have shown that the Wasserstein barycenter of the μ^k with weights $\{\lambda_k\}_k \in \Sigma_K$ for the quadratic Euclidean distance ground cost is

$$\mu_\lambda := \sum_{j=(j_1,j_2,\ldots,j_K)} \mu_j \delta_{\mathcal{B}_j(x)} \tag{7.40}$$

where $A_j(x) := \sum_k \lambda_k x_{j_k}$ is the Euclidean barycenter and $\gamma \in \mathbb{R}_+^{N^K}$ is an optimal multi-marginal coupling that solves (7.34) for the following cost

$$C_j = \sum_{1 \leqslant k \leqslant K} \frac{\lambda_k}{2} \|x_{j_k} - \mathcal{B}_j(x)\|^2.$$

An important point to note is that the measure barycenter (7.40) is in general composed of more than M Diracs, and that these Diracs are not constrained to be on the discretization grid $(x_i)_i$. In particular, the obtained result is different from the one obtained by solving (4.1), which computes a barycenter that lies on the same grid as the input measures. In some sense, formulation (7.40) is able to compute the "true" barycenter of measures, whereas (4.1) computes an approximation on a fixed grid, but the price to pay is the resolution of a high-dimensional multi-marginal program.

Figure 7.1 shows an histogram depiction of the measure μ_λ defined in (7.40), for the iso-barycenter (i.e. $\lambda_k = 1/K$ for all k). It is computed by first solving (7.34) with the same three marginals used in Figure 4.1. The histogram $\mu_\lambda \in \Sigma_N$ computed on a grid of $N = 60 \times 60$ points. Each μ_i is the total mass of μ_λ in the discretization square S_i of size $1/\sqrt{N} \times 1/\sqrt{N}$, i.e. $\mu_i = \mu_\lambda(S_i)$.

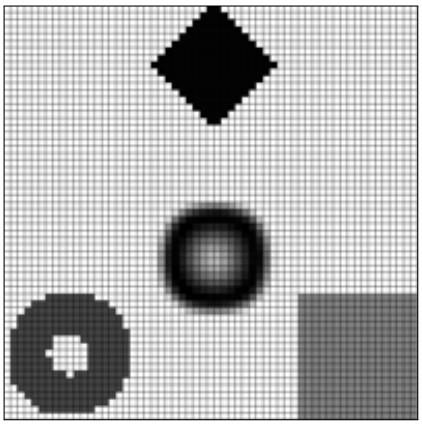

Figure 7.1: *Barycenter computed by solving the multi-marginal problem with three marginals (annulus, diamond and square) discretized on an uniform 2-D grid of $N = 60 \times 60$ points in $[0, 1]^2$ and $\varepsilon = 0.005$. See the main text body for details about how the display of the barycenter measure is performed.*

7.5.2 Partial Optimal Transport

In [77] Pass and Kitagawa studied the multi-marginal partial transport problem and, as a natural extension, the partial barycenter problem. Let us consider

K marginals $\{\mu_k\}_{k=1}^K$ and a transport plan $\gamma \in \mathbb{R}_+^{N^K}$. We now combine the (regularized) partial optimal transport and the "standard" multi-marginal problem, as described in Sections 4.3 and 7.4 respectively. We obtain the following problem

$$\min_{\gamma} \{\mathrm{KL}(\gamma|\overline{\gamma}) \mid \gamma \in \mathcal{C}_1 \cap \mathcal{C}_2 \cap \ldots \cap \mathcal{C}_{K+1}\} \quad \text{where} \quad \overline{\gamma} := \exp(-\frac{C}{\varepsilon}) \tag{7.41}$$

where

$$\begin{aligned} \mathcal{C}_k &:= \left\{\gamma \in \mathbb{R}_+^{N^K} \mid \pi_k(\gamma) \leqslant \mu^k\right\} \quad k = 1, \ldots, K, \\ \mathcal{C}_{K+1} &:= \left\{\gamma \in \mathbb{R}_+^{N^K} \mid \textstyle\sum_j \gamma_j = m\right\}, \end{aligned}$$

where $m \in [0, \min_k(\langle \mu_k, \mathbf{1}\rangle)]$ and $\pi_k : \mathbb{R}_+^{N^K} \to \mathbb{R}_+^N$ denotes the usual canonical projection.

The KL projections on these convex sets are detailed in the following proposition.

Proposition 7.5.1 ([BCC+15]). *For any $k = 1, \ldots, K+1$, denoting $\gamma^k = P_{\mathcal{C}_k}^{\mathrm{KL}}(\bar{\gamma})$, one has*

$$\forall\, k = 1, \ldots, K,\ \forall\, j = (j_1, \ldots, j_K), \quad \gamma_j^k = \min\left(\frac{(\mu^k)_{j_k}}{\pi_k(\bar{\gamma})_{j_k}}, 1\right)\bar{\gamma}_j$$

$$\gamma^{K+1} = \frac{m}{\sum_j \bar{\gamma}_j}\bar{\gamma}.$$

Once again the sets $\mathcal{C}_k$ are not affine, so one needs to use Dykstra iterations (3.19).

Figure 7.2 shows the results obtained when solving (7.41) with the same three marginals (μ_1, μ_2, μ_3) used in Figure 4.1, using the cost

$$C_{j_1, j_2, \ldots, j_K} = \sum_{1 \leqslant s,t \leqslant K} \frac{1}{2}\|x_{j_s} - x_{j_t}\|^2, \tag{7.42}$$

The computation is performed on an uniform 2D-grid of $N = 60 \times 60$ points in $[0,1]^2$, $\varepsilon = 0.005$ and $m = 0.7 \min_k(\langle \mu_k, \mathbf{1}\rangle)$.

7.5.3 Generalized Solutions of Euler Equations

As explained in section 6.3, if we consider a fixed uniform discretization of $[0,1]^d$ with points $\{x_i|_{i=1}^N$ and of $[0,T]$ (assume for simplicity $T = 1$) with $K+1$ steps in time, we recover a discrete multi-marginal problem with the specific cost function

$$C_{j_0, \ldots, j_K} = \frac{K}{2\,T} \sum_{k=0,\ldots,K-1} \|x_{j_{k+1}} - x_{j_k}\|^2 \tag{7.43}$$

for the discretized kinetic energy. The coupling $\gamma_{j_0,\ldots,j_K}$ is the probability matrix to find a "generalized particle" on the discrete time path $x_{j_0}, \ldots, x_{j_K}$. Because the fluid is incompressible the k^{th} "time" marginal, or the probability to find a

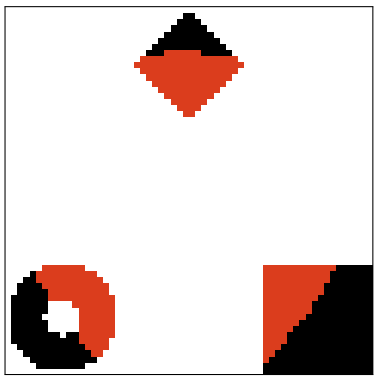

Figure 7.2: *Multi-marginal partial transport. The active regions are displayed in red.*

path at time k at any point of the domain x_{j_k} is uniform, i.e we have the usual marginals constraints with $\mu^k = \mathbf{1}/K$ for all k.

For each $k \in \{0, \dots, K\}$, the transition probability from "time" 0 to "time" k : $\gamma_{0,k} \in \mathbb{R}^{N \times N}$ is defined as

$$\forall\, (s,w) \in \{1,\dots,N\}^2, \quad (\gamma_{0,k})_{s,w} = \sum_{j_i \neq j_0, j_k} \gamma_{s,j_2,\dots,j_{k-1},w,j_{k+1},\dots,j_K}. \tag{7.44}$$

It represents the probability to find a "generalized particle" initially at x_s to be at x_w at time k.

Brenier initial and final constraints take the form of deterministic values for the matrix $\gamma_{0,K}$. Given a permutation of the grid points, i.e. a discrete bijection $\sigma : \{1,\dots,N\} \to \{1,\dots,N\}$, we have the additional constraint

$$(\gamma_{0,K})_{s,w} = \delta_{\sigma(s),w}. \tag{7.45}$$

Where δ is the Kronecker symbol. This is an additional linear constraint on the coupling π and the Bregman approach would imply to compute the projection on this set. Another possibility, simpler to implement, is to include this constraint by adding a term (which acts as a penalization) to the cost function (7.43) :

$$C_{j_0,\dots,j_K} = \sum_{k=0,\dots,K-1} \frac{K}{2T} \|x_{j_{k+1}} - x_{j_k}\|^2 + p\|x_{\sigma(j_0)} - x_{j_K}\|^2,$$

where p is a penalization parameter (for all the following simulations we take $p = 50$).

Brenier's numerical method [23] is based on an approximation of the measure preserving map by a one to one permutation. The domain and the representation of the diffuse coupling therefore needs a large number of particles.

Our resolution method is different and computes a space discretization of the coupling matrix and naturally encodes non-diffeomorphic volume preserving maps. The coupling γ is an array of size $(N^d)^K$ where the d-dimensional physical domain is discretized on N^d points and we have K times steps. However, as explained in Remark 7.5.2 below, thanks of the separable structure of the cost we only need to store and multiply matrices of size $(N^d)^2$.

Remark 7.5.2. [Reduction to Transitions probabilities] As detailed in proposition 7.4.2, the resolution of the regularized K-marginal OT problem boils down

to the computation of a KL projection of $\overline{\gamma} = \exp(-\frac{C}{\varepsilon})$. We can rewrite the coupling using only 2 smaller matrices $\overline{\gamma}^0, \overline{\gamma}^1 \in \mathbb{R}^{N\times N}$ since

$$\overline{\gamma}_{j_0,\dots,j_K} = \left(\prod_{k=0}^{K-1} \overline{\gamma}^0_{j_k,j_{k+1}}\right) \overline{\gamma}^1_{j_K\sigma(j_1)} \tag{7.46}$$

$$\text{where} \quad \overline{\gamma}^0_{\alpha,\beta} = \exp(-\frac{D_{\alpha\beta}}{\varepsilon}), \qquad \overline{\gamma}^1_{\beta,\alpha} = \exp(-\frac{D_{\beta\sigma(\alpha)}}{\varepsilon}).$$

and $D_{\alpha\beta} = \|x_\alpha - x_\beta\|^2$. We recall that all the marginals are equal to (a discretization of) the Lebesgue measure and $\{x_i\}_i$ are discretized on the unit cube $[0,1]^d$. It is obvious that we can apply the IPFP procedure described in (7.39) since all the sets $\mathcal{C}_k$ are affine. However, one can notice that the sum in (7.39), namely the push-forward S_k could be computationally onerous, but thanks to (7.46) we can rearrange it as

$$a^{k,(n)}_{j_k} = \frac{1/K}{B_{j_k,j_k}}$$

where $a^{k,(n)}$ is the k^{th} vector at step (n) and B is the the product of $K+1$ smaller $N \times N$ matrices

$$B = \overline{\gamma}^{\text{init}} \bigotimes_{\ell=1}^{K-1} \tilde{\overline{\gamma}}_\ell \quad \text{with} \quad \overline{\gamma}^{\text{init}} = \begin{cases} \overline{\gamma}^0 & \text{for} \quad k \neq K, \\ \overline{\gamma}^1 & \text{otherwise} \end{cases}$$

$$\text{and} \quad \tilde{\overline{\gamma}}_\ell = \begin{cases} \text{diag}(a^{\sigma^k(\ell),(n)}) \otimes \overline{\gamma}^0 & \text{for} \quad \sigma^k(\ell) \neq K \quad \text{and} \quad \sigma^k(\ell) < k, \\ \text{diag}(a^{\sigma^k(\ell),(n-1)}) \otimes \overline{\gamma}^0 & \text{for} \quad \sigma^k(\ell) \neq K \quad \text{and} \quad \sigma^k(\ell) > k, \\ \text{diag}(a^{K,(n-1)}) \otimes \overline{\gamma}^1 & \text{otherwise,} \end{cases}$$

where $\otimes$ is the standard matrix product and we use the convention that diag of vector is the diagonal matrix with vector values and diag of matrix is the vector of its diagonal. We also highlight that, to use the simplification the a^ℓ must be ordered in the correct way so that the computation of the sum for the k^{th} update starts at $k+1$ and finishes at $k-1$. We have introduced the circular permutations $\sigma^k(\ell) = (\ell + k \mod K)$ which returns the $(\sigma^k(\ell))^{\text{th}}$ term at the ℓ^{th} position of the product.

Each iteration of the IPFP procedure therefore only involves $(2K)$ 2-coupling matrices multiplications and only requires storing K vectors and the 2-coupling cost matrices $\overline{\gamma}^0$ and $\overline{\gamma}^1$. The computation of the 2-coupling maps (7.44) can be simplified with the same remark.

7.5.4 1 dimension experiments

Figures 7.3, 7.4 and 7.5 show $\gamma_{0,k}$ for three test cases in dimension $d = 1$ proposed in [23]. The computation is performed with a uniform discretization $(x_i)_i$ of $[0,1]$ with $N = 200$ points, $\varepsilon = 10^{-3}$ and $K + 1 = 16$. They agree with the solutions produced by Brenier and the mass spreading of the generalized flow is nicely captured by the 2 marginals couplings (7.44). In figure 7.6 we show the displacement of the mass originally located at a fixed point $\overline{x}_s$ when the final configuration is given by $g^\star(x) = 1 - x$. In particular we are plotting the set $\Gamma_s := \{(x_i, t_k) \in [0,1]^2 \mid (\gamma_{1,k})_{s,i} > 0\}$. Notice that this is the case presented in remark 6.2.10 and that we retrieve, taking into account the effect of the entropy, the analytical solution (figure 6.2) found by Brenier.

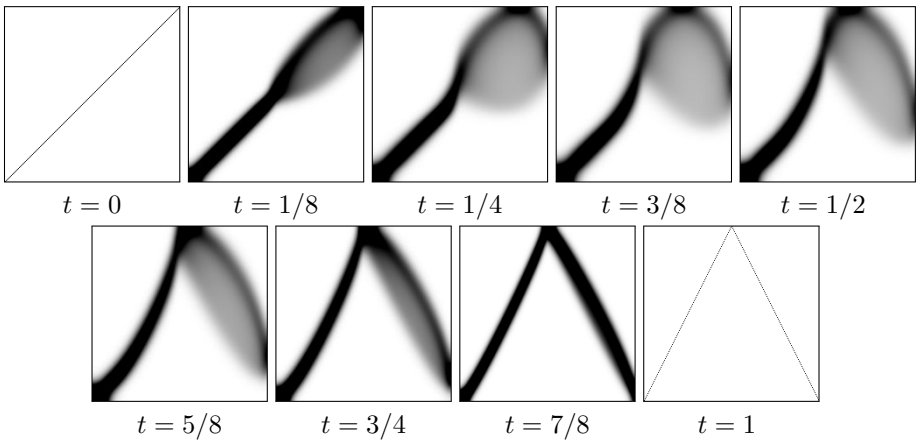

Figure 7.3: *Display of $\gamma_{0,k}$ showing the evolution of the fluid particles from x to $g^\star(x) = \min(2x, 2-2x)$ for $x \in [0,1]$. The corresponding time is $t = \frac{k-1}{K-1} \in [0,1]$.*

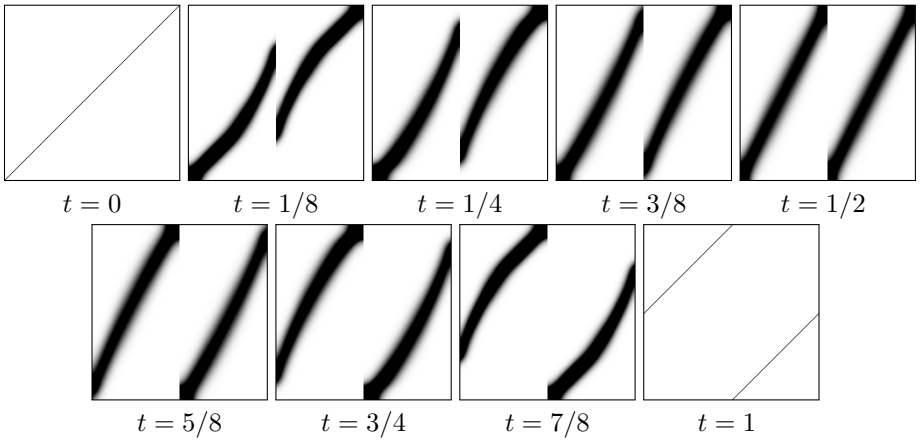

Figure 7.4: *Same as Figure 7.3 for the map $g^\star(x) = (x + 1/2)$ mod 1 for $x \in [0,1]$.*

7.5.5 2 dimension experiment: the Beltrami flow

Consider the unit square $\mathcal{D} = [0,1]^2$ and the Beltrami flow obtained from the following time-independent velocity and pressure fields (one can verify that they solve the steady Euler equations):

$$u(x_1, x_2) = (-\cos(\pi x_1)\sin(\pi x_2), \sin(\pi x_1)\cos(\pi x_2)),$$
$$p(x_1, x_2) = \frac{1}{2}(\sin(\pi x_1)^2 + \sin(\pi x_2)^2).$$

Then one can compute the Hessian of the pressure $\nabla^2 p$ and find that the maximum eigenvalue is π^2 which suggests that the critical time is $T_{max} = 1$. Indeed we remind that we have deterministic solutions when all the eigenvalues of $\nabla^2 p$ are strictly smaller than $\dfrac{\pi^2}{T}$ for a given final time T. The matrix $\overline{\gamma}^1_{ij}$ is now given by $\overline{\gamma}^1_{ij} = \exp\left(\frac{\|g^\star(x_1) - x_K\|^2}{\varepsilon}\right)$ where $g^\star$ is the solution to the Cauchy prob-

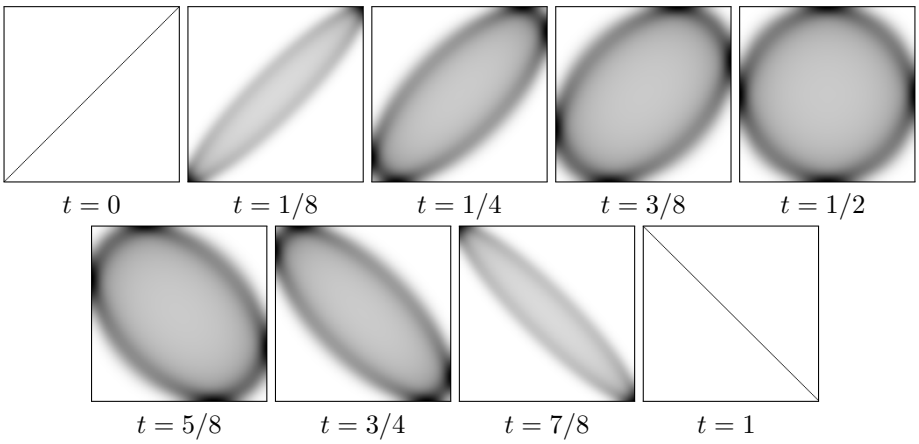

Figure 7.5: *Same as Figure 7.3 for the map* $g^\star(x) = 1 - x$ *for* $x \in [0, 1]$.

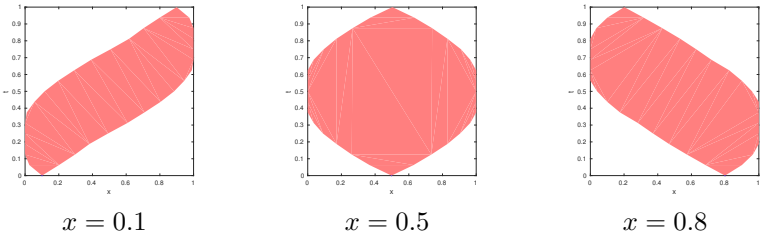

Figure 7.6: *Displacement of the mass initially located at* $x = 0.1$, $x = 0.5$ *and* $x = 0.8$ *for* $g^\star(x) = 1 - x$ *(third row)*

lem (6.2) at the given final time T. In this case, we cannot simply visualize the matrix $\gamma_{1,k}$ as it is a 4-dimension matrix, so we consider the following quantities:

$$(\gamma_k^1)_j = \sum_{i \in I_1} (\gamma_{1,k})_{ij}, \quad (\gamma_k^2)_j = \sum_{i \in I_2} (\gamma_{1,k})_{ij}, \quad (\gamma_k^3)_j = \sum_{i \in I_3} (\gamma_{1,k})_{ij}, \tag{7.47}$$

where I_1, I_2 and I_3 are defined as follows

$$I_1 := \{i \in \{1, \cdots N\} \mid (x_1^i, x_2^i) \in \left[0, \frac{1}{3}\right] \times [0, 1]\},$$
$$I_2 := \{i \in \{1, \cdots N\} \mid (x_1^i, x_2^i) \in \left(\frac{1}{3}, \frac{2}{3}\right] \times [0, 1]\},$$
$$I_3 := \{i \in \{1, \cdots N\} \mid (x_1^i, x_2^i) \in \left(\frac{2}{3}, 1\right] \times [0, 1]\},$$

where $\{((x_1^i, x_2^i)\}_{i=1}^N$ is a discretization of $[0, 1]^2$. As one can see in figures 7.7, 7.11 and 7.15, we plot the support of the quantities γ_k^1, γ_k^2 and γ_k^3 by using three different colors; moreover if mixture of mass occurs (which means that the solution γ is not deterministic) then we expect overlaps of the supports of γ_k^ℓ. In figures 7.8, 7.9 and 7.10 we show the support of γ_k^1 (red), γ_k^2 (green) and γ_k^3 (blue) for $T = 0.9$; notice that no overlaps among the three supports occur (excluding the diffusion effect due both to the discretization and the regularization) On the contrary if we look at figures 7.12, 7.13, 7.14 and 7.16, 7.17 and 7.18, we can see, as expected, and overlap among the supports. Figures 7.7, 7.11 and 7.15

show γ_k^1, γ_k^2 and γ_k^3 for three test cases and the solution of the corresponding Cauchy problem. We remark that a small error appear at the boundaries of the domain if we compare the solution of the Cauchy problem with the generalized one at the last time step, this probably due to the discretization used to obtain the final $g^\star$; a finer grid could provide a better result. All the computations are performed with a uniform discretization of $[0,1]^2$ with $N = 64 \times 64$, $\varepsilon = 10^{-4}$ and $K + 1 = 16$. The solution of the Cauchy problem are computed by using an explicit Euler method for the time derivative and a discretization of $[0,1]^2$ with $N = 500 \times 500$. The simulation in figure 7.7 has been obtained by taking a final time $T = 0.9$, which means that the inequality (6.20) is satisfied. Indeed we can observe that no mixture of mass happens. On the contrary, simulations in 7.11 and 7.15 are performed by taking $T = 1.3$ and $T = \pi$ respectively ($T > T_{max}$) and we can notice that a split of mass occurs (although the solution appears "more deterministic" than the one to the unit disk that we present in the next paragraph); moreover the generalized solutions differ from the one of the Cauchy problem as we can see a clockwise rotation in the middle of the square and a counterclockwise rotation near the boundary. Notice that our solutions are in accordance with ones provided in [93] (see also [64] where the authors provide a numerical method to solve the Cauchy problem). All these simulation take approximately a CPU time of 3 hours, this means that the code must be parallelized in order to become competitive.

7.5.6 2 dimension experiment: the unit disk

On the unit disk $\mathcal{D} := \{(x_1, x_2) \in \mathbb{R}^2 \mid x_1^2 + x_2^2 \leqslant 1\}$, a solution to stationary Euler equations is given by the following pressure and velocity field

$$p(x_1, x_2) = \frac{1}{2}(x_1^2 + x_2^2), \tag{7.48}$$

$$u(x_1, x_2) = (-x_2, x_1), \tag{7.49}$$

and if we solve the Cauchy problem (6.2), the corresponding flow map $g(t)$ is the rotation of angle t.

It is easy to see that the generalized incompressible flow $\gamma_{g_\pm}$ induced by the clockwise and counterclockwise rotations of angle $t \in [0, \pi]$,

$$g_\pm(t) = (x_1 \cos(t) \mp x_2 \sin(t), \pm x_1 \sin(t) + x_2 \cos(t)),$$

connect $g_\star = \mathrm{Id}_\mathcal{D}$ to $g^\star = -\mathrm{Id}_\mathcal{D}$ at time $T = \pi$ and are concentrated on the solution of

$$\ddot{x}(t) = -x(t)$$

, which is exactly the ODE (6.19) for the pressure field in (7.48). As the maximum eigenvalue of the $\nabla^2 p$ is 1 at every point in $\mathcal{D}$ then the inequality (6.20) is satisfied for any final time T such that $T \leqslant T_{max}$ where $T_{max} = \pi$. Then, by applying theorem 6.2.15 one can deduce that both γ_{g_+} and γ_{g_-} are minimizers of (6.10); moreover, thanks to corollary 6.2.16 we have that for any $T < T_{max}$ the flows γ_{g_+} and γ_{g_-} are the unique minimizers of problem (6.10) between $g_\star = \mathrm{Id}_\mathcal{D}$ and $g^\star = g_+(T, \cdot)$ and $g^\star = g_-(T, \cdot)$, respectively. As $T = \pi$ the loss of uniqueness is not limited to the previous example ($\gamma_\pm$ are both solutions of (6.10) at $T = \pi$), but it is also due to the existence of non-deterministic solution. An explicit example of non-deterministic generalized solution was already

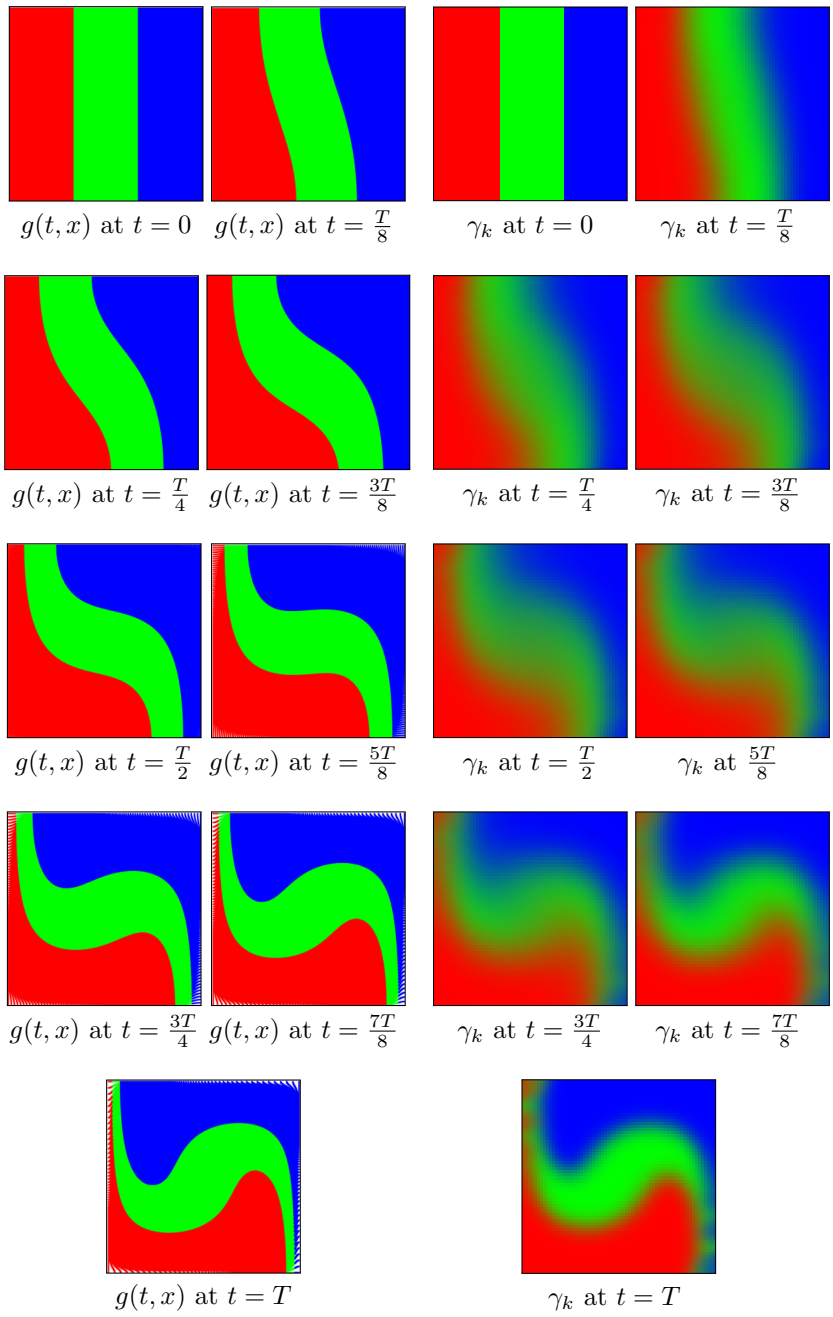

Figure 7.7: *Display the evolution of the fluid particles from $x \in [0,1]^2$ to the solution of the Cauchy problem at $T = 0.9$ for the Beltrami's flow. We plot the solution of the Cauchy problem $g(t,x)$ and the support of γ_k^1 (red), γ_k^2 (green) and γ_k^3 (blue).*

discovered by Brenier in [20]: given a point $x \in \mathcal{D}$ and a velocity field u, denote by $\omega_{x,u}$ the curve $\omega_{x,u}(t) = x\cos(t) + u\sin(t)$, $t \in [0,1]$. Then, the solution is obtained as the push-forward by the map $(x,u) \mapsto \omega_{x,u}$ of the following measure

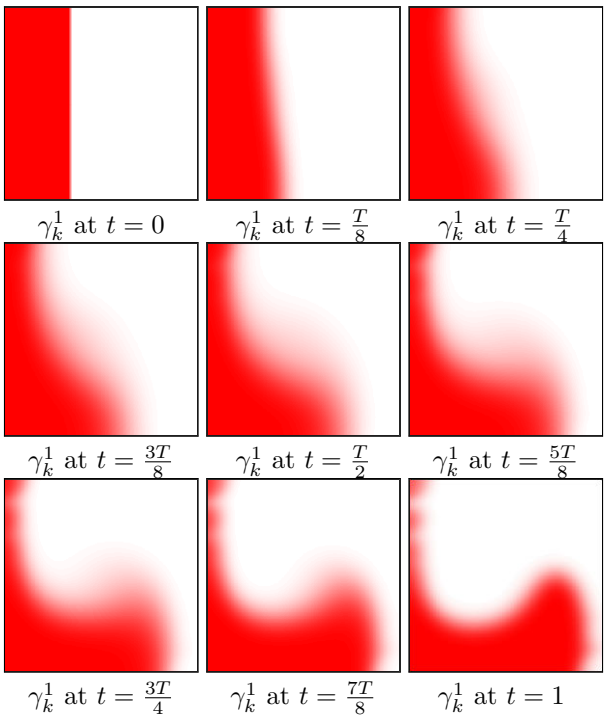

Figure 7.8: *Display the support* γ_k^1 *at each timestep* $t = \frac{kT}{K}$ *for* $T = 0.9$.

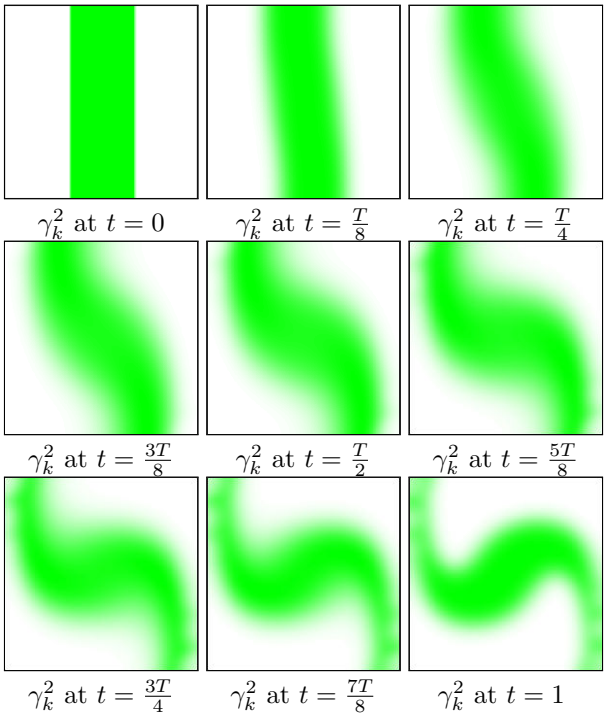

Figure 7.9: *Display the support* γ_k^2 *at each timestep* $t = \frac{kT}{K}$ *for* $T = 0.9$.

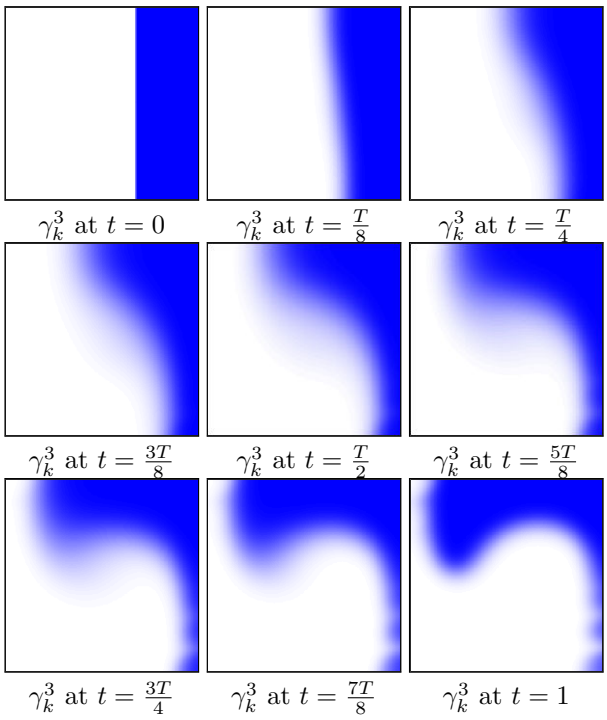

Figure 7.10: *Display the support γ_k^3 at each timestep $t = \frac{kT}{K}$ for $T = 0.9$.*

on $\mathcal{D} \times \mathbb{R}^2$

$$\gamma(dx, du) = \frac{1}{\pi}\mathcal{H}^2(dx) \otimes \frac{1}{2\pi\sqrt{1-|x|^2}}\mathcal{H}^1|_{\{|u|=\sqrt{1-|x|^2}\}}(du), \tag{7.50}$$

where $\mathcal{H}^\ell$ denotes the $\ell-$dimensional Hausdorff measure. Notice that this non-deterministic flow spreads each particle of fluid uniformly in all directions, see figure 7.19. Moreover, Bernot et al. (see [11]) proved that the set of solutions to (6.10) is very rich.. In order to visualize the solution, we consider the coupling $\gamma_{1,k}$, we fix a position $\overline{x}_{\bar{i}} = (x_1^{\bar{i}}, x_2^{\bar{i}})$ at $t = 0$ and we look at the evolution of the quantity $(\gamma_{1,k}^{\overline{x}})_j = (\gamma_{1,k})_{\bar{i}j}$. So it is clear that if the solution is deterministic then we should visualize a dirac by plotting $\gamma_{1,k}^{\overline{x}}$. On the contrary if the solution is not deterministic then $\gamma_{1,k}^{\overline{x}}$ represents how the mass is displaced between the initial and the final configuration. Figures 7.20 and 7.21 show the support and the surface of $\gamma_{1,k}^{\overline{x}}$ for two different $\overline{x}$. The simulations are performed on a discretization $\{x_i := (x_1^i, x_2^i)\}_{i=1}^N$ of $\mathcal{D}$ with $N = 64 \times 64$, $\varepsilon = 10^{-4}$, $T = \pi$ and $K + 1 = 17$. As expected the solution is not deterministic; indeed we retrieve a solution, among all the possible ones, which spread the mass as much as possible: we remind that if non-uniqueness holds for the OT problem then the solution of the regularized problem converges toward the one with minimal entropy, namely the "most diffuse".

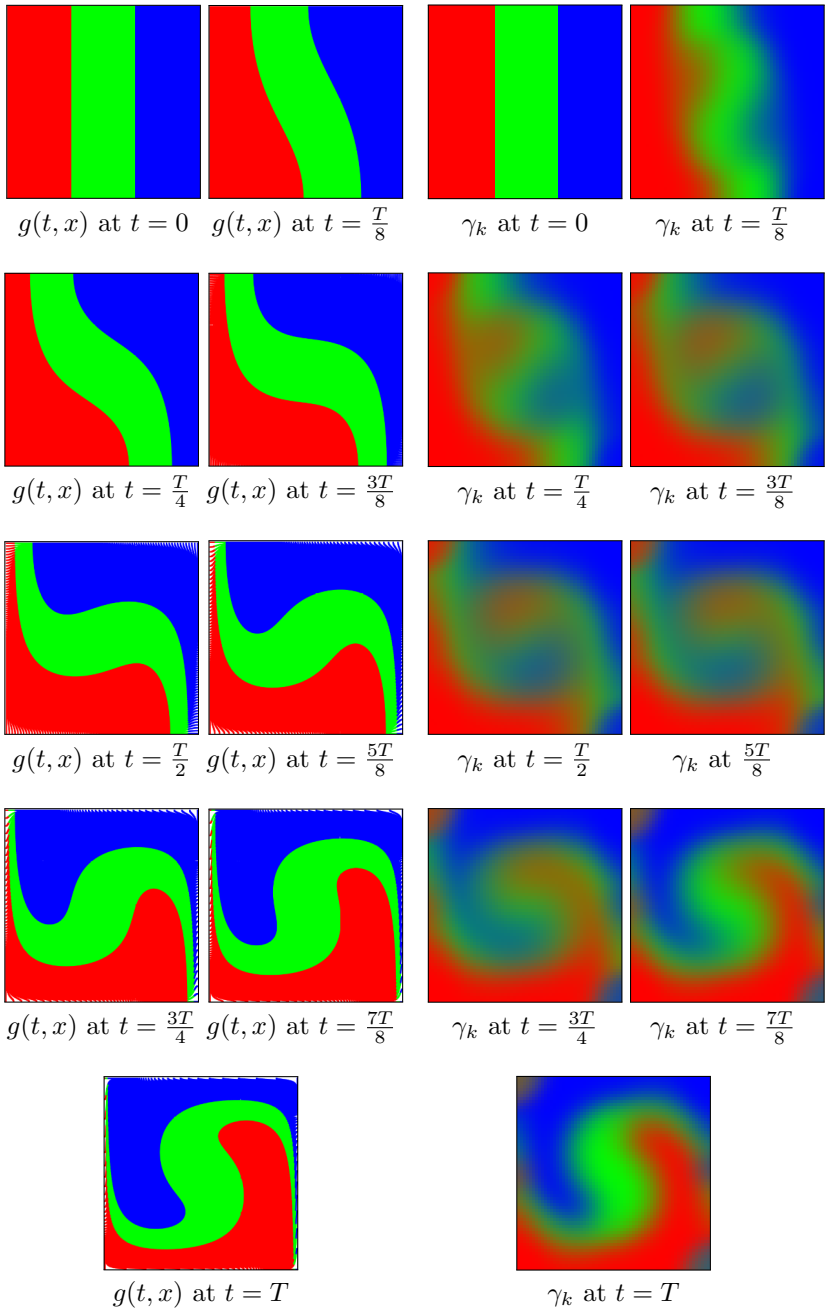

Figure 7.11: *Display the evolution of the fluid particles from $x \in [0,1]^2$ to the solution of the Cauchy problem at $T = 1.3$ for the Beltrami's flow. We plot the solution of the Cauchy problem $g(t,x)$ and the support of γ_k^1 (red), γ_k^2 (green) and γ_k^3 (blue).*

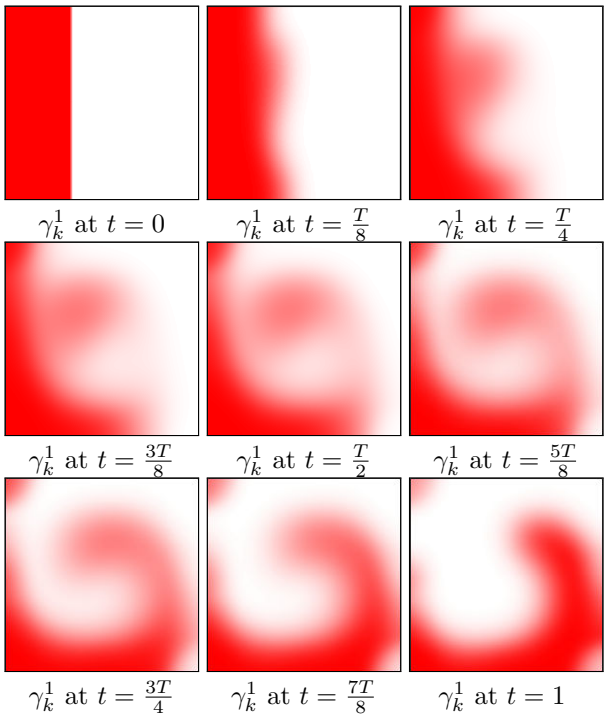

Figure 7.12: *Display the support* γ_k^1 *at each timestep* $t = \frac{kT}{K}$ *for* $T = 1.3$.

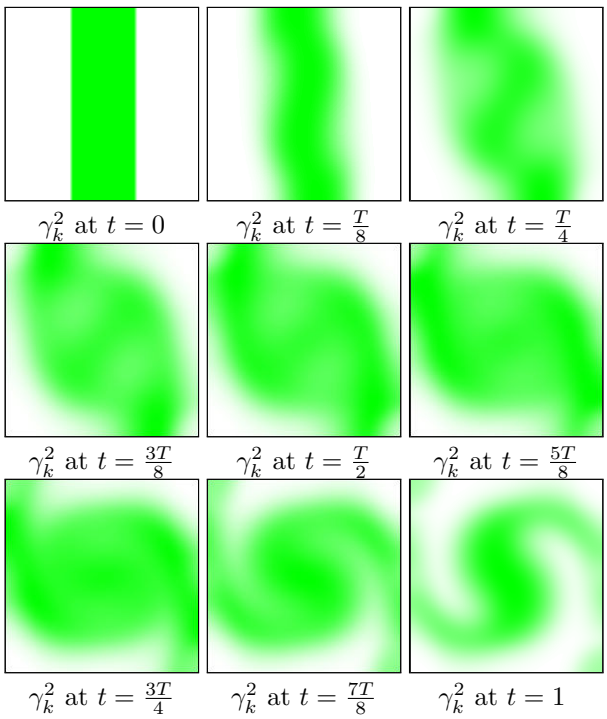

Figure 7.13: *Display the support* γ_k^2 *at each timestep* $t = \frac{kT}{K}$ *for* $T = 1.3$.

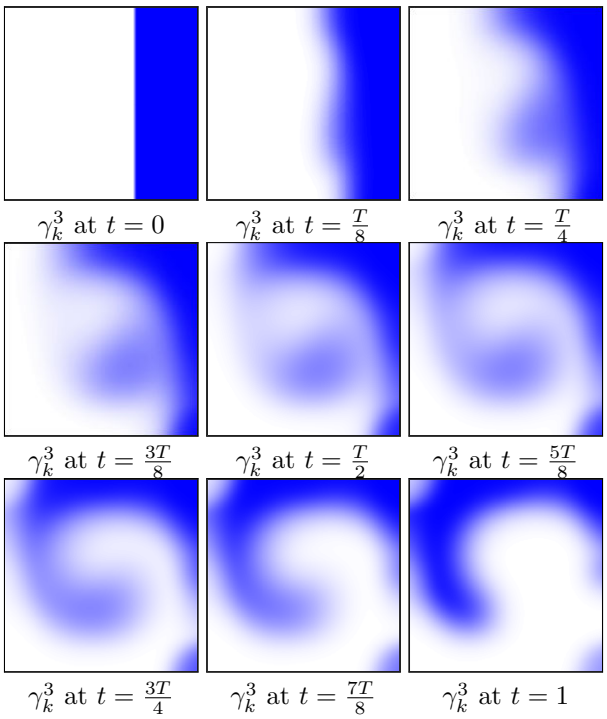

Figure 7.14: *Display the support γ_k^3 at each timestep $t = \frac{kT}{K}$ for $T = 1.3$.*

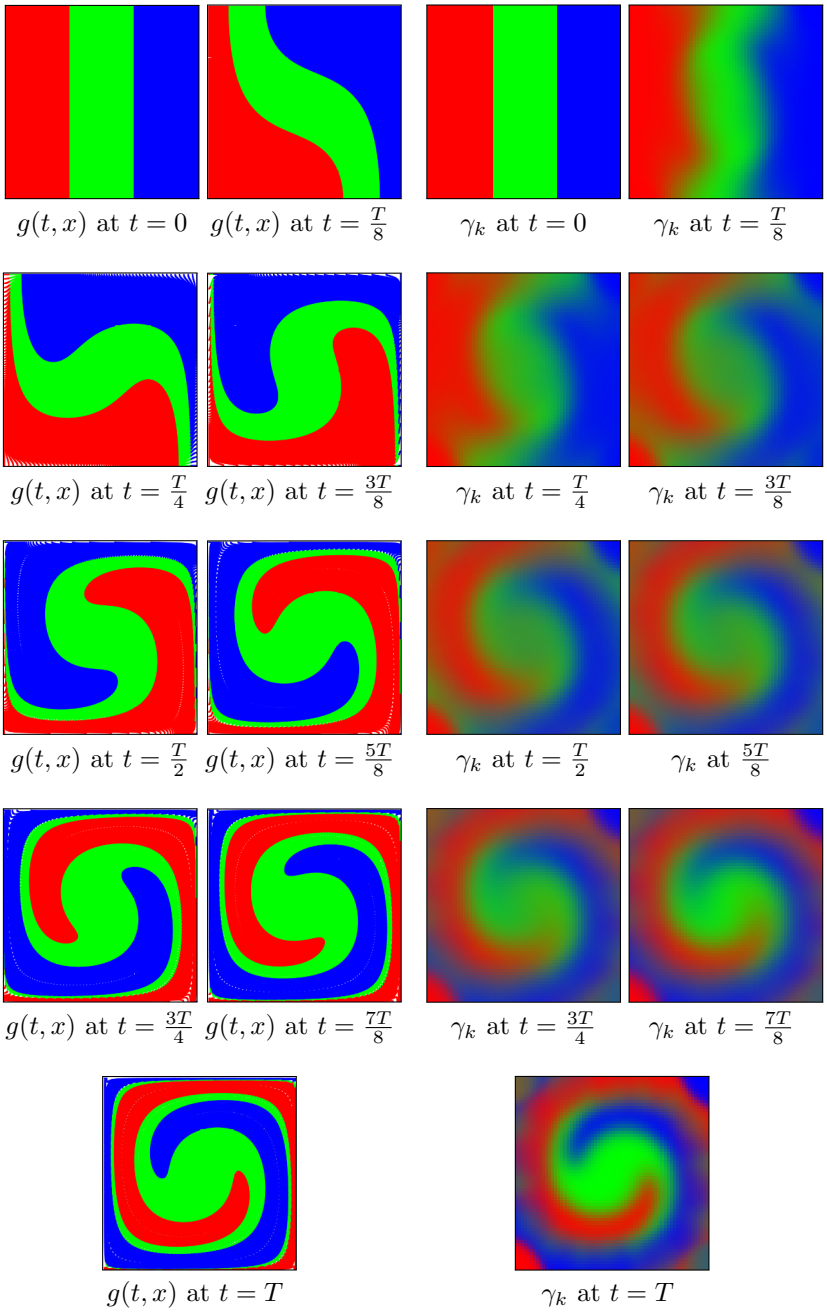

Figure 7.15: *Display the evolution of the fluid particles from $x \in [0,1]^2$ to the solution of the Cauchy problem at $T = \pi$ for the Beltrami's flow. We plot the solution of the Cauchy problem $g(t,x)$ and the support of γ_k^1 (red), γ_k^2 (green) and γ_k^3 (blue).*

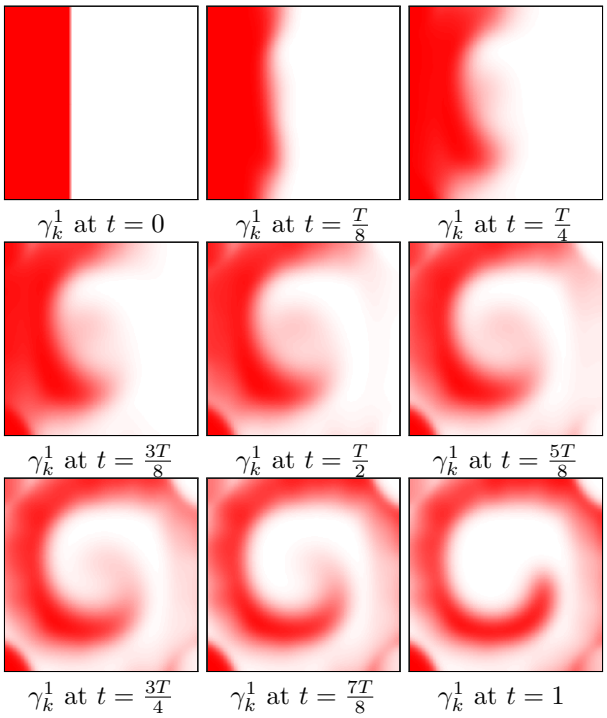

Figure 7.16: *Display the support γ_k^1 at each timestep $t = \frac{kT}{K}$ for $T = 1.3$.*

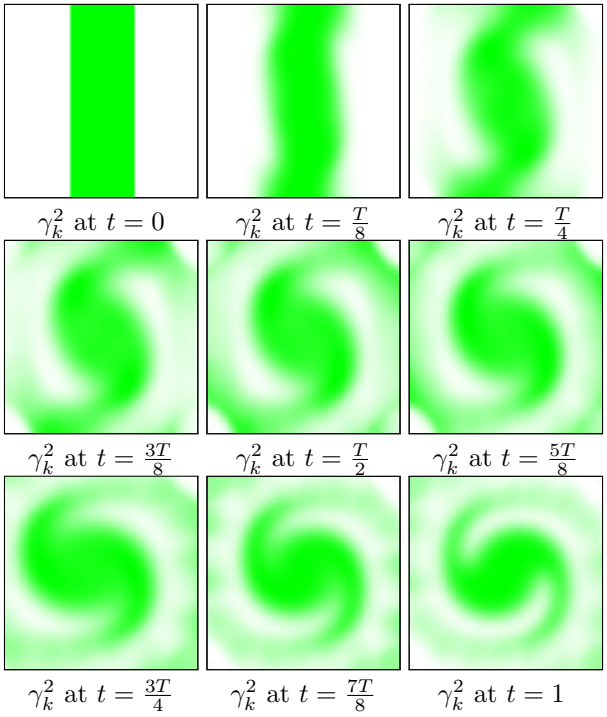

Figure 7.17: *Display the support γ_k^2 at each timestep $t = \frac{kT}{K}$ for $T = 1.3$.*

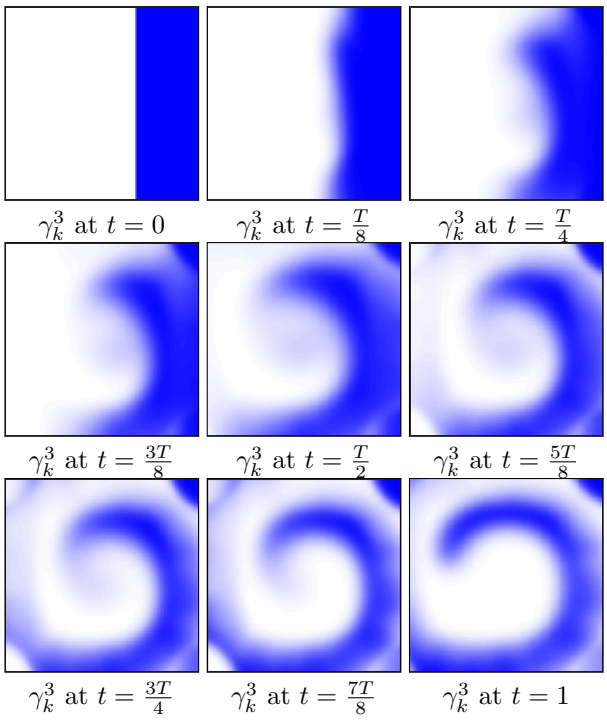

Figure 7.18: *Display the support* γ_k^3 *at each timestep* $t = \frac{kT}{K}$ *for* $T = \pi$.

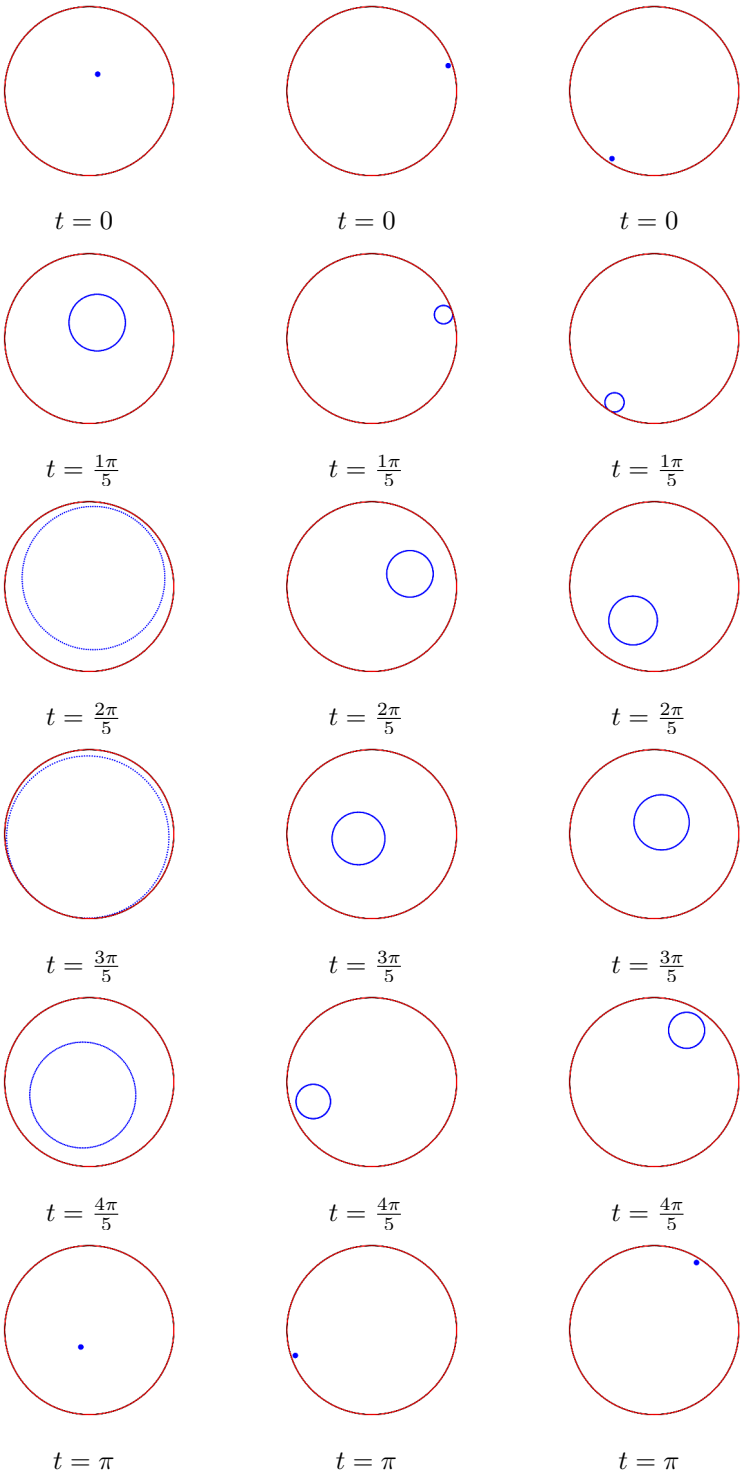

Figure 7.19: *Display the trajectories of three particles initally located at* x_i, $i = 1, 2, 3$ *at different time* t.

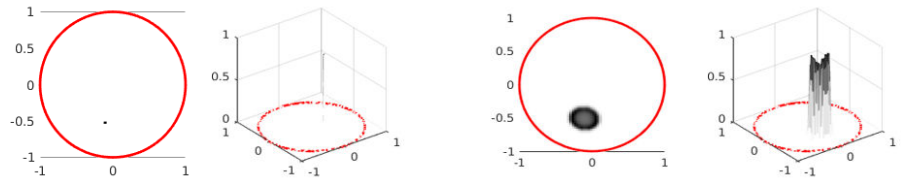

Support at $t = 0$ Surface at $t = 0$ Support at $t = \frac{2\pi}{K}$ Surface at $t = \frac{2\pi}{K}$

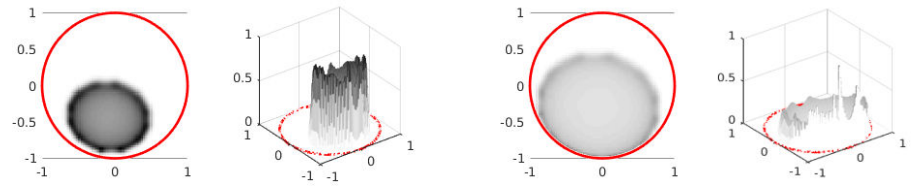

Support at $t = \frac{4\pi}{K}$ Surface at $t = \frac{4\pi}{K}$ Support at $t = \frac{6\pi}{K}$ Surface at $t = \frac{6\pi}{K}$

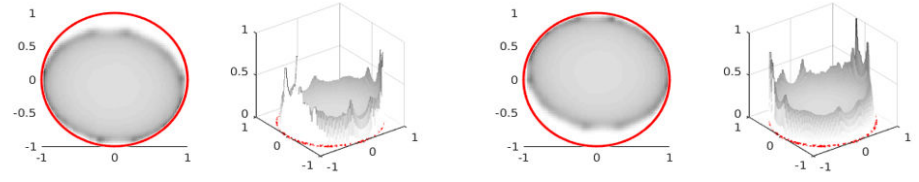

Support at $t = \frac{8\pi}{K}$ Surface at $t = \frac{8\pi}{K}$ Support at $t = \frac{10\pi}{K}$ Surface at $t = \frac{10\pi}{K}$

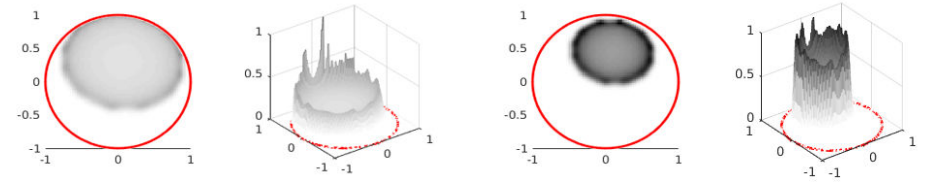

Support at $t = \frac{12\pi}{K}$ Surface at $t = \frac{12\pi}{K}$ Support at $t = \frac{14\pi}{K}$ Surface at $t = \frac{14\pi}{K}$

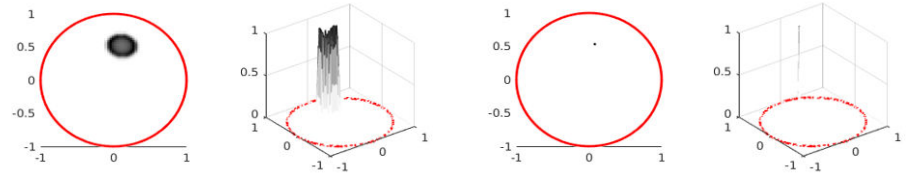

Support at $t = \frac{16\pi}{K}$ Surface at $t = \frac{16\pi}{K}$ Support at $t = \frac{K\pi}{K}$ Surface at $t = \frac{K\pi}{K}$

Figure 7.20: *Display the support and the surface of* $\gamma^{\overline{x}}_{1,k}$ *for a particle at* $\overline{x}$ *at* $t = 0$.

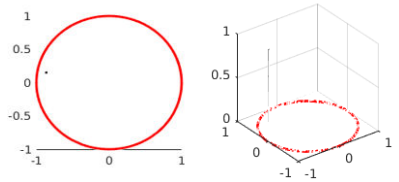

Support at $t = 0$ Surface at $t = 0$

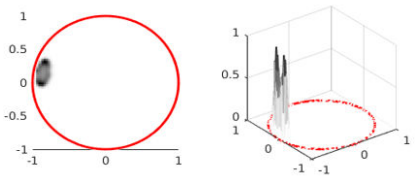

Support at $t = \frac{2\pi}{K}$ Surface at $t = \frac{2\pi}{K}$

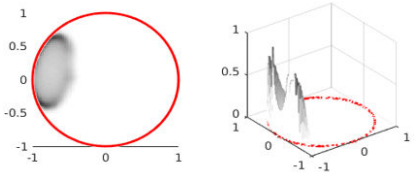

Support at $t = \frac{4\pi}{K}$ Surface at $t = \frac{4\pi}{K}$

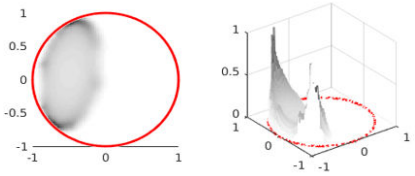

Support at $t = \frac{6\pi}{K}$ Surface at $t = \frac{6\pi}{K}$

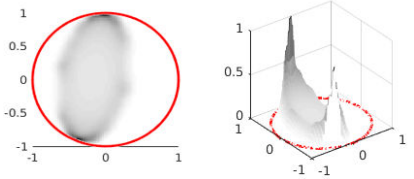

Support at $t = \frac{8\pi}{K}$ Surface at $t = \frac{8\pi}{K}$

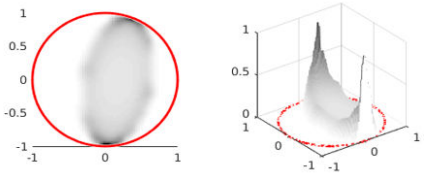

Support at $t = \frac{10\pi}{K}$ Surface at $t = \frac{10\pi}{K}$

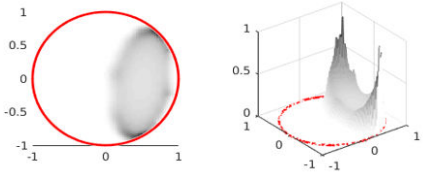

Support at $t = \frac{12\pi}{K}$ Surface at $t = \frac{12\pi}{K}$

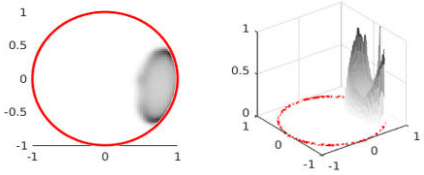

Support at $t = \frac{14\pi}{K}$ Surface at $t = \frac{14\pi}{K}$

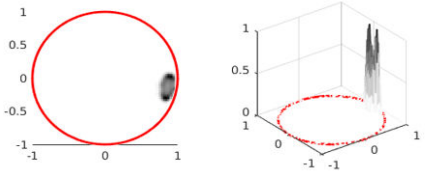

Support at $t = \frac{16\pi}{K}$ Surface at $t = \frac{16\pi}{K}$

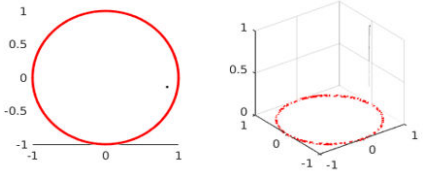

Support at $t = \frac{K\pi}{K}$ Surface at $t = \frac{K\pi}{K}$

Figure 7.21: *Display the support and the surface of* $\gamma_{1,k}^{\overline{x}}$ *for a particle at* $\overline{x}$ *at* $t = 0$.

Chapter 8

Repulsive Optimal Transport

In this chapter we want to introduce a particular class of cost functions, the so-called repulsive costs. As we will explain in the last part of this thesis, the main motivation which led us to study this kind of optimal transport problem arises from the Density Functional Theory where some interesting costs, as the Coulomb one or the repulsive harmonic, play a central role. From a mathematical perspective the interesting case is when all marginals of the coupling γ in $(\mathcal{MK}_K)$ are absolutely continuous with respect to Lebesgue measure and are all the same. In particular, since the cost functions are *"repulsive"*, if Monge-type solutions exists, they should follow the rule *"the further, the better!"*, which means that we want to move the mass as much as we can. In other words, in the present case, optimal transport plans tend to be as spread as possible. Before introducing the repulsive optimal transport, it would be interesting to have a formal definition of *repulsive cost*. Indeed this is quite difficult since usually this concept is based on the intuition that comes solving the particular problem. Anyway, we can try to define a repulsive cost as follows

Definition 8.0.1 (Repulsive cost)**.** *Given a cost $c : \mathbb{R}^{dK} \to \mathbb{R}$, we say that it is repulsive if it satisfies the following condition for all the possible pair (x_i, x_j) with $i \neq j$*

$$c(x_1, \cdots, x_i, \cdots, x_i, \cdots, x_K) + c(x_1, \cdots, x_j, \cdots, x_j, \cdots, x_K) \geqslant$$
$$c(x_1, \cdots, x_i, \cdots, x_j, \cdots, x_K) + c(x_1, \cdots, x_j, \cdots, x_i, \cdots, x_K).$$

Here we will treat only the case of the repulsive harmonic cost and the determinant cost, showing that the set of optimal solutions can be very rich, where as we will devote the last part of the thesis to the physical motivation and to the study of the Coulomb cost.

8.1 Multi-marginal OT with repulsive Harmonic Cost

This section is devoted to the study of the repulsive harmonic cost.

More precisely, we are interested in characterizing the minimizers of the following problem

$$(\mathcal{MK}_{weak}) \qquad \min_{\gamma\in\Pi(\mathbb{R}^{dK};\mu_1,\cdots,\mu_K)} \int_{\mathbb{R}^{dN}} \sum_{i,j=1}^{K} -|x_j - x_i|^2 d\gamma(x_1,\dots,x_K), \qquad (8.1)$$

where $\mu_1,\dots,\mu_K$ are absolutely continuous probability measures in $\mathbb{R}^d$.

From a mathematical viewpoint this cost has some advantages compared to some others repulsive cost as the Coulomb one. Indeed, from a technical point of view, this problem is an interesting toy model to approach the case of Coulomb cost. From applications, some minimizers of (8.1) seem to have no particular relevance in physics because, as we will see in the examples 8.1.10, 8.1.11 and 8.1.12 below, certain optimal γ of (8.1) allow particles to overlap.

We will see that the set of solutions has a very rich structure which is different from the standard 2-marginal case. From now on we consider only marginals $\mu_i \in \mathcal{P}(\mathbb{R}^d)$ having finite second moment. First of all we notice that minimizers of this problem are also minimizers of the problem with the cost $c(x_1,\dots,x_n) = |x_1+\dots+x_n|^2$; in fact we have that

$$\int_{\mathbb{R}^{dK}} \sum_{i,j=1}^{K} -|x_i - x_j|^2 \, d\gamma = 2\int_{\mathbb{R}^{dK}} c\, d\gamma - (K+1)\sum_{i=1}^{K}\int_{\mathbb{R}^d} |x|^2 \, d\mu_i,$$

but this last additive term depends only on the marginals and not on the specific plan γ. The cost c is very particular since it has a wide class of "trivial" optimal plans, that is the ones that are concentrated on $x_1+\dots+x_K=0$; however the structure is very rich, see Lemma 8.1.3.

Concerning the existence of minimizers of (8.1), we will assume that the measures μ_i have finite second moments; then existence follows immediately from the equality

$$\operatorname*{argmin}_{\gamma} \int -\sum_{i=1}^{K}\sum_{j=i+1}^{K} |x_j - x_i|^2 d\gamma = \operatorname*{argmin}_{\gamma} \int |x_1+\dots+x_K|^2 d\gamma.$$

In particular, Corollary 7.1.26 holds in this case too. Notice that the fact that the repulsive harmonic cost is smooth and has linear gradient does not make the Multi-marginal Optimal Transportation problem easier compared to the Coulomb cost. In fact, in this case the problem is that if we write down the optimality conditions for the potentials, in the case described in Lemma 8.1.3, we simply find the condition $x_1+\dots+x_K = const$, since in this case the potentials are linear functions.

However, we can enjoy the symmetries of this problem and build easy Monge solutions for some particular cases of (8.1), see examples 8.1.9, 8.1.10, 8.1.11, 8.1.12 and 8.1.14 below.

Before stating the main result in the multi-marginal setting, we start analyzing the problem (8.1) in the 2-marginals case, where everything seems to work fine, just as in the square distance case.

Proposition 8.1.1 ([DMGN15]). *Let $\mu,\nu\in\mathcal{P}(\mathbb{R}^d)$ and $c(x,y) = -|x-y|^2$ be the opposite of the square-distance in $\mathbb{R}^d$. Suppose that μ is absolutely continuous*

with respect to the Lebesgue measure in $\mathbb{R}^d$ and ν has no atoms. Then, there exists a unique optimal transport map $T : \mathbb{R}^d \to \mathbb{R}^d$ for the problem

$$\min\left\{\int c(x,y)d\gamma \mid \gamma \in \Pi(\mathbb{R}^d;\mu,\nu)\right\} = \inf\left\{\int c(x,T(x))d\mu \mid T_\sharp\mu = \nu\right\}$$

Moreover, $T = \nabla\varphi$, where $\varphi : \mathbb{R}^d \to \mathbb{R}$ is a concave function and there exists a unique optimal transport plan $\overline{\gamma}$, that is $\overline{\gamma} = (\mathrm{Id}, T)_\sharp\mu$.

Proof. This result is an easy consequence of the Brenier's theorem. Indeed, it is enough to verify that, taking $C = 2\int |x|^2\, d\mu + 2\int |x|^2\, d\nu$, we have

$$C + \inf_{T_\sharp\mu=\nu}\int -|x - T(x)|^2 d\mu(x) = \inf_{G_\sharp\mu=\tilde{\nu}}\int |x - G(x)|^2 d\mu(x)$$

where $G = -T$ and $\tilde{\nu} = (-\mathrm{Id})_\sharp\nu$. Then by Brenier's theorem there exists an unique optimal map G which can be written as $G(x) = \nabla\psi(x)$, and $\psi : \mathbb{R}^d \to \mathbb{R}$ is a convex map. In other words, T is a gradient of a concave function. □

Notice that if we suppose $\mu = f(x)dx$ and $\nu = g(x)dx$ are probability measures with densities f, g concentrated, respectively, on convex sets Ω_f, Ω_g and assume there exits a constant $\lambda > 0$ such that $\lambda \leqslant f, g \leqslant 1/\lambda$, then T is a $C^{1,\alpha}$ function inside Ω_f [28, 29].

Example 8.1.2 (2 marginals case, uniform measure in the d-dimensional cube)**.** *Suppose that $\mu = \nu = \mathcal{L}\big|_{[0,1]^d}$. In this case, we can verify easily that the optimal map $T : [0,1]^d \to [0,1]^d$ is given by the anti-monotone map $T(x) = (1,\dots,1) - x$.*

Surprisingly, the next theorem says that we can not always expect Caffarelli's regularity for the optimal transport maps for the repulsive harmonic cost with finitely many marginals $K > 2$ even when the support of the measures has convex interior (see corollary 8.1.8 below). Before stating the theorem we will prove a lemma that characterizes the optimal plans:

Lemma 8.1.3 ([DMGN15])**.** *Let $\{\mu_i\}_{i=1}^K$ be probability measures on $\mathbb{R}^d$ and $h : \mathbb{R}^d \to \mathbb{R}$ be a strictly convex function and suppose $c : ([0,1]^d)^K \to \mathbb{R}$ a cost function of the form $c(x_1,\dots,x_K) = h(x_1 + \cdots + x_K)$. Consider a plan $\gamma \in \Pi(\mu_1,\dots,\mu_K)$, then $\mathrm{supp}(\gamma) \subset \{x_1 + \ldots + x_K = a\}$ (with $a \in \mathbb{R}$) is a necessary and sufficient condition for γ to be optimal. In this case we will say that γ is a flat optimal plan and $\{\mu_i\}_{i=1}^K$ is a flat K-tuple of measures.*

Proof. First of all we show that k is fixed by the marginals μ_i, and it is in fact the sum of the barycenters of these measures. Let $c_i = \int x\, d\mu_i$; then let us suppose that there exists $\gamma \in \Pi(\mathbb{R}^{dK};\mu_1,\cdots,\mu_K)$ that is concentrated on $\{x_1 + \ldots + x_K = a\}$. Then, using that the i-th marginal of γ is μ_i, we can compute

$$k = \int (x_1 + \ldots + x_K)\, d\gamma = \sum_{i=1}^K \int x_i\, d\gamma = \sum_{i=1}^K \int x\, d\mu_i = \sum_{i=1}^K c_i.$$

In particular we notice also that for every admissible plan $\tilde{\gamma}$ we have $\int (x_1 + \ldots + x_K)\, d\tilde{\gamma} = a$ and so by Jensen inequality we have

$$\int h(x_1{+}\ldots{+}x_K)\, d\tilde{\gamma} \geqslant h\left(\int (x_1 + \ldots + x_K)\, d\tilde{\gamma}\right) = h(a) = \int h(x_1{+}\ldots{+}x_K)\, d\gamma.$$

This proves that γ is an optimal plan. Thanks to the strict convexity of h, this shows also that if $\tilde{\gamma}$ is optimal then $\tilde{\gamma}$-a.e. we should have $x_1 + \ldots + x_K = a$. □

This reveals a very large class of minimizers in some cases, as we will see later. However not every K-tuple of measures is flat: it is clear that we can have marginals such that there is no plan with such property:

Remark 8.1.4. Let $K = 3$ and $\mu_i = \mu$ for every $i = 1, 2, 3$ with $\mu = \nu_1 + \nu_2$ with $\nu_1 = (-\mathrm{Id})_\sharp \nu_2$ and ν_1 concentrated on $[2, 3]$. Now it is clear that the barycenter of μ is 0 but for every 3 points x_1, x_2, x_3 in the support of μ we cannot have $x_1 + x_2 + x_3 = 0$: two of them have the same sign, let's say x_1 and x_2, but then we have $|x_1 + x_2| \geqslant 4 > 3 \geqslant |x_3|$, which contradicts $x_1 + x_2 = -x_3$. So there is no admissible plan concentrated on $H_0 = \{x_1 + x_2 + x_3 = 0\}$; in fact we showed that for every $\gamma \in \Pi(\mu)$ we have $\mathrm{supp}(\gamma) \cap H_0 = \emptyset$.

Remark 8.1.5. In the case $K = 2$ the condition for which there exists an admissible plan γ concentrated on an hyperplane of the form $x_1 + x_2 = k$ implies that the two measures μ and $\tilde{\nu} = (-\mathrm{Id})_\sharp \nu$ are equal up to translation. This condition is in fact very restrictive. However when we think at the DFT problem (see part III) and in particular we assume that $\mu = \nu$ then the said condition amounts to have that μ is centrally symmetric about its barycenter and in the context of density of 2 electrons around a nucleus this seems a fairly natural condition.

Theorem 8.1.6 ([DMGN15])**.** *Let $\mu_i = \mu = \mathcal{L}^d\big|_{[0,1]^d}, \forall i = 1, \ldots, K$ be the uniform measure on the d-dimensional cube $[0, 1]^d \subset \mathbb{R}^d$, $h : \mathbb{R}^d \to \mathbb{R}$ a convex function and suppose $c : ([0, 1]^d)^K \to \mathbb{R}$ a cost function such that $c(x_1, \ldots, x_K) = h(x_1 + \cdots + x_K)$. Then, there exits a transport map $T : [0, 1]^d \to [0, 1]^d$ such that $T_\sharp \mu = \mu$, $T^{(K)}(x) = x$ and*

$$\min_{\gamma \in \Pi_K(\mu)} \int c d\gamma = \min_{\substack{T_\sharp \mu = \mu, \\ T^{(K)} = \mathrm{Id}}} \int c(x, T(x), \ldots, T^{(K-1)}(x)) d\mu,$$

which means that the optimal plan γ has the form $\gamma_T = (\mathrm{Id}, T, \cdots, T^{(K-1)})_\sharp \mu$. Moreover, T is not differentiable at any point and it is a fractal map, meaning that it is the unique fixed point of a "self-similar" linear transformation $\mathcal{F}$ acting on $L^\infty([0, 1]^d; [0, 1]^d)$.

Proof. We express every $z \in [0, 1]$ by its base-K system, $z = \sum_{k=1}^{\infty} \frac{a_k}{K^k}$ with $a_k \in \{0, 1 \ldots, K - 1\}$. Consider the map given by $S(z) = \sum_{k=1}^{\infty} \frac{\sigma(a_k)}{K^k}$, where σ is the permutation of K symbols such that $\sigma(i) = i + 1, \forall \{i = 0, 1, \ldots, K - 2\}$ and $\sigma(K - 1) = 0$. A straightforward computation shows that

$$z + \sum_{i=1}^{K} S^{(i)}(z) = \frac{K}{2} \tag{8.2}$$

Let $T : \mathbb{R}^d \to \mathbb{R}^d$ be a map defined by $T(x) = T(z_1, \ldots, z_d) = (S(z_1), \ldots, S(z_d))$ and denote by $T^{(j)}(x) = (S^{(j)}(z_1), \ldots, S^{(j)}(z_d))$, $j = 1, \ldots, K - 1$. We will first show that S is a measure-preserving map. In fact, we can show that there exist functions $S_k : [0, 1] \to [0, 1]$ defined recursively by

$$S_0(x) = x, \quad \text{and} \quad S_{k+1}(x) = T_{k+1}(S_k(x))$$

where T_k acts only of the k-th digit: $T_k(x) = x - (K-1)\cdot K^{-k}$ if $x \in C_k$ and $T_k(x) = x + K^{-k}$ if $x \in [0,1] \setminus C_k$. The sets C_k are defined by

$$C_k = \bigcup_{j=1}^{K^{k-1}} \left(\frac{j}{K^{k-1}} - \frac{1}{K^k}, \frac{j}{K^{k-1}} \right].$$

In order to understand how the T_k acts we have plotted in figure 8.1 the first three iterations T_1, T_2 and T_3 for $K = 2$ and $K = 3$.

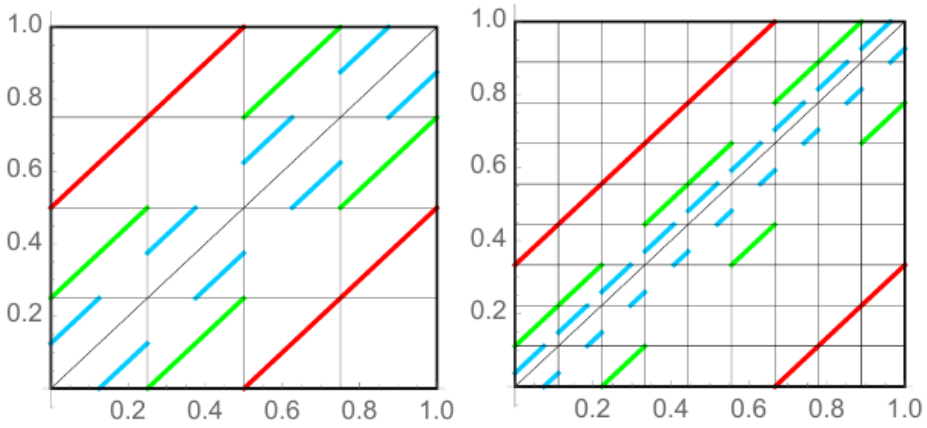

Figure 8.1: *The functions $T_1(x), T_2(x)$ and $T_3(x)$ (in red, green and blue, respectively) for the case $K = 2$ (left) and $K = 3$ (right).*

Moreover, it is easy to see that

$$(T_k)_\sharp \mathcal{L}_{[0,1]} = \mathcal{L}_{[0,1]} \ \forall k \in \mathbb{N}, \quad \text{and} \quad S_k \to S \text{ uniformly.}$$

Hence

$$\int f(x) S_\sharp \mathcal{L}^d = \int f(x) dx, \quad \forall f \in C_0([0,1]).$$

Figure 8.2 clearly illustrates for $K = 2$ that $S_k(x) \to 1 - x$ as $k \to \infty$, while for $K = 3$ the graph of $S_3(x)$ becomes a fractal in that limit.

Now, it remains to show that T is optimal. But this is true thanks to the fact that (8.2) implies that the plan induced by T satisfies the hypothesis of Lemma 8.1.3.

It is clear that we can reduce to prove the non-differentiability and the fractal properties only for the map S. The non-differentiability comes from the fact that for each $z \in [0,1]$, we have that the base-K representation $z = \sum_{k=1}^{\infty} \frac{a_k}{K^k}$ is such that a_k can't be definitively $K-1$. Now it is sufficient to choose those k_j such that $a_{k_j} \neq K-1$ and consider the numbers $z_j = z + (K - 1 - a_{k_j})/K^{k_j}$ and $z'_j = z \pm 1/K^{k_j}$ (depending on whether $a_{k_j} = 0$ or not) which have the same digits as z apart from the j_k-th digit. Then it is straightforward to see that $S(z_j) - S(z) = -(a_{k_j} + 1)/K^{k_j}$ while $S(z'_j) - S(z) = z'_j - z$; in particular we have $\frac{S(z'_j) - S(z)}{z'_j - z} = 1$ while $\frac{S(z_j) - S(z)}{z_j - z} \leqslant -\frac{1}{K}$ and so, letting $j \to \infty$, we get that S is not differentiable at the point z.

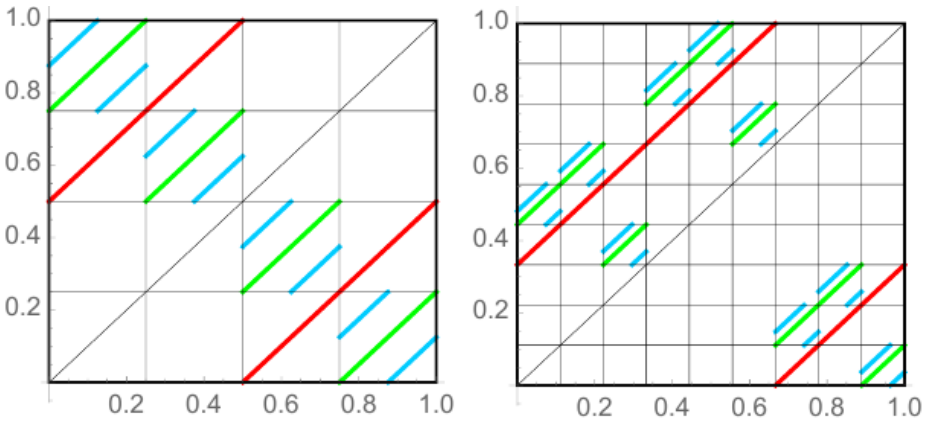

Figure 8.2: *The functions $S_1(x), S_2(x)$ and $S_3(x)$ (in red, green and blue, respectively) for the case $K = 2$ (left) and $K = 3$ (right).*

As for the fractal property: we consider the transformation

$$\mathcal{F}(g)(x) = \begin{cases} \frac{1}{K} g(Kx - i) + \frac{i+1}{K} & \text{for } \frac{i}{K} \leqslant x < \frac{i+1}{K}, \text{ with } i = 0, \dots, K-2 \\ \frac{1}{K} g(Kx - K - 1) & \text{for } \frac{K-1}{K} \leqslant x < 1. \end{cases}$$

In order to see what the construction is doing we imagine to divide $[0,1]^2$ in a grid $K \times K$ of squares and then we are putting scaled copies (by a factor K) of the original function in the above diagonal squares and in the rightmost bottom one. Now it is easy to see that S is the unique[1] fixed point of $\mathcal{F}$, and this gives the property of self-similarity. □

Remark 8.1.7. Another proof of Theorem 8.1.6 can be done noticing that the transformation $\mathcal{F}$ (the one defined in the proof) acts as a $1/K$-contraction in the space of measures preserving L^∞-bijections from $[0,1)$ to $[0,1)$.

Corollary 8.1.8 ([DMGN15])**.** *Let $\mu = \mathcal{L}^d\big|_{[0,1]^d}$ be the uniform measure on the d-dimensional cube $[0,1]^d$ in $\mathbb{R}^d$ and suppose $c : ([0,1]^d)^K \to \mathbb{R}$ the K-dimensional repulsive harmonic cost*

$$c(x_1, \dots, x_K) = -\sum_{i=1}^{K} \sum_{j=i+1}^{K} |x_j - x_i|^2, \qquad (x_1, \dots, x_K) \in ([0,1]^d)^K$$

Then, there exists an optimal cyclical transport map $T : [0,1]^d \to [0,1]^d$: in particular

$$\min_{\gamma \in \Pi_K(\mu)} \int c d\gamma = \min_{\substack{T_\sharp \mu = \mu, \\ T^{(K)} = I}} \int c(x, T(x), T^{(2)}(x), \dots, T^{(K-1)}(x)) d\mu.$$

Moreover, T is not differentiable at any point.

Proof. As we already observed, the problem with the cost c is equivalent to the problem with the cost $|x_1 + \ldots + x_K|^2$ and the result follows from the Theorem 8.1.6. □

[1] We notice that $\mathcal{F}$ is a contraction: $\|\mathcal{F}(g) - \mathcal{F}(g')\|_\infty \leqslant \frac{1}{K} \|g - g'\|_\infty$

We remark the construction of T in the proof of the Theorem 8.1.6 also works if $K = 2$ and T is exactly the optimal transport map described in the example (8.1.2).

The unexpected aspect of Corollary 8.1.8 is the existence - for $K \geqslant 3$ - of an optimal transport map which is not differentiable almost everywhere. It turns out that this optimal map T could be not unique if $d > 1$ and $K \geqslant 3$ and, in that case, we can construct explicitly a regular optimal map. This kind of richness appears already in the case $d = 1$ with the Coulomb cost; however in that case we have uniqueness if we restrict ourselves to the symmetric optimal plan. Here this is not the case as it is easy to see that modifying the action $\mathcal{S}$ on the digits (the important thing is that when we see $\mathcal{S}$ as a permutation, it is a cycle), we obtain another map, and the symmetrized plan is not equal to the one generated by the map described before.

In the following, we are going to present some concrete examples where we have other explicit solutions for such kind of optimal maps for $(\mathcal{MK}_{weak})$ in (8.1). For these examples the goal is to show that there can be smooth optimal maps but they don't necessarily satisfy the "group rule", that is, we can find maps $T_2, \dots T_K$ such that $(\mathrm{Id}, T_1, T_2, \dots, T_{K-1})_\sharp \mu_1$ is an optimal plan but $T_1 \circ T_1 \neq T_i$ for any index $i \in \{1, \dots, K-1\}$.

Example 8.1.9 (3 particles, asymmetric)**.** *Consider the case when three particles are distributed in* $\mathbb{R}^3$ *as Gaussians,* $\mu_1 = \mu_2 = \frac{1}{(2\pi)^{3/2}} \exp(-\frac{1}{2}(x_1^2+x_2^2+x_3^2))$ *and* $\mu_3 = \frac{1}{2\pi^{3/2}} \exp(-(x_1^2+x_2^2+x_3^2))$*. In this case, we can verify that the couple* (T_1, T_2) *of maps* $T_1, T_2 : \mathbb{R}^d \to \mathbb{R}^d$*,* $T_1(x) = x$ *a.e. and* $T_2(x) = -2x$ *a.e. is admissible and it is optimal since* $x + T_1(x) + T_2(x) = 0$*.*

Example 8.1.10 (2K particles on S^1,)**.** *Suppose* $\mu_1, \dots, \mu_{2K}$ *uniform probability measures on the circle* S^1*. The rotation map* $R_\theta : \mathbb{R}^2 \to \mathbb{R}^2$ *with angle* $\theta = \pi/K$ *is an optimal transport map. Also, the maps* $R_{k\theta}$*,* $k = 2, \dots, K$*, are optimal transport maps for the repulsive harmonic cost.*

Example 8.1.11 (2K particles, breathing map)**.** *Suppose* $\mu_1, \dots, \mu_{2K}$ *uniform probability measures on* $S^2 \subset \mathbb{R}^3$*. Consider a vector* v*,* $A : \mathbb{R}^3 \to \mathbb{R}^3$ *the antipodal map* $A(x) = -x$ *and* $R_\theta^v : \mathbb{R}^3 \to \mathbb{R}^3$ *the rotation of angle* $\theta = \pi/K$ *and direction* v*. Then,* $T = A \circ R_\theta^v$ *is a cyclic optimal transport map.*

The optimal solution $\gamma = (x, T, T^{(2)}, \dots, T^{(2K-1)})_\sharp \mu_1$ *is called "breathing" solution [110]: the coupling* γ *represent the configuration where the* $2K$ *electrons are always at the same distance from the center, opposite to each other in the equilibrium configuration.*

Example 8.1.12 (2K particles in $\mathbb{R}^d$, symmetric ρ)**.** *In this case, on can consider the maps* $T(x) = x$ *a.e. and* $S(x) = -x$ *a.e. which are such that*

$$c(T(x), S(x), \dots, T(x), S(x)) = 0.$$

We notice that in this case we have $S^{(2)}(x) = T(x) = x$ *and so in particular this solution has the cyclic structure*

$$(T(x), S(x), \dots, T(x), S(x)) = (x, S(x), S^{(2)}(x), \dots, S^{(2K-1)}).$$

Example 8.1.13 (Optimal Maps which do not satisfy a group law)**.** *Let us consider the case* $d = 1$ *and* $K = 3$ *where the measures are* $\mu_1 = \mu_2 = \mu_3 = \frac{1}{2}\mathcal{L}|_{[-1,1]}$*.*

Then we define the maps

$$T(x) = \begin{cases} x+1 & \text{if } x \leqslant 0 \\ x-1 & \text{if } x > 0, \end{cases} \qquad S(x) = \begin{cases} -1-2x & \text{if } x \leqslant 0 \\ 1-2x & \text{if } x > 0. \end{cases}$$

We have that $T_\sharp \mu = \mu$ *and* $S_\sharp \mu = \mu$*, and moreover* $x + T(x) + S(x) = 0$*; in particular* $(\mathrm{Id}, S, T)_\sharp \mu$ *is a flat optimal plan and so the thesis.*

Example 8.1.14 (Optimal Transport diffuse plan)**.** *Let us consider the same problem as in Example 8.1.13. Now we consider a general symmetric plan* $\gamma = \frac{1}{2}\mathcal{H}^2|_H f(\max\{|x|,|y|,|z|\})$*, where* H *is defined as* $H = \{x+y+z=0\} \cap \{|x| \leqslant 1, |y| \leqslant 1, |z| \leqslant 1\}$ *and* f *is a function to be chosen later. This is a symmetric flat optimal plan; now we compute the marginals. Since it is clear that* γ *is invariant under* $x \mapsto -x$*, it is sufficient to consider the marginal on the set* $x > 0$*. But then we can make the computation*

$$\begin{aligned} \int_{x\geqslant 0} \varphi(x)\, d\gamma(x,y,z) &= \iint_{\substack{|x|,|y|,|x+y|\leqslant 1,\\ x\geqslant 0}} \sqrt{3}\varphi(x) f(\max\{|x|,|y|,|x+y|\})\, dxdy \\ &= \int_0^1 \int_0^{1-x} \sqrt{3}\varphi(x) f(x+y)\, dy\, dx + \sqrt{3}\int_0^1 \int_{-x}^0 \varphi(x) f(x)\, dy\, dx \\ &\quad + \sqrt{3}\int_0^1 \int_{-1}^{-x} \varphi(x) f(|y|)\, dy\, dx \\ &= \int_0^1 \sqrt{3}\varphi(x) \left(x f(x) + 2\int_x^1 f(t)\, dt \right) dx. \end{aligned}$$

In particular the choice $f(x) = \frac{\sqrt{3}}{6}x$ *gives the marginals equal to* $\frac{1}{2}\mathcal{L}|_{[-1,1]}$*. We notice also that any even density* $\rho = h(|x|)$ *for some decreasing function* $h : [0,1] \to [0,\infty)$ *can be represented in this way: in fact it is sufficient to choose* $f(x) = \frac{1}{\sqrt{3}}\Big(\frac{h(x)}{x} - 2x\int_x^1 \frac{h(t)}{t^3}\, dt\Big)$*.*

Remark 8.1.15 (A Counterexample on the uniqueness $K > 3$)*.* As mentioned in corollary 7.1.17 and in [60], it was already understood by Pass that in these high dimensional cases, the solution of repulsive costs may also be non unique, as opposite to the two marginals case. On a higher dimensional surface there can be enough wiggle room to construct more than one measure with common marginals, as shown in the examples 8.1.9–8.1.14. In most of the cases, the non-uniqueness seems to be given by the symmetries of the problem, but in Example 8.1.14 and Corollary 8.1.8 this is not the case, as we exploit the fact that the dimension of the set $c(x+y+z) - \varphi(x) - \varphi(y) - \varphi(z) = 0$, is greater than the minimal one.

Finally, the last proposition of this section states that when $d = 1$ and odd K we have no hope in general to find piecewise regular cyclic optimal transport maps.

Proposition 8.1.16 ([DMGN15])**.** *Let* $\mu = \mathcal{L}|_{[0,1]}$ *and* $K \geqslant 3$ *be an odd number. Then, the infimum*

$$\inf\left\{ \int c(x, T(x), T^{(2)}(x), \dots, T^{(K-1)}) d\mu \ : \ \begin{array}{c} T_\sharp \mu = \mu, \\ T^K = \mathrm{Id} \end{array} \right\}.$$

is not attained by a map T *which is differentiable almost everywhere.*

Proof. First of all we notice that if T is differentiable almost everywhere then also $T^{(2)}$ has the same property, thanks to the fact that $T_\sharp\mu = \mu$. In particular, since the Lusin property holds true for $T^{(i)}$ for every $i = 1, \dots, K$ and $T_\sharp\mu = \mu$, the change of variable formula holds and in particular we have that $(T^{(i)})'(x) = \pm 1$ for almost every x (notice also that T is bijective almost everywhere since $T^{(K)}(x) = x$).

Since μ is K-flat we have that the condition on T in order to be an optimal cyclical map is $x + T(x) + T^{(2)}(x) + \ldots + T^{(K-1)}(x) = K/2$; now we can differentiate this identity and so we will get

$$1 + T'(x) + (T^{(2)})'(x) + \ldots + (T^{(K-1)})'(x) = 0 \qquad \text{for a.e. } x.$$

But this is absurd since on the left hand side we have an odd number of ± 1 and their sum will be an odd number. □

In conclusion, also in the case of the repulsive harmonic cost, the picture is far from being clear: an interesting structure appears when $\{\mu_i\}_{i=1}^K$ is a flat K-tuple of measures but we still can't characterize this property. Moreover, in the flat case in which $\mu_i = \mu$, for example when $\mu = \frac{1}{2}\mathcal{L}^1|_{[-1,1]}$, we have both diffuse optimal plan and a cyclical optimal map.

An interesting open problem is whether for any K-flat measure μ, say absolutely continuous with respect to the Lebesgue measure, we have a cyclical optimal map and a diffuse plan.

8.2 Numerical Results: MM-OT with repulsive Harmonic Cost

As shown in section 8.1 the minimizers of the OT problem with the harmonic cost are also minimizers of the problem with $c(x_1, \cdots, x_K) = |x_1 + \cdots + x_K|^2$, so for the discrete problem (7.22) we take $c_{j_1 \cdots j_K} = |x_{j_1} + \cdots + x_{j_K}|^2$. Let us first consider the two marginals case and the uniform density on $[0, 1]$ (see example 8.1.2), and, as expected, we find a deterministic coupling given by $\gamma(x, y) = \mu(x)\delta(y - T(x))$ where $T(x) = 1 - x$, see figure 8.3. The simulation in figure 8.3 has been performed on a discretization of $[0, 1]$ with $N = 1000$ gridpoints and $\varepsilon = 0.005$.

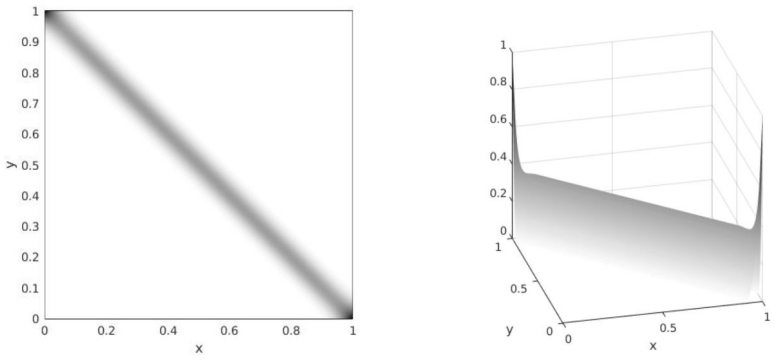

Figure 8.3: *Left: support of the optimal coupling. Right: optimal coupling.*

The multi-marginals case is more delicate to treat: the original OT problem does not admit a unique solution whereas the regularized problem does. As we have explained in section 2.2 the regularized problem is a strongly convex problem which admits a unique solution and the resulting coupling is the one with the minimal entropy. However we are able to make the IPFP algorithm converge to a selected coupling among the optimal ones for the original problem. Let us focus on the example 8.1.13. In this case we have all marginals equal to $\mu = \frac{1}{2}\mathcal{L}|_{[-1,1]}$ and we can find a deterministic coupling given by $\gamma(x,y,z) = \mu(x)\delta(y-T(x))\delta(z-S(x))$ for the maps $T(x)$ and $S(x)$. In order to select this coupling, the idea is to modify the cost function by adding a penalization term $p(x,y) = \frac{\tau}{|x-y|}$ which makes μ_1 and μ_2 be *as far as possible* (if we consider μ_1 and μ_2 as particles). Thus, the discretized cost now reads as

$$c_{j_1,j_2,j_3} = |x_{j_1} + x_{j_2} + x_{j_3}|^2 + \frac{\tau}{|x_{j_1} - x_{j_2}|}. \tag{8.3}$$

Then we expect, as shown in figure 8.4, that the projection $\tilde{\gamma}_{12}(x,y) = (e_1,e_2)\gamma(x,y,z)$ and $\tilde{\gamma}_{13}(x,z) = (e_1,e_3)\gamma(x,y,z)$ of the computed coupling are induced by map T and S respectively. The simulation has been performed on a discretization of $[-1,1]$ with $N = 1000$ gridpoints, $\varepsilon = 0.0005$ and $\eta = 0.1$.
We, finally, take the same marginals as in the previous example, but we do not

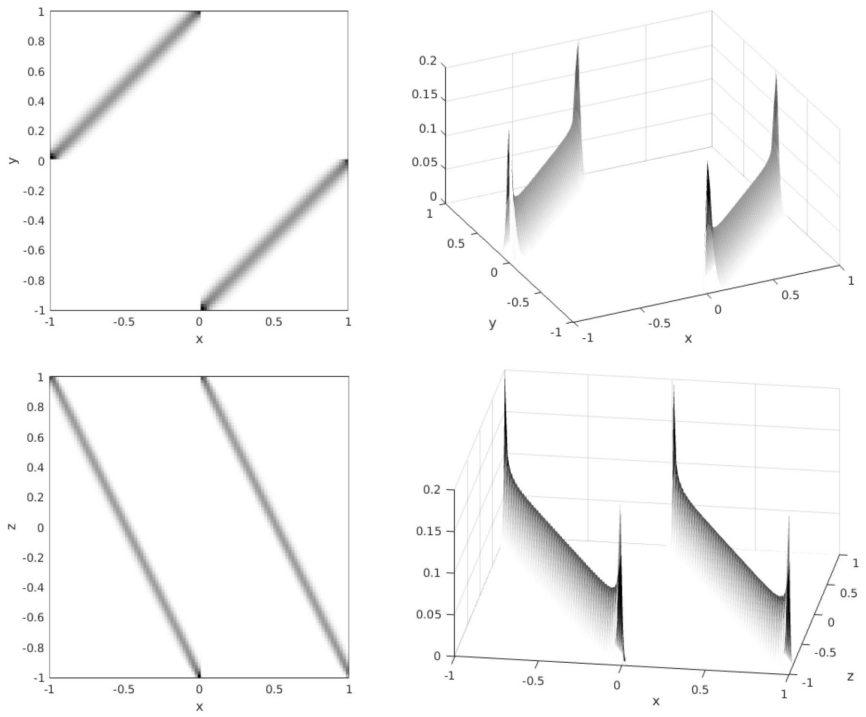

Figure 8.4: *Top-Left: support of the optimal coupling $\tilde{\gamma}_{12}(x,y)$. Top-Right: optimal coupling $\tilde{\gamma}_{12}(x,y)$. Bottom-Left: support of the optimal coupling $\tilde{\gamma}_{13}(x,z)$. Bottom-Right: optimal coupling $\tilde{\gamma}_{13}(x,z)$.*

add the penalization. In this case we expect a diffuse plan since, if we forget

about the marginal constraint, it is simple to show that the second order Γ-limit of the regularized problem as $\varepsilon \to 0$ is the relative entropy of γ with respect to $\mathcal{H}^2|_{\{x+y+z=0\}}$; we expect that the Γ-limit is the same also when we add the marginal constraint.

In figure 8.5 we present the projection $\tilde{\gamma}_{12}(x,y) = (e_1,e_2)\gamma(x,y,z)$ of the computed coupling (it is enough to visualize only this projection because of the symmetries of the problem) and, as expected, we observe a diffuse plan. . The simulation has been performed on a discretization of $[-1,1]$ with $N = 1000$ gridpoints, $\varepsilon = 0.0005$.

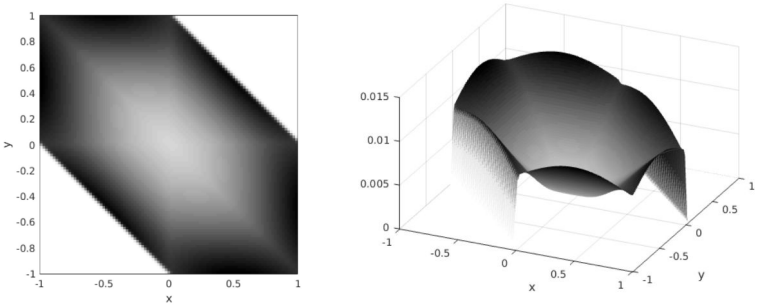

Figure 8.5: *Left: support of the optimal coupling $\tilde{\gamma}_{12}(x,y)$. Right: optimal coupling $\tilde{\gamma}_{12}(x,y)$.*

8.3 Multi-marginal OT for the Determinant

We are going to give a short overview of the main results in [36], where Carlier and Nazaret consider the following optimal transport problems for the determinant:

$$(\mathcal{MK}_{Det}) \qquad \sup_{\gamma\in\Pi((\mathbb{R}^d)^d,\mu_1,\dots,\mu_d)} \int_{(\mathbb{R}^d)^d} \det(x_1,\dots,x_d)d\gamma(x_1,\dots,x_d) \tag{8.4}$$

and

$$(\mathcal{MK}_{|Det|}) \qquad \sup_{\gamma\in\Pi((\mathbb{R}^d)^d,\mu_1,\dots,\mu_d)} \int_{(\mathbb{R}^d)^d} |\det(x_1,\dots,x_d)|d\gamma(x_1,\dots,x_d), \tag{8.5}$$

where $\mu_1,\dots,\mu_d$ are absolutely continuous probability measures in $\mathbb{R}^d$. In addition, in order to guarantee existence of a solution, we assume that there exist $p_1,\dots,p_d \in [1,\infty[$ such that

$$\sum_{i=1}^d \frac{1}{p_i} = 1, \quad \text{and} \quad \sum_{i=1}^d \int_{\mathbb{R}^d} \frac{|x_i|^{p_i}}{p_i} d\mu(x_i) < +\infty.$$

Notice that for this particular cost the problem (7.1) makes sense only when $K = d$. In the following, we will focus on problem (8.4) and exhibit explicit minimizers γ in the radial case. Clearly, the difference between (8.4) and (8.5) is that the second one admits positively and negatively oriented basis of vectors,

while the first one "chooses" only the positive ones. Moreover, if we assume that among marginals $\mu_1, \dots, \mu_d$ there exist two symmetric probability measures $\mu_i, \mu_j, i \neq j$, *i.e.* $\mu_i = (\text{-Id})_\sharp \mu_i$ and $\mu_j = (\text{-Id})_\sharp \mu_j$, then any solution γ of (8.4) satisfies $\det(x_1, \dots, x_d) \geqslant 0$ γ-almost everywhere and so solves also (8.5) (Proposition 6, [36]).

Similarly to the Gangbo-Święch cost [66], the Monge-Kantorovich problem for the determinant (8.4) can be seen as a natural extension of classical optimal transport problem with two marginals and so, it is equivalent to the 2-marginals repulsive harmonic cost (8.1).

Indeed, we can write in the two marginals case, $\det(x_1, x_2) = \langle x_1, Rx_2 \rangle$, where $R : \mathbb{R}^2 \to \mathbb{R}^2$ is the rotation of angle $-\pi/2$. Hence, since μ_1 and μ_2 have finite second moments, up to a change of variable $\tilde{x}_2 = Rx_2$, the problem $(\mathcal{MK}_{Det})$ in (8.4) is equivalent to the classical Brenier's optimal transportation problem:

$$\begin{aligned}
\operatorname*{argmax}_{\gamma \in \Pi(\mu_1, \mu_2)} \int_{\mathbb{R}^2} \det(x_1, x_2) d\gamma(x_1, x_2) &= \operatorname*{argmax}_{\gamma \in \Pi(\mu_1, \mu_2)} \int_{\mathbb{R}^2} \langle x_1, \tilde{x}_2 \rangle d\gamma(x_1, x_2) \\
&= \operatorname*{argmax}_{\tilde{\gamma} \in \Pi(\mu_1, \tilde{\mu}_2)} \int_{\mathbb{R}^2} \langle x_1, x_2 \rangle d\tilde{\gamma} \\
&= \operatorname*{argmin}_{\gamma \in \Pi(\mu_1, \tilde{\mu}_2)} \int_{\mathbb{R}^2} \frac{|x_1 - x_2|^2}{2} d\gamma(x_1, x_2) - C
\end{aligned}$$

where $C = 1/2(\int |x_1|^2 \, d\mu_1 + \int |x_2|^2 \, d\mu_2)$ and $\tilde{\mu}_2 = R_\sharp \mu_2$.

In the sequel, we are going to construct maximizers for (8.4), thanks to some properties of the Kantorovich potentials of the dual problem associated to (8.4) (see theorem 8.3.1 bellow),

$$(\mathcal{K}_K^{Det}) \quad \inf \left\{ \int_{\mathbb{R}^d} \sum_{i=1}^d u_i(x_i) d\mu_i(x_i) : \det(x_1, \dots, x_d) \leqslant \sum_{i=1}^K u_i(x_i) \right\}. \tag{8.6}$$

In [36], the authors provide a useful characterization of optimal transport plans through the potentials u_i, given by theorem 8.3.1 . In addition, by means of a standard convexification trick we obtain regularity results on the Kantorovich potentials.

Theorem 8.3.1 ([36])**.** *A coupling $\gamma \in \Pi((\mathbb{R}^d)^d, \mu_1, \dots, \mu_d)$ is optimal in* (8.4) *if and only if there exists lower semi-continuous convex functions $u_i : \mathbb{R}^d \to \mathbb{R} \cup \{\infty\}$ such that for all $i \in \{1, \dots, d\}$,*

$$\sum_{j=1, j \neq i}^d u_j(x_j) \geqslant u_i^*((-1)^{i+1} \bigwedge_{j \neq i} x_j), \quad \text{on} \quad (\mathbb{R}^d)^d;$$

$$\sum_{j=1, j \neq i}^d u_j(x_j) = u_i^*((-1)^{i+1} \bigwedge_{j \neq i} x_j), \quad \gamma - \textit{almost everywhere};$$

$$(-1)^{i+1} \bigwedge_{j \neq i} x_j \in \partial u_i(x_i), \quad \gamma - \textit{almost everywhere}.$$

where $\bigwedge_{i=1}^{d} x_j$ *denotes the wedge product and, for every* i, u_i^* *is the convex dual of the Kantorovich potential* u_i.

Now, the main idea is to use the geometrical constraints on the Kantorovich potentials u_i (8.6), given by the theorem (8.3.1), in order to construct an explicit solution.

We illustrate the theorem (8.3.1) and explain how to construct a particular optimal γ for (8.4) by an example in the three marginals case. Let $\mu_i = \rho_i \mathcal{L}^3$, $i = 1, 2, 3$ radially symmetric probability measures on the 3-dimensional ball B.

In this particular situation, the optimizers of (8.4) and (8.5) have a natural geometric interpretation: what is the best way to place three random vectors x, y, z, distributed by probability measures μ_1, μ_2, μ_3 on the sphere, such that the simplex generated by those three vectors (x, y, z) has maximum average volume?

Suppose $\gamma \in \Pi(B, \mu_1, \mu_2, \mu_3)$ optimal in (8.4) when $d = 3$. From optimality of γ, we have

$$u_1(x) + u_2(y) + u_3(z) = det(x, y, z), \quad \gamma - almost\ everywhere.$$

Applying the theorem (8.3.1), we get

$$\begin{cases} u_2(y) + u_3(z) = u_1^*(y \wedge z) \\ u_1(x) + u_3(z) = u_2^*(-x \wedge z) \\ u_1(x) + u_2(y) = u_3^*(x \wedge y) \end{cases}, \quad \gamma - almost\ everywhere,$$

and,

$$\begin{cases} \nabla u_1(x) = y \wedge z \\ \nabla u_2(y) = -x \wedge z \\ \nabla u_3(z) = x \wedge y \end{cases}, \quad \gamma - almost\ everywhere. \tag{8.7}$$

It follows from (8.7), given a vector x in the ball, the conditional probability of y given x is supported in a *"meridian"* $M(x)$

$$M(x) = \{y \in S^2 : \langle \nabla u_1(x), y \rangle = 0\},$$

where S^2 is the $2-$sphere. Finally, assuming that $\langle x, \nabla u_1(x) \rangle \neq 0$, the conditional probability of z given the pair (x, y) is simply given by a delta function on z

$$z = \frac{\nabla u_1(x) \wedge \nabla u_2(y)}{\langle x, \nabla u_1(x) \rangle};$$

In particular, we have

$$\langle x, \nabla u_1(x) \rangle + \langle y, \nabla u_2(y) \rangle + \langle z, \nabla u_3(z) \rangle = \det(x, y, z) = \det(\nabla u_1(x), \nabla u_2(y), \nabla u_3(z)).$$

Example 8.3.2 (An explicit solution in the ball $B \subset \mathbb{R}^3$, see also [36])**.** *Suppose* $\mu_i = \mathcal{L}^3_B$, $i = 1, 2, 3$, *the 3-dimensional Lebesgue measure in the ball* $B \subset \mathbb{R}^3$. *The following coupling* γ^*

$$\int_{B^3} f d\gamma^* = \frac{1}{\mathcal{L}^3(B)} \int_B \left(\int_{M(x)} f(x, |x|y, x \wedge y) \frac{d\mathcal{H}^1(y)}{2\pi} \right) dx, \ \forall f \in C(B^3, \mathbb{R}). \tag{8.8}$$

is an optimizer for (8.4) *with* $d = 3$. *Indeed, from we can show explicit potentials* $u_1^*(x) = u_2^*(x) = u_3^*(x) = |x|^3/3$; *clearly we have*

$$\det(x, y, z) \leqslant |x||y||z| \leqslant |x|^3/3 + |y|^3/3 + |z|^3/3, \quad \forall\ (x, y, z) \in B,$$

with equality when $|x| = |y| = |z|$ *and* x, y, z *are orthogonal. Since* γ^* *is concentrated on this kind of triples of vector we have the optimality. Finally, by a suitable change of variable, it is easy to see that* $\gamma^* \in \Pi_3(\mathcal{L}^3_B)$.

Some comments on the radially symmetric d-marginals case: In [36], for d radially symmetric probability measures, the authors exhibit explicit optimal couplings γ^*. In their proof, two aspects were crucial: the first one is remark that if $\{\mu_i\}_{i=1}^d$ are radially symmetric measures in $\mathbb{R}^d$, then the optimal Kantorovich potentials $u_i(x_i) = u_i(|x_i|)$ are also radially symmetric; in particular the system (8.7) for general d implies that the support of γ^* is contained in the set of an orthogonal basis. The second observation is to notice that in the support of γ^* we have $G_i(|x_1|) = |x_i|$, where G_i is the unique monotone increasing map such that $(\tilde{G}_i)_\sharp \mu_1 = \mu_i$, where $\tilde{G}_i(x) = \frac{x}{|x|} G_i(|x|)$. This is done analyzing the corresponding radial problem (with cost $c(r_1, \dots, r_d) = r_1 \cdots r_d$), using the optimality condition $\varphi_i'(r_i) = \partial_i c$ and the fact that in this case $r_i \varphi_i'(r_i) = r_1 \varphi_1'(r_1) = c \geqslant 0$; then, exploiting the convexity of φ_i we get $r_i = G_i(r_1)$ for some increasing function G_i, that is uniquely determined.

Existence of Monge-type solutions: In the 3-marginals case in the unit ball, by construction of the coupling γ^* in (8.8) or, more generally, the optimal coupling in the d-marginal case (see theorem 4 in [36]), we can see that their support are not concentrated in the graph of cyclic maps $T, T^2, \dots, T^{d-1}$ or simply on the graph of maps $T_1, \dots, T_{d-1}$ as we could expect from corollary (7.1.26). In other words, γ^* in (8.8) is not Monge-type solution.

The existence of Monge type solutions for the determinant cost is still an open problem for odd number of marginals. From the geometric conditions we discussed above, in the case in which $\mu_i = \mu$ a radial measure, if Monge solutions exists then, for every $x \in \mathbb{R}^d$, $(x, T_1(x), \dots, T_{d-1}(x))$ should be an orthogonal basis, and $|T_i(x)| = |x|$, $i = 1, \dots, d-1$.

For the interesting even dimensional case, we can observe a similar phenomena remarked in the repulsive harmonic costs, concerning the existence of trivial even dimensional solutions for the Monge problem in (8.4). We expect the existence of non-regular optimal transport map also to this case.

Example 8.3.3 (Carlier & Nazaret, [36])**.** *The even dimensional phenomenon: as in the repulsive harmonic cost, it is easy to construct Monge minimizers for the determinant cost for even number of marginals* $\geqslant 4$. *For instance, suppose* $c(x_1, x_2, x_3, x_4) = \det(x_1, x_2, x_3, x_4)$, *alle the marginals equal to the uniform measure* μ *on the ball, define transport maps* $T_1, T_2, T_3 : B \to \mathbb{R}^4$ *by, for* $x = (x_1, x_2, x_3, x_4) \in B$

$$T_1(x) = \begin{pmatrix} -x_2 \\ x_1 \\ -x_4 \\ x_3 \end{pmatrix}, \qquad T_2(x) = \begin{pmatrix} -x_3 \\ x_4 \\ x_1 \\ -x_2 \end{pmatrix}, \qquad T_3(x) = \begin{pmatrix} -x_4 \\ -x_3 \\ x_2 \\ x_1 \end{pmatrix}.$$

We can see that $\gamma_T = (\mathrm{Id}, T_1, T_2, T_3)_\sharp \mu$ *is a Monge-type optimal transport plan for* (8.4) *and* (8.5).

8.4 Numerical Results: MM-OT with Determinant Cost

Numerical simulations for the multi-marginal problem with the determinant cost present an obvious computational difficulty: in order to compute the solution just for the 3-marginals case, we have to introduce a discretization of $\mathbb{R}^3$ (as the cost function now is $c(x_1, \cdots, x_K) = det(x_1, \cdots, x_K)$ with $x_i \in \mathbb{R}^K$). However if we take radially symmetric densities μ_i as marginals (see section 8.3 for a more complete description of the problem in the measure framework), Carlier and Nazaret show that $(\mathcal{MK})$ can be reduced to a 1-dimensional problem: the only unknowns are the relations between the norms $r_i = \|x_i\|$ of each vector. These relations can be obtained by solving the following problem

$$\min_{\gamma \in \Pi(\lambda_1(r), \cdots, \lambda_K(r))} - \int (\prod_{i=1}^{K} r_i) \gamma(r_1, \cdots, r_K) dr_1 \cdots dr_K, \tag{8.9}$$

where $\lambda_i(r) = \sigma(r)\mu_i(\mathbf{r})$ (e.g. $K = 3$ then $\mathbf{r} = (r, \theta, \varphi)$ and $\sigma(r) = 4\pi r^2$). Moreover, for this problem we know that there exists a unique (deterministic) optimal coupling (see Proposition 5 in [36]). The discretized cost now reads $c_{j_1 \cdots j_K} = \prod_{k=1}^{K} r_{j_k}$. Let us consider the 3-marginals case and all densities λ_i equal to the uniform density on the ball $\mathcal{B}_{0.5} = \{x \in \mathbb{R}^3 | \|x\| \leqslant 0.5\}$. As proved in [36], the optimal coupling is actually supported by the graph of maps which rearrange measure (see figure 8.6). The simulation in figure 8.6 has been performed on a discretization of $[0, 0.5]$ with $N = 100$ and $\varepsilon = 0.01$. In

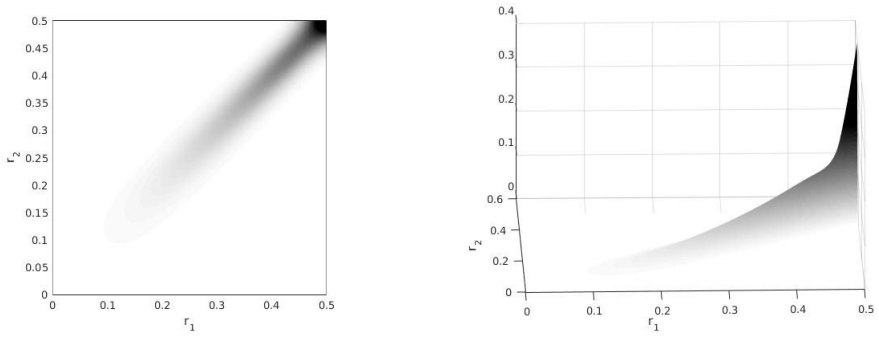

Figure 8.6: *(Uniform density) Left: support of the optimal coupling $\tilde{\gamma}_{12}(r_1, r_2)$. Right: optimal coupling $\tilde{\gamma}_{12}(r_1, r_2)$.*

the same way we can take all marginals $\lambda_i(r) = 4\pi r^2 e^{-4r}$ and we obtain again a deterministic coupling, figure 8.7. The simulation has been performed on a discretization of $[0, 3]$ with $N = 300$ and $\varepsilon = 0.05$.

We, finally, present a simulation (see figure 8.9) with three different marginals λ_i (see figure 8.8). As one can observe we obtain that the projections of the optimal coupling are concentrated on the graph of a map which rearranges the densities in a monotone way. The simulation has been performed on a discretization of $[0, 4]$ with $N = 300$ and $\varepsilon = 0.07$.

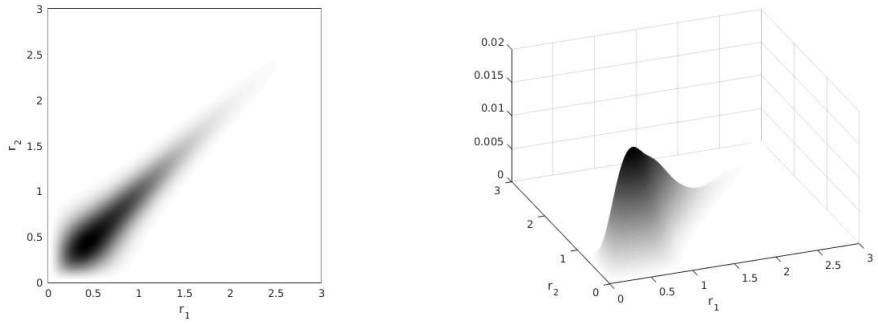

Figure 8.7: *(Exponential density)Left: support of the optimal coupling* $\tilde{\gamma}_{12}(r_1, r_2)$*. Right: optimal coupling* $\tilde{\gamma}_{12}(r_1, r_2)$*.*

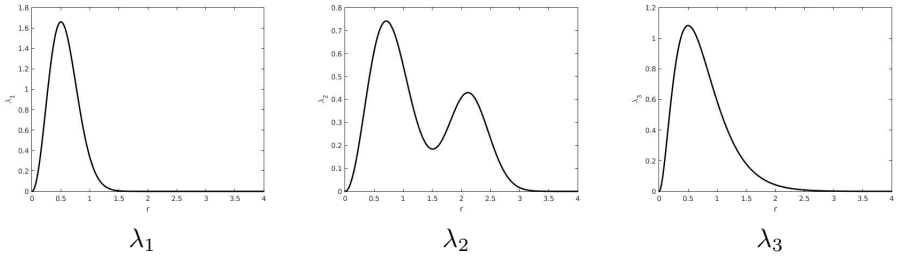

λ_1 λ_2 λ_3

Figure 8.8: *Densities* λ_1*,* λ_2 *and* λ_3*.*

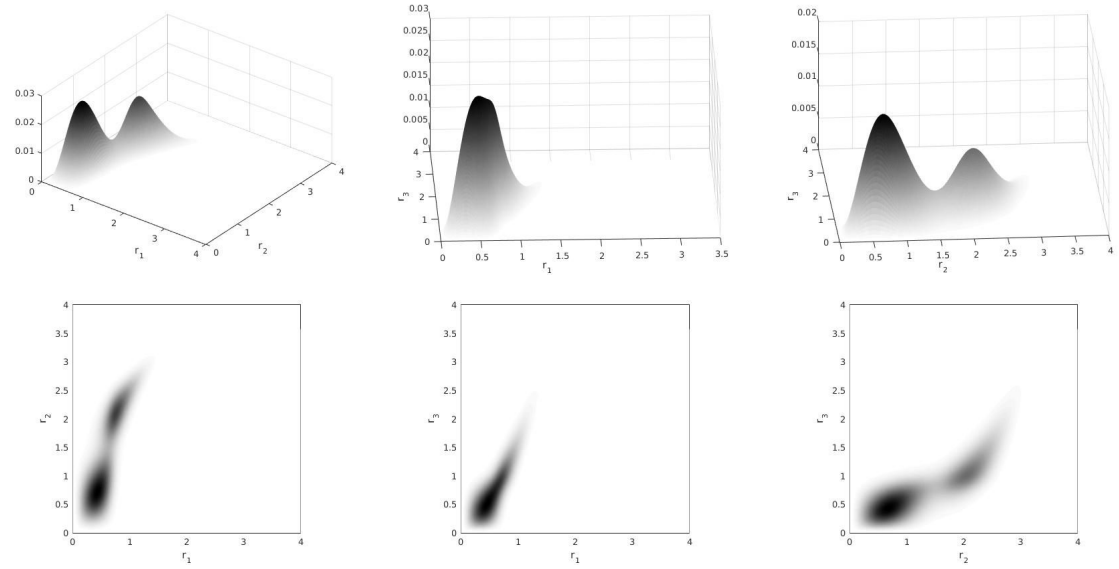

Figure 8.9: *Top-Left: optimal coupling* $\tilde{\gamma}_{12}(r_1, r_2)$*. Top-Center: optimal coupling* $\tilde{\gamma}_{13}(r_1, r_3)$*. Top-Right: optimal coupling* $\tilde{\gamma}_{23}(r_2, r_3)$*. Bottom: supports of those couplings.*

Part III

Application to Density Functional Theory

Résumé

Dans cette partie nous présentons la théorie de fonctionnelle de la densité (TFD). Nous montrons que la résolution du problème de minimisation de l'énergie de répulsion interne de K électrons dans un densité donnée μ, est equivalent à trouver la meilleure façon de transporter $K-1$ fois la densité μ sur elle-même, avec le coût repulsif coulombien. Cela signifie que nous étudions un problème du transport optimal multi-marges. Nous soulignons également que la régularisation entropique du problème peut être vu comme une borne inférieure de la fonctionnelle de Hohenberg-Kohn. On se concentre sur les résultats rigoureux et les conjectures sur l'existence et la caractérisation géométrique des transports optimaux, pour le problème (TOMM) avec le coût de Coulomb. En particulier, nous fournissons des contre-exemples théoriques ainsi que numériques (voir aussi [41]) à la conjecture de Seidl. Cette partie est basée sur des travaux en commun avec Jean-David Benamou, Guillaume Carlier, Simone Di Marino, Augusto Gerolin, Klass Giesbertz, Paola Gori-Giorgi et Michael Seidl: [BCN15], [DMGN15] et [SDMG$^+$].

Abstract

In this part we introduce the Density Functional Theory (DFT). We show that solving the problem of finding the minimum internal repulsion energy for K electrons in a given density μ is equivalent to find the optimal way of transporting $K-1$ times the density μ into itself, with cost function given by the Coulomb repulsion. This means that we finally deal with a multi-marginal optimal transport problem. We also highlight that the entropic regularized problem can be seen as a lower bound of the Hohenberg-Kohn functional. We focus on rigorous results and conjectures on the existence and the geometrical characterization of optimal transport maps for the MMOT problem with Coulomb cost. In particular we provide both theoretical and numerical counterexamples (for other counterexamples we refer the reader to [41]) to the so-called Strong Seidl's conjecture. This part is based on joint works with Jean-David Benamou, Guillaume Carlier, Simone Di Marino, Augusto Gerolin, Klass Giesbertz, Paola Gori-Giorgi and Michael Seidl: [BCN15], [DMGN15] and [SDMG$^+$].

Chapter 9

Density Functional Theory and Multi-Marginal Optimal Transport

9.1 Brief introduction to Quantum Mechanics of K-body systems

Energies and geometries of a molecule depend on the kind of atom and the chemical environment. Semi-empirical models as *Lewis structure* explain some aspects, but they are far from being satisfactory, mostly because they are not quantitative.

Classical behavior of atoms and molecules is described accurately, at least from a theoretical point of view, by quantum mechanics. However, in order to predict the chemical behavior of a molecule with a large number of electrons we need to deal with computational aspects and approximations. For example, if we use a direct approximation of 10 grid points in $\mathbb{R}$ of the time-dependent Schrödinger equation in order to simulate the chemical behavior of the water molecule (H_2O), which has 10 electrons and its position is represented in the space $\mathbb{R}^{30}$, then we need to compute the solution over 10^{30} grid points.

Quantum Chemistry studies the ground state of individual atoms and molecules, the excited states and the transition states that occur during chemical reactions. Many systems use the so-called *Born-Oppenheimer approximation* and many computations involve iterative and other approximation methods.

The main goal of Quantum Chemistry is to to predict the evolution of a molecular system. Classical models consider a molecule with K electrons and M nuclei. We denote by a point $x_i \in \mathbb{R}^3$ the position coordinates of the i-th electron of mass m_e and by s_i its i-th electron spin. The charges, the masses and the positions of the α-th nucleus are represented, respectively, by $Z_\alpha \in \mathbb{R}^M$, $m_\alpha \in \mathbb{R}_+^M$ and $R_\alpha \in (\mathbb{R}^3)^M$

The state of the system is described by a time-dependent wave function $\psi \in \mathrm{L}^2([0,T]; \otimes_{i=1}^K \mathrm{L}^2(\mathbb{R}^3 \times \mathbb{Z}_2) \times \otimes_{\alpha=1}^M \mathrm{L}^2(\mathbb{R}^3))$, $\psi(x_1, s_1, \cdots, x_K, s_K; R_1, \cdots, R_M, t)$. The group $\mathbb{Z}_2 = \{\uparrow, \downarrow\}$ represents the spin of a particle.

We say that a wave function is antisymmetric or *fermionic* if it changes

sign under a simultaneous exchange of two electrons i and j with the space coordinates x_i and x_j and spins s_i and s_j, that is,

$$\psi(x_{\sigma(1)}, s_{\sigma(1)}, \cdots, x_{\sigma(K)}, s_{\sigma(K)}) = \text{sign}(\sigma)\psi(x_1, s_1, \cdots, x_K, s_K) \quad \sigma \in \mathscr{S}_K$$

where $\mathscr{S}_K$ denotes the permutation set of K elements.

In physics literature, the *Fermionic* wave function obeys the *Fermi-Dirac statistics* and, in particular, the *Pauli exclusion principle*. On the other hand, a wave function is called symmetric or *bosonic* when it obeys *Bose-Einstein statistics* which also implies that when one swaps two bosons, the wave function of the system is unchanged.

If it is not mentioned explicitly, we will suppose that the wave function is spinless, i.e. ψ is a function depending only on time, electrons and nuclei position $\psi(t, x_1, x_2, \cdots, x_K, R_1, \cdots, R_M)$.

The evolution of a wave function ψ is modeled by a (time-dependent) Schrödinger Equation

$$i\partial_t\psi = H\psi \quad , \quad H = T_n + T_e + V_{ne} + V_{ee} + V_{nn} \tag{9.1}$$

where the operators T_n, T_e, V_{ne}, V_{ee} and V_{nn} are defined by

$$T_n = -\hbar \sum_{\alpha=1}^{M} \frac{1}{2m_\alpha}\Delta_{R_\alpha} \quad \textit{(Nuclei Kinetic Energy)}$$

$$T_e = -\hbar \sum_{i=1}^{K} \frac{1}{2m_e}\Delta_{x_i} \quad \textit{(Electron Kinetic Energy)}$$

$$V_{ne} = -\sum_{i=1}^{K} v(x_i) = -\sum_{i=1}^{K}\left(\sum_{\alpha=1}^{M} \frac{Z_\alpha}{|x_i - R_\alpha|}\right) \qquad \left(\begin{array}{l}\textit{Potential Energy of Inte-}\\ \textit{raction Nuclei-Electron}\end{array}\right)$$

$$V_{ee} = \sum_{i=1}^{K}\sum_{j=1, j\neq i}^{K} \frac{1}{|x_i - x_j|} \quad \textit{(Interaction Electron-Electron)}$$

$$V_{nn} = \sum_{\alpha=1}^{M}\sum_{\beta=1, \beta\neq\alpha}^{M} \frac{Z_\alpha Z_\beta}{|R_\alpha - R_\beta|} \quad \textit{(Interaction Nuclei-Nuclei)}$$

Born-Oppenheimer Approximation: The Born-Oppenheimer approximation (named for its original inventors, Max Born and Robert Oppenheimer) is based on the fact that nuclei are several thousand times heavier than electrons. The proton, itself, is approximately 2000 times more massive than an electron. Roughly speaking, in the Born-Oppenheimer approximation we suppose that nuclei behave as point classical particles. This is reasonable, since typically $2000m_e \leqslant m_\alpha \leqslant 100000m_e$.

In other words, we suppose $m_\alpha \gg m_e$, we fix $m_e = 1$ and we consider an *ansatz* of type $\psi(x, R, t) = \psi_e(x, R)\chi(R, t)$, which physically means that the dynamics of the electron ψ_e are decoupled from the dynamics of the atomic nuclei χ. Substituting that *ansatz* in (9.1), we can show that the electronic part $\psi_e(x, R)$ solves the following eigenvalue problem, so-called *Electronic Schrödinger Equation*

$$H_e\psi_e = \lambda_e\psi_e, \qquad H_e = T_e + V_{ne} + V_{ee} + V_{nn} \tag{9.2}$$

where the eigenvalue $\lambda_e = \lambda_e(R)$ depends on the position vector $R = (R_1, \cdots, R_M)$ of the atomic nuclei. The function $H_e = H_e(R)$ is called *Electronic Hamiltonian*. From the other side, through a formal argument, the nuclei wave function $\chi(R,t)$ is a solution of a Schrödinger Equation restricted to the nuclei with potential energy λ_e,

$$i\partial_t \chi(R) = (T_n + \lambda_e(R))\chi(R).$$

We refer to [16] for all computations and formal deduction of those formulas. Another consequence of that approximation is that the nuclear components of the wave function are spatially more localized than the electronic component of the wave function. In the classical limit, the nuclei are fully localized at single points representing classical point particles.

In Quantum Chemistry it is interesting to study the so called *Geometric Optimization Problem*.

The Geometric Optimization Problem: Compute the following minimizer

$$\inf \left\{ E_0(R_1, \cdots, R_M) + \sum_{\alpha=1}^{M} \sum_{\beta=1, \beta\neq\alpha}^{M} \frac{Z_\alpha Z_\beta}{|R_\alpha - R_\beta|} \mid (R_1, \cdots, R_M) \in \mathbb{R}^{3M} \right\} \quad (9.3)$$

where

- The second term is the nuclei-nuclei iteration V_{nn}, as defined in (9.1).
- The function $E_0(R) = E_0(R_1, \cdots, R_M)$ corresponds to the effective potential created by the electrons and is, itself, given by a minimization problem (see *Electronic minimization problem* below).

The value of the potential $E_0 = E_0(R_1, \cdots, R_M)$ for given fixed positions of the nuclei is obtained by solving the electronic problem:

The Electronic minimization problem: Compute the lowest eingenvalue (*"ground state energy"*) E_0 of the following linear operator, called *Electronic Hamiltonian*

Definition 9.1.1 (Electronic Hamiltonian)**.** *The Electronic Hamiltonian is a linear operator* $H_{el} : L^2_{anti}(\mathbb{R}^{3K}) \to L^2_{anti}(\mathbb{R}^{3K})$,

$$H_{el} = -\frac{\hbar^2}{2} \sum_{i=1}^{K} \Delta_{x_i} + \sum_{i=1}^{K} v(x_i) + \sum_{i=1}^{K} \sum_{j=i+1}^{K} f(x_j - x_i),$$

where $L^2_{anti}(\mathbb{R}^{3K})$ denotes the set of square-integrable antisymmetric functions $\psi : \mathbb{R}^{3K} \to \mathbb{R}$, $v : \mathbb{R}^3 \to \mathbb{R}$ is a $\mathrm{L}^2(\mathbb{R}^{3K})$ function and $f : \mathbb{R} \to \mathbb{R}$ is a continuous function.

The first term of the Electronic Hamiltonian is the Kinetic Energy and the second term, the function $v(x_i)$, depends only on the single electron. Typically, $v(x_i) = -\sum_{\alpha=1}^{M} \frac{Z_\alpha}{|x_i - R_\alpha|}$ is the interaction electron-nuclei energy of the single electron. The function f depends only on the distance of two electrons and measures the electron-electron potential interaction; typically f is the Coulomb Interaction $f(x_j - x_i) = 1/|x_j - x_i|$ or the repulsive harmonic interaction $f(x_j -$

$x_i) = -|x_j - x_i|^2$. From both mathematical and physical viewpoint, it may be also useful to study more general convex and concave functions.

The *ground state* of the functional (9.1.1) is given by the *Rayleigh-Ritz variational principle*

$$E_0 = E_0(R_1, \cdots, R_M) = \min\{\langle \psi, H_{el}\psi\rangle \mid \psi \in \mathcal{H}\},$$

where $\mathcal{H} = \{\psi \in \mathrm{H}^1(\mathbb{R}^{3K}) : \psi \text{ is antisymmetric and } \|\psi\| = 1\}$. Equivalently,

$$E_0 = \min\Big\{T_e(\psi) + V_{ne}(\psi) + V_{ee}(\psi) \mid \psi \in \mathcal{H}\Big\} \tag{9.4}$$

where $T_e(\psi)$ is the *Kinetic energy*,

$$T_e(\psi) = \frac{\hbar^2}{2} \sum_{s_1 \in \mathbb{Z}_2} \int_{\mathbb{R}^3} \cdots \sum_{s_K \in \mathbb{Z}_2} \int_{\mathbb{R}^3} \sum_{i=1}^{K} |\nabla_{x_i} \psi(x_1, s_1 \cdots, x_K, s_K)|^2 dx_1 \cdots dx_K$$

$V_{ne}(\psi)$ is the electron-nuclei interaction energy,

$$V_{ne}(\psi) = \sum_{s_1 \in \mathbb{Z}_2} \int_{\mathbb{R}^3} \cdots \sum_{s_K \in \mathbb{Z}_2} \int_{\mathbb{R}^3} \sum_{i=1}^{K} v(x_i) |\psi(x_1, s_1 \cdots, x_K, s_K)|^2 dx_1 \cdots dx_K$$

and, $V_{ee}(\psi)$ is the electron-electron interaction energy

$$V_{ee}(\psi) = \sum_{s_1 \in \mathbb{Z}_2} \int_{\mathbb{R}^3} \cdots \sum_{s_K \in \mathbb{Z}_2} \int_{\mathbb{R}^3} \sum_{i=1}^{K} \sum_{j=i+1}^{K} f(x_j - x_i) |\psi(x_1, s_1 \cdots, x_K, s_K)|^2 dx_1 \cdots dx_K$$

Notice that, with a slightly abuse of notations, we denote in the same way operators and energies. Here, the ground state quantum K-body problem refers to the problem of finding equilibrium states for system of type (9.1). A theorem proved first by Zhislin [119], guarantees the existence of the minimum in (9.4). Some variants can be found in the literature due, for instance, to Lieb & Simon [90], Lions [91] and Friesecke [59].

In computational chemistry, the most computationally practicable methods are not numerical (in the sense in which this terminology is used in mathematics), but power series of analytical solutions of reduced models.

9.2 Probabilistic Interpretation and Marginals

The square norm of the wave function $\psi(x_1, s_1, \cdots, x_K, s_K)$ can be interpreted as a K-point probability density distribution for the electrons to be in the points x_i with spins s_i.

$$\int_{\mathbb{R}^{3K}} \sum_{s_1, \cdots, s_K \in \mathbb{Z}_2} |\psi(x_1, s_1, \cdots, x_K, s_K)|^2 dx = 1.$$

If ψ is a $\mathrm{L}^2(\mathbb{R}^{3K})$ function we can define the single particle density by

$$\rho(x_1) = K \int_{\mathbb{R}^{3(K-1)}} \gamma_K(x_1, s_1, \cdots, x_K, s_K) dx_2, \cdots dx_K, \tag{9.5}$$

where γ_K represents the K-point position density

$$\gamma_K(x_1, \cdots, x_K) = \sum_{s_1, \cdots, s_K \in \mathbb{Z}_2} |\psi(x_1, s_1, \cdots, x_K, s_K)|^2. \tag{9.6}$$

Analogously, we can define the k-density

$$\gamma_k(x_1, \cdots, x_k) = \binom{K}{k} \int_{\mathbb{R}^{3(K-k)}} \gamma_K(x_1, s_1, \cdots, x_K, s_K) dx_{k+1}. \cdots dx_K \tag{9.7}$$

We remark that when the particle is spinless the single particle density (9.5) can be simply be written as

$$\rho(x_1) = K \int_{\mathbb{R}^{3(K-1)}} |\psi(x_1, \cdots, x_K)|^2 dx_2, \cdots dx_K.$$

The relevance of ρ and γ_2 to compute the ground state energy (9.4) is due to the fact that the interaction nuclei-nuclei energy $V_{ne}(\psi)$ and electron-electron energy $V_{ee}(\psi)$ depends only on these.

Lemma 9.2.1 ([43]). *If $\psi, \nabla\psi \in \mathrm{L}^2((\mathbb{R}^3 \times \mathbb{Z}_2)^K, \mathbb{R})$, ψ antisymmetric and $\|\psi\|_2 = 1$, then*

$$V_{ne}(\psi) = \int_{\mathbb{R}^3} v(x)\rho(x)dx, \quad V_{ee}(\psi) = \int_{\mathbb{R}^6} \frac{1}{|x-y|}\gamma_2(x,y)dxdy.$$

It is natural to wonder about the space of those densities arising from such a wave-function ψ: the space $\mathcal{A}$ of densities $\rho : \mathbb{R}^3 \to \mathbb{R}$ verifying (9.5) for an antisymmetric ψ such that $\psi, \nabla\psi \in \mathrm{L}^2((\mathbb{R}^3 \times \mathbb{Z}_2)^K, \mathbb{R})$ and $\|\psi\|_2 = 1$. The following explicit characterization has been given by Lieb in [88]):

$$\mathcal{A} = \left\{ \rho : \mathbb{R}^3 \to \mathbb{R} \mid \rho \geqslant 0, \sqrt{\rho} \in \mathrm{H}^1(\mathbb{R}^3) \text{ and } \int_{\mathbb{R}^3} \rho(x)dx = K \right\}. \tag{9.8}$$

9.3 Density Functional Theory (DFT)

The Density Functional Theory is the standard approximation to quantum mechanics. It can be used for simulations of a system with more than a dozen electrons and showed to be successful in many instances but has rare drastic failures as, for instance, in predicting the behavior of Cr_2 molecules [39]. DFT theory approximates quantum mechanics via variational principle on the marginal density

$$\rho(x_1) := \int_{\mathbb{R}^{d(K-1)}} |\psi(x_1, \cdots, x_K)|^2 dx_2 \cdots dx_K, \tag{9.9}$$

where ψ is a wave function associated to the K-body quantum problem as in equation (9.5). Roughly speaking, DFT models are semi-empirical models of the pair density

$$\gamma_2(x_1, x_2) := \int_{\mathbb{R}^{3(K-2)}} |\psi(x_1, \cdots, x_K)|^2 dx_3 \cdots dx_K. \tag{9.10}$$

in terms of its marginal ρ. We simply write $\psi \to \rho$ and $\psi \to \gamma_2$ to denote the relation between ψ and ρ, and ψ and γ_2. This means, respectively, that ψ has single particle density ρ and pair density γ_2.

Concerning the ground state problem (9.4), we the following result which let us split the minimization problem into two problems

Theorem 9.3.1 ([73],[86],[88])**.** *Let $\rho \in \mathcal{P}(\mathbb{R}^3)$ be a probability density such that $\rho \in \mathrm{H}^1(\mathbb{R}^3)$ and $f : \mathbb{R} \to \mathbb{R}$ be a continuous function. There exists a functional $F^{HK} : \mathcal{P}(\mathbb{R}^3) \to \mathbb{R}$ depending only on the single-particle density ρ such that for any potential V_{nn}, the exact Quantum Mechanics ground state energy (9.4) satisfies*

$$E_0 = \min\left\{\left(F^{HK}(\rho) + K\int_{R^3} v(x)\rho(x)dx\right) \mid \rho \in \mathcal{P}(\mathbb{R}^3)\right\} \tag{9.11}$$

Moreover, $F^{HK}(\rho)$ is given itself as a minimum problem

$$F^{HK}(\rho) = \min\left\{\left\langle\psi, \Big(-\frac{\hbar^2}{2}\Delta + \sum_{i=1}^{K}\sum_{j=i+1}^{K} f(x_j - x_i)\Big)\psi\right\rangle \;\mid\; \psi \in \mathcal{H}, \psi \to \rho\right\}$$

where, $\psi \to \rho$ means that ψ has single-particle density ρ and $\mathcal{A}$ is the set of $\rho : \mathbb{R}^3 \to \mathbb{R}$ such that $\rho \geqslant 0$, $\sqrt{\rho} \in \mathrm{H}^1(\mathbb{R}^3)$ and $\int_{\mathbb{R}^3}\rho(x)dx = K$.

We refer to F^{HK} as the *Hohenberg-Kohn* functional. The Hohenberg-Kohn theorem states that the functional F^{HK} is *universal* in the sense that it does not depend on the molecular system under consideration. From a Physics point of view, it guarantees that in a molecular system of K electrons, the single electron density ρ determines the pair density of the system (see corollary 9.3.2). From a mathematical perspective, the proof of this theorem is a functional analysis exercise that, for sake of completeness, we are going to present in a version we learnt from Gero Friesecke.

Proof. Firstly we remark that the electron-nuclei interaction only depends on ρ:

$$\langle\psi, \sum_{i=1}^{K} v(x_i)\psi\rangle = \int_{\mathbb{R}^{3K}}\sum_{i=1}^{K} v(x_i)|\psi(x_1, \cdots, x_K)|^2 d\mathbf{x} = K\int_{\mathbb{R}^3} v(x)\rho(x)dx$$

Then, we rewrite problem (9.4) as a double inf problem

$$\begin{aligned} E_0 &= \inf_{\psi}\left(\langle\psi, \mathrm{H}_{el}\,\psi\rangle + K\int v(r)\rho(r)dr\right) \\ &= \inf_{\rho}\left(\inf_{\psi\mapsto\rho}\left(\langle\psi, \mathrm{H}_{el}\,\psi\rangle\right) + K\int v(r)\rho(r)dr\right) \\ &= \inf_{\rho}\left(F^{HK}(\rho) + K\int v(r)\rho(r)dr\right) \end{aligned}$$

where $F^{HK}(\rho) = \inf_{\psi\mapsto\rho}\left(\langle\psi, \mathrm{H}_{el}\,\psi\rangle\right)$. □

The present version stated in theorem 9.3.1 is due to Levy [86] and Lieb [88]. The next corollary contains the main physical and mathematical consequence of the Hohenberg-Kohn theorem (9.3.1).

Corollary 9.3.2 (HK Theorem and Coupling problem)**.** *Let $\rho \in \mathcal{P}(\mathbb{R}^3)$ be a measure and $\psi \in \mathrm{H}^1(\mathbb{R}^{3K})$ be an antisymmetric function with $\|\psi\|_2 = 1$. There exists a universal map from single-particle density $\rho(x_1)$ to a pair densities $\gamma_2(x_1, x_2)$ - or even k-density $\gamma_k(x_1, \cdots, x_k)$ - which gives the exact pair density of any K-electron molecular ground state $\psi(x_1, \cdots, x_K)$ in terms of its single-particle density.*

Proof. Consider

$$\overline{\psi} \in \operatorname{argmin}\{\langle \psi, H_{el}\psi\rangle \mid \psi \to \rho\}$$

and define by γ_k the universal k-point density of that minimizer, i.e.

$$\gamma_k(x_1, \cdots, x_k) = \int |\overline{\psi}(x_1, \cdots, x_K)|^2 d_{k+1} \cdots dx_K$$

□

9.4 "Semi-classical limit" and Optimal Transport problem

A natural approach to understand the behavior of the Hohenberg-Kohn functional $F^{HK}(\rho)$ (**??**) is to study separately the contributions of the kinetic energy and electron-electron repulsion (namely the Coulomb interaction). Consider the Hohenberg-Kohn functional where the electron-electron interaction is rescaled by a real parameter λ while keeping the density ρ fixed [82, 118]

$$F_\lambda^{HK}(\rho) = \min_{\substack{\psi \in \mathcal{H} \\ \psi \to \rho}} \left\{ \langle \psi, \big(-\frac{\hbar^2}{2}\Delta + \sum_{i=1}^{K} \sum_{j=i+1}^{K} \frac{\lambda}{|x_j - x_i|} \big)\psi \rangle \right\}. \tag{9.12}$$

The strictly correlated electron limit ($\lambda \to \infty$), up to relaxing in the space of probability measures, was first considered by two papers in physics literature: Seidl [109] and Seidl, Gori-Giorgi & Savin [110]. In [71], Gori-Giorgi, Seidl and Vignale interpreted the strong-interaction regime as a mass transportation problem with a Coulomb cost.

Later, an equivalent limit, so-called *"semi-classical limit"*, was made mathematically rigorous in the two particles case by Cotar, Friesecke & Klüppelberg [43]. They considered the Hohenberg-Kohn functional $F^{HK} = F_\hbar^{HK}$ as a function of both ρ and $\hbar$ ($\lambda = 1$) and proved that - up to passage to the limit $\hbar \to 0$ - the functional F^{HK} reduces to the following one

$$\tilde{F}(\rho) = \inf \left\{ \int_{\mathbb{R}^6} \frac{1}{|x-y|} \gamma_2(x, y) dx dy \mid \gamma_2 \in \mathcal{A}_2, \gamma_2 \to \rho \right\}, \tag{9.13}$$

where $\gamma_2 \to \rho$ means that γ_2 satisfies the equation (9.7), and the set $\mathcal{A}_2$ of admissible pair density functions is defined by the image of $\mathcal{A}$ under the map $\psi \to \gamma_2$. As pointed out in [43], contrary to the corresponding single particle density case, we do not know any characterization of the space of admissible pair density function $\mathcal{A}_2$.

We state in the next theorem the semi-classical limit for the 2-particles case. The general case of K particles is still an open problem.

Theorem 9.4.1 ("Semi-classical limit" for $K = 2$, Cotar-Friesecke-Klüppelberg, [43])**.** *Let $\rho : \mathbb{R}^3 \to [0, \infty]$ be a probability density such that $\sqrt{\rho} \in \mathrm{H}^1(\mathbb{R}^3)$, $K = 2$ and $f : \mathbb{R} \to \mathbb{R}$ be the Coulomb or the repulsive harmonic interaction potentials. Then,*

$$\begin{aligned} F_\hbar^{HK}(\rho) &= \min_{\psi \in \mathrm{H}^1(\mathbb{R}^6), \psi \to \rho} \langle \psi, \big(-\tfrac{\hbar^2}{2}\Delta + f(x_2 - x_1)\big)\psi \rangle \\ &\underset{\hbar \to 0}{\to} \min_{\gamma \in \Pi_2(\mathbb{R}^6, \rho)} \int_{\mathbb{R}^{3K}} f(x_2 - x_1) d\gamma(x_1, x_2) =: F^{OT}(\rho), \end{aligned} \tag{9.14}$$

where the set $\Pi_2(\mathbb{R}^6, \rho)$ denotes the set of measures $\gamma \in \mathcal{P}(\mathbb{R}^6)$ having ρ as marginals, i.e. $(\pi_i)_\sharp \gamma = \rho$ where, for $i = 1, 2$, $\pi_i : \mathbb{R}^3 \times \mathbb{R}^3 \to \mathbb{R}^3$ are the canonical projections.

Remark 9.4.2 (F^{OT} and Monge-Kantorovich). Notice that F^{OT} coincides with the two marginal Monge-Kantorovich problem.

The main difficulty in proving Theorem 9.4.1 is that for any transport plan given by a density ψ, $\gamma = |\psi(x_1, \cdots, x_K)|^2 dx_1 \cdots x_K$, it may be that $\psi \notin \mathrm{H}^1(\mathbb{R}^{3K}), \psi \notin \mathrm{L}^2(\mathbb{R}^{3K})$ and $T(\psi) = \infty$. Moreover, smoothing the optimal γ does not work at this level, because this may change the marginals of the problem (9.14). Cotar, Friesecke & Klüppelberg developed a smoothing technique in order to deal with this problem without changing the marginals. A complete proof of the previous theorem can be found in [43].

Let us precise somewhat the terminology. In Quantum Mechanics, the *"semi-classical limit"* has a precise meaning: it is an asymptotic regime for the Hamiltonian dynamics of a Quantum system defined in a Hilbert space and it is given by a *Weyl-Wigner quantization* (or *quantization by deformation* studied in the more abstract context of Poisson manifolds). In those specific cases, the limit $\hbar \to 0$ is called *"semi-classical"* limit, because the first and second order terms of an asymptotic expansion of the Hamiltonian operator is given by *"classical"* terms, functions of the Hamiltonian function in a symplectic manifold [53, 103].

In DFT context, that limit seems to be up to now merely a question of re-scaling. The minimizers of $F^{OT}(\rho)$ are candidates of *ansatz* to develop approximating methods to compute the ground state energy of the *Electronic Hamiltonian*.

At this point, it is natural to define the *DFT-Optimal Transportation ground state* E_0^{DFT-OT} [43],

$$\begin{aligned} E_0^{DFT-OT}(\rho) &= \inf \Big\{ T_e(\psi) + V_{ne}(\psi) + E^{OT}(\psi) \mid \psi \in \mathcal{H} \Big\} \\ &= \inf \Big\{ T_{QM}(\rho) + V_{ne}(\rho) + E^{OT}(\rho) \mid \rho \in \mathcal{A} \Big\}. \end{aligned} \tag{9.15}$$

where ρ represents the single particle density (see (9.5)), T_{QM} and E^{OT} are defined, respectively, by

$$T_{QM}(\rho) = \inf \Big\{ T_e(\psi) \mid \psi \in \mathcal{H}, \psi \to \rho \Big\} \quad \text{and}$$

$$E^{OT}(\rho) = \inf\left\{ \int_{\mathbb{R}^{3K}} \sum_{i=1}^{K}\sum_{i=1}^{K} f(x_j - x_i) d\gamma(x_1, \cdots, x_K) \mid \gamma \in \Pi_K(\mathbb{R}^{dK}; \rho) \right\}, \tag{9.16}$$

where $\Pi_K(\mathbb{R}^{dK}; \rho)$ denotes the set of probability measures $\gamma : (\mathbb{R}^d)^K \to \mathbb{R}_+$ having ρ as marginals.

The problem of minimizing E_0^{DFT-OT} in (9.15) is called DFT-OT problem. Finally, we have

Theorem 9.4.3 (Cotar-Friesecke-Klüppelberg, [43]). *Consider $f(|x_j - x_i|) = 1/|x_j - x_i|$. For every K, and any potential $v \in L^{3/2} + L^\infty(\mathbb{R}^3)$, the density functional with electron-electron interaction energy (9.16) is a rigorous lower bound of the Electronic minimization problem* (9.4)

$$E_0 \geqslant E_0^{DFT-OT}$$

One of the central question of DFT-OT problem with Coulomb potentials is to characterize the minimizers γ of $E^{OT}(\rho)$. Those minimizers could be used as *ansatz* in order to find minimizers of the Hohenberg-Kohn $F^{HK}(\rho)$. In [109], the physicist Seidl formulated the following conjecture.

Conjecture 9.4.4 (Weak Seidl Conjecture [109]). *There exists a deterministic minimizer of $E^{OT}(\rho)$ with Coulomb potential/cost*

$$c(x_1, \cdots, x_K) = \sum_{i=1}^{K}\sum_{j=i+1}^{K} \frac{1}{|x_i - x_j|}.$$

In other words, for Coulomb-type electron-electron interactions, Seidl conjectures[1] state that, at least for radially symmetric measures ρ, there exists an optimal measure γ for E^{OT} of the form $\gamma = (\mathrm{Id}, T_1, \cdots, T_{K-1})_\sharp \rho$, with $T_1, \cdots, T_{K-1} : \mathbb{R}^3 \to \mathbb{R}^3$. These maps T_i are called co-motion functions and, due to the symmetries of the problem, a natural group law is required for them, namely that for every i, j there exists k such that $T_i \circ T_j = T_k$; this is satisfied if for example $T_i = T^{(i)}$ (cyclical case, see Equation (7.14)).

It is natural to ask the same kind of question for other cost functions. In the following we mention some interesting results:

(i) In the 2-electrons case, the minimizers of E_0^{DFT-OT} are well-understood [43] and there exists a map which correlates the density of a given minimization plan of $E^{OT}(\rho)$, see Theorem 10.1.1.

(ii) Gangbo & Święch (without being aware of Seidl) reinforces the conjecture 9.4.4 showing in [66] that for the attractive harmonic cost $c(x_1, \cdots, x_K) = \sum_{i,j=1}^{K} |x_i - x_j|^2$ there exists a unique optimal plan, and it is a deterministic one.

(iii) Colombo, De Pascale & Di Marino [49] answer affirmatively the (strong) Seidl conjecture in the one dimensional case ($d = 1$), as we will describe in section 9.5.

[1] There is also a stronger version of the conjecture, the Strong Seidl Conjecture, where the author describes explicitly a possible optimal map in the radially symmetric case: for the precise statement see the conjecture 10.1.4 and the lemma 10.1.3 in section 9.5.

(iv) *"Seidl's conjecture"* is not true for the repulsive harmonic cost $c(x_1, \cdots, x_K) = \sum_{i,j=1}^{K} -|x_i - x_j|^2$ (see theorem 8.1.6). Moreover, for the same cost and for a particular single particle density, there exists *"fractal-like"* optimal transport maps, i.e. an optimal map T which are not differentiable at every point, see section 8.1.

Remark 9.4.5 (Warning: notations). From now on we refer to $F^{OT}(\rho)$ and $E^{OT}(\rho)$ as $\mathcal{MK}(\rho)$ and $\mathcal{MK}_K(\rho)$ (which are actually the notations for the Monge-Kantorovich problem in the 2-marginals case and in the $K-$marginals used throughout all the thesis), respectively.

9.5 Multi-marginal OT with Coulomb Cost

This section is devoted to the summary of the results present in literature on the multi marginal optimal transport with Coulomb cost. We already highlighted the fact that the interesting case is when all the marginals are equal, since this is the physical case. We point out that, as always, the focus will be on characterizing the optimal plans as well as looking for cyclical transport maps: in this direction an important conjecture has been made by Seidl in his seminal paper [109], where he gave an explicit construction of a map for measures with radial symmetry in $\mathbb{R}^d$. In the last years the conjecture was proven to be true in the 1D case when μ is the uniform measure on an interval, and then generalized to any diffuse measure on the real line. However, quite recently various authors disproved the conjecture in the case $\mathbb{R}^d$ for $d \geqslant 2$ and for $K = 3$ marginals, yet the Seidl map is still optimal for some class of measures.

We begin by analyzing the general problem, and then we will proceed to look at the radial case.

9.5.1 General theory: duality, equivalent formulations and many particles limit

We begin by stating the duality theorem in this case proved by De Pascale [48], by means of Γ-convergence of finite dimensional problems for which the duality is classical.

Theorem 9.5.1 ([48]). *Let $\mu \in \mathcal{P}(\mathbb{R}^d)$ be a measure that is not concentrated on a set of cardinality smaller or equal than $K-1$. Then the duality* (7.7) *holds and the dual problem has a bounded maximizer.*

The boundedness of the maximizer u can let us prove also some regularity properties. The first one is the fact that any optimal plan is supported away from the diagonals, while the second one proves second order regularity of u.

Lemma 9.5.2 (Corollary 3.13 in [48]). *Let μ as in Theorem 9.5.1; then there exists $\alpha > 0$ such that for every optimal plan γ we have* $\mathrm{supp}(\gamma) \subseteq \{(x_1, \ldots, x_K) : |x_i - x_j| \geqslant \alpha, \ \forall\, i \neq j\}$.

Lemma 9.5.3 ([DMGN15]). *Let μ as in Theorem 9.5.1 and u be a bounded maximizer in the dual problem in* (7.7)*; then u has a μ-representative that is Lipschitz and semi concave.*

Proof. As in the classical case we first prove a structural property of the maximizer u, namely that the constraint (7.8) is saturated, that is $(u, \dots, u)$ is a c-conjugate K-tuple. Let us consider

$$w(x_1) = \operatorname*{ess\text{-}inf}_{(x_2,\dots,x_K)\in\mathbb{R}^{d(K-1)}} \left\{ \sum_{1\leqslant i<j\leqslant K} \frac{1}{|x_i - x_j|} - \sum_{i=2}^{K} u(x_i) \right\},$$

where the ess-inf is made with respect to the measure $\mu^{\otimes K-1}$. It is obvious that $w(x_1) \geqslant u(x_1)$ for μ-a.e x_1, thanks to (7.8). Suppose that $w > u$ in a set of positive measure; but then $(w, u, \dots, u)$ would be a better competitor in the (not symmetric) dual problem contradicting the fact that u is a maximizer (we use the fact that the symmetric dual problem and the not symmetric one have the same values). Now we have that w is defined everywhere and so we can talk about its regularity.

Let $d > 0$ be a number such that there exists points $p_1, \dots p_K$ in the support of μ such that $|p_i - p_j| \geqslant d$; this number exists as long as $\sharp\mathrm{supp}(\mu) \geqslant K$. Let us fix $\varepsilon > 0$ such that $\frac{1}{2\varepsilon} > \frac{2K(K-1)}{d} + 2K\|u\|_\infty$ and $\varepsilon \leqslant d/8$; in this way it is true that if we define

$$w_{x_0}(x_1) = \operatorname*{ess\text{-}inf}_{|x_i - x_0|\geqslant\varepsilon,\, i=2,\dots,K} \left\{ \sum_{1\leqslant i<j\leqslant K} \frac{1}{|x_i - x_j|} - \sum_{i=2}^{K} u(x_i) \right\},$$

we have $w_{x_0} = w$ on $B(x_0, \varepsilon)$. In fact in the definition of w we can choose x_i among the p_i (or very close to them, as they belong to the support) such that $|x_i - x_j| > d/2 - 2\varepsilon \geqslant d/4$ for every $i \neq j$, and so we have that $w \leqslant \frac{2K(K-1)}{d} + K\|u\|_\infty$ but then it is clear that for any $(x_2, \dots, x_K)$ such that $|x_i - x_0| \leqslant \varepsilon$ we will have

$$\sum_{1\leqslant i<j\leqslant K} \frac{1}{|x_i - x_j|} - \sum_{i=2}^{K} u(x_i) \geqslant \frac{1}{2\varepsilon} > w(x_1) \qquad \forall x_1 \in B(x_0, \varepsilon);$$

this proves that in fact $w_{x_0} = w$ on the set $B(x_0, \varepsilon)$ and so in particular also in $B(x_0, \varepsilon/2)$. But in this set w_{x_0} is Lipschitz and semi concave since it is an infimum of uniformly C^∞ functions on $B(x_0, \varepsilon/2)$. Moreover the bounds on the first and second derivatives don't depend on x_0 but only on ε, that is fixed a priori, and so by a covering argument we obtain the thesis. □

Another interesting reformulation of the Coulomb-like problem, or more generally when we have only interaction between two particles, can be found in [60] where, seeking a dimensional reduction of the problem, the authors use the fact that if $\gamma \in \Pi_K(\mathbb{R}^{dK}; \mu)$ is a symmetric plan then

$$\int_{\mathbb{R}^{dK}} \sum_{1\leqslant i<j\leqslant K} \frac{1}{|x_i - x_j|}\, d\gamma = \binom{K}{2} \int_{\mathbb{R}^{2d}} \frac{1}{|x - y|}\, d(\pi_1, \pi_2)_\sharp \gamma,$$

that is, since the electrons are indistinguishable, it is sufficient to look at the potential energy of a couple of electrons and then multiply it by the number of couples of electrons. It is clear that $\gamma_2 = (\pi_1, \pi_2)_\sharp \gamma$ is a 2-plan whose marginals are still μ; we will say that $\eta \in \Pi_2(\mathbb{R}^{d2}; \mu)$ is K-representable whenever it exists

$\gamma \in \Pi_K(\mathbb{R}^{dK};\mu)$ such that $\eta = (\pi_1,\pi_2)_\sharp\gamma$. The equivalent formulation they give is

$$\min_{\gamma\in\Pi_K(\mathbb{R}^{dK};\mu)} \int_{\mathbb{R}^{dK}} \sum_{1\leqslant i<j\leqslant K} \frac{1}{|x_i-x_j|}\,d\gamma = \min_{\substack{\eta\in\Pi_2(\mathbb{R}^{d2};\mu)\\ \eta \text{ is } K\text{-representable}}} \binom{K}{2} \int_{\mathbb{R}^{2d}} \frac{1}{|x-y|}\,d\eta.$$

Unfortunately the conditions for being K-representable are not explicit and they are very difficult to handle; this is correlated to the K-representability for matrices, but here, since we are in the semiclassical limit, we deal with densities instead. In [60] the authors propose, as a method for reducing the dimension of the problem, to substitute the condition of being K-representable with that of being k-representable with $k \leqslant K$; the resulting problem will give a lower bound to the SCE functional .

We present also a general theorem regarding the many particles limit, that embodies the well-known fact that when $K\to\infty$ then the solution is the mean field one

Theorem 9.5.4 ([44])**.** *Let $\mu\in\mathcal{P}(\mathbb{R}^d)$. Then we have that*

$$\lim_{K\to\infty} \frac{1}{\binom{K}{2}} \min_{\gamma\in\Pi_K(\mathbb{R}^{dK};\mu)} \int_{\mathbb{R}^{dK}} \sum_{1\leqslant i<j\leqslant K} \frac{1}{|x_i-x_j|}\,d\gamma = \int_{\mathbb{R}^{2d}} \frac{1}{|x-y|}\,d\mu\otimes\mu.$$

In terms of DFT we are saying that $E^{OT}(\mu) = \binom{K}{2}E^{MF}(\mu) + o(K^2)$, where E^{MF} is the normalized mean field energy $E^{MF}(\mu) = \int \frac{1}{|x-y|}\,d\mu(x)\,d\mu(y)$.

Remark 9.5.5. The statement about the Coulomb cost in the physical case is quite classical. In fact, for a measure $\rho\in L^{4/3}(\mathbb{R}^3)$ the Lieb-Oxford bound holds [87, 89]:

$$\binom{K}{2}E^{MF}(\mu) \geqslant \mathcal{MK}_K(\mu) \geqslant K^2E^{MF}(\mu) - CK^{4/3}\int_{\mathbb{R}^3}\mu^{4/3}(x)\,dx,$$

and so the conclusion is immediate. However, in [44] the proof is completely different and relies on the fact that a measure $\gamma\in\Pi_2(\mathbb{R}^{d2};\mu)$ that is K-representable for every K must be in the convex envelope of measures of the type $\nu\otimes\nu$, and then on a direct computation using the Fourier transform. In particular, aside from the Coulomb cost in dimension 3 they prove the theorem for more general costs with binary interaction of the form $\sum_{1\leqslant i<j\leqslant K} f(x_i-x_j)$, where $f\in\mathcal{C}_b(\mathbb{R}^d)\cap \mathrm{L}^1(\mathbb{R}^d)$ satisfies $f(z)=f(-z)$ and also $\hat{f}\geqslant 0$.

9.5.2 Regularized Optimal Transport and Hohenberg-Kohn functional

Consider now the $K-$marginals Monge-Kantorovich problem with the Coulomb cost and all marginals equal to $\mu_i(x) = \rho(x)\mathcal{L}^d$ (w.l.o.g. we will identify the measure μ with its density ρ)

$$(\mathcal{MK}_K)\quad \min\left\{\int_{\mathbb{R}^{dK}}\sum_{i<j}\frac{1}{|x_i-x_j|}\gamma(x_1,\cdots,x_K)dx_1,\cdots,dx_K \mid \gamma\in\Pi_K(\mathbb{R}^{dK};\rho)\right\}, \tag{9.17}$$

and the entropic regularization

$$\mathscr{S}_{K,\varepsilon}(\rho) := \min\left\{\mathrm{H}(\gamma|\eta_\varepsilon) \mid \gamma \in \Pi_K(\mathbb{R}^{dK};\rho)\right\}, \tag{9.18}$$

where $\eta_\varepsilon := \frac{1}{L}\exp\left(-\sum_{i<j}\frac{1}{\varepsilon|x_i-x_j|}\right)\otimes_{i=1}^K dx_i$ (L is the normalization constant) and the entropy is defined as in (2.2). We show now that problem (9.18) with a fixed parameter ε is a lower bound of the Hohenberg-Kohn functional. Take a plan $\gamma(x_1,\cdots,x_K) = \sum_{s_1,\cdots,s_K\in\mathbb{Z}_2}|\psi(x_1,s_1,\cdots,x_K,s_K)|^2$ (it is obvious that $\sqrt{\gamma}\in \mathrm{H}^1(\mathbb{R}^{dK})$), then the Hohenberg-Kohn functional $F^{HK}(\rho)$ reads as

$$F^{HK} = \inf\Bigg\{\frac{\hbar^2}{2}\int_{\mathbb{R}^{dK}}|\nabla\sqrt{\gamma(x_1\cdots x_K)}|^2 dx_1\cdots dx_K + \int_{\mathbb{R}^{dK}}\sum_{i<j}\frac{1}{|x_i-x_j|}\gamma(x_1\cdots x_K)dx_1\cdots dx_K \mid \gamma\in\Pi_K(\mathbb{R}^{dK};\rho)\Bigg\}. \tag{9.19}$$

We can establish the following result

Theorem 9.5.6 (Entropy Lower bound,[DMN]). *Let be $\rho\in\mathcal{P}(\mathbb{R}^d)$ and $\psi\in \mathrm{H}^1((\mathbb{R}^d\times\mathbb{Z}_2)^K;\mathbb{R})$, then the following inequality holds*

$$F^{HK}(\rho)\geqslant \mathscr{S}_{K,\varepsilon}(\rho), \tag{9.20}$$

with $\varepsilon = \dfrac{\pi\hbar^2}{2}$.

In order to prove theorem 9.5.6 we need some useful results on the logarithmic Sobolev inequality for the Lebesgue measure.

Corollary 9.5.7 (Corollary 7.3, [72]). *Let us consider $\nu\in\mathcal{P}(\mathbb{R}^d)$ such that $\nu(x)=e^{-V(x)}$ with $\mathrm{D}^2V\geqslant\kappa Id$. Then, for every $f\geqslant 0$ such that $f\nu\in\mathcal{P}(\mathbb{R}^d)$ we have that*

$$\mathrm{H}(f\nu|\nu)\leqslant\frac{2}{\kappa}\int_{\mathbb{R}^d}|\nabla\sqrt{f}|^2\,d\nu. \tag{9.21}$$

Notice that, thanks to the 1-homogeneity of both sides of the inequality with respect to f, one can forget the constraint $f\nu\in\mathcal{P}(\mathbb{R}^d)$. Now we are ready to state our result for the Lebesgue measure:

Theorem 9.5.8 (LSI,[DMN]). *Let $f\geqslant 0$ be a function such that $\sqrt{f}\in\mathrm{H}^1(\mathbb{R}^d)$ and $f\mathcal{L}^d\in\mathcal{P}(\mathbb{R}^d)$. Then the following holds:*

$$\mathrm{H}(f\mathcal{L}^d|\mathcal{L}^d)\leqslant\frac{1}{\pi}\int_{\mathbb{R}^d}|\nabla\sqrt{f}|^2\,dx. \tag{9.22}$$

Proof. The proof is rather simple: it relies on the observation that if $\int f\,d\nu\leqslant 1$ then $\mathrm{H}(f\nu|\nu)\geqslant\int f\log f\,d\nu$. In particular we can consider the measure $\nu_y = e^{-\pi|x-y|^2}$. It is clear that, since $\nu_y\leqslant\mathcal{L}^d$, we have that $\int f\,d\nu_y\leqslant 1$ for every y. In particular, we have that

$$\int f\log f\,d\mu_y\leqslant\mathrm{H}(f\nu_y|\nu_y).$$

Now we can integrate this with respect to y and use that $\int e^{-\pi|x-y|^2} dy = 1$ to obtain

$$\int f \log f \, dx \leqslant \int \mathrm{H}(f\nu_y|\nu_y)\, dy.$$

Now considering $V(x) = \pi|x-y|^2$, we have $\mathrm{D}^2 V = 2\pi Id$ and in particular we have that (9.21) holds with $\kappa = 2\pi$ and so we conclude

$$\begin{aligned} &\mathrm{H}(f\mathcal{L}^d|\mathcal{L}^d) = \int_{\mathbb{R}^d} f \log f \, dx \leqslant \\ &\frac{1}{\pi}\int_{\mathbb{R}^d}\int_{\mathbb{R}^d} |\nabla\sqrt{f}|^2 \, d\mu_y \, dy = \\ &\frac{1}{\pi}\int_{\mathbb{R}^d} |\nabla\sqrt{f}|^2 \, dx. \end{aligned} \tag{9.23}$$

□

Proof Theorem 9.5.6. Notice that by definition $\gamma \geqslant 0$ and $\gamma \in \mathrm{H}^1(\mathbb{R}^{dK})$ so we can apply theorem 9.5.8 and we have

$$\frac{\hbar^2}{2}\int_{\mathbb{R}^{dK}} |\nabla_x\sqrt{\gamma}|^2 dx_1\cdots dx_K \geqslant \varepsilon\, \mathrm{H}(\gamma|\mathcal{L}^{dK}), \tag{9.24}$$

where $\varepsilon := \dfrac{\pi\hbar^2}{2}$. It follows that

$$\begin{aligned} &\int_{\mathbb{R}^{dK}} |\nabla_x\sqrt{\gamma(x_1\cdots x_K)}|^2 dx_1\cdots dx_K + \int_{\mathbb{R}^{dK}} \sum_{i<j} \frac{1}{|x_i - x_j|}\gamma(x_1\cdots x_K) dx_1\cdots dx_K \geqslant \\ &\varepsilon\, \mathrm{H}(\gamma|\mathcal{L}^{dK}) + \int_{\mathbb{R}^{dK}} \sum_{i<j} \frac{1}{|x_i - x_j|}\gamma(x_1\cdots x_K) dx_1\cdots dx_K = \\ &\mathrm{H}(\gamma|\eta_\varepsilon), \end{aligned} \tag{9.25}$$

where $\eta_\varepsilon = \exp\left(-\sum_{i<j}\frac{1}{\varepsilon|x_i-x_j|}\right)\otimes_{i=1}^K dx_i$ (notice that w.l.o.g. we can normalize η_ε in order to have a probability measure). Then, the inequality (9.20) easily follows. □

Remark 9.5.9. Since we obtain the plan γ by symmetrizing ψ, we cannot distinguish a γ induced by a symmetric ψ from the one induced by an antisymmetric wave-function. Anyway the inequality (9.20) still holds; moreover we have the following chain of inequalities

$$F^{HK}_{anti}(\rho) \geqslant F^{HK}_{sym}(\rho) \geqslant \mathscr{S}_{K,\varepsilon}(\rho). \tag{9.26}$$

Remark 9.5.10 (Logarithmic Sobolev exponential Inequality). For the sake of completeness we give also a stronger inequality, the *logarithmic Sobolev exponential inequality*, exploiting the fact that the Lebesgue measure is scale invariant. We will use repeatedly the fact that $\int g(kx)dx = k^{-d}\int g(x)dx$.

Theorem 9.5.11 (LSEI,[DMN]). *Let us assume that* $f \geqslant 0$, $\int_{\mathbb{R}^d} f(x)dx = 1$ *and* $f \in \mathrm{H}^1(\mathbb{R}^d)$. *Then we have that*

$$d \exp\left(\frac{2\,\mathrm{H}(f\mathcal{L}^d|\mathcal{L}^d)}{d}\right) \leqslant \frac{2e}{\pi} \int |\nabla\sqrt{f}|^2\,dx. \tag{9.27}$$

Proof. Let us consider $f_k(x) = k^d f(kx)$ and let us do the calculation for the scaling of the quantities involved:

$$\begin{aligned}\mathrm{H}(f_k(x)\mathcal{L}^d|\mathcal{L}^d) &= k^d \int f(kx)(\log(k^d f(kx)) - 1)\,dx + 1\\ &= \int f(\log(f) - 1)\,dx + 1 + d\log(k)\\ &= \mathrm{H}(f\mathcal{L}^d|\mathcal{L}^d) + d\log(k).\end{aligned}$$

Instead we have that

$$\int_{\mathbb{R}^d} |\nabla\sqrt{f_k}(x)|^2\,dx = \int_{\mathbb{R}^d} k^{2d}|\nabla\sqrt{f}|^2(kx)\,dx = k^2 \int_{\mathbb{R}^d} |\nabla\sqrt{f}|^2\,dx;$$

In particular considering (9.22) for f_k we obtain

$$\mathrm{H}(f\mathcal{L}^d|\mathcal{L}^d) \leqslant \frac{k^2}{\pi} \int_{\mathbb{R}^d} |\nabla\sqrt{f}|^2\,dx - d\log(k).$$

Now we want to minimize the right hand side in k: let us consider the function $ak^2 - b\log(k)$. Its minimum is reached for $k = \sqrt{b/(2a)}$, and so the minimum is

$$a \cdot \left(\sqrt{\frac{b}{2a}}\right)^2 - b\log\left(\sqrt{\frac{b}{2a}}\right) = \frac{b}{2}(1 + \log(2a) - \log(b)).$$

Thus we get, denoting $\mathrm{H}(f\mathcal{L}^d|\mathcal{L}^d) = \mathrm{H}$

$$\begin{aligned}\mathrm{H} &\leqslant \frac{b}{2}(\log(2ea) - \log(b))\\ be^{2\,\mathrm{H}/b} &\leqslant 2ea\end{aligned}$$

that is precisely our conclusion. □

Chapter 10

The Seidl's Conjecture and Counterexamples

In the previous chapter we have given the weak Seidl's conjecture which inquires the existence of optimal maps for the multi-marginal problem with the Coulomb cost. In [110], Seidl, Gori-Giorgi and Savin go a step further and formulate, in the case of a radial symmetric measure, a conjecture (we refer to it as *Strong Seidl Conjecture*) in which they establish the existence of optimal maps and also give a geometric characterization of the maps. Here, we explain this strong conjecture and we also give a counterexample which disproves it. Moreover, we show that, in the framework of this counterexample, high non-uniqueness of optimal solutions holds and that fractal maps, as for the repulsive harmonic cost, appears.

10.1 The Monge problem: deterministic examples and counterexamples

In this section we will illustrate the cases in which we know that there exists a deterministic solution; in those cases moreover there is also a result of uniqueness. We remark that these are two extreme cases, namely the case $K = 2$ (and any d) and the case $d = 1$ (and any K). We will just sketch the proofs in order to make clear the method used here, and why it is difficult to generalize it. We begin with the 2-particles case, in every dimension d: this result was proved in [43] by means of standard optimal transport techniques.

Theorem 10.1.1 ([43])**.** *Let $\mu \in \mathcal{P}(\mathbb{R}^d)$ be a probability measure that is absolutely continuous with respect to the Lebesgue measure. Then there exists a unique optimal plan $\gamma_O \in \Pi_2(\mathbb{R}^{d2}; \mu)$ for the problem*

$$\min\left\{\int_{\mathbb{R}^{2d}} \frac{1}{|x_1 - x_2|}\, d\gamma \mid \gamma \in \Pi_2(\mathbb{R}^{d2}; \mu)\right\}.$$

Moreover this plan is induced by an optimal map T, that is, $\gamma = (\mathrm{Id}, T)_\sharp \mu$, and $T(x) = x + \frac{\nabla\varphi}{|\nabla\varphi|^{3/2}}$ μ-almost everywhere, where φ is a Lipschitz maximizer for the dual problem.

Proof. Let us consider γ a minimizer for the primal problem and φ a bounded and Lipschitz maximizer of the dual problem (it exists thanks to Lemma 9.5.3). Then we know that

$$F(x_1, x_2) = \varphi(x_1) + \varphi(x_2) - \frac{1}{|x_1 - x_2|} \leqslant 0 \qquad \text{for } \mu \otimes \mu\text{-almost every } (x_1, x_2),$$

and we know also that $F = 0$ γ-almost everywhere. But then F has a maximum on the support of γ and so $\nabla F = 0$ in this set; in particular we have that $\nabla\varphi(x_1) = -\frac{x_1 - x_2}{|x_1 - x_2|^3}$ on the support of γ. Finding x_2 we have that $x_2 = x_1 - \frac{\nabla\varphi}{|\nabla\varphi|^{3/2}}(x_1) = T(x_1)$ on the support of γ and this implies $\gamma = (\mathrm{Id}, T)_\sharp\mu$ as we wanted to show. □

The first positive K-marginal result for the Coulomb cost is instead shown in [49] where, in dimension $d = 1$, the authors can prove that for non-atomic measure an optimal plan is always "induced" by a cyclical optimal map T.

Theorem 10.1.2 ([49])**.** *Let $\mu \in \mathcal{P}(\mathbb{R})$ be a diffuse probability measure. Then there exists a unique optimal symmetric plan $\gamma_O \in \Pi_K(\mathbb{R}^K; \mu)$ that solves*

$$\min\left\{ \int_{\mathbb{R}^K} \sum_{1 \leqslant i < j \leqslant K} \frac{1}{|x_j - x_i|}\, d\gamma \mid \gamma \in \Pi_K(\mathbb{R}^K; \mu) \right\}.$$

Moreover this plan is induced by an optimal cyclical map T, that is, $\gamma_O = \frac{1}{K!}\sum_{\sigma \in \mathscr{S}_K} \sigma_\sharp \gamma_T$, where $\gamma_T = (\mathrm{Id}, T, T^{(2)}, \dots, T^{(K-1)})_\sharp\mu$. An explicit optimal cyclical map is

$$T(x) = \begin{cases} F_\mu^{-1}(F_\mu(x) + 1/K) & \text{if } F_\mu(x) \leqslant (K-1)/K \\ F_\mu^{-1}(F_\mu(x) + 1 - 1/K) & \text{otherwise.} \end{cases}$$

Here $F_\mu(x) = \mu(-\infty, x]$ is the distribution function of μ, and F_μ^{-1} is its lower semicontinuous left inverse.

Proof. We begin by observing that if γ is a symmetric optimal plan then a stronger statement than Proposition 7.1.13 holds, namely we have that for every $x, y \in \mathrm{supp}(\gamma)$:

$$c(x) + c(y) = \min\{c(X(x, \sigma(y), p)) + c(Y(x, \sigma(y), p)) : \ \forall p \subset \{1, \dots, K\}, \forall \sigma \in \mathscr{S}_K\},$$

where c is the Coulomb cost on the K-tuple of points $x = (x_1, \dots, x_K)$ and σ acts on the indices. The key point here is that one can show (Proposition 2.4 [49]) that this property holds if and only if a more geometric condition holds true for x and y: they are well-ordered. This property amounts to the fact that, up to permute the coordinates of both points, we have

$$x_1 \leqslant y_1 \leqslant x_2 \leqslant \cdots \leqslant x_K \leqslant y_K,$$

or the other way around. Once this property is proven the rest of proof is rather straightforward, since we proved that the support of $(e_1, e_2)_\sharp\gamma|_D$, where $D = \{x_i \leqslant x_j \text{ and } y_i \leqslant y_j, \ \forall\, i < j\}$, is monotone in the usual sense. We remark that the key property does not easily generalize to $d > 1$ since it (heavily) uses the ordered structure of $\mathbb{R}$. □

Let us notice that in this case we don't have uniqueness of optimal plan neither of cyclical optimal maps, as pointed out in Remark 1.2 in [49].

For the general case we thus have to assume $d > 1$ and $K > 2$: from now on we will look at the case in which the measure μ has radial symmetry. As we have seen in section 7.1.3 we can reduce our problem to a multi-marginal problem in $\mathbb{R}$.

Lemma 10.1.3 (Radial case)**.** *Let $\mu \in \mathcal{P}(\mathbb{R}^d)$ be a radially symmetric measure. In particular μ is determined by $\rho = |\cdot|_\sharp\mu$. Then for every optimal plan $\gamma \in \Pi_K(\mathbb{R}^{dK};\mu)$, if we consider $\gamma_r = R_\sharp\gamma$, where $R : (x_1,\dots,x_K) \mapsto (|x_1|,\dots,|x_K|)$, we have that γ_r is an optimal plan for the $1D$ multi marginal problem*

$$\min\left\{\int_{\mathbb{R}^K_+} \tilde{c}(r_1,\dots,r_K)\,d\eta \mid \eta \in \Pi_K(\mathbb{R}^d_+;\rho)\right\}. \tag{10.1}$$

where $\tilde{c}$ is the reduced Coulomb cost

$$\tilde{c}(r_1,\dots,r_K) = \min\left\{\sum_{1\leqslant i<j\leqslant K} \frac{1}{|x_j - x_i|} \;:\; |x_i| = r_i\ \forall i = 1,\dots,K\right\}. \tag{10.2}$$

Moreover

$$\int_{\mathbb{R}^{dK}} \sum_{1\leqslant i<j\leqslant K} \frac{1}{|x_i - x_j|}\,d\gamma = \int_{\mathbb{R}^K_+} \tilde{c}(r_1,\dots r_K)\,d\gamma_r.$$

Proof. See proof of lemma 7.1.18. □

Given the one dimensional character of this problem, one could expect that the solution is similar to the one depicted in Theorem 10.1.2. In fact in [110] the authors conjecture a similar structure:

Conjecture 10.1.4 (Strong Seidl Conjecture, [110])**.** *Let $\mu \in \mathcal{P}(\mathbb{R}^d)$ be an absolutely continuous measure with respect to the Lebesgue measure, with radial symmetry, and let $\rho(r) = |\cdot|_\sharp\mu$. Let $0 = r_0 < r_1 < \ldots < r_{K-1} < r_K = \infty$ such that the intervals $A_i = [r_i, r_{i+1})$ have all the same radial measure $\rho(A_i) = 1/K$. Then let $F(r) = \rho(0,r]$ be the cumulative radial function and let $S : [0,\infty) \to [0,\infty)$ be defined piecewise such that the interval A_i is sent in the interval A_{i+1} in an anti monotone way:*

$$S(r) = F^{-1}(2i/K - F(r)) \qquad \text{if } r_{i-1} \leqslant r < r_i \text{ and } i < K \tag{10.3}$$

$$S(r) = \begin{cases} F^{-1}(F(r) + 1/K - 1) & \text{if } K \text{ is odd} \\ F^{-1}(1 - F(r)) & \text{if } K \text{ is even,} \end{cases} \qquad \text{if } r_{K-1} \leqslant r < r_K. \tag{10.4}$$

Then S is an optimal cyclical map for the problem (10.1).

Remark 10.1.5 (Notations). Form now on ρ stands for both the measure and its density.

Example 10.1.6 (Example for $K = 5$)**.** *Consider the density*

$$\rho(r) = \frac{1}{4\pi}\exp -r, \tag{10.5}$$

In this case, $r_0 = 0$, $r_N = \infty$, *and*

$$F(r) = (1 - e^{-r}), \qquad F^{-1}(y) = -\log\Big(1 - y\Big). \tag{10.6}$$

For $K = 5$, *Eqs.* (10.3) *and* (10.4) *yield the functions*

$$S(r) = -\log(\frac{2(K-i)}{K} - \exp(-r)) \qquad \text{if } r_{i-1} \leqslant r < r_i \text{ and } i < 5 \tag{10.7}$$

$$S(r) = -\log(\frac{1}{5} - \exp(-r)) \qquad \text{if } r_{K-1} \leqslant r < r_K \tag{10.8}$$

and the maps $T_1(r) = r$, $T_i(r) = S^{(i-1)}(r)$ *for* $i = 2, \cdots, K$ *are plotted in the right panel of figure 10.1*

Remark 10.1.7 (Seidl's notations). In Physics the map T_i are usually referred as *co-motion* functions or SGS maps (where SGS stands for Seidl, Gori-Giorgi and Savin [110]) f_i and are defined in the following way

- for even $i \in \{2, ..., N\}$

$$f_i(r) = \begin{cases} F^{-1}\big(i/K - F(r)\big) & r \leq r_i, \\ F^{-1}\big(F(r) - i/K\big) & r \geq r_i. \end{cases} \tag{10.9}$$

  Since $r \leqslant r_K$, this implies $f_K(r) = F^{-1}\big(K - F(r)\big)$ when K is even.

- for odd $i \in \{1, ..., K\}$, we define

$$f_i(r) = \begin{cases} F^{-1}\big(F(r) + i/K - 1\big) & r < r_{K-i+1}, \\ F^{-1}\big(2 + (1-i)/K - F(r)\big) & r > r_{K-i+1}, \end{cases} \tag{10.10}$$

  generally implying that $f_1(r) = r$.

Then if we consider the density in example 10.1.6, the maps f_i are plotted in the left panel of figure 10.1.

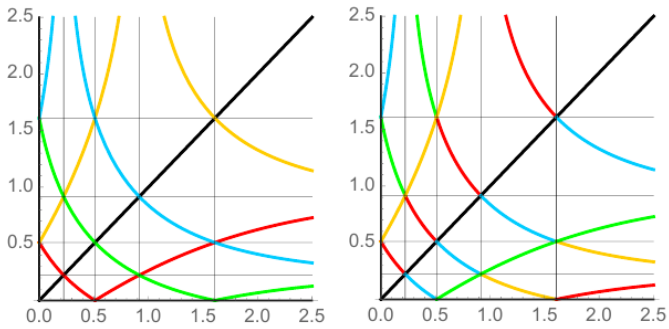

Figure 10.1: *The co-motion functions* $f_i(r)$ *(left) and the maps* T_i *(right) for density 10.5 with* $K = 5$ *marginals. Colors: black, red, yellow, green, blue, respectively for i=1,2,3,4,5.*

In the following section we present a (counter)example (from [SDMG$^+$]) which disproves conjecture 10.1.4. For the sake of completeness we refer the reader to [41] where Maria Colombo and Federico Stra propose some other counterexamples. Moreover, they also give a positive example, namely a class of measures for which the conjecture holds:

Proposition 10.1.8 (Proposition 2.2, [41]). *There exists $M > 0$ such that for any probability measure ρ, such that $\rho([1,2]) = \rho([3,4]) = \rho([M, +\infty[) = \frac{1}{3}$, the conjecture 10.5 holds.*

10.2 Counterexample

Counterexample 10.2.1 (Thin Shell, [SDMG$^+$]). *Let be $\delta > 0$, $K = 3$ and $\rho_\delta(r)$ the density given by*

$$\rho_\delta(r) = \begin{cases} \dfrac{1}{a\delta} & r \in [a, a + a\delta], \\ 0 & \textit{otherwise}, \end{cases} \tag{10.11}$$

then for δ sufficiently small, the conjecture 10.1.4 does not hold.

Remark 10.2.2. We remind that $\rho_\delta = |\cdot|_\sharp \mu_\delta = 4\pi r^2 \mu_\delta(|x|) =$ if $d = 3$, where $\mu_\delta(|x|) = \dfrac{1}{4\pi a\delta |x|^2}$.

For simplicity we take $a = 1$.

Remark 10.2.3 (Optimal maps). In this case the cumulative function $F(r)$ is given by

$$F(r) = \begin{cases} 0 & r < 1, \\ \dfrac{1}{\delta}(r-1) & r \in [1, 1+\delta] \\ 1 & r > +\infty, \end{cases} \tag{10.12}$$

and $r_1 = 1 + \frac{\delta}{3}$, $r_2 = 1 + \frac{2\delta}{3}$. Then the map $S(r)$ is

$$S(r) = \begin{cases} 2(\dfrac{\delta}{3} + 1) - r & r \in [1, r_1[, \\ 2(\dfrac{2\delta}{3} + 1) - r & r \in [r_1, r_2[, \\ r - \dfrac{2\delta}{3} & r \in [r_2, 1+\delta[, \end{cases} \tag{10.13}$$

and the optimal maps T_i are plotted in the right panel of figure 10.2

The proof of counterexample 10.2.1 relies on the following proposition

Proposition 10.2.4 ([SDMG$^+$]). *Consider the cost c_δ defined as*

$$c_\delta(x_1, x_2, x_3) := \tilde{c}(1 + \delta\tilde{x}_1, 1 + \delta\tilde{x}_2, 1 + \delta\tilde{x}_3),$$

where $\tilde{c}$ is the reduced cost (10.2) and the functionals $\mathcal{F}_\delta, \mathcal{F}$

$$\mathcal{F}_\delta(\gamma) := \begin{cases} \displaystyle\int_{[0,1]^3} c_\delta(x_1, x_2, x_3) d\gamma(x_1, x_2, x_3) & \gamma \in \Pi_3([0,1]^3; \mathcal{L}_{[0,1]}), \\ +\infty & \textit{otherwise}, \end{cases}$$

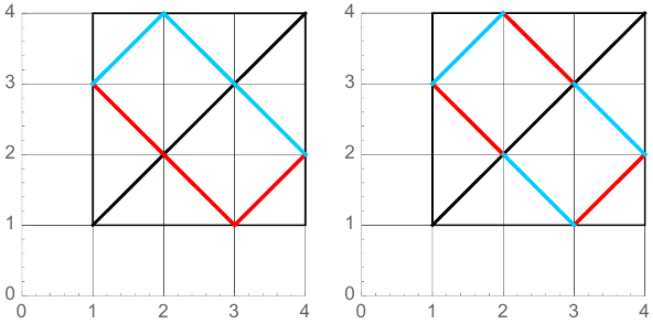

Figure 10.2: *The co-motion functions $f_i(r)$ (left) and the maps T_i (right) for density 10.11 with $K = 3$ marginals and $\delta = 3$. Colors: black, red and blue for i=1,2,3.*

$$\mathcal{F}(\gamma) := \begin{cases} \int_{[0,1]^3} c(x_1, x_2, x_3) d\gamma(x_1, x_2, x_3) & \gamma \in \Pi_3([0,1]^3; \mathcal{L}_{[0,1]}), \\ +\infty & \text{otherwise}, \end{cases}$$

where $c(x_1, x_2, x_3) = |x_1 + x_2 + x_3|^2$. Then,

$$\lim_{\delta \to 0} \mathcal{F}_\delta(\gamma_\delta) = \mathcal{F}(\gamma)$$

for every $\{\gamma_\delta\} \in \Pi_3([0,1]^3; \mathcal{L}_{[0,1]})$ such that $\gamma_\delta \rightharpoonup \gamma$. Moreover, the minimizers of $\mathcal{F}_\delta$ converge to the minimizers of $\mathcal{F}$.

Before proving proposition 10.2.4 we need the following result dealing with the Taylor expansion of the reduced cost at (a, a, a) with $a \neq 0$:

Lemma 10.2.5 (Taylor Expansion of $\tilde{c}(r_1, r_2, r_3)$ at $r_1 = r_2 = r_3 = a$)**.** *Let $\tilde{c}(r_1, r_2, r_3)$ the reduced cost, then the Taylor expansion of $\tilde{c}$ at $r_1 = r_2 = r_3 = a$ is given by*

$$\begin{aligned} \tilde{c}(r_1, r_2, r_3) &= \frac{\sqrt{3}}{a}\Big[1 - \frac{u_1 + u_2 + u_3}{3a} \\ &+ \frac{u_1u_2 + u_1u_3 + u_2u_3}{5a^2} + 2\frac{u_1^2 + u_2^2 + u_3^2}{15a^2} \\ &+ O\Big(\frac{u_1}{a}, \frac{u_2}{a}, \frac{u_3}{a}\Big)^3\Big], \end{aligned} \tag{10.14}$$

where $u_i = r_i - a$.

Remark 10.2.6. Here we present a simplified proof of lemma 10.2.5; notice that near a point (a, a, a) the reduced cost is $\mathcal{C}^3$ so that we can compute the Taylor expansion (see [41]).

Proof. In the case $K = 3$, a minimum-energy configuration has the three charges on a plane containing the origin. For $k = 1, 2$, let θ_k be the angle between x_k and x_3. Then,

$$\tilde{c}(r_1, r_2, r_3) = \min_{\theta_1, \theta_2} c(r_1, r_2, r_3, \theta_1, \theta_2), \tag{10.15}$$

where, due to the cosine theorem,

$$\begin{aligned} c(r_1, r_2, r_3, \theta_1, \theta_2) &= \Big[r_1^2 + r_2^2 - 2r_1 r_2 \cos(\theta_1 + \theta_2)\Big]^{-1/2} \\ &+ \sum_{k=1}^{2} \Big[r_k^2 + r_3^2 - 2r_k r_3 \cos\theta_k\Big]^{-1/2}. \end{aligned} \tag{10.16}$$

In the trivial case $r_3 = 0$, we find $\theta_1 + \theta_2 = \pi$ and

$$\tilde{c}(r_1, r_2, 0) = \frac{1}{r_1 + r_2} + \frac{1}{r_1} + \frac{1}{r_2}. \tag{10.17}$$

Finding the general function $\tilde{c}(r_1, r_2, r_3)$ explicitly seems to be a difficult task.

Instead, we shall now evaluate $\tilde{c}$ and its partial derivatives $\tilde{c}_i$ and $\tilde{c}_{ij}$ for the case $r_1, r_2, r_3 = a$, when the $K = 3$ charges occupy one sphere with radius a and at equilibrium make an equilateral triangle with side length $a\sqrt{3}$,

$$\tilde{c}(a, a, a) = \frac{\sqrt{3}}{a}. \tag{10.18}$$

The symmetry of this problem implies for $i = 1, 2, 3$

$$\begin{aligned} \tilde{c}_i(a, a, a) &= \frac{1}{3}\sum_{k=1}^{3} \tilde{c}_k(a, a, a) \\ &= \frac{1}{3}\frac{d}{da}\tilde{c}(a, a, a) = -\frac{1}{\sqrt{3}}\, a^{-2}, \end{aligned} \tag{10.19}$$

and, since $\tilde{c}_{12}(a, a, a) = \tilde{c}_{23}(a, a, a) = \tilde{c}_{13}(a, a, a)$, as well as $\tilde{c}_{11}(a, a, a) = \tilde{c}_{22}(a, a, a) = \tilde{c}_{33}(a, a, a)$,

$$\begin{aligned} \frac{2}{\sqrt{3}}\, a^{-3} &\equiv \frac{d}{da}\tilde{c}_i(a, a, a) \\ &= \sum_{k=1}^{3} V_{ik}(a, a, a) \\ &= \tilde{c}_{33}(a, a, a) + 2\tilde{c}_{12}(a, a, a). \end{aligned} \tag{10.20}$$

Since $\tilde{c}_{33}(a, a, a) = \frac{4}{5\sqrt{3}}\, a^{-3}$, Eq. (10.29) below, we have

$$\tilde{c}_{12}(a, a, a) = \frac{3}{5\sqrt{3}}\, a^{-3}. \tag{10.21}$$

We obtain the Taylor expansion

$$\begin{aligned} \tilde{c}(r_1, r_2, r_3) &= \frac{\sqrt{3}}{a}\Big[1 - \frac{u_1 + u_2 + u_3}{3a} \\ &+ \frac{u_1u_2 + u_1u_3 + u_2u_3}{5a^2} + 2\frac{u_1^2 + u_2^2 + u_3^2}{15a^2} \\ &+ O\Big(\frac{u_1}{a}, \frac{u_2}{a}, \frac{u_3}{a}\Big)^3\Big], \end{aligned} \tag{10.22}$$

where $u_i = r_i - a$.

To find $\tilde{c}_{33}(a,a,a) = \frac{d^2}{dr^2}\tilde{c}(a,a,r)|_{r=a}$, we observe that any equilibrium configuration with $r_1 = r_2 = a$ has equal angles $\theta_1 = \theta_2 = \theta$. In this case, Eq. (10.16) reads

$$c(r_1,r_2,r_3,\theta_1,\theta_2) = \frac{1}{a}\Big\{\frac{1}{2\sin\theta} + \frac{2}{\sqrt{1+s^2-2s\cos\theta}}\Big\} =: \frac{\widetilde{W}(s,\theta)}{a}, \qquad (10.23)$$

with the new variable $s = \frac{r_3}{a}$. For $s = 1$, the equilibrium angle is $\theta = \frac{2\pi}{3}$. For $\widetilde{W}(s, \frac{2\pi}{3} + \alpha) \equiv W(s,\alpha)$, the addition theorems yield

$$\begin{aligned} W(s,\alpha) &= \frac{1}{\sqrt{3}\cos\alpha - \sin\alpha} \\ &\quad +2\Big[1+s^2+s\big(\cos\alpha+\sqrt{3}\sin\alpha\big)\Big]^{-1/2} \\ &= W(s,0) + \sum_{n=1}^{\infty} W_n(s)\alpha^n. \end{aligned} \qquad (10.24)$$

The equilibrium angle $\alpha(s)$ is fixed by $\frac{\partial}{\partial\alpha}W(s,\alpha) = 0$,

$$0 = W_1(s) + 2W_2(s)\alpha(s) + 3W_3(s)\alpha(s)^2 + \cdots \qquad (10.25)$$

Taking the derivative $\frac{d}{ds}$ yields

$$\begin{aligned} 0 &= W_1'(s) + 2\Big[W_2'(s)\alpha(s) + W_2(s)\alpha'(s)\Big] \\ &+ 3\Big[W_3'(s)\alpha(s) + 2W_3(s)\alpha'(s)\Big]\alpha(s) + \cdots \end{aligned} \qquad (10.26)$$

Setting $s = 1$ and using $\alpha(1) = 0$, we obtain

$$\alpha'(1) = -\frac{W_1'(1)}{2W_2(1)} = -\frac{\sqrt{3}}{15}, \qquad (10.27)$$

where we have used $W_1(s) = \frac{1}{3} - s\sqrt{3}(1+s+s^2)^{-3/2}$ and $W_2(s) = \frac{5}{6\sqrt{3}} + \frac{1}{4}(2s + 11s^2 + 2s^3)(1+s+s^2)^{-5/2}$. Eventually, we find

$$\begin{aligned} \tilde{c}_{33}(a,a,a) &\equiv \frac{d^2}{dr^2}\tilde{c}(a,a,r)\Big|_{r=a} \\ &= \frac{1}{a^2}\frac{d^2}{ds^2}\frac{W\big(s,\alpha(s)\big)}{a}\Big|_{s=1} \\ &= \frac{1}{a^3}\Big[\frac{\partial^2 W}{\partial s^2} + 2\frac{\partial^2 W}{\partial s\partial\alpha}\alpha'(s) + \\ &\quad \frac{\partial^2 W}{\partial\alpha^2}\alpha'(s)^2 + \frac{\partial W}{\partial\alpha}\alpha''(s)\Big]\Big|_{s=1}. \end{aligned} \qquad (10.28)$$

The partial derivatives of $W = W(s,\alpha)$ are readily evaluated from Eq. (10.24). As expected, $\frac{\partial W}{\partial\alpha}|_{s=1} = 0$. With Eq. (10.27), the remaining three terms in Eq. (10.28) yield

$$\tilde{c}_{33}(a,a,a) = \frac{4}{5\sqrt{3}}a^{-3}. \qquad (10.29)$$

□

Proof of proposition 10.2.4. Notice that thanks to lemma 10.2.5 we have that

$$\begin{aligned}\tilde{c}(1,1,1) =&\sqrt{3}[1-\delta\frac{1}{3}(\tilde{x}_1+\tilde{x}_2+\tilde{x}_3)+\delta^2\frac{2}{15}(\tilde{x}_1^2+\tilde{x}_2^2+\tilde{x}_3^2)+\\ &\delta^2\frac{1}{5}(\tilde{x}_1\tilde{x}_2+\tilde{x}_1\tilde{x}_3+\tilde{x}_2\tilde{x}_3)+O(\delta\tilde{x}_1,\delta\tilde{x}_2,\delta\tilde{x}_3)].\end{aligned} \tag{10.30}$$

It follows that c_δ converges pointwise to $c(1,1,1)$. Take now a sequence of plan $\gamma_\delta \in \Pi_3([0,1]^3;\mathcal{L}_{[0,1]})$ such that $\gamma_\delta \rightharpoonup \gamma \in \mathcal{P}([0,1]^3)$, then by compactness of $\Pi_3([0,1]^3;\mathcal{L}_{[0,1]})$ we have that γ still belongs to $\Pi_3([0,1]^3;\mathcal{L}_{[0,1]})$. Then, it is easy to prove that $\mathcal{F}_\delta(\gamma_\delta) \to \int_{[0,1]^3}\tilde{c}(1,1,1)d\gamma$, where $\tilde{c}$ is given by (10.30). Moreover, we have that the minimizers of $\inf(\mathcal{F}_\delta(\gamma))$ converges to the minimizers of

$$\inf\{\int_{[0,1]^3}\tilde{c}(1,1,1)d\gamma \mid \gamma\in\Pi_3([0,1]^3;\mathcal{L}_{[0,1]})\}. \tag{10.31}$$

Notice now that $\tilde{c}(1,1,1)$ can be decomposed into two terms

$$\tilde{c}(1,1,1) = c_{sep}(\tilde{x}_1,\tilde{x}_2,\tilde{x}_3)+\kappa\delta^2(\tilde{x}_1\tilde{x}_2+\tilde{x}_1\tilde{x}_3+\tilde{x}_2\tilde{x}_3)+O(\delta^3),$$

where $\kappa=\frac{\sqrt{3}}{5}$ and

$$c_{sep}(\tilde{x}_1,\tilde{x}_2,\tilde{x}_3) := \sum_{i=1}^{3}\frac{1}{\sqrt{3}}(1-\delta\tilde{x}_i+\delta^2\frac{2}{5}\tilde{x}_i^2).$$

This means that in minimization (10.31) the term c_{sep} depends only on the fixed marginals of γ, $O(\delta^3)$ is negligible at the limit and problem (10.31) is equivalent to

$$\inf\{\int_{[0,1]^3}c(\tilde{x}_1,\tilde{x}_2,\tilde{x}_3)d\gamma \mid \gamma\in\Pi_3([0,1]^3;\mathcal{L}_{[0,1]})\},$$

which ends the proof. □

Proof of Counterexample 10.2.1. We are given the following minimization problem

$$\inf\left\{\int_{[1,1+\delta]^3}\tilde{c}(r_1,r_2,r_3)d\gamma(r_1,r_2,r_3) \mid \gamma\in\Pi_3([1,1+\delta]^3;\mathcal{L}_{[1,1+\delta]})\right\}. \tag{10.32}$$

By setting $r_i = 1+\delta x_i$ with $x_i\in[0,1]$ for $i=1,2,3$, the cost becomes $\tilde{c}(r_1,r_2,r_3)=\tilde{c}(1-\delta x_1,1-\delta x_2,1-\delta x_3)$ and the marginals $\rho_\delta=\mathcal{L}_{[0,1]}$. Thus, problem (10.32) can be rewritten as

$$\inf\left\{\int_{[0,1]^3}\tilde{c}(1-\delta x_1,1-\delta x_2,1-\delta x_3)d\gamma(x_1,x_2,x_3) \mid \gamma\in\Pi_3([0,1]^3;\mathcal{L}_{[0,1]})\right\} \tag{10.33}$$

and by applying proposition 10.2.4 we have that for $\delta\to 0$ problem (10.33) collapses to

$$\inf\left\{\int_{[0,1]^3}|x_1+x_2+x_3|^2d\gamma(x_1,x_2,x_3) \mid \gamma\in\Pi_3([0,1]^3;\mathcal{L}_{[0,1]})\right\}. \tag{10.34}$$

In section 8.1 we have showed that high non-uniqueness holds for problem (10.34). Moreover, thanks to theorem 8.1.6 we know that in this case fractal like maps exist.
We show now that the SGS maps are never optimal and so that the Seidl's conjecture does not hold. If we consider the limit problem with the cost $|x_1 + x_2 + x_3|^2$, we know that a necessary and sufficient condition for a plan γ being optimal (see lemma 8.1.3) is

$$|x_1 + x_2 + x_3| = k \quad \gamma - a.e,$$

where k is a constant. This means that the Seidl's maps T_i, associated to density (10.2.1) are optimal if and only if the induced plan $\gamma = (\mathrm{Id}, T_2, T_3)_\sharp \mathcal{L}_{[0,1]}$ satisfies the condition above. The maps T_i can be easily computed as follows

$$T_2(x) = S(x),$$

where $S(x)$ is given by equation (10.13) and

$$T_3(x) = S(S(x)) = \begin{cases} r + \dfrac{2\delta}{3} & r \in [1, r_1[, \\ 2(\dfrac{\delta}{3} + 1) - r & r \in [r_1, r_2[, \\ 2(\dfrac{2\delta}{3} + 1) - r & r \in [r_2, 1 + \delta[. \end{cases}$$

It is now clear that the plan induced by these maps never satisfies the condition for being optimal. □

Remark 10.2.7 (Fractal map for the Thin Shell). In figure 10.3 we plot the fractal maps defined in theorem 8.1.6 for the density (10.2.1)

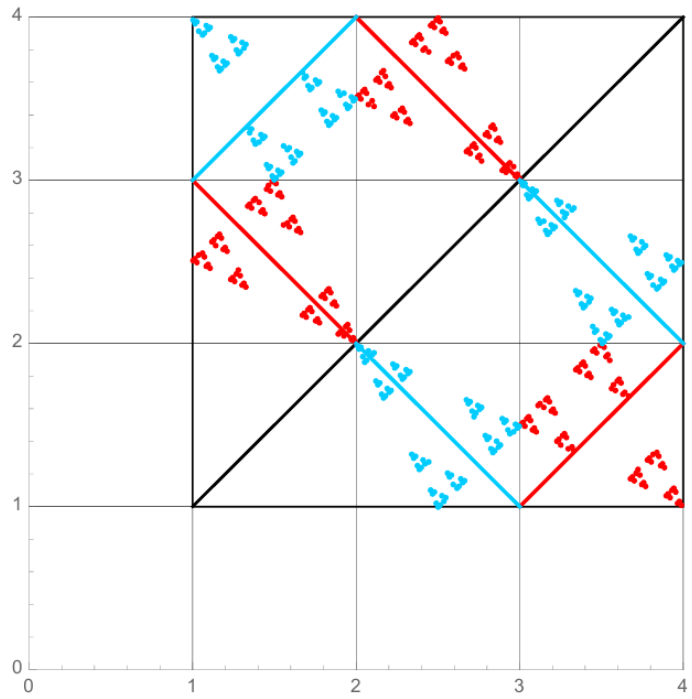

Figure 10.3: *The fractal co-motion functions $f_i(r)$ for density (10.2.1), with $a = 1$ and $\delta = 3$. Colors: black, red (dots) and blue (dots) for $i = 1, 2, 3$, respectively. For comparison we have also plotted the maps T_i from the right panel of figure 10.2*

Chapter 11

Numerical Results

11.1 1−dimensional density: analytical solutions and numerical examples

In this section we treat some simple 1−dimensional case for which we can compute the analytical solutions and then we compare them with the numerical ones obtained by using the IPFP procedure.

11.1.1 1−dimensional for $K = 2$

Let us consider 2 particles in one dimension and marginal densities

$$\mu_1(x) = \mu_2(x) = \begin{cases} a & if\ |x| \leqslant a/2 \\ 0 & otherwise. \end{cases} \tag{11.1}$$

After a few computations, we obtain the following associated co-motion function

$$T(x) = \begin{cases} x + \frac{a}{2} & if\ x \leqslant 0 \\ x - \frac{a}{2} & otherwise \end{cases} \quad . \tag{11.2}$$

If we take

$$\mu_1(x) = \mu_2(x) = \frac{a - |x|}{a^2} \quad defined \quad in \quad [-a, a], \tag{11.3}$$

we get

$$T(x) = \frac{x}{|x|}(\sqrt{2a|x| - x^2} - a) \quad on \quad [-a, a] \tag{11.4}$$

Figure 11.1 shows the co-motion functions for (11.1) and (11.3).

We want now to compare the analytical solutions in figure 11.1 with the ones obtained numerically. Thus consider a uniform density (as (11.1) with $a = 2$) in $1D$. In table 11.1, we analyze the performance of the numerical method by varying the parameter ε. We notice that the error becomes smaller by decreasing the regularizing parameter, but the drawback is that the method needs more

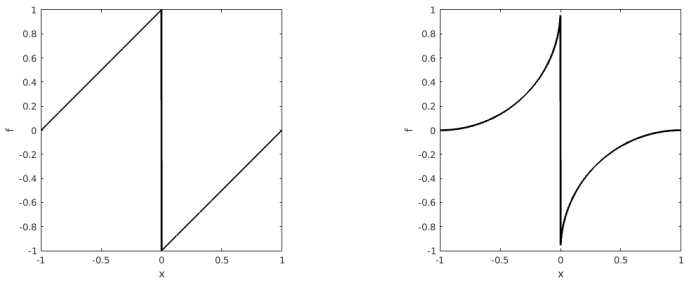

Figure 11.1: *Right: Co-motion function for (11.1) with $a = 2$. Left: Co-motion function for (11.3) with $a = 1$.*

iterations to converge. Figure 11.2 shows the Kantorovich potential, the co-motion function which can be recovered from the potential and the transport plan. The simulation is performed with a discretization of (11.1) with $a = 2$, $N = 1000$ (gridpoints) and $\varepsilon = 0.004$.

Remark 11.1.1. One can notice that, in the case of a uniform density, the transport plan presents a concentration of mass on the boundaries. This is a combined effect of the regularization and of the fact that the density has a compact support.

ε	Error ($\|u^\varepsilon - u\|_\infty / \|u\|_\infty$)	Iteration	CPU time (s)
0.256	0.1529	11	0.4017
0.128	0.0984	16	0.5977
0.064	0.0578	25	0.9282
0.032	0.0313	38	1.4411
0.016	0.0151	66	2.4297
0.008	0.0049	114	4.2674
0.004	0.0045	192	7.0638

Table 11.1: *Numerical results for uniform density in 1D. u^ε is the numerical Kantorovich potential and u is the analytical one.*

11.1.2 1−dimensional for $K \geqslant 3$

We now consider the 3−marginal case and a uniform density ρ on the unit interval. By applying theorem 10.1.2 we show that we can easily recover the following optimal maps.

$$\begin{aligned} T_2(x) &= \begin{cases} x + 1/3 & if \quad x \leqslant 2/3 \\ x - 2/3 & if \quad x > 2/3 \end{cases}, \\ T_3(x) = T_2(T_2(x)) &= \begin{cases} x + 2/3 & if \quad x \leqslant 1/3 \\ x - 1/3 & if \quad x > 1/3 \end{cases}. \end{aligned} \tag{11.5}$$

Furthermore, we know that the Kantorovich potential u satisfies the relation (here we take $K = 3$)

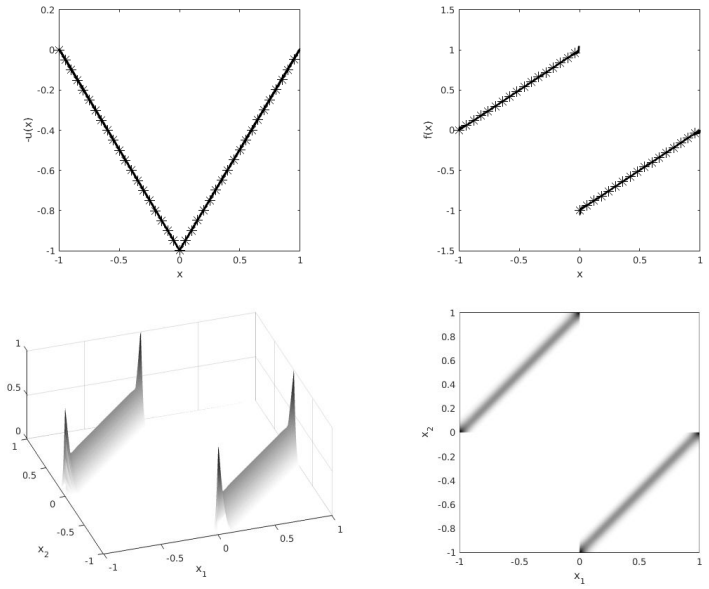

Figure 11.2: *Top-Left: Kantorovich Potential $u(x)$. Top-Right: Numerical co-motion function (solid line) and analytical co-motion (star-solid line) . Bottom-Left: Transport plan $\tilde{\gamma}$. Bottom-Right: Support of $\tilde{\gamma}$.*

$$u'(x) = -\sum_{i=2}^{K} \frac{x - T_i(x)}{|x - T_i(x)|^3} \tag{11.6}$$

and by substituting the optimal maps in (11.6) (and integrating it) we get

$$u(x) = \begin{cases} \frac{45}{4}x & 0 \leqslant x \leqslant 1/3 \\ \frac{15}{4} & 1/3 \leqslant x \leqslant 2/3 \\ -\frac{45}{4}x + \frac{45}{4} & 2/3 \leqslant x \leqslant 1 \end{cases} \tag{11.7}$$

Figure 11.3 illustrates this example.

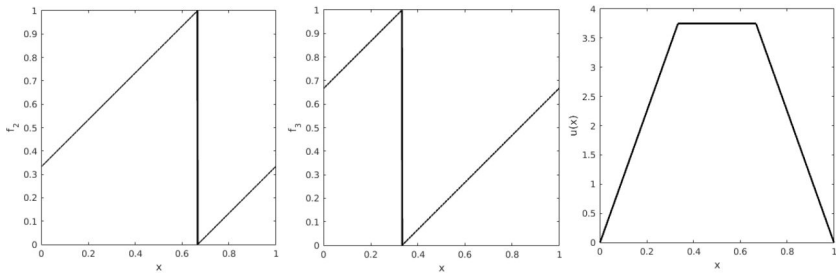

Figure 11.3: *Right: co-motion function T_2 for (11.5). Center: co-motion function T_3 for (11.5). Left: Kantorovich Potential $u(x)$ (11.7).*

As we have done in the previous section, we compare the analytical results with the numerical ones. In table 11.2, we present the performance of the

method for a uniform density on $[0,1]$ by varying ε and, as expected, we see the same behavior as in the 2 marginals case. Figure 11.4 shows the Kantorovich potential and the projection of the transport plan onto two marginals (namely $\gamma^2 = \pi_{12}(\gamma^\varepsilon)$). The support gives the relative positions of two electrons.

The simulation is performed on a discretization of $[0,1]$ with a uniform density, $N = 1000$ and $\varepsilon = 0.02$. If we focus on the support of the projected transport plan we can notice that the numerical solution correctly reproduces the prescribed behavior. The concentration of mass is again due to the compact support of the density.

ε	Error ($\|u^\varepsilon - u\|_\infty / \|u\|_\infty$)	Iteration	CPU time (s)
0.32	0.0658	15	5.8372
0.16	0.0373	27	20.061
0.08	0.0198	64	55.718
0.04	0.0097	178	194.22
0.02	0.0040	374	542.63

Table 11.2: *Numerical results for uniform density in 1D and three electrons. u^ε is the numerical Kantorovich potential and u is the analytical one.*

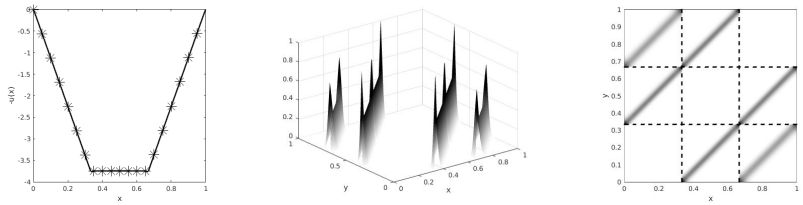

Figure 11.4: *Left: Numerical Kantorovich potential $u(x)$ (solid line) and analytical potential (star-solid line). Center: Projection of the transport plan $\pi_{12}(\gamma(x,y,z))$. Right: Support of $\pi_{12}(\gamma(x,y,z))$ The dot-dashed lines delimit the intervals where ρ_i, with $i = 1, \cdots, 3$, are defined.*

We finally present some simulations for densities which have not a compact support to show that we have not the same concentration of mass at the boundary as for the uniform density. The simulations in figure 11.5 are all performed on a discretization of $[-5,5]$ with $N = 200$, with marginals $\mu_i = \mu(x) = \frac{K}{10}(1 + \cos(\frac{\pi}{5}x)) \quad i = 1, \cdots, K$ and $\varepsilon = 0.02$. If we focus on the support of the coupling $\tilde{\gamma}_{12}(x,y) = \pi_{12}\gamma(x,y,z)$, where $\pi_{12} : \mathbb{R}^{KN} \to \mathbb{R}^N$ is the canonical projection, we can notice that the numerical solution correctly reproduces the prescribed behavior: the transport plan is induced by a cyclical optimal map.

Remark 11.1.2. Theorem 10.1.2 actually works also for other costs functions as $c(x_1, \cdots, x_K) = \sum_{i<j}^K -\log(|x_i - x_j|)$. This means that if we use the density $\mu(x) = \frac{K}{10}(1 + \cos(\frac{\pi}{5}x))$, we expect to obtain the same solution as for the Coulomb cost. Thus if we now consider the 3-marginals case and the discretized cost $c_{j_1,j_2,j_3} = -\log(|x_{j_1} - x_{j_2}|) - \log(|x_{j_1} - x_{j_3}|) - \log(|x_{j_2} - x_{j_3}|)$, we can notice

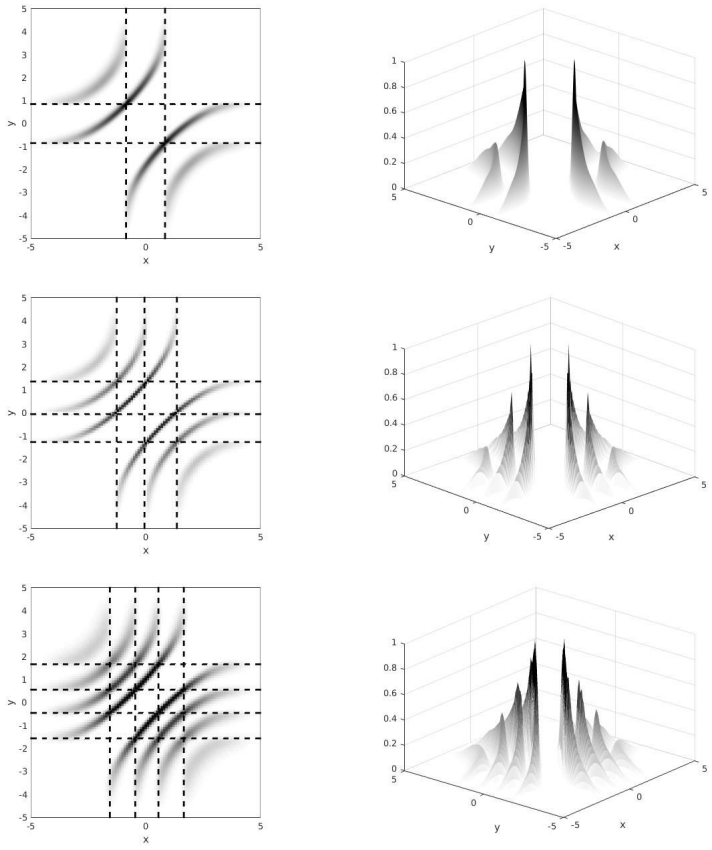

Figure 11.5: *On the Left: support of the optimal coupling* $\tilde{\gamma}_{12}(x, y)$*, on the Right: graph of the optimal coupling* $\tilde{\gamma}_{12}(x, y)$ *, in the cases* $K = 3$ *(1st Row),* $K = 4$ *(2nd Row),* $K = 5$ *(3rd Row). The dashed lines delimit the supports of* $\tilde{\mu}_i$ *, with* $i = 1, \cdots, K$*.*

(see figure 11.6) that we recover the same optimal coupling as the corresponding case for Coulomb (first row of figure 11.5). The simulation is performed on a discretization $[-5, 5]$ with $N = 200$, with marginals $\mu(x) = \frac{K}{10}(1+\cos(\frac{\pi}{5}x))$ $K = 3$ and $\varepsilon = 0.01$.

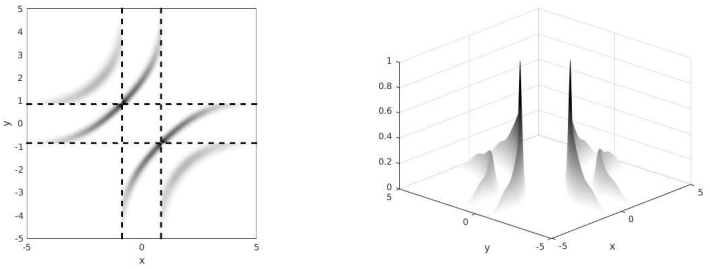

Figure 11.6: *(logarithmic cost) Left: support of the optimal coupling $\tilde{\gamma}_{12}(x, y)$ for $K = 3$. Right: support of the optimal coupling $\tilde{\gamma}_{12}(x, y)$ for $K = 3$. The dashed lines delimit the intervals where $\tilde{\mu}_i$, with $i = 1, \cdots, 3$, are defined.*

11.2 $d-$dimensional radial symmetric density

11.2.1 $N = 2$ electrons in dimension $d \geqslant 3$: analytical examples

As explained in section 7.1.3, we can also compute the co-motion for a radially symmetric density. We have tested the method in $2D$ and $3D$, figure 11.7 and 11.8 respectively, by using the normalized uniform density on the unit ball. Moreover, in the radial case we have proved that the OT problem can be reduced to a $1-$dimensional problem by computing $\tilde{c}$ which is trivial for the 2 electrons case: let us set the problem in $2D$ in polar coordinates (r_1, θ_1) and (r_2, θ_2), for the first and the second electron respectively (without loss of generality we can set $\theta_1 = 0$), then it is easy to verify that the minimum is achieved with $\theta_2 = \pi$. Figure 11.7 shows the Kantorovich potential (the radial component $v(r)$ as defined in section 7.1.3), the co-motion and the transport plan for the $2-$dimensional case, the simulation is performed with $N = 1000$ and $\varepsilon = 0.002$. In figure 11.8 we present the result for th $3-$dimensional case, the simulation is performed with $N = 1000$ and $\varepsilon = 0.002$.

11.2.2 $K = 2$ electrons in dimension $d = 3$: Helium atom

Once we have validated the method with some analytical examples, we solve the regularized problem for the Helium atom by using the electron density computed in [58]. In figure 11.9, we present the electron density, the Kantorovich potential and the transport plan. The simulation is performed with a discretization of $[0, 4]$ with $N = 1000$ and $\varepsilon = 5\,10^{-3}$. We can notice the potential correctly fits the asymptotic behavior from [110], namely $v(r) \sim \dfrac{K-1}{|r|}$ for $r \to \infty$, where K is the number of electrons.

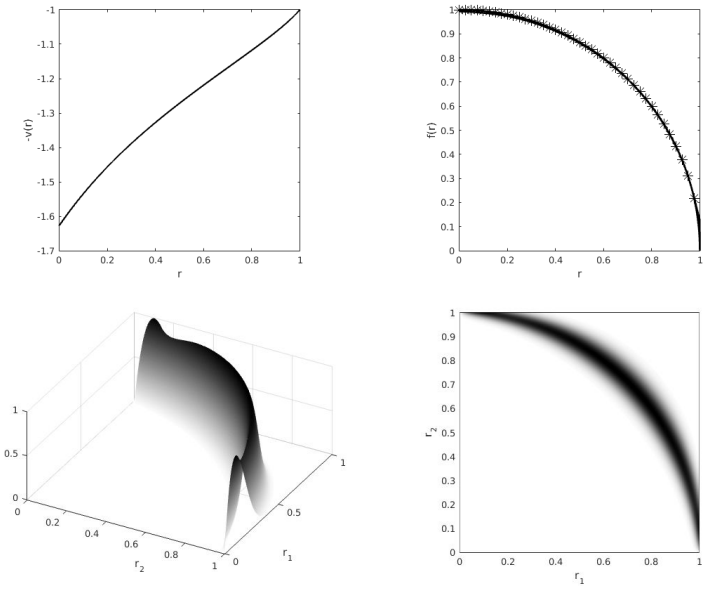

Figure 11.7: *Top-Left: Kantorovich Potential $v(r)$. Top-Right: Numerical co-motion function (solid line) and analytical co-motion (star-solid line) . Bottom-Left: Transport plan $\tilde{\gamma}$. Bottom-Right: Support of $\tilde{\gamma}$.*

11.2.3 $K = 3$ electrons in dimension $d = 3$ radial case : Lithium atom

We finally perform some simulations for the radial $3-$dimensional case for $K = 3$. As for the $3-$dimensional case with 2 marginals we solve the reduced problem: let us consider the spherical coordinates $(r_i, \theta_i, \varphi_i)$ with $i = 1, \cdots, 3$ and we fix $\theta_1 = 0$ and $\varphi_1 = \varphi_2 = 0$ (the first electrons defines the z axis and the second one is on the xz plane). We then notice that $\varphi_3 = 0$ as the electrons must be on the same plane of the nucleus to achieve compensation of forces (one can see it by computing the optimality conditions), so we have to minimize on θ_2 and θ_3 in order to obtain $\tilde{c}$.

Figure 11.10 shows the electron density of the Lithium (computed in [24]), the Kantorovich Potential (and the asymptotic behavior) and the projection of the transport plan onto two marginals $\tilde{\gamma}^2 = \pi_{12}(\tilde{\gamma}^\varepsilon)$. The support gives the relative positions of two electrons.

The simulation is performed on a discretization of $[0, 8]$ with $N = 300$ and $\varepsilon = 0.007$. Our results show (taking into account the regularization effect) a concentrated transport plan for this kind of density and they match analogous result obtained in [110].

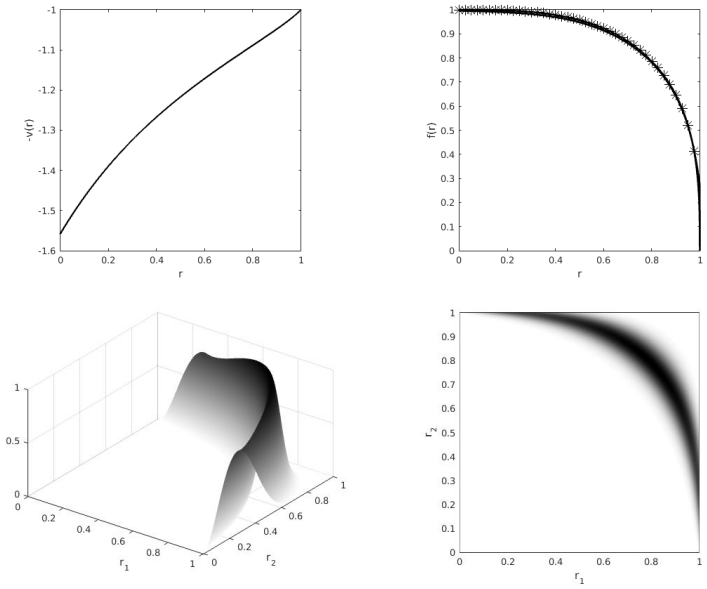

Figure 11.8: *Top-Left: Kantorovich Potential $v(r)$. Top-Right: Numerical co-motion function (solid line) and analytical co-motion (star-solid line) . Bottom-Left: Transport plan $\tilde{\gamma}$. Bottom-Right: Support of $\tilde{\gamma}$.*

11.3 Numerical Counterexamples to Seidl's conjecture

In this section we provide some numerical experiments, by using different methods, to disprove Seidl's conjecture. We firstly consider the density (10.2.1) of the thin shell counterexample we have previously treated

11.3.1 The Thin Shell

Hessian matrix of classical potential energy

We define the potential energy as follows:

Definition 11.3.1 (Potential energy)**.** *Let $c : \mathbb{R}^{dK} \to \mathbb{R}$ be the Coulomb cost (or the reduced cost in case of radial symmetric marginals), μ the marginals and u the optimal Kantorovich potential then the potential energy $E_{\text{pot}}[\rho] : \mathbb{R}^{dK} \to \mathbb{R}$ is*

$$E_{\text{pot}}[\mu](x_1, \cdots, x_K) = c(x_1, \cdots, x_K) - \sum_{i=1}^{K} u(x_i). \tag{11.8}$$

Remark 11.3.2 (Optimal solution and Potential energy). We know that $E_{\text{pot}}[\mu]$ is actually non-negative as u is the optimal Kantorovich potential; moreover if we evaluate the potential energy at $(x_1, \cdots, x_K)$, where $(x_1, \cdots, x_K)$ belongs to the support of the optimal γ, then we have $E_{\text{pot}}[\mu](x_1, \cdots, x_K) = L$ (L is a constant).

For a density ρ, for which the Seidl's maps are optimal, the potential energy function $E_{\text{pot}}[\rho](x_1, \ldots, x_K)$ must be minimum, and therefore constant,

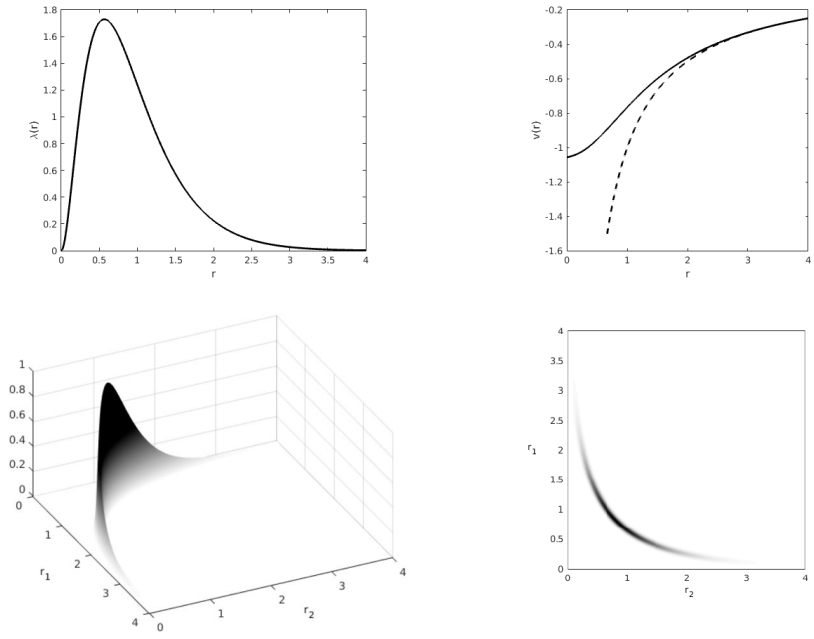

Figure 11.9: *Top-Left: Helium density* $\lambda(r) = 4\pi r^2\rho(r)$. *Top-Right: Kantorovich Potential* $v(r)$ *(solid line) and asymptotic behavior (dashed line)* $v(r) \sim \frac{1}{r} \quad r \to \infty$. *Bottom-Left: Transport plan* $\tilde{\gamma}$. *Bottom-Right: Support of* $\tilde{\gamma}$. *All quantities are in Hartree atomic units.*

on a d-dimensional subset (namely the support of the optimal plan γ which is concentrated on the optimal maps) of the Kd-dimensional configuration space. Consequently, the $(Kd \times Kd)$ Hessian matrix of this function,

$$H(x_1, \ldots, x_K) = \mathrm{D}^2 E_{\mathrm{pot}}[\rho](x_1, \ldots, x_K), \tag{11.9}$$

evaluated at any $(x_1, \cdots, x_K) \in \operatorname{supp}\gamma$, where $\gamma = (\mathrm{Id}, T_2, \cdots, T_K)_\sharp\rho$ (T_i are the Seidl's maps for ρ),

$$\widetilde{H}(x) = H(x, T_2(x), \ldots, T_K(x)), \tag{11.10}$$

should always have $p \geq d$ eigenvectors to the eigenvalue 0, while all the other $Kd - p$ eigenvalues must be > 0.

For the density ρ_δ of eq. (10.2.1), with $d = K = 3$, the $Kd = 9$ eigenvalues $\lambda_q[\rho](r)$ (where $r = |x|$), $q = 1, \ldots, 9$, are plotted versus $r \in [1, 1 + \delta]$ in figure 11.11. The persistence of at least one significantly negative eigenvalue, for all different values of the parameter $\delta > 0$ considered here, is indicating that, for this particular set of densities, the Seidl's maps T_i do not yield the true minimum.

LP and Entropic approach

In this section we compare the results obtained by using the IPFP and a standard Linear Programming approach (LP). Since the marginals are radially symmetric we can solved the discretized problem in $1-$dimension and precompute the reduced cost $\tilde{c}_{ijk}$. Notice that only three marginals are involved so

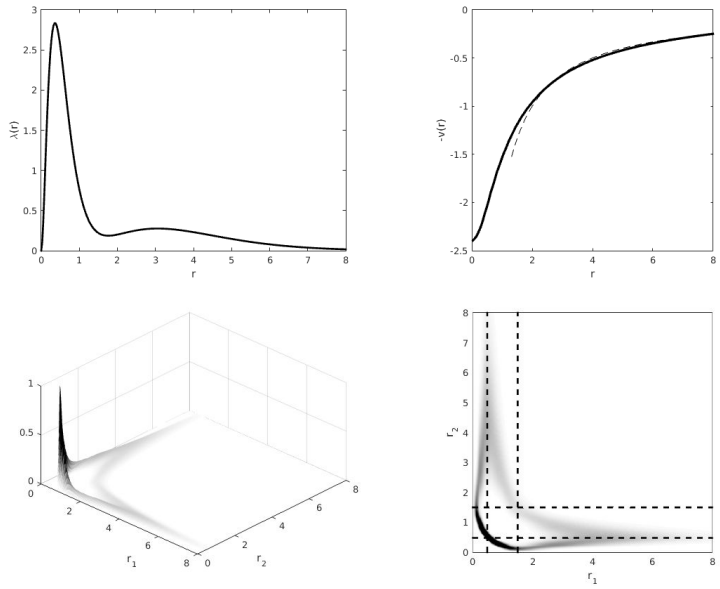

Figure 11.10: *Top-Left: lithium density* $\rho(r) = 4\pi r^2\rho(r)$. *Top-Right: Kantorovich Potential* $v(r)$ *(solid line)) and asymptotic behavior (dashed line)* $v(r) \sim \frac{2}{r} \quad r \to \infty$. *Bottom-Left: Projection of the Transport plan* $\tilde{\gamma}^2 = \pi_{12}(\tilde{\gamma}^\varepsilon)$. *Bottom-Right: Support of the projected transport plan* $\tilde{\gamma}^2$. *The dot-dashed lines delimit the three regions that the electrons must occupy, we computed them numerically following the idea in [110]. All quantities are in Hartree atomic units.*

the standard problem without entropic regularization can be easily solved by using a simplex method. For the simulations we have used a uniform discretization of $[1, 1+\delta]$ with 100 gridpoints. In table 11.3 we report the values of the Monge-Kantorovich problem obtained by using the Seidl's maps $((\mathcal{MK})_{SGS})$, the LP approach $((\mathcal{MK})_{LP})$ and the entropic regularization $((\mathcal{MK})_{entropic})$. In figure 11.12 we compare $(\mathcal{MK})_{LP} - (\mathcal{MK})_{SGS}$ and $(\mathcal{MK})_{entropic} - (\mathcal{MK})_{SGS}$: notice that, as expected, the values of Monge-Kantorovich obtained with LP are smaller than the ones associated to the Seidl's maps. In figure 11.13 we plot an isosurface of the optimal plan obtained by using the LP approach; we can see that as δ becomes smaller, the plan tends to concentrate on the hyperplane $|x_1 + x_2 + x_3|$, namely the optimal γ is converging towards a solution of $(\mathcal{MK})$ with the cost $c(x_1, x_2, x_3) = |x_1 + x_2 + x_3|^2$.

11.3.2 Some others numerical counterexamples

In this final section we show some further numerical counterexamples to Seidl's conjecture. In section 11.2.3 we have seen that for the Lithium density the conjectures holds (from a numerical point of view). Here we present the evolution of the optimal transport plan by considering the following family of densities

$$\rho_\alpha(r) = \alpha\rho(r)_{lithium} + (1-\alpha)\rho_{exp}(r), \quad \alpha \in [0,1]$$

where $\rho_{lithium}$ is the density used in section 11.2.3 and $\rho_{exp}(r) = \frac{3}{\pi}\exp(-2r)$ In figure 11.14 we plot the support and the surface of the projection $\tilde{\gamma}^2 := \pi_{12}(\tilde{\gamma}^\varepsilon)$

δ	SGS	LP	H
0.1	1.6497	1.6497	1.6500
0.3	1.5071	1.5070	1.5079
0.5	1.3877	1.3875	1.3885
0.7	1.2862	1.2858	1.2870
0.9	1.1987	1.1983	1.1995
1.1	1.1226	1.1221	1.1232
1.3	1.0557	1.0551	1.0560
1.5	0.9964	0.9957	0.9966
1.7	0.9434	0.9427	0.9436
1.9	0.8959	0.8951	0.8960
2.1	0.8529	0.8521	0.8530
2.3	0.8139	0.8130	0.8139
2.5	0.7783	0.7774	0.7783
2.7	0.7457	0.7448	0.7457
2.9	0.7158	0.7148	0.7157
3.1	0.6881	0.6872	0.6881
3.3	0.6626	0.6616	0.6625
3.5	0.6388	0.6379	0.6388

Table 11.3: *Values of the Monge-Kantorovich problem obtained by using the Seidl's maps (SGS), the Linear Programming approach (LP) and the entropic one for different δ*

of the optimal plan obtained by using the entropic regularization; notice that as $\alpha \to 1$ the plan tends to concentrate on the Seidl's maps. This becomes more clear if we look at the values (see table 11.4) of the Monge-Kantorovich problem: when the plan is spread the entropic regularization returns a value smaller than the Seidl's maps. If the SGS maps were optimal, then the associated value of $(\mathcal{MK})$ would be smaller than the one of the entropic regularization. In table 11.4 we report also the values obtained via an LP approach; notice that one the Seidl's map appear the LP returns a values larger than the one computed by using the map, this is due to the discretization: as the Seidl's maps can be easily computed we can use a finer grid than the one for the LP problem. This implies that when the Seidl's maps are optimal, they provide a fast computational method to compute the value of $(\mathcal{MK})$.

We end this section by showing, in figure 11.15, the transition of the transport plans γ obtained by using the entropic regularization and the LP approach. We remark that, as expected, the LP plan concentrates on the graph of the transport maps, where as the entropic plan stays more spread because of the regularization

α	LP	H	SGS
0	1.2109	1.2122	1.2178
0.1429	1.2270	1.2284	1.2325
0.2857	1.2471	1.2506	1.2499
0.4286	1.2723	1.2741	1.2723
0.5714	1.3045	1.3064	1.3026
0.7143	1.3462	1.3483	1.3434
0.8571	1.3989	1.4019	1.3902
1	1.4663	1.469	1.4624

Table 11.4: *Values of the Monge-Kantorovich problem obtained by using the Seidl's maps (SGS), the Linear Programming approach (LP) and the entropic one for different* α

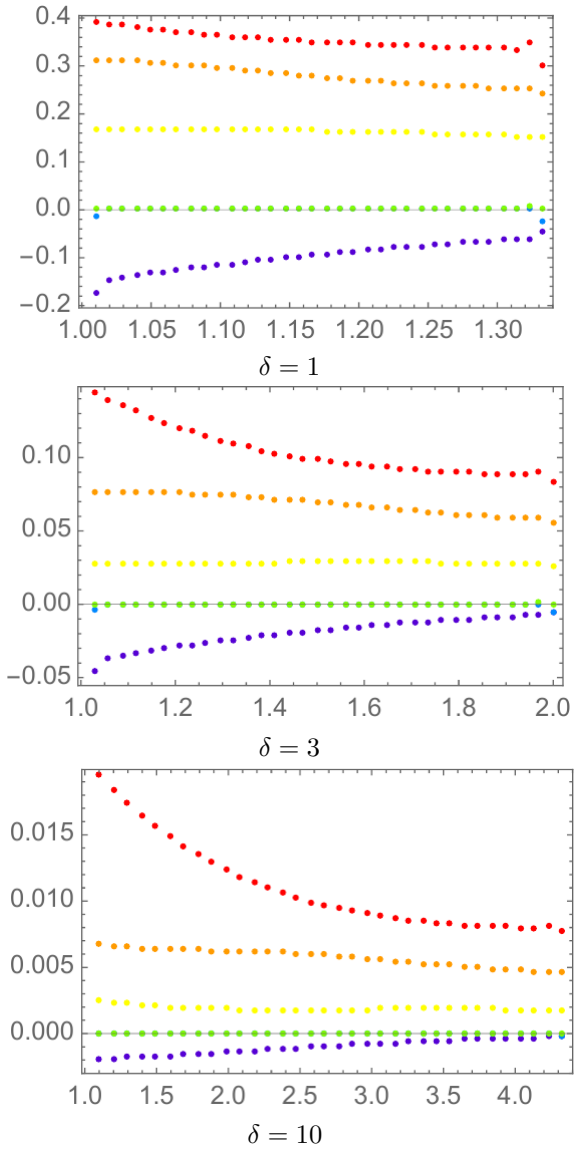

Figure 11.11: *Eigenvalues of the Hessian (11.10) for the density (10.2.1).*

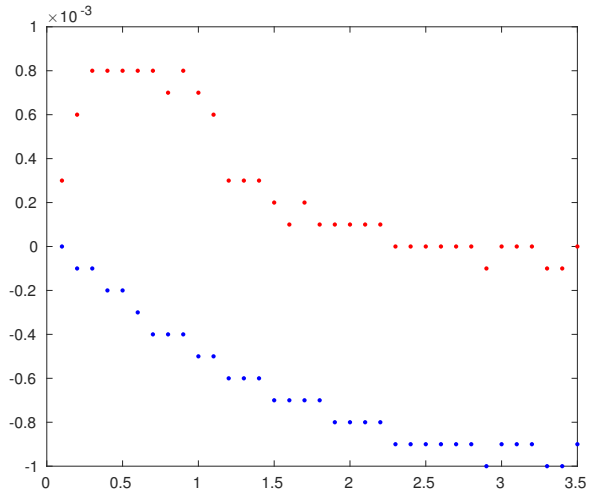

Figure 11.12: *Comparison between* $(\mathcal{MK})_{LP} - (\mathcal{MK})_{SGS}$ *(blue dots) and* $(\mathcal{MK})_{entropic} - (\mathcal{MK})_{SGS}$ *(red dots).*

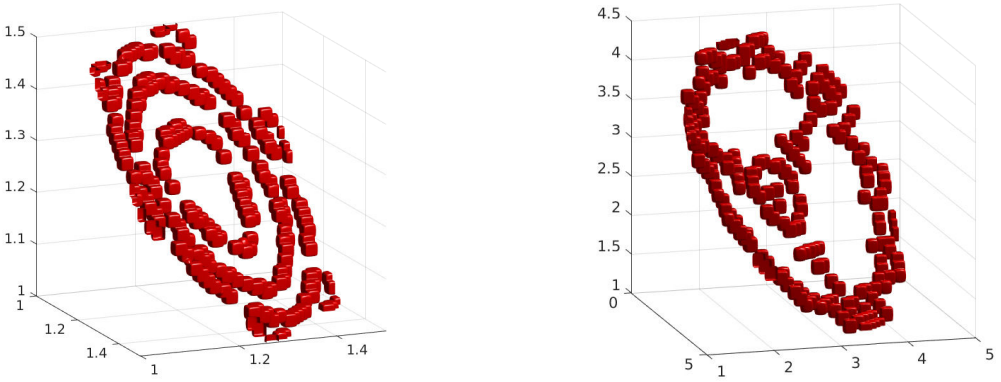

Figure 11.13: *Isosurface of the optimal plan* γ*, solution of the LP problem, for* $\delta = 0.5$ *(left) and* $\delta = 3.5$ *(right).*

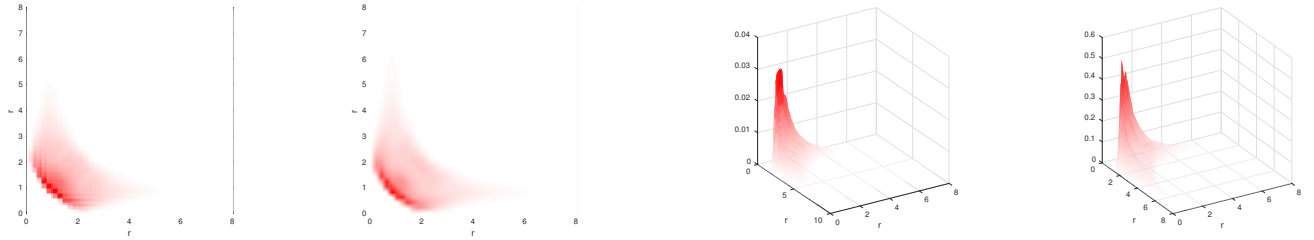

$\mathrm{supp}(\tilde{\gamma}^2)$ for $\alpha = 0$ | $\mathrm{supp}(\tilde{\gamma}^2)$ for $\alpha = 0.1429$ | $\tilde{\gamma}^2$ for $\alpha = 0$ | $\tilde{\gamma}^2$ for $\alpha = 0.1429$

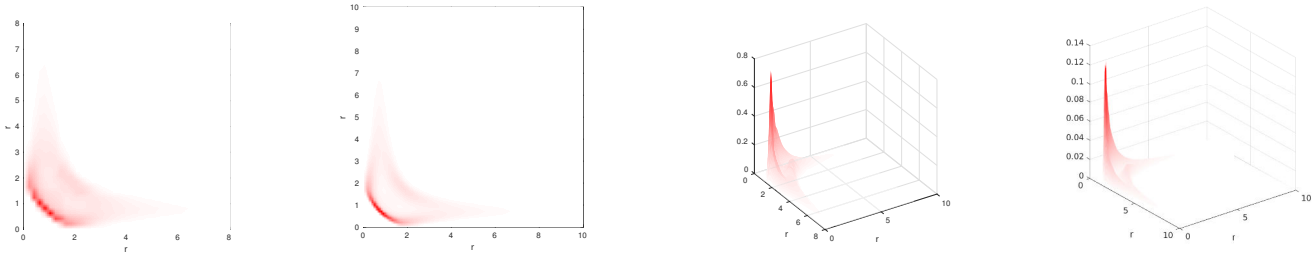

$\mathrm{supp}(\tilde{\gamma}^2)$ for $\alpha = 0.2857$ | $\mathrm{supp}(\tilde{\gamma}^2)$ for $\alpha = 0.4286$ | $\tilde{\gamma}^2$ for $\alpha = 0.2857$ | $\tilde{\gamma}^2$ for $\alpha = 0.4286$

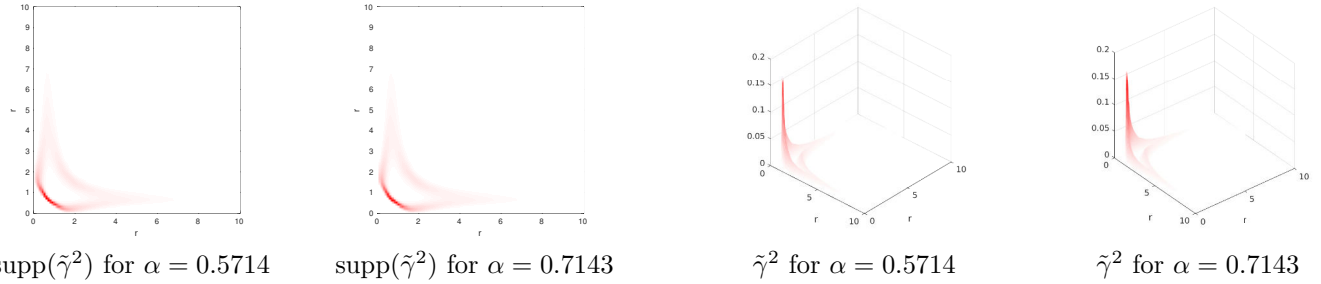

$\mathrm{supp}(\tilde{\gamma}^2)$ for $\alpha = 0.5714$ | $\mathrm{supp}(\tilde{\gamma}^2)$ for $\alpha = 0.7143$ | $\tilde{\gamma}^2$ for $\alpha = 0.5714$ | $\tilde{\gamma}^2$ for $\alpha = 0.7143$

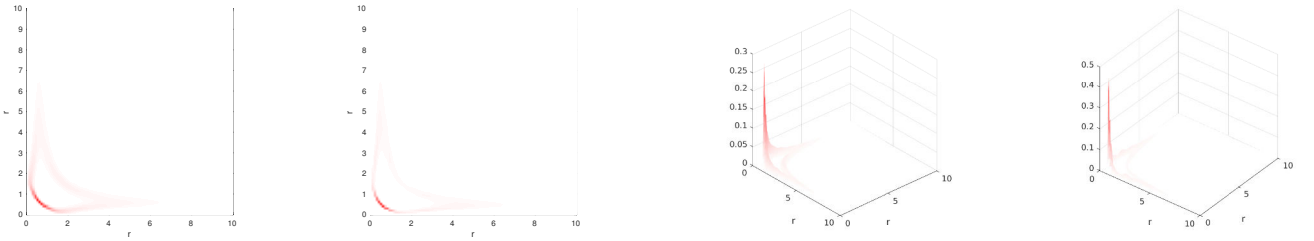

$\mathrm{supp}(\tilde{\gamma}^2)$ for $\alpha = 0.8571$ | $\mathrm{supp}(\tilde{\gamma}^2)$ for $\alpha = 1$ | $\tilde{\gamma}^2$ for $\alpha = 0.8571$ | $\tilde{\gamma}^2$ for $\alpha = 1$

Figure 11.14: *Display the support (left) and the surface (right) of the projection $\tilde{\gamma}^2$ for different values of the parameter α.*

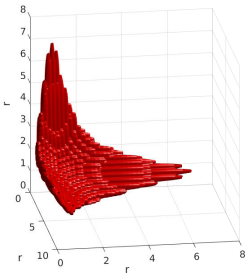

optimal plan γ^{ε} for $\alpha = 0$

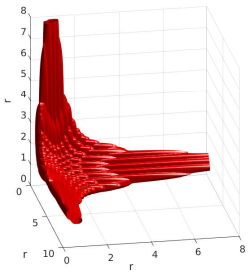

optimal plan γ^{ε} for $\alpha = 0.2857$

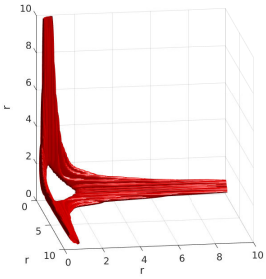

optimal plan γ^{ε} for $\alpha = 1$

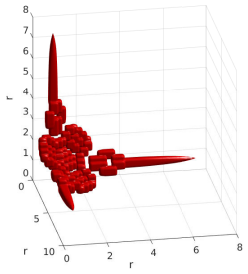

optimal plan γ^{LP} for $\alpha = 0$

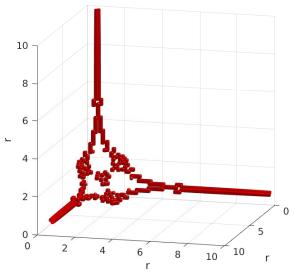

optimal plan γ^{LP} for $\alpha = 0.2857$

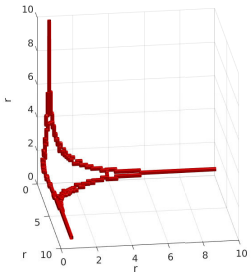

optimal plan γ^{LP} for $\alpha = 1$

Figure 11.15: *Display the support (left) and the surface (right) of the projection $\tilde{\gamma}^2$ for different values of the parameter α.*

Contributions

[BCC+15] Jean-David Benamou, Guillaume Carlier, Marco Cuturi, Luca Nenna, and Gabriel Peyré. Iterative Bregman projections for regularized transportation problems. *SIAM Journal on Scientific Computing*, 37(2):A1111–A1138, 2015.

[BCN15] Jean-David Benamou, Guillaume Carlier, and Luca Nenna. A numerical method to solve optimal transport problems with Coulomb cost. *arXiv preprint arXiv:1505.01136, to appear as a chapter in "Splitting Methods in Communication and Imaging, Science and Engineering", Editors R. Glowinski, S. Osher, and W. Yin., Springer*, 2015.

[BCN16a] Jean-David Benamou, Guillaume Carlier, and Luca Nenna. Multimarginal optimal transportation and incompressible Euler equations. *in preparation*, 2016.

[BCN16b] Adrien Blanchet, Guillaume Carlier, and Luca Nenna. Computation of Cournot-Nash equilibria by entropic regularization. September 2016. working paper or preprint.

[DMGN15] Simone Di Marino, Augusto Gerolin, and Luca Nenna. Optimal transportation theory with repulsive costs. *arXiv preprint arXiv:1506.04565*, 2015.

[DMN] Simone Di Marino and Luca Nenna. *in preparation.*

[SDMG+] Michael Seidl, Simone Di Marino, Augusto Gerolin, Luca Nenna, Klaas Giesbertz, and Paola Gori-Giorgi. The strictly-correlated electron functional for spherically symmetric systems revisited. *in preparation.*

Bibliography

[1] M. Agueh and G. Carlier. Barycenters in the Wasserstein space. *SIAM J. on Mathematical Analysis*, 43(2):904–924, 2011.

[2] Luigi Ambrosio and Alessio Figalli. Geodesics in the space of measure-preserving maps and plans. *Archive for rational mechanics and analysis*, 194(2):421–462, 2009.

[3] Luigi Ambrosio, Nicola Gigli, and Giuseppe Savaré. *Gradient flows: in metric spaces and in the space of probability measures*. Springer Science & Business Media, 2006.

[4] Marc Arnaudon, Ana Bela Cruzeiro, and Shizan Fang. Generalized stochastic lagrangian paths for the navier-stokes equation. *arXiv preprint arXiv:1509.03491*, 2015.

[5] Marc Arnaudon, Ana Bela Cruzeiro, Christian Léonard, and Jean-Claude Zambrini. An entropic interpolation problem for incompressible viscid fluids. *private communication*.

[6] Vladimir Arnold. Sur la géométrie différentielle des groupes de lie de dimension infinie et ses applications à l'hydrodynamique des fluides parfaits. In *Annales de l'institut Fourier*, volume 16, pages 319–361, 1966.

[7] H. H. Bauschke and A. S. Lewis. Dykstra's algorithm with Bregman projections: a convergence proof. *Optimization*, 48(4):409–427, 2000.

[8] Mathias Beiglböck and Claus Griessler. An optimality principle with applications in optimal transport. *arXiv preprint arXiv:1404.7054*, 2014.

[9] Mathias Beiglböck, Christian Léonard, and Walter Schachermayer. A general duality theorem for the monge–kantorovich transport problem. *arXiv preprint arXiv:0911.4347*, 2009.

[10] Jean-David Benamou and Yann Brenier. A computational fluid mechanics solution to the monge-kantorovich mass transfer problem. *Numerische Mathematik*, 84(3):375–393, 2000.

[11] Marc Bernot, Alessio Figalli, and Filippo Santambrogio. Generalized solutions for the euler equations in one and two dimensions. *Journal de mathématiques pures et appliquées*, 91(2):137–155, 2009.

[12] Dimitri P Bertsekas. The auction algorithm: A distributed relaxation method for the assignment problem. *Annals of operations research*, 14(1):105–123, 1988.

[13] Garrett Birkhoff. Extensions of jentzsch's theorem. *Transactions of the American Mathematical Society*, 85(1):219–227, 1957.

[14] Adrien Blanchet and Guillaume Carlier. From Nash to Cournot-Nash equilibria via the Monge-Kantorovich problem. *Philos. Trans. R. Soc. Lond. Ser. A Math. Phys. Eng. Sci.*, 372(2028):20130398, 11, 2014.

[15] Adrien Blanchet and Guillaume Carlier. Optimal transport and Cournot-Nash equilibria. *Mathematics of Operations Research*, 41(1):125–145, 2015.

[16] Enrico Bodo. Applicazioni di meccanica quantistica: appunti per le lezioni. lecture notes for a course in quantum chemistry. *Available (April/2015) at http://w3.uniroma1.it/bodo/dispense/appl.pdf*, 2008.

[17] Jonathan M Borwein, Adrian Stephen Lewis, and Roger D Nussbaum. Entropy minimization, dad problems, and doubly stochastic kernels. *Journal of Functional Analysis*, 123(2):264–307, 1994.

[18] L. M. Bregman. The relaxation method of finding the common point of convex sets and its application to the solution of problems in convex programming. *USSR computational mathematics and mathematical physics*, 7(3):200–217, 1967.

[19] Y Brenier. The dual least action problem for an ideal, incompressible fluid. *Archive for rational mechanics and analysis*, 122(4):323–351, 1993.

[20] Yann Brenier. The least action principle and the related concept of generalized flows for incompressible perfect fluids. *Journal of the American Mathematical Society*, 2(2):225–255, 1989.

[21] Yann Brenier. Polar factorization and monotone rearrangement of vector-valued functions. *Communications on pure and applied mathematics*, 44(4):375–417, 1991.

[22] Yann Brenier. Minimal geodesics on groups of volume-preserving maps and generalized solutions of the euler equations. *Communications on pure and applied mathematics*, 52(4):411–452, 1999.

[23] Yann Brenier. Generalized solutions and hydrostatic approximation of the euler equations. *Physica D: Nonlinear Phenomena*, 237(14):1982–1988, 2008.

[24] C. Bunge. The full ci density of the li atom has been computed with a very large basis set with 8 s functions and up to k functions. *private communication*.

[25] Peter J Bushell. Hilbert's metric and positive contraction mappings in a banach space. *Archive for Rational Mechanics and Analysis*, 52(4):330–338, 1973.

[26] Giuseppe Buttazzo, Luigi De Pascale, and Paola Gori-Giorgi. Optimal-transport formulation of electronic density-functional theory. *Physical Review A*, 85(6):062502, 2012.

[27] L. A. Caffarelli and R. J. McCann. Free boundaries in optimal transport and Monge-Ampère obstacle problems. *Ann. of Math. (2)*, 171(2):673–730, 2010.

[28] Luis A Caffarelli. A localization property of viscosity solutions to the monge-ampere equation and their strict convexity. *Annals of Mathematics*, pages 129–134, 1990.

[29] Luis A Caffarelli. Some regularity properties of solutions of monge ampere equation. *Communications on pure and applied mathematics*, 44(8-9):965–969, 1991.

[30] Luis A Caffarelli. The regularity of mappings with a convex potential. *Journal of the American Mathematical Society*, 5(1):99–104, 1992.

[31] Luis A Caffarelli. Boundary regularity of maps with convex potentials–ii. *Annals of mathematics*, 144(3):453–496, 1996.

[32] G. Carlier and I. Ekeland. Matching for teams. *Econom. Theory*, 42(2):397–418, 2010.

[33] G. Carlier, A. Oberman, and E. Oudet. Numerical methods for matching for teams and Wasserstein barycenters. Preprint, Ceremade, 2014.

[34] Guillaume Carlier. *Duality and existence for a class of mass transportation problems and economic applications*, pages 1–21. Springer Japan, Tokyo, 2003.

[35] Guillaume Carlier, Vincent Duval, Gabriel Peyré, and Bernhard Schmitzer. Convergence of entropic schemes for optimal transport and gradient flows. *arXiv preprint arXiv:1512.02783*, 2015.

[36] Guillaume Carlier and Bruno Nazaret. Optimal transportation for the determinant. *ESAIM: Control, Optimisation and Calculus of Variations*, 14(04):678–698, 2008.

[37] Guillaume Carlier, Adam Oberman, and Edouard Oudet. Numerical methods for matching for teams and wasserstein barycenters. *arXiv preprint arXiv:1411.3602*, 2014.

[38] Yongxin Chen, Tryphon T Georgiou, and Michele Pavon. Entropic and displacement interpolation: a computational approach using the hilbert metric. *arXiv preprint arXiv:1506.04255*, 2015.

[39] Aron J Cohen, Paula Mori-Sánchez, and Weitao Yang. Challenges for density functional theory. *Chemical Reviews*, 112(1):289–320, 2011.

[40] Maria Colombo and Simone Di Marino. Equality between monge and kantorovich multimarginal problems with coulomb cost. *Annali di Matematica Pura ed Applicata*, pages 1–14, 2013.

[41] Maria Colombo and Federico Stra. Counterexamples in multimarginal optimal transport with coulomb cost and spherically symmetric data. *Mathematical Models and Methods in Applied Sciences*, 26(06):1025–1049, 2016.

[42] Roberto Cominetti and Jaime San Martín. Asymptotic analysis of the exponential penalty trajectory in linear programming. *Mathematical Programming*, 67(1-3):169–187, 1994.

[43] Codina Cotar, Gero Friesecke, and Claudia Klüppelberg. Density functional theory and optimal transportation with coulomb cost. *Communications on Pure and Applied Mathematics*, 66(4):548–599, 2013.

[44] Codina Cotar, Gero Friesecke, and Brendan Pass. Infinite-body optimal transport with coulomb cost. *Calculus of Variations and Partial Differential Equations*, pages 1–26, 2013.

[45] M. Cuturi and A. Doucet. Fast computation of Wasserstein barycenters. In *Proceedings of the 31st International Conference on Machine Learning (ICML), JMLR W&CP*, volume 32, 2014.

[46] Marco Cuturi. Sinkhorn distances: Lightspeed computation of optimal transport. In *Advances in Neural Information Processing Systems*, pages 2292–2300, 2013.

[47] Sara Daneri and Alessio Figalli. Variational models for the incompressible euler equations. *HCDTE Lecture Notes. Part II. Nonlinear HYperboliC PDEs, Dispersive and Transport Equations. AIMS Book Series, Applied Mathematics, to appear*, 2012.

[48] Luigi De Pascale. Optimal transport with coulomb cost. approximation and duality. *arXiv preprint arXiv:1503.07063*, 2015.

[49] Simone Di Marino, Luigi De Pascale, and Maria Colombo. Multimarginal optimal transport maps for 1-dimensional repulsive costs. *CANADIAN JOURNAL OF MATHEMATICS-JOURNAL CANADIEN DE MATHEMATIQUES*, 67:350–368, 2015.

[50] R. L. Dykstra. An algorithm for restricted least squares regression. *J. Amer. Stat.*, 78(384):839–842, 1983.

[51] David G Ebin and Jerrold Marsden. Groups of diffeomorphisms and the motion of an incompressible fluid. *Annals of Mathematics*, pages 102–163, 1970.

[52] L Euler. Principes generaux de l'etat d'equilibre des fluides; principes generaux du mouvement des fluides; continuation des recherches sur la theorie du mouvement des fluides. *Histoire de l'Acacdernie de Berlin*, 1755.

[53] Lawrence C Evans and Maciej Zworski. Lectures on semiclassical analysis, 2007.

[54] A. Figalli. The optimal partial transport problem. *Arch. Ration. Mech. Anal.*, 195(2):533–560, 2010.

[55] Hans Föllmer. Random fields and diffusion processes. In *École d'Été de Probabilités de Saint-Flour XV–XVII, 1985–87*, pages 101–203. Springer, 1988.

[56] J. Franklin and J. Lorentz. On the scaling of multidimensional matrices. *Linear Algebra and its Applications*, 114–115:717–735, 1989.

[57] Joel Franklin and Jens Lorenz. Special issue dedicated to alan j. hoffman on the scaling of multidimensional matrices. *Linear Algebra and its Applications*, 114:717 – 735, 1989.

[58] David E. Freund, Barton D. Huxtable, and John D. Morgan. Variational calculations on the helium isoelectronic sequence. *Phys. Rev. A*, 29:980–982, Feb 1984.

[59] Gero Friesecke. The multiconfiguration equations for atoms and molecules: charge quantization and existence of solutions. *Archive for Rational Mechanics and Analysis*, 169(1):35–71, 2003.

[60] Gero Friesecke, Christian B Mendl, Brendan Pass, Codina Cotar, and Claudia Klüppelberg. N-density representability and the optimal transport limit of the hohenberg-kohn functional. *The Journal of chemical physics*, 139(16):164109, 2013.

[61] A. Galichon. *Optimal Transport Methods in Economics*. Princeton University Press, 1st edition, 2016.

[62] Alfred Galichon and Nassif Ghoussoub. Variational representations for n-cyclically monotone vector fields. *Pacific Journal of Mathematics*, 269(2):323–340, 2014.

[63] Alfred Galichon and Bernard Salanié. Matching with trade-offs: Revealed preferences over competing characteristics. 2010.

[64] Thomas Gallouët and Quentin Mérigot. A lagrangian scheme for the incompressible euler equation using optimal transport. *arXiv preprint arXiv:1605.00568*, 2016.

[65] Wilfrid Gangbo and Robert J McCann. The geometry of optimal transportation. *Acta Mathematica*, 177(2):113–161, 1996.

[66] Wilfrid Gangbo and Andrzej Swiech. Optimal maps for the multidimensional monge-kantorovich problem. *Communications on pure and applied mathematics*, 51(1):23–45, 1998.

[67] Tryphon T Georgiou and Michele Pavon. Positive contraction mappings for classical and quantum schrödinger systems. *Journal of Mathematical Physics*, 56(3):033301, 2015.

[68] Nassif Ghoussoub and Bernard Maurey. Remarks on multi-marginal symmetric monge-kantorovich problems. *arXiv preprint arXiv:1212.1680*, 2012.

[69] Nassif Ghoussoub and Abbas Moameni. Symmetric monge–kantorovich problems and polar decompositions of vector fields. *Geometric and Functional Analysis*, 24(4):1129–1166, 2014.

[70] Nassif Ghoussoub and Brendan Pass. Decoupling of degiorgi-type systems via multi-marginal optimal transport. *Communications in Partial Differential Equations*, 39(6):1032–1047, 2014.

[71] Paola Gori-Giorgi, Michael Seidl, and Giovanni Vignale. Density-functional theory for strongly interacting electrons. *Physical review letters*, 103(16):166402, 2009.

[72] Nathael Gozlan and Christian Léonard. Transport inequalities. a survey. *arXiv preprint arXiv:1003.3852*, 2010.

[73] P. Hohenberg and W. Kohn. Inhomogeneous electron gas. *Phys. Rev.*, 136:B864–B871, Nov 1964.

[74] Leonid Kantorovich. On a problem of monge. *Journal of Mathematical Sciences*, 133(4):1383–1383, 2006.

[75] Leonid Vitalievich Kantorovich. On the translocation of masses. 37:199–201, 1942.

[76] Hans G Kellerer. Duality theorems for marginal problems. *Zeitschrift für Wahrscheinlichkeitstheorie und verwandte Gebiete*, 67(4):399–432, 1984.

[77] Jun Kitagawa and Brendan Pass. The multi-marginal optimal partial transport problem. *arXiv preprint arXiv:1401.7255*, 2014.

[78] W. Kohn and L. J. Sham. Self-consistent equations including exchange and correlation effects. *Phys. Rev.*, 140:A1133–A1138, Nov 1965.

[79] Jonathan Korman and Robert McCann. Optimal transportation with capacity constraints. *Transactions of the American Mathematical Society*, 367(3):1501–1521, 2015.

[80] Jonathan Korman and Robert J McCann. Insights into capacity-constrained optimal transport. *Proceedings of the National Academy of Sciences*, 110(25):10064–10067, 2013.

[81] Harold W Kuhn. The hungarian method for the assignment problem. *Naval research logistics quarterly*, 2(1-2):83–97, 1955.

[82] David C Langreth and John P Perdew. The exchange-correlation energy of a metallic surface. *Solid State Communications*, 17(11):1425–1429, 1975.

[83] M. LeBreton and S. Weber. Games of social interactions with local and global externalities. *Econ. Letters*, 111:88–90, 2011.

[84] Christian Léonard. From the Schrödinger problem to the monge–kantorovich problem. *Journal of Functional Analysis*, 262(4):1879–1920, 2012.

[85] Christian Léonard. A survey of the Schrödinger problem and some of its connections with optimal transport. *arXiv preprint arXiv:1308.0215*, 2013.

[86] Mel Levy. Universal variational functionals of electron densities, first-order density matrices, and natural spin-orbitals and solution of the v-representability problem. *Proceedings of the National Academy of Sciences*, 76(12):6062–6065, 1979.

[87] Elliott H Lieb. A lower bound for coulomb energies. *Physics Letters A*, 70(5):444–446, 1979.

[88] Elliott H Lieb. Density functionals for coulomb systems. In *Inequalities*, pages 269–303. Springer, 2002.

[89] Elliott H Lieb and Stephen Oxford. Improved lower bound on the indirect coulomb energy. *International Journal of Quantum Chemistry*, 19(3):427–439, 1981.

[90] Elliott H Lieb and Barry Simon. The hartree-fock theory for coulomb systems. *Communications in Mathematical Physics*, 53(3):185–194, 1977.

[91] Pierre-Louis Lions. Solutions of hartree-fock equations for coulomb systems. *Communications in Mathematical Physics*, 109(1):33–97, 1987.

[92] Robert J McCann. A convexity principle for interacting gases. *Advances in mathematics*, 128(1):153–179, 1997.

[93] Quentin Mérigot and Jean-Marie Mirebeau. Minimal geodesics along volume preserving maps, through semi-discrete optimal transport. *arXiv preprint arXiv:1505.03306*, 2015.

[94] Gaspard Monge. *Mémoire sur la théorie des déblais et des remblais*. De l'Imprimerie Royale, 1781.

[95] John Von Neumann. On rings of operators. reduction theory. *Annals of Mathematics*, 50(2):pp. 401–485, 1949.

[96] B. Pass. Uniqueness and Monge solutions in the multimarginal optimal transportation problem. *SIAM Journal on Mathematical Analysis*, 43(6):2758–2775, 2011.

[97] Brendan Pass. *Structural results on optimal transportation plans*. PhD thesis, University of Toronto, 2011.

[98] Brendan Pass. On the local structure of optimal measures in the multi-marginal optimal transportation problem. *Calculus of Variations and Partial Differential Equations*, 43(3-4):529–536, 2012.

[99] Brendan Pass. Remarks on the semi-classical Hohenberg–Kohn functional. *Nonlinearity*, 26(9):2731, 2013.

[100] Gabriel Peyré. Entropic approximation of wasserstein gradient flows. *SIAM Journal on Imaging Sciences*, 8(4):2323–2351, 2015.

[101] Aldo Pratelli. On the equality between monge's infimum and kantorovich's minimum in optimal mass transportation. In *Annales de l'Institut Henri Poincare (B) Probability and Statistics*, volume 43, pages 1–13. Elsevier, 2007.

[102] Aldo Pratelli. On the sufficiency of c-cyclical monotonicity for optimality of transport plans. *Mathematische Zeitschrift*, 2007.

[103] Didier Robert. *Autour de l'approximation semi-classique*, volume 68. Birkhäuser Basel, 1987.

[104] Ludger Rüschendorf. Convergence of the iterative proportional fitting procedure. *The Annals of Statistics*, pages 1160–1174, 1995.

[105] Filippo Santambrogio. *Optimal transport for applied mathematicians*. Progress in Nonlinear Differential Equations and their Applications, 87. Birkhäuser/Springer, Cham, 2015. Calculus of variations, PDEs, and modeling.

[106] Walter Schachermayer and Josef Teichmann. Characterization of optimal transport plans for the monge-kantorovich-problem. *proceedings of the A.M.S.*, Vol. 137.(2):519–529, 2009.

[107] Erwin Schrödinger. *Über die umkehrung der naturgesetze*. Verlag Akademie der wissenschaften in kommission bei Walter de Gruyter u. Company, 1931.

[108] Erwin Schrödinger. Sur la théorie relativiste de l'électron et l'interprétation de la mécanique quantique. In *Annales de l'institut Henri Poincaré*, volume 2, pages 269–310, 1932.

[109] Michael Seidl. Strong-interaction limit of density-functional theory. *Physical Review A*, 60(6):4387, 1999.

[110] Michael Seidl, Paola Gori-Giorgi, and Andreas Savin. Strictly correlated electrons in density-functional theory: A general formulation with applications to spherical densities. *Physical Review A*, 75(4):042511, 2007.

[111] AI Shnirelman. Generalized fluid flows, their approximation and applications. *Geometric and Functional Analysis*, 4(5):586–620, 1994.

[112] Alexander I Shnirelman. On the geometry of the group of diffeomorphisms and the dynamics of an ideal incompressible fluid. *Mathematics of the USSR-Sbornik*, 56(1):79, 1987.

[113] R. Sinkhorn. Diagonal equivalence to matrices with prescribed row and column sums. *Amer. Math. Monthly*, 74:402–405, 1967.

[114] Cyril Smith and Martin Knott. On hoeffding-fréchet bounds and cyclic monotone relations. *Journal of multivariate analysis*, 40(2):328–334, 1992.

[115] C. Villani. *Topics in Optimal Transportation*, volume 58 of *Graduate Studies in Mathematics*. American Mathematical Society, Providence, 2003.

[116] Cédric Villani. *Optimal transport: old and new*, volume 338. Springer Science & Business Media, 2008.

[117] John von Neumann. *Functional Operators. Vol. 1: Measures and integrals. Vol 2: The geometry of orthogonal spaces*. Number 21, 22. 1950–1951.

[118] Weitao Yang. Generalized adiabatic connection in density functional theory. *The Journal of chemical physics*, 109(23):10107–10110, 1998.

[119] Grigorii M. Zhislin. Discussion of the spectrum of schrödinger operators for systems of many particles. *Trudy Moskovskogo matematiceskogo obscestva*, 9:81–120, 1960.

Résumé

Dans cette thèse, notre but est de donner un cadre numérique général pour approcher les solutions des problèmes du transport optimal (TO). L'idée générale est d'introduire une régularisation entropique du problème initial. Le problème régularisé correspond à minimiser une entropie relative par rapport à une mesure de référence donnée. En effet, cela équivaut à trouver la projection d'un couplage par rapport à la divergence de Kullback-Leibler. Cela nous permet d'utiliser l'algorithme de Bregman/Dykstra et de resoudre plusieurs problèmes variationnels liés au TO. Nous nous intéressons particulièrement à la résolution des problèmes du transport optimal multi-marges (TOMM) qui apparaissent dans le cadre de la dynamique des fluides (équations d'Euler incompressible à la Brenier) et de la physique quantique (la théorie de fonctionnelle de la densité). Dans ces cas, nous montrons que la régularisation entropique joue un rôle plus important que de la simple stabilisation numérique. De plus, nous donnons des résultats concernant l'existence des transports optimaux (par exemple des transports fractals) pour le problème TOMM.

Abstract

In this thesis we aim at giving a general numerical framework to approximate solutions to optimal transport (OT) problems. The general idea is to introduce an entropic regularization of the initial
problems. The regularized problem corresponds to the minimization of a relative entropy with respect a given reference measure. Indeed, this is equivalent to find the projection of the joint coupling with respect the Kullback-Leibler divergence. This allows us to make use the Bregman/Dykstra's algorithm and solve several variational problems related to OT. We are especially interested in solving multi-marginal optimal transport problems (MMOT) arising in Physics such as in Fluid Dynamics (e.g. incompressible Euler equations à la Brenier) and in Quantum Physics (e.g. Density Functional Theory). In these cases we show that the entropic regularization plays a more important role than a simple numerical stabilization. Moreover, we also give some important results concerning existence of optimal transport maps (e.g. fractal maps) for MMOT .

Mots Clés

Transport optimal, Transport Optimal Multi-Marges, régularisation entropique, algorithme de Bregman, algorithme de Dykstra, équations d'Euler, TFD, problème de Schrödinger, map fractale, Cournot-Nash, Transport Partiel, Contarinte de capacité, barycentre de Wasserstein

Keywords

Optimal transport, Multi-Marginal Optimal transport, Entropic regularization, Dykstra algorithm, Bregman algorithm, Euler equations, DFT, Schrödinger problem, fractal map, Cournot-Nash, Partial transport, Capacity constraint, Wasserstein barycenter